WHEN THE SIGNAL IS LOST

IMPROVING MOLECULAR DIAGNOSTICS OF RENAL CILIOPATHIES

Marijn F. Stokman

when the signal is lost_marijn_8072018.indd 1 08/07/2018 10:50

When the signal is lost
Improving molecular diagnostics of renal ciliopathies

Copyright © Marijn F. Stokman 2018

All rights reserved. No part of this thesis may be reproduced or transmitted, in any form or by any means, without prior written permission of the author and corresponding journal.

ISBN: 978-94-930-1919-5
Design and layout: Jan Willem Deiman
Layout: Jan Willem Deiman
Printed by: ProefschriftMaken || www.proefschriftmaken.nl

The research described in this thesis was financially supported by the Dutch Kidney Foundation under grant agreement CP11.18 Kouncil.

When the signal is lost

Improving molecular diagnostics of renal ciliopathies

Als het signaal verloren gaat

Het verbeteren van de moleculaire diagnostiek van renale ciliopathieën
(met een samenvatting in het Nederlands)

Proefschrift

ter verkrijging van de graad van doctor aan de Universiteit Utrecht op gezag van de rector magnificus, prof. dr. H.R.B.M. Kummeling, ingevolge het besluit van het college voor promoties in het openbaar te verdedigen op donderdag 30 augustus 2018 des middags te 12.45 uur

door

Marijn Fijke Stokman
geboren op 26 februari 1987
te Utrecht

when the signal is lost_marijn_8072018.indd 3 08/07/2018 10:50

Promotor: Prof. dr. V.V.A.M. Knoers

Copromotoren: Dr. R.H. Giles
Dr. M.R. Lilien

when the signal is lost_marijn_8072018.indd 4 08/07/2018 10:50

CONTENTS

CHAPTER 1
Introduction and outline: Genetic etiology of nephronophthisis-related ciliopathies 7

PART 1
CLINICAL, GENETIC AND FUNCTIONAL ASPECTS OF CILIOPATHIES

CHAPTER 2
Clinical and genetic analyses of a Dutch cohort of 40 patients with a nephronophthisis-related ciliopathy 19

CHAPTER 3
De novo 14q24.2q24.3 microdeletion including *IFT43* is associated with intellectual disability, skeletal anomalies, cardiac anomalies and myopia 53

CHAPTER 4
Compound heterozygous *NEK1* variants in two sibs with oral-facial-digital syndrome II (Mohr syndrome) 73

CHAPTER 5
Mutations in *KIF14* cause Meckel-Gruber syndrome and cytokinesis defects 103

PART 2
NOVEL APPROACHES TO KIDNEY DISEASE DIAGNOSTICS

CHAPTER 6
Changes in the urinary extracellular vesicle proteome are associated with nephronophthisis-related ciliopathies 125

CHAPTER 7
The expanding phenotypic spectra of kidney diseases: insights from genetic studies 163

CHAPTER 8
General discussion 187

APPENDICES
Nederlandse samenvatting 202
References 206
Acknowledgments / Dankwoord 246
List of publications 250
Curriculum vitae 252

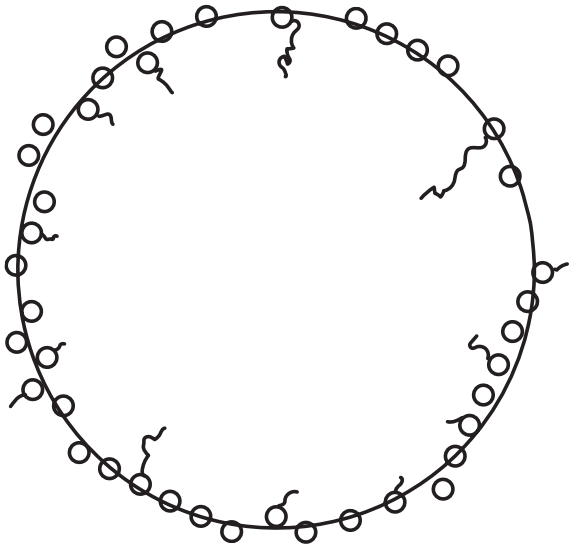

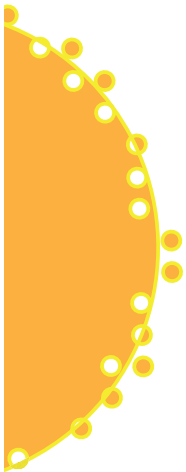

CHAPTER 1

Introduction and outline: Genetic etiology of nephronophthisis-related ciliopathies

Adapted from:
Stokman MF, Lilien MR, Knoers NVAM. 2016. Nephronophthisis. GeneReviews® [Internet]. Seattle Univ. Washington, Seattle: 1-40.
And:
Renkema KY, Stokman MF, Giles RH, Knoers NVAM. 2014. Next-generation sequencing for research and diagnostics in kidney disease. Nat. Rev. Nephrol. 10: 433-444.
DOI:10.1038/nrneph.2014.95

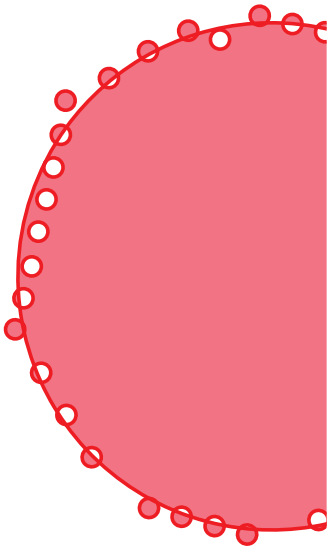

1.1 WASTING OF THE KIDNEYS

Nephronophthisis is a hereditary kidney disease. 'Nephronophthisis' literally means 'wasting of the kidneys'. The name is derived from the ancient Greek '*nephrós*', meaning 'kidney', and '*phthinein*', meaning 'to waste away'. Nephronophthisis is the most important monogenic cause of end-stage renal disease (ESRD) in childhood, accounting for 2.4% to 15% of cases [Hildebrandt et al., 1993; Hamiwka et al., 2008; Hildebrandt et al., 2009]. It is characterized by reduced urine concentrating ability of the kidney, chronic tubulointerstitial nephritis, and progression to ESRD before the age of 30 years [Hildebrandt and Zhou, 2007].

Three clinical subtypes of nephronophthisis are recognized based on the age of ESRD onset. It should be noted that there is considerable inter- and intrafamilial variability in the rate of progression to ESRD within subtypes [Caridi et al., 2006a]:

1. Infantile nephronophthisis can present in utero with an oligohydramnios (Potter) sequence (i.e. limb contractures, pulmonary hypoplasia and facial dysmorphisms) or in the first years of life with severe renal failure. Hypertension can present secondary to renal failure [Haider et al., 1998; Otto et al., 2003]. ESRD develops before the age of three years [Haider et al., 1998; Otto et al., 2003].

2. Juvenile nephronophthisis is the most prevalent form of nephronophthisis. Juvenile nephronophthisis typically presents with polydipsia and polyuria, growth retardation, or chronic iron-resistant anemia [Ala-Mello et al., 1996; Hildebrandt et al., 2009; Soliman et al., 2012]. Other findings related to chronic kidney disease (CKD) may include metabolic bone disease, metabolic acidosis, uremic symptoms (e.g. nausea, anorexia and weakness), and proteinuria due to secondary glomerulosclerosis. Hypertension is typically absent because of salt wasting [Hildebrandt et al., 2009; Niaudet, 2013]. ESRD develops at a median age of 13 years [Hildebrandt et al., 1997b, 2009; Soliman et al., 2012; Wolf, 2015].

3. Adolescent/ adult nephronophthisis. Clinical features are similar to juvenile nephronophthisis. ESRD develops at a median age of 19 years [Omran et al., 2000; Olbrich et al., 2003].

The diagnosis of nephronophthisis is currently based on clinical findings, ultrasound findings (including increased echogenicity, reduced corticomedullary differentiation and renal cysts in 50% of patients), and a family history compatible with autosomal recessive inheritance. However, there is significant diagnostic delay in most patients. As a result of variable and aspecific presentation, the diagnosis is made an average of 3.5 years after the onset of symptoms [Soliman et al., 2012]. As a result, kidney damage is often severe and irreversible by the time nephronophthisis is detected. Thus, studies investigating early diagnostic markers for nephronophthisis are warranted.

when the signal is lost_marijn_8072018.indd 8 08/07/2018 10:50

1.1.1 Terminology used in this thesis

Approximately 80%-90% of individuals with nephronophthisis have isolated nephronophthisis. The remaining 10%-20% of individuals have extrarenal manifestations [Hildebrandt et al., 2009; Wolf, 2015]. The term 'nephronophthisis-related ciliopathies' (NPH-RC) is used to describe isolated nephronophthisis, nephronophthisis with extrarenal features that do not constitute a recognizable syndrome, and syndromic nephronophthisis (e.g. Senior-Løken syndrome, Joubert syndrome, Meckel-Gruber syndrome, Sensenbrenner syndrome and Jeune syndrome) [Halbritter et al., 2013]. Renal ciliopathies include NPH-RC and ciliopathies with other renal manifestations, for example Bardet-Biedl syndrome, which can be associated with congenital abnormalities of the kidney and urinary tract (CAKUT).

1.2 GENETIC HETEROGENEITY IN NPH-RC

Nephronophthisis is considered a ciliopathy, or a disease involving the cilia. The primary cilium is a sensory organelle present on the apical surface of nearly all cell types, including renal tubular epithelial cells. It is involved in the detection and the transmission of signals from and towards the cell. Nephronophthisis is classified as a ciliopathy because almost all nephronophthisis-related genes encode proteins that localize to the primary cilium: at the ciliary transition zone, the inversin compartment, the centrosome or subunits of the intraflagellar transport (IFT) complexes (**Figure 1**) (among other localizations such as cell-cell junctions) [Fliegauf et al., 2006; Omran, 2010; Novarino et al., 2011; Sang et al., 2011; van Reeuwijk et al., 2011; Donaldson et al., 2002; Delous et al., 2009; Hurd and Hildebrandt, 2011]. Moreover, mutations in nephronophthisis-related genes often result in defects in ciliogenesis or ciliary protein trafficking [Bredrup et al., 2011].

The genetic cause of nephronophthisis can be established in approximately 40%-50% of individuals with nephronophthisis by identifying biallelic pathogenic variants in one of the 20 known nephronophthisis-related genes (**Table 1**) [Schueler et al., 2016; Kang et al., 2016]. Mutations in a few nephronophthisis-related genes are associated with a distinct phenotype, for example patients with mutations in *SDCCAG8* (*NPHP10*) often have nephronophthisis and retinal degeneration [Otto et al., 2010; Schaefer et al., 2011; Chaki et al., 2011; Billingsley et al., 2012]. However, there is substantial phenotypic overlap between renal ciliopathies and genotype-phenotype correlations are currently not clear-cut [Chaki et al., 2011]. This hampers targeted genetic testing and prognostic counseling of patients. Genetic diagnostic algorithms for nephronophthisis have been proposed by several groups [Chaki et al., 2011; Simms et al., 2011; Braun et al., 2016]; however, consensus diagnostic criteria have not been established. **Figure 2** depicts the genetic testing strategy used for the research described in this thesis.

when the signal is lost_marijn_8072018.indd 9 08/07/2018 10:50

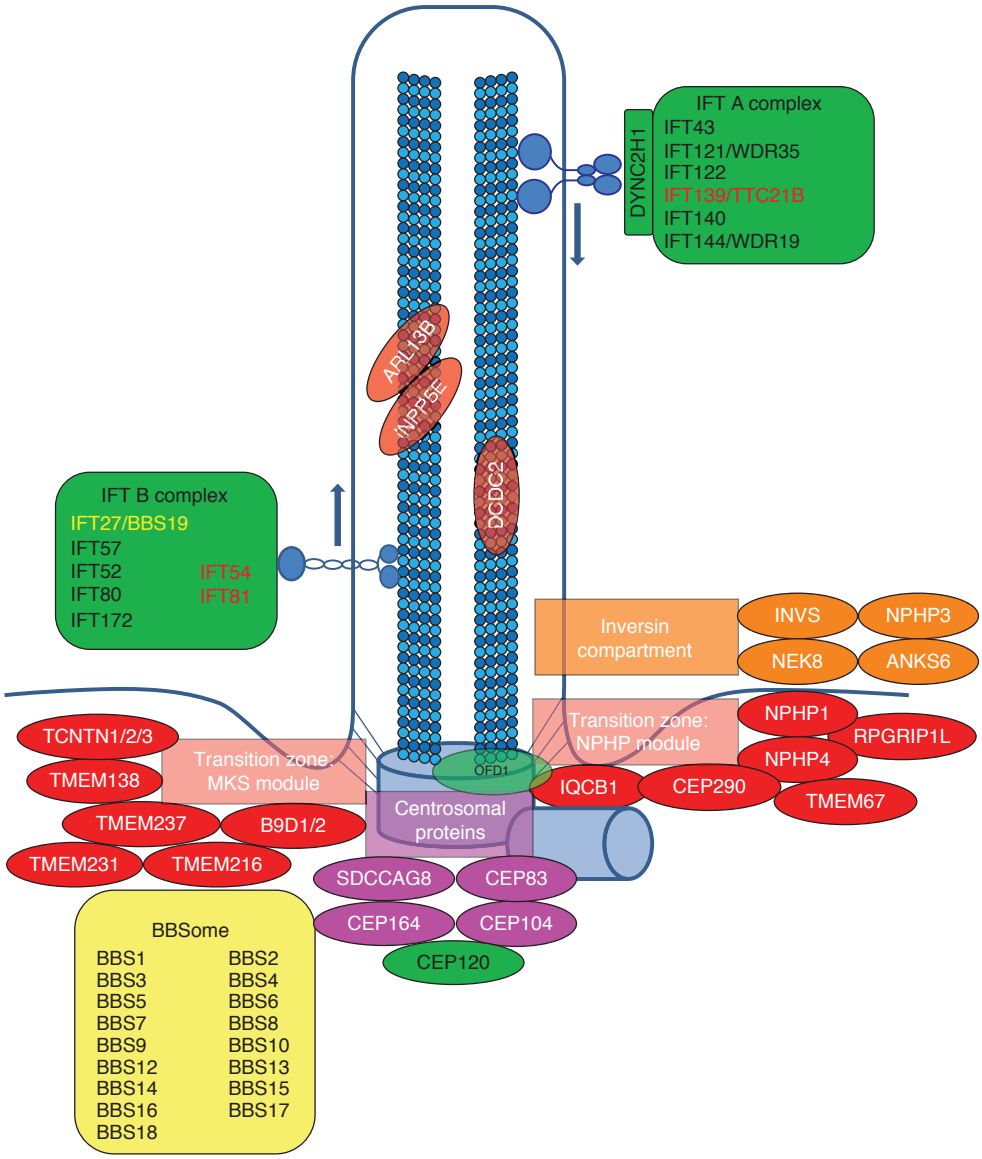

Figure 1. Ciliary localization of proteins encoded by genes associated with nephronophthisis-related ciliopathies. Proteins associated with nephronophthisis, Senior-Løken syndrome, Joubert syndrome and Meckel-Gruber syndrome localize primarily to the transition zone, inversin compartment and centrosome (red, orange and purple). Proteins associated with Bardet-Biedl syndrome form the BBSome (yellow) and proteins associated with skeletal ciliopathies localize to the intraflagellar transport (IFT) complexes (green). Reprinted with permission from Cold Spring Harbor Laboratory Archives (© 2017 Cold Spring Harbor Laboratory Press) [Braun and Hildebrandt, 2017].

when the signal is lost_marijn_8072018.indd 10 08/07/2018 10:50

Table 1. Nephronophthisis genes

Locus name	Gene	Chromosome locus	Protein
NPHP1	*NPHP1*	2q13	Nephrocystin-1
NPHP2	*INVS*	9q31.1	Inversin
NPHP3	*NPHP3*	3q22.1	Nephrocystin-3
NPHP4	*NPHP4*	1p36.31	Nephrocystin-4
NPHP5	*IQCB1*	3q13.33	IQ calmodulin-binding motif-containing protein 1
NPHP6	*CEP290*	12q21.32	Centrosomal protein of 290 kDa
NPHP7	*GLIS2*	16p13.3	Zinc finger protein GLIS2
NPHP8	*RPGRIP1L*	16q12.2	Protein fantom
NPHP9	*NEK8*	17q11.2	Serine/threonine-protein kinase Nek8
NPHP10	*SDCCAG8*	1q43-q44	Serologically defined colon cancer antigen 8
NPHP11	*TMEM67*	8q22.1	Meckelin
NPHP12	*TTC21B*	2q24.3	Tetratricopeptide repeat protein 21B
NPHP13	*WDR19*	4p14	WD repeat-containing protein 19
NPHP14	*ZNF423*	16q12.1	Zinc finger protein 423
NPHP15	*CEP164*	11q23.3	Centrosomal protein of 164 kDa
NPHP16	*ANKS6*	9q22.33	Ankyrin repeat and SAM domain-containing protein 6
NPHP17	*IFT172*	2p23.3	Intraflagellar transport protein 172 homolog
NPHP18	*CEP83*	12q22	Centrosomal protein of 83 kDa
NPHP19	*DCDC2*	6p22.3	Doublecortin domain-containing protein 2
NPHP20	*MAPKBP1*	15q15.1	Mitogen-activated protein kinase-binding protein 1

Additional genes associated with nephronophthisis are not currently classified as nephronophthisis-related genes in the Online Mendelian Inheritance of Man (OMIM®) database. These include genes associated with ciliopathies in which nephronophthisis is a non-obligatory feature (e.g. *AHI1* and *OFD1*) and newly discovered NPH-RC genes (e.g. *IFT140*, *TRAF3IP1* and *IFT81*) [Perrault et al., 2012; Schmidts et al., 2013; Bizet et al., 2015; Perrault et al., 2015; Xu et al., 2015]. Moreover, more than 90 genes have been identified as disease causing in the broader category of NPH-RC [Braun and Hildebrandt, 2017]. Considering the current 40%-50% mutation detection rate, many more nephronophthisis-related genes have yet to be identified [Hildebrandt et al., 2009; Otto et al., 2011; Wolf and Hildebrandt, 2011; Arts and Knoers, 2013b]. However, the relative paucity of novel (isolated-) nephronophthisis genes discovered in recent years causes researchers to consider variants in non-coding and regulatory regions [Elumalai et al., 2014b; Merta et al., 2002], and different modes of inheritance, including oligogenic inheritance [Katsanis, 2001; Bandano et al., 2003; Baala et al., 2007b; Helou et al., 2007; Tory et al., 2007; Leitch et al., 2008; Louie et al., 2010; Davis et al., 2011; Lin et al., 2013; Zhang et al., 2014; Lindstrand et al., 2014]. Consequently, the use of new genetic techniques including whole-genome sequencing, which enables detection of non-coding variants, is necessary to study the genetic etiology of NPH-RC in unsolved cases.

when the signal is lost_marijn_8072018.indd 11 08/07/2018 10:50

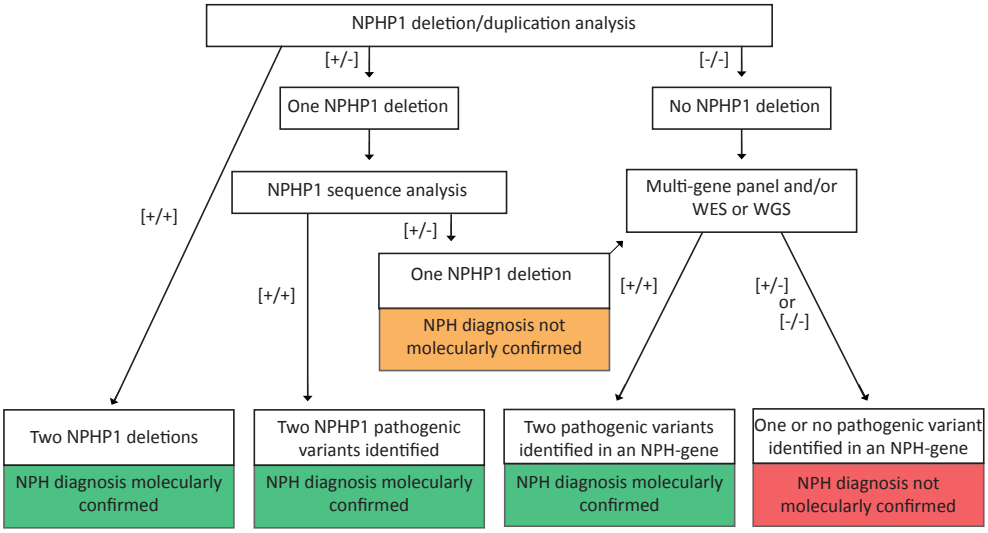

Figure 2. Current strategy to identify the genetic cause of nephronophthisis. *NPHP1*-targeted deletion/duplication analysis is performed first because deletions in *NPHP1* are detected in 20%-25% of patients with isolated nephronophthisis. If only one allele is determined to have an *NPHP1* deletion, sequence analysis of *NPHP1* is performed. If only one *NPHP1* pathogenic variant is found, a multi-gene panel of ciliary genes, WES or WGS may be considered because the *NPHP1* pathogenic variant could be acting as a genetic modifier in combination with biallelic pathogenic variants in another NPH-related gene. Of note, to date no heterozygous *NPHP1* pathogenic variant has been identified as a modifier of isolated nephronophthisis caused by biallelic pathogenic variants in another NPH-related gene. WES: whole-exome sequencing; WGS: whole-genome sequencing. Reprinted with permission from Genereviews (© 1993-2017 University of Washington) [Stokman et al., 2016a].

1.3 NEXT-GENERATION SEQUENCING AND FUNCTIONAL STUDIES IN NPH-RC

By enabling cost-effective analysis of multiple (or all) disease-associated genes simultaneously [Drmanac, 2011; Need et al., 2012; Yang et al., 2013b; Sun et al., 2015], next-generation sequencing (NGS) has boosted gene discovery and increased diagnostic yield in NPH-RC during the past ten years. *SDCCAG8* (*NPHP10*) was the first nephronophthisis gene to be identified by using a combination of homozygosity mapping and targeted exome sequencing [Otto et al., 2010]. *WDR19* (*NPHP13*), *ZNF423* (*NPHP14*) and *CEP164* (*NPHP15*) were subsequently identified using whole-exome sequencing (WES) [Bredrup et al., 2011; Chaki et al., 2012]. WES in consanguineous or familial cases with pediatric-onset CKD suspected of NPH-RC based on renal ultrasound criteria yielded etiological diagnoses in 63.3% of patients, one-third of which were reclassifications of other kidney diseases including renal tubulopathies and Alport syndrome

when the signal is lost_marijn_8072018.indd 12 08/07/2018 10:50

[Braun et al., 2016]. These examples illustrate the utility of WES in gene discovery and diagnostics of NPH-RC.

Whole-genome sequencing will likely replace targeted NGS including WES in the near future because of decreasing costs, better coverage of the exome [Meienberg et al., 2016; Sun et al., 2015], increasingly reliable detection of copy number variations (CNVs) and somatic mosaicism [King et al., 2016], as well as variant detection in non-coding and regulatory regions [Elumalai et al., 2014b; Merta et al., 2002].

Increasingly untargeted sequencing approaches have resulted in the detection of increasing amounts of variants with an unclear relation to the clinical phenotype. In other words: the more of the genome we investigate, the more variants we find. Variants detected with NGS require proof of causality, either through identification of additional patients with a similar genotype and phenotype or through functional validation in model systems. Model systems frequently used in kidney disease are *in silico* prediction models, *in vitro* renal cell models, *ex vivo* kidney explant models and a variety of *in vivo* models including zebrafish [Otto et al., 2010; Chaki et al., 2012; Sang et al., 2011; Choi et al., 2013; Van De Hoek et al., 2015]. Frequently used assays include cellular reporter assays, electrophysiological assays, cilia- and reconstitution assays in 2-D or 3-D cell culture (used in **Chapters 3-5**) and tubulogenesis assays. The recent advent of genome-editing technologies such as the CRISPR-Cas9 system facilitates high-throughput functional validation of NPH-RC-associated variants. Only validated variants can be used for reliable (reproductive) counseling of patients or testing of family members.

1.4 HOW DO NPH-RC ARISE?

The mechanisms by which disruption in NPH-RC-associated genes described above lead to nephronophthisis are largely unknown, although recent studies have shed light on nephrocystin functions and associated pathways. Nephrocystins are implicated in important signaling pathways, such as the Wnt pathway (involved in apical-basolateral polarity of renal tubular cells in response to tubular flow) [Simons et al., 2005], the Hedgehog pathway (involved in mesenchymal-to-epithelial transition in renal tubulogenesis) [Yu et al., 2002; Attanasio et al., 2007] and the Hippo pathway (involved in regulation of tissue growth) [Benzing and Schermer, 2012; Barker et al., 2014; Wolf, 2015]. Cilia defects can therefore lead to disruption of ciliary signaling pathways, which in turn can disrupt kidney development and maintenance of normal kidney architecture.

In addition, the nephronophthisis-related genes *NEK8*, *CEP164*, *SDCCAG8*, *CEP290* and *ZNF423* play a dual role in the nucleus and have been implicated in DNA damage response (DDR) signaling and cell-cycle checkpoint control [Chaki et al., 2012; Zalli et al., 2012; Choi et al., 2013; Yuan and Sun, 2013; Airik et al., 2014; Slaats et al., 2014; Slaats and Giles, 2015; Slaats et al., 2015]. It has

when the signal is lost_marijn_8072018.indd 13 08/07/2018 10:50

been hypothesized that mutations in cilia genes causing a severe disruption of DDR signaling early in development lead to depletion of progenitor cells and consequent renal developmental phenotypes (e.g. renal dysplasia), while milder disruptions cause degenerative phenotypes in childhood (e.g. nephronophthisis) [Chaki et al., 2012]. As pathogenic variants in *CEP164* induce epithelial-to-mesenchymal transition and a profibrotic response [Slaats et al., 2014], the DDR pathway may be most closely linked to tubulointerstitial fibrosis, which is a hallmark feature of nephronophthisis [Slaats and Giles, 2015]. Consequently, measures for DNA double-strand breaks, cell cycle defects and fibrosis can also be used as functional readouts in (a subset of) ciliopathies [Slaats et al., 2014]. Moreover, exploration of the role of cilia proteins in DDR signaling and fibrosis can reveal new mechanisms for targeted treatment in renal ciliopathies [Slaats et al., 2016b].

1.5 SCOPE AND OUTLINE OF THIS THESIS

In this thesis, I present research aimed at improving early diagnostics, prognostics and clinical care for patients with NPH-RC. **Chapter 1** introduces the NPH-RC phenotypes and the methods used to investigate the underlying molecular mechanisms.

The first part of this thesis focuses on clinical, genetic and functional aspects of ciliopathies. In **Chapter 2**, I describe the Nephronophthisis Registry containing 40 Dutch patients with NPH-RC and explore associations between genotypes and renal and extrarenal phenotypes, and presenting signs and symptoms of nephronophthisis. **Chapters 3, 4** and **5** focus on the functional validation of candidate genetic variants in the cilia genes *IFT43*, *NEK1* and *KIF14* using cell models. The pathophysiological insight gained from studying the role of the encoded proteins in the cilium and in the nucleus is discussed.

Part two describes novel approaches to diagnostics of kidney diseases. In **Chapter 6**, untargeted proteomics of urinary extracellular vesicles is used to identify diagnostic and prognostic biomarkers for nephronophthisis, and to analyze pathways involved in ciliopathies. In **Chapter 7**, I discuss the contribution of NGS techniques to our understanding of genotype-phenotype correlations and nosology in NPH-RC and other kidney diseases.

Finally, **Chapter 8** summarizes the scientific and clinical implications of the studies described in this thesis. The main results are discussed in the context of renal ciliopathy research and the changing clinical genetics landscape.

when the signal is lost_marijn_8072018.indd 14 08/07/2018 10:50

when the signal is lost_marijn_8072018.indd 15 08/07/2018 10:50

PART 1

CLINICAL, GENETIC AND FUNCTIONAL ASPECTS OF CILIOPATHIES

when the signal is lost_marijn_8072018.indd 16 08/07/2018 10:50

when the signal is lost_marijn_8072018.indd 17 08/07/2018 10:50

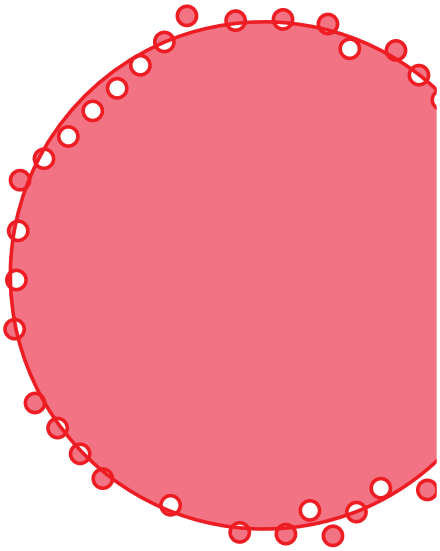

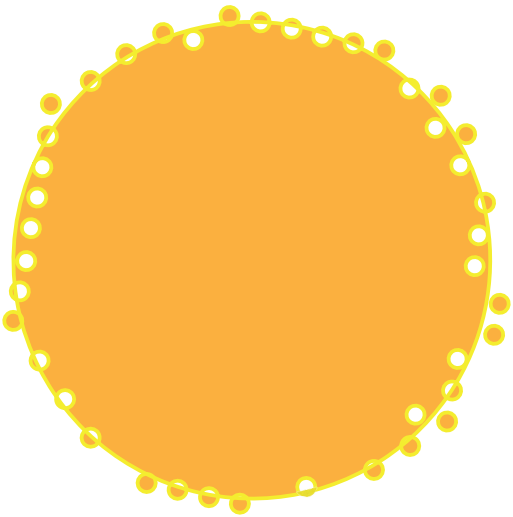

CHAPTER 2

Clinical and genetic analyses of a Dutch cohort of 40 patients with a nephronophthisis-related ciliopathy

Stokman MF, Van der Zwaag B, Van de Kar NCAJ, Van Haelst MM, Van Eerde AM, Van der Heijden JW, Kroes HY, Ippel E, Schulp JA, Van Gassen KL, Van Rooij IALM, Giles RH, Beales PL, Roepman R, Arts HH, Bongers EMHF, Renkema KY, Knoers NVAM, Van Reeuwijk J*, Lilien MR*

* These authors contributed equally

2018. Pediatr. Nephrol.
DOI:10.1007/s00467-018-3958-7

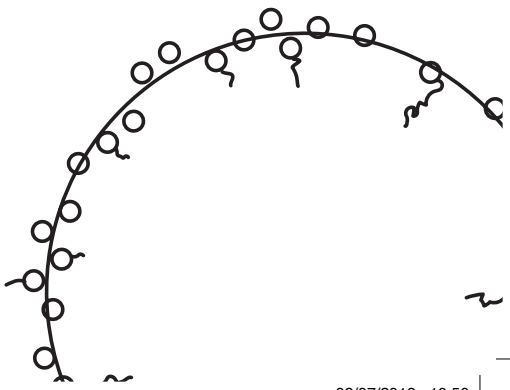

ABSTRACT

Nephronophthisis is an autosomal recessive ciliopathy and an important cause of end-stage renal disease in children and young adults. Diagnostic delay is frequent in nephronophthisis. The aim of this study was to gain insight in the clinical characteristics, initial symptoms and genetic defects associated with nephronophthisis in a Dutch cohort of 40 patients with a nephronophthisis-related ciliopathy, to improve early detection and genetic counseling. A cohort of 40 patients from 36 families with a nephronophthisis-related ciliopathy was recruited at eight university medical centers in The Netherlands and via the webpage www.kouncil.nl. Comprehensive clinical and genotypic data were recorded in the Nephronophthisis Registry. Thirteen patients with a nephronophthisis-related ciliopathy without a molecular diagnosis were analyzed for deletion/duplication of the *NPHP1* gene, and gene panel sequencing and/or whole-exome sequencing were performed. Of 40 patients with a nephronophthisis-related ciliopathy, 45% had isolated nephronophthisis, 48% had a syndromic diagnosis and 7% had nephronophthisis with extrarenal features that did not constitute a recognizable syndrome. Patients developed end-stage renal disease at a median age of 13 years (range 5-47 years). The median age of symptom onset was 9 years in both isolated and syndromic forms of NPH (range 5-26 vs. 5-33 respectively). The most frequently reported presenting signs and symptoms were fatigue (42%), polydipsia and polyuria (33%) and hypertension (21%), which should prompt evaluation of renal function. Renal ultrasound showed small to normal-sized kidneys, increased echogenicity (65%), cysts (43%) and abnormal corticomedullary differentiation (32%). Renal biopsies were performed in eight patients and showed nonspecific signs of chronic kidney disease. Of 40 patients, 23 (58%) had a genetic diagnosis upon inclusion. Thirteen out of 17 patients without a genetic diagnosis upon inclusion gave consent for genetic testing. The genetic cause was identified in 5 (38%) of the patients tested within this study. In conclusion, nephronophthisis is a genetically and phenotypically heterogeneous disorder that should be considered in children and young adults presenting with persistent fatigue and polyuria, and in all patients with unexplained chronic kidney disease. Because symptom onset can occur well into in adulthood, presymptomatic monitoring of kidney function in syndromic ciliopathy patients should be continued until at least age 30 years.

when the signal is lost_marijn_8072018.indd 20 08/07/2018 10:50

2.1 INTRODUCTION

Nephronophthisis (NPH) is an autosomal recessive kidney disease that is responsible for up to 15% of pediatric patients with end-stage renal disease (ESRD) [Hildebrandt et al., 1993; Hamiwka et al., 2008; Hildebrandt et al., 2009]. In The Netherlands, this corresponds to an estimated one to five children with ESRD per year [Van Huis, 2016]. NPH is characterized by a renal concentration defect, chronic tubulointerstitial nephritis, renal cysts in 50% of patients and progression to ESRD before age 30 years [Hildebrandt and Zhou, 2007; König et al., 2017; Soliman et al., 2012]. Three clinical subtypes are recognized based on age of onset. The most prevalent form, juvenile NPH, results in ESRD at a median age of 13 years [Hildebrandt et al., 1997, 2009; Soliman et al., 2012; Wolf, 2015]. NPH can occur in an isolated form and, in 10 to 15% of cases, as part of a multisystem disorder, for example Senior-Løken syndrome and Joubert syndrome. Both isolated and syndromic NPH are caused by mutations in genes encoding proteins that localize to primary cilia. These mutations result in structural and functional ciliary defects, and disruption of essential ciliary and nuclear signaling pathways. Hence, NPH is considered a ciliopathy.

The diagnosis of NPH is based on clinical findings, renal ultrasound findings and a family history compatible with autosomal recessive inheritance. The average diagnostic delay in isolated NPH is 3.5 years because of nonspecific presenting symptoms including polydipsia and polyuria, secondary enuresis, growth retardation and anemia refractory to iron therapy [Soliman et al., 2012]. In addition, causal mutations in one of the 20 NPH-associated genes are detected in less than 50% of patients [Halbritter et al., 2013; Braun et al., 2016; Schueler et al., 2016]. Although recent progress has been made in characterizing the clinical spectrum of NPH [Tory et al., 2009; Soliman et al., 2012; Chaki et al., 2011; König et al., 2017], the absence of solid genotype-phenotype correlations currently limits prognostic counseling of NPH patients. Therefore, analysis of presenting symptoms, renal and extrarenal phenotypes and associated genetic defects in a well-defined population of NPH patients is warranted.

Here we report clinical characteristics and genetic findings in a cohort of 40 Dutch patients from 36 families with a nephronophthisis-related ciliopathy (NPH-RC). We assess progression of CKD in isolated and syndromic forms of NPH and discuss the initial signs and symptoms of kidney disease that could point towards NPH in an early disease stage. Renal and extrarenal phenotypes and associated genetic defects are analyzed. Finally, our results suggest the limited diagnostic value of a renal biopsy in advanced stages of CKD and point towards the utility of early molecular testing in diagnostics of NPH.

when the signal is lost_marijn_8072018.indd 21 08/07/2018 10:50

2.2 METHODS

2.2.1 Patients

Patients were recruited at all eight university medical centers in The Netherlands, via the Dutch Kidney Patient Association and the Dutch Joubert Syndrome Patient and Parents' Network, and via the webpage www.kouncil.nl. Patients were included in the AGORA (Aetiologic research into Genetic and Occupational/environmental Risk factors for Anomalies in children) data- and biobank from March 2014 until May 2017 at the Department of Genetics and the Department of Pediatric Nephrology of the University Medical Center Utrecht, the Department of Human Genetics of the Radboudumc Nijmegen and the Department of Nephrology of the VU University Medical Center Amsterdam. Approval by the regional Committee on Research involving Human Subjects (CMO Arnhem-Nijmegen 2006/048) was obtained. Informed consent was available for all subjects for access to medical records, DNA testing and/or collection of biomaterial including urine, fibroblasts and/or deciduous teeth.

Inclusion criteria were a molecularly confirmed diagnosis of NPH-RC or suspected NPH-RC. NPH-RC was defined as isolated NPH, NPH with extrarenal features that do not constitute a recognizable syndrome, and syndromic NPH. Suspected NPH-RC was based on the presence of chronic kidney disease (CKD) stage 2-5 in all patients [Kidney Disease: Improving Global Outcomes (KDIGO) CKD Work Group, 2013], a family history compatible with autosomal recessive inheritance, and additional extrarenal features associated with a ciliopathy and/or clinical characteristics of NPH including signs of a renal concentration defect (e.g. polyuria), renal ultrasound showing parenchymal damage (e.g. increased echogenicity) but absence of congenital anomalies of the kidneys and urinary tract that could explain the phenotype, urinalysis showing absence of hematuria, erythrocyte casts and proteinuria in the nephrotic range, absence of recurrent urinary tract infections, and exclusion of other causes of early-onset renal failure. Cases in which the clinical diagnosis was ambiguous were discussed with a pediatric nephrologist (M.L.) and a clinical geneticist (N.K.) until consensus was reached. We included five patients with Bardet-Biedl syndrome and a nephronophthisis phenotype, however, the classification of Bardet-Biedl syndrome as NPH-RC is not consistent across literature [Braun et al., 2016; König et al., 2017]. Siblings of patients with molecularly confirmed NPH-RC who had the same biallelic mutations in an NPH-RC-associated gene and who showed some but not all clinical features were included for the analysis of initial phenotypic features of NPH. In addition to 40 patients with NPH-RC, we included twelve patients with a ciliopathy and renal features that did not fulfill clinical criteria of NPH to assess the phenotypic spectrum of renal ciliopathies.

2.2.2 The Nephronophthisis Registry

To record detailed clinical and genetic data from patients with NPH-RC, we developed a multicenter Nephronophthisis Registry using Castor EDC (Castor Electronic Data Capture, Ciwit BV, Amsterdam, The Netherlands). Access to

when the signal is lost_marijn_8072018.indd 22 08/07/2018 10:50

electronic medical records or paper copies of medical records were requested for all patients. For standardized data collection, a set of clinical parameters and definitions was established by a team of clinical experts from relevant fields including pediatric nephrology, clinical genetics and clinical molecular genetics. Consensus was reached on all parameters. Human Phenotype Ontology (HPO) terms were used for most of the clinical terms recorded to phenotype the patients, thereby also providing a basis for future integration with clinical data from other nephronophthisis registries and for clinical matching of patients in HPO-centered registries of rare diseases [Köhler et al., 2017]. Case report forms were structured in categories including medical history, physical examination, ophthalmological examination, and genetic analysis. For longitudinal data, we developed report forms for laboratory results, medication, physical re-examination, histological examination, and imaging. Syndrome diagnoses were based on clinical data on renal and extrarenal phenotypes (e.g. presence of molar tooth sign on brain imaging in Joubert syndrome) according to internationally recognized diagnostic criteria [Parisi and Glass, 2017; Forsythe and Beales, 2015; Arts and Knoers, 2013; Stokman et al., 2016a], in combination with the assessment of the referring physician.

2.2.3 Genetic analyses

Of 17 patients without a molecular diagnosis upon inclusion, 13 patients from 12 families gave consent for genetic testing. Targeted deletion/duplication analysis was performed to assess the occurrence of *NPHP1* deletions in patients with isolated NPH, Senior-Løken syndrome and Joubert syndrome, and to assess copy number variations in ciliary genes in which we identified single heterozygous point mutations (**Supplementary Methods S1**). Targeted next-generation sequencing using a gene panel containing 15 genes associated with NPH was performed in one patient (10:44). Whole-exome sequencing (**Supplementary Methods S2**) was subsequently performed in this patient and 10 additional patients with no deletion or a heterozygous deletion in *NPHP1*, including a patient with Bardet-Biedl-like syndrome in whom biallelic *NPHP1* deletions were unlikely to be causal.

2.2.4 Statistical analyses

Clinical and genetic data from the Nephronophthisis Registry were exported to Excel and analyzed using GraphPad Prism (Version 7.02).

2.3 RESULTS

2.3.1 Phenotypic variability in renal ciliopathies

Forty patients from 36 families with NPH-RC were recruited, including patients with isolated NPH (n=18), Joubert syndrome (n=8), Bardet-Biedl syndrome (n=5), Senior-Løken syndrome (n=4), cranioectodermal dysplasia (n=2), and NPH-RC phenotypes that did not constitute a recognizable syndrome (n=3) (**Figure 1**). Twenty-two out of 40 patients (55%) had extrarenal ciliopathy-associated features

when the signal is lost_marijn_8072018.indd 23 08/07/2018 10:50

including impaired vision (16/40; 40%), oculomotor abnormalities (10/33; 30%) and developmental delay (13/36; 36%), indicating enrichment of syndromic forms of NPH-RC in our cohort (**Supplementary Table S1**). **Table 1** depicts the frequency of occurrence of clinical features per causative gene for 40 patients.

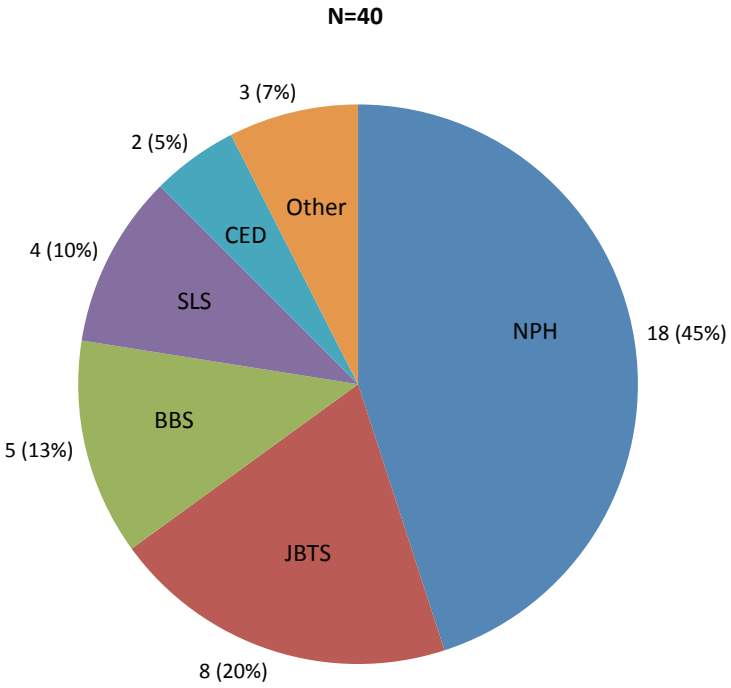

Figure 1. Relative frequencies of NPH-RC phenotypes in the cohort

Patients developed ESRD at a median age of 13 years (range 5-33 years). The median age of symptom onset was 9 years in both isolated and syndromic forms of NPH (range 5-26 vs. 5-33 years respectively). Median time between reported symptom onset and ESRD was 1 year (range 0-8 years) in patients with isolated NPH (n=11) and 5.5 years (range 0-14 years) in patients with syndromic forms of NPH (n=4). Four out of 18 patients with isolated NPH (22%) did not yet have ESRD at the time of inclusion (median age 21 years; range 17-41 years), although two patients had at least CKD stage 3. In contrast, 10/20 patients with syndromic forms of NPH (50%) did not have ESRD at the time of inclusion (median age 15.5 years; range 10-25 years) and three patients had at least CKD stage 3. More longitudinal data will be collected to determine the rate of CKD progression in patients with isolated and syndromic forms of NPH.

To evaluate the range of renal ciliopathy-associated phenotypes, we included 12 patients with a renal ciliopathy without sufficient evidence for NPH. Phenotypes included perinatally lethal renal cystic hypodysplasia and renal insufficiency with proteinuria (**Supplementary Results S1** and **Supplementary Table S2**).

when the signal is lost_marijn_8072018.indd 24 08/07/2018 10:50

when the signal is lost_marijn_8072018.indd 25

Table 1. Genetic and phenotypic findings in 40 patients with NPH-RC

Gene	Patients	Families	Median age (range)[1] (yrs)	Median age symptom onset (range)[1] (yrs)	Median age ESRD (range)[1,2] (yrs)	Median time to ESRD (range)[1,2] (yrs)	Polyuria	Polydipsia	Enuresis	Renal ultrasound findings		
										Cysts	Abnormal corticomedullary differentiation	Increased echogenicity
NPHP1	n=16	n=14	21 (9-62)	9 (6-26)	14 (7-28)	1 (0-8)	90% (9/10)	80% (8/10)	38% (3/8)	33% (4/12)	38% (3/8)	70% (7/10)
NPHP4	n=3	n=3	19 (11-41)	16 (8-24)	8	0	33% (1/3)	67% (2/3)	0% (0/3)	50% (1/2)	50% (1/2)	100% (2/2)
WDR35	n=3	n=2	17 (12-33)	9	12	3	67% (2/3)	50% (1/2)	0% (0/2)	67% (2/3)	33% (1/3)	100% (2/2)
BBS1	n=2	n=1	18 (16-20)	NA	-	NA	0% (0/1)	0% (0/1)	0% (0/1)	50% (1/2)	0% (0/2)	0% (0/2)
AHI1	n=1	n=1	25	14	-	NA	0% (0/1)	0% (0/1)	0% (0/1)	0% (0/1)	0% (0/1)	0% (0/1)
BBS10	n=1	n=1	13	NA	-	NA	100% (1/1)	100% (1/1)	0% (0/1)	100% (1/1)	100% (1/1)	100% (1/1)
IQCB1	n=1	n=1	29	NA	10	NA	NA	NA	NA	NA	NA	NA
OFD1	n=1	n=1	12	5	5	0	NA	NA	NA	0% (0/1)	0% (0/1)	100% (1/1)
Unknown	n=11	n=11	21 (15-54)	13 (5-33)	14 (8-47)	11 (8-14)	33% (2/6)	86% (6/7)	33% (1/3)	50% (4/8)	17% (1/6)	57% (4/7)
Total	n=40	n=36	19 (9-62)	9 (5-33)	13 (5-47)	1 (0-14)	60% (15/25)	72% (18/25)	21% (4/19)	43% (13/30)	32% (7/22)	65% (17/26)

ESRD: end-stage renal disease, -: absent (no ESRD), NA: not available.

[1]When range is not reported, the value is based on one patient.

[2]Patient age at CKD stage 5 was used as the age at ESRD. If this was not available, the youngest reported age at the start of dialysis/transplantation was used. Median time to ESRD could be an underestimate because patients who did not develop ESRD were not included in this calculation.

08/07/2018 10:50

2.3.2 Fatigue and polyuria are presenting symptoms of NPH

To assess presenting symptoms of NPH, we reviewed medical records and conducted patient interviews. Presenting symptoms were documented for 24/40 patients. The most frequently reported initial signs and symptoms were fatigue (10/24; 42%), polydipsia and polyuria (8/24; 33%) and hypertension (5/24; 21%) (**Figure 2** and **Supplementary Table S3**). Anemia (2/24; 8%), growth retardation (2/24; 8%), enuresis (2/24; 8%) and uremic symptoms (1/24; 4%) occurred less frequently. Novel reported presenting symptoms included muscle cramps and injuries (n=2), dizziness (n=1), red patches on the skin (n=1) and weight loss (n=1). In addition, a patient with Joubert syndrome caused by *NPHP1* mutations (34:73) reported muscle cramps after NPH was diagnosed. Based on these findings, persistent fatigue and muscle complaints in children should prompt evaluation of kidney function in addition to the classic presenting symptoms of NPH.

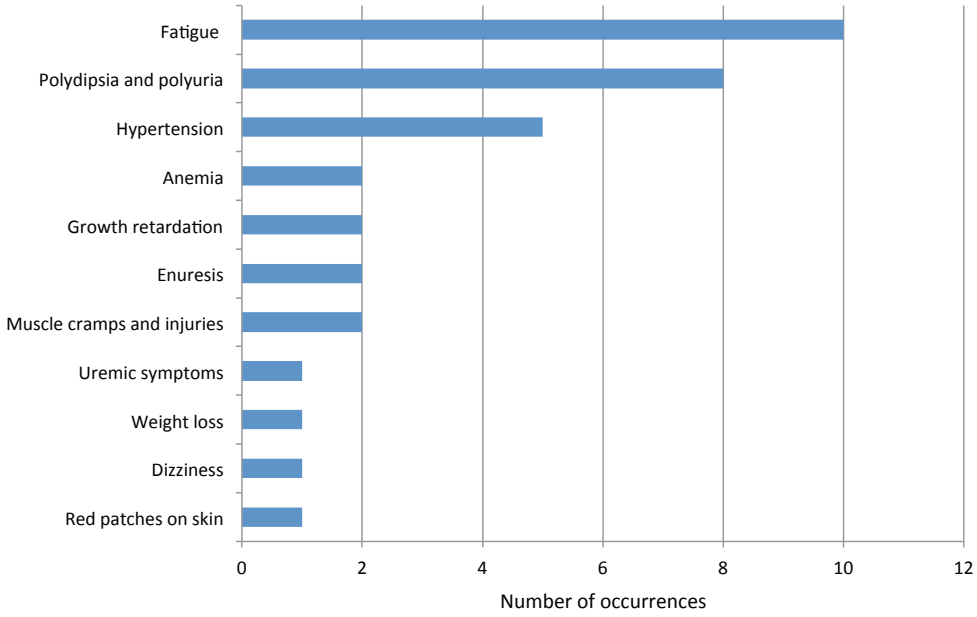

Figure 2. Presenting signs and symptoms of NPH by frequency of occurrence. Data was available for 24 patients. For ten patients, more than one presenting sign or symptom was reported.

when the signal is lost_marijn_8072018.indd 26 08/07/2018 10:50

when the signal is lost_marijn_8072018.indd 27

Table 2. Associations between gene and renal phenotype

Gene	Patients	Families	Median age (range)[1] (yrs)	Median age symptom onset (range)[1] (yrs)	Median age ESRD (range)[1,2] (yrs)	Median time to ESRD (range)[1,2] (yrs)	Polyuria	Polydipsia	Enuresis	Renal ultrasound findings		
										Cysts	Abnormal corticomedullary differentiation	Increased echogenicity
NPHP1	n=16	n=14	21 (9-62)	9 (6-26)	14 (7-28)	1 (0-8)	90% (9/10)	80% (8/10)	38% (3/8)	33% (4/12)	38% (3/8)	70% (7/10)
NPHP4	n=3	n=3	19 (11-41)	16 (8-24)	8	0	33% (1/3)	67% (2/3)	0% (0/3)	50% (1/2)	50% (1/2)	100% (2/2)
WDR35	n=3	n=2	17 (12-33)	9	12	3	67% (2/3)	50% (1/2)	0% (0/2)	67% (2/3)	33% (1/3)	100% (2/2)
BBS1	n=2	n=1	18 (16-20)	NA	-	NA	0% (0/1)	0% (0/1)	0% (0/1)	50% (1/2)	0% (0/2)	0% (0/2)
AHI1	n=1	n=1	25	14	-	NA	0% (0/1)	0% (0/1)	0% (0/1)	0% (0/1)	0% (0/1)	0% (0/1)
BBS10	n=1	n=1	13	NA	-	NA	100% (1/1)	100% (1/1)	0% (0/1)	100% (1/1)	100% (1/1)	100% (1/1)
IQCB1	n=1	n=1	29	NA	10	NA	NA	NA	NA	NA	NA	NA
OFD1	n=1	n=1	12	5	5	0	NA	NA	NA	0% (0/1)	0% (0/1)	100% (1/1)
Unknown	n=11	n=11	21 (15-54)	13 (5-33)	14 (8-47)	11 (8-14)	33% (2/6)	86% (6/7)	33% (1/3)	50% (4/8)	17% (1/6)	57% (4/7)
Total	n=40	n=36	19 (9-62)	9 (5-33)	13 (5-47)	1 (0-14)	60% (15/25)	72% (18/25)	21% (4/19)	43% (13/30)	32% (7/22)	65% (17/26)

ESRD: end-stage renal disease, -: absent (no ESRD), NA: not available.

[1]When range is not reported, the value is based on one patient.

[2]Patient age at CKD stage 5 was used as the age at ESRD. If this was not available, the youngest reported age at the start of dialysis/transplantation was used. Median time to ESRD could be an underestimate because patients who did not develop ESRD were not included in this calculation.

08/07/2018 10:50

2.3.3 Increased echogenicity is a more prevalent finding than renal cysts in NPH-RC

Overall occurring symptoms were analyzed in 40 patients with NPH-RC. The most frequently reported symptoms were polydipsia and polyuria (18/25; 72% and 15/25; 60%, respectively) and enuresis (4/19; 21%) (**Table 2** and **Supplementary Table S3**). Fifteen out of 23 patients (65%) had normal-sized kidneys on renal ultrasound and eight patients (35%) had at least one small kidney (size <5th percentile) (reference values: [Kulon, 2016; Kadioglu, 2010]). Small to normal-sized kidneys is a typical finding in NPH [Blowey et al., 1996; Soliman et al., 2012; König et al., 2017]. Additional ultrasound findings included increased echogenicity (17/26; 65%), renal cysts (13/30; 43%) and abnormal corticomedullary differentiation (7/22; 32%). Increased echogenicity was the most prevalent finding on renal ultrasound and could therefore be considered a more sensitive finding for nephronophthisis than renal cysts.

2.3.4 Histological findings are frequently nonspecific in NPH

Renal biopsy was performed in 8/40 patients. Insufficient material was obtained from two patients, resulting in a second biopsy for one patient. Tubulointerstitial nephritis was a finding in 4/7 biopsies and tubular atrophy in 3/7. Renal cysts were reported in none of the patients. Instead, glomerulosclerosis was seen in 5/7 biopsies. Biopsies were taken in advanced stages of NPH (CKD stage ≥3 for all patients except patient 11:45), when differentiating findings such as thickening of tubular basement membranes and cysts on the corticomedullary border were expected to be no longer detectable. These findings suggest that the diagnostic value of a renal biopsy is limited in advanced stages of CKD, which is often already present when the diagnosis of NPH is first suspected.

2.3.5 NPHP1 mutations in thirty-eight percent of tested patients

Twenty-three out of 40 patients (58%) had a (likely) molecular diagnosis at the time of inclusion (**Supplementary Table S4**). We performed genetic testing for 13 patients from 12 families without a molecular diagnosis, including genotyping, bioinformatics analysis and/or functional assays for the interpretation of genetic variants (**Figure 3a**). A biallelic mutation in *NPHP1* was detected in five out of 13 patients (38%), of whom two patients had a homozygous deletion and three patients had a compound heterozygous deletion and mutation (**Table 3**). Consequently, *NPHP1* was the most frequently mutated gene in our cohort (16/36 patients (44%); **Figure 3b**), which is consistent with literature [Halbritter et al., 2013].

Additional biallelic variants were detected in *TMEM67* in one patient with Bardet-Biedl-like syndrome (23:58). Two unrelated patients with Joubert syndrome (1:34 and 5:38) harbored a compound heterozygous known pathogenic variant and the same missense variant of unknown significance (c.[628T>C] p.[Ser210Pro]) in *TMEM67*, suggesting a possible founder effect. This variant represents a novel candidate variant for NPH-RC. Interestingly, the latter two patients had progressive liver fibrosis, liver function abnormalities and hepatomegaly, which is consistent with reports of liver involvement in patients with mutations in *TMEM67* [Chaki et al., 2011; König et al., 2017].

when the signal is lost_marijn_8072018.indd 28 08/07/2018 10:50

a

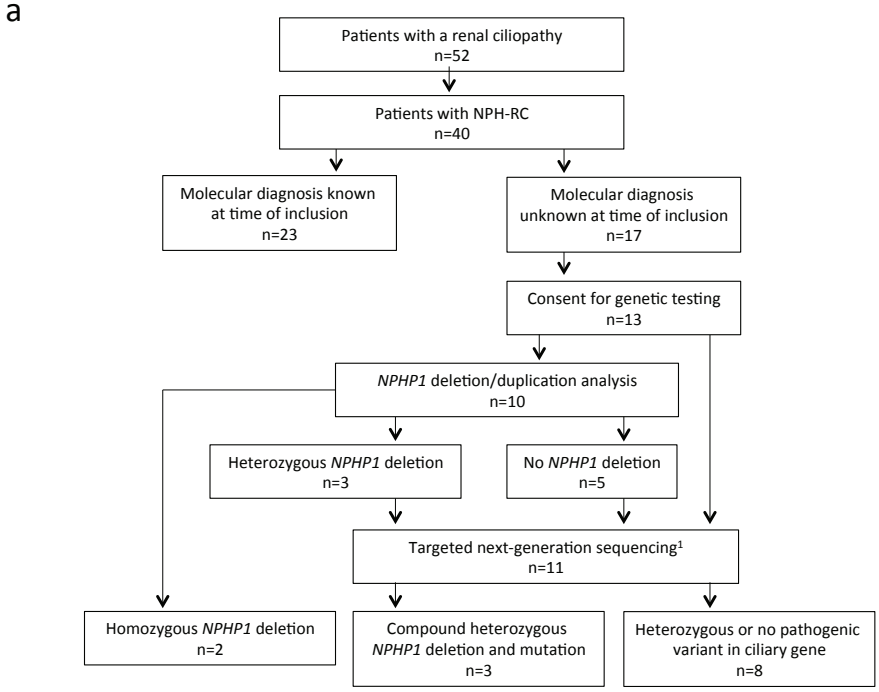

b

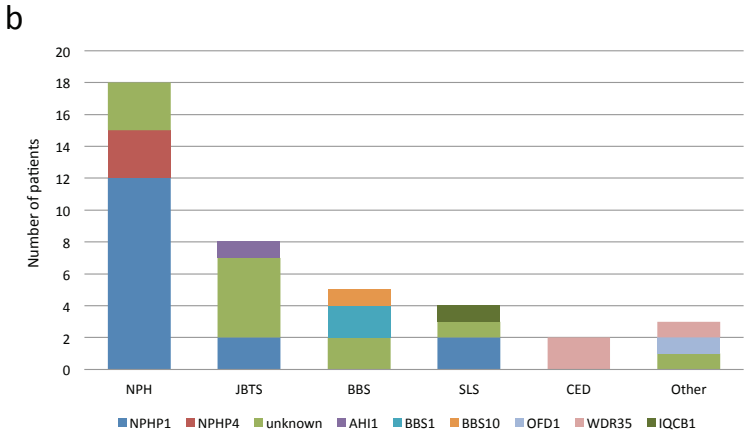

Figure 3. Clinical and genetic characterization of the cohort. **A.** Genetic diagnostic testing strategy. Targeted next-generation sequencing included a multi-gene panel and/or whole-exome sequencing. **B.** Prevalence of causal genes per NPH-RC phenotype. NPH: isolated nephronophthisis, JBTS: Joubert syndrome, BBS: Bardet-Biedl syndrome, SLS: Senior-Løken syndrome, CED: cranioectodermal dysplasia.

when the signal is lost_marijn_8072018.indd 29 08/07/2018 10:50

Table 3. Genetic findings in 13 NPH-RC patients

ID	Gene	Zygosity	Accession #	c.Position	p.Position	HGMD accession	Polyphen-2	Mut Tast	SIFT	Gerp	ExAC[1]	Clinical diagnosis
6:39	*NPHP1*	Hom	NM_000272.3	c.1-?_2034+?del	p.(?)	NA	NA	NA	NA	NA	NA	NPH
24:60	*NPHP1*	Hom	NM_000272.3	c.1-?_2034+?del	p.(?)	NA	NA	NA	NA	NA	NA	NPH
9:42	*NPHP1*	Comp het	NM_000272.3	c.1-?_2034+?del;	p.(?)	NA	NA	NA	NA	NA	NA	NPH
9:43				c.1039C>T	p.Arg347*	CM080456	NA	DC	NA	NA	NA	
11:45	*NPHP1*	Comp het	NM_000272.3	Deletion;	p.(?);	NA	NA	NA	NA	NA	NA	SLS
				c.1027G>A	p.Gly343Arg	CM066932	Probably damaging	DC	NA	5.79	13/0/119452	
23:58	*TMEM67*	Comp het	NM_153704.5	c.870-5del[2];	p.(?)	NA	NA	NA	NA	NA	NA	Other (BBS-like)
				c.1379G>C	p.Arg460Thr	NA	Benign	DC	NA	NA	36/0/120958	
1:34	*TMEM67*	Comp het	NM_153704.5	c.1843T>C;	p.Cys615Arg;	CM094694	Possibly damaging	DC	Deleterious	4.16	29/0/121374	JBTS
				c.628T>C	p.Ser210Pro	NA	Benign	P	Tolerated	4.45	1/0/121256	
	IQCB1	Het	NM_001023571.2	c.59delA	NA	NA	NA	NA	NA	4.45	NA	
5:38	*TMEM67*	Comp het	NM_153704.5	c.2498T>C;	p.Ile833Thr	CM090682	Probably damaging	DC	Deleterious	3.49	4/0/121114	JBTS
				c.628T>C	p.Ser210Pro	NA	Benign	P	Tolerated	4.45	1/0/121256	
3:36	*CEP290*	Het	NM_025114.3	c.6320A>G	p.Lys2107Arg	NA	Probably damaging	DC	Tolerated	4.65	2/0/56244	JBTS
	KIF7	Het	NM_198525.2	c.505C>T	p.Arg169Trp		Probably damaging	DC	Deleterious	3.42	1/0/21750	
2:35	*CEP164*	Het	NM_014956.4	c.151C>T	p.Arg51*	NA	NA	DC	NA	-2.37	2/0/106462	JBTS
29:65	*NINL*	Het	NM_025176.5	c.1318G>C	p.Glu440Gln	NA	Probably damaging	DC	Damaging	4.6	NA	NPH
4:37	NA											JBTS
10:44	NA											NPH

No candidate variants were identified for two patients (4:37 and 10:44) with Joubert syndrome and isolated nephronophthisis, respectively. Hom: homozygous, Het: heterozygous, Comp het: compound heterozygous, NA: not available, DC: disease causing, P: polymorphism, NPH: isolated nephronophthisis, BBS: Bardet-Biedl syndrome, JBTS: Joubert syndrome.

[1]ExAC: allele count/number of homozygotes/allele number [Lek et al., 2016].

[2]Predicted attenuation of canonical splice acceptor site (Human Splicing Finder version 3.0) [Desmet et al., 2009].

when the signal is lost_marijn_8072018.indd 30 08/07/2018 10:50

2.3.6 Gene-phenotype associations

NPHP1 (n=16)

Biallelic mutations in *NPHP1* were detected in patients with isolated NPH (n=12), Joubert syndrome (n=2) and Senior-Løken syndrome (n=2). Median reported age of symptom onset was 9 years (range 6-26 years) and median age of ESRD was 14 years (range 7-28 years). Patients with *NPHP1* mutations had higher reported frequencies of polyuria (9/10; 90%), polydipsia (8/10; 80%) and enuresis (3/8; 38%) compared to all patients. Strikingly, renal cysts were present in only 4/12 patients (33%) with *NPHP1* mutations, while hyperechogenicity (7/10; 70%) and abnormal corticomedullary differentiation (3/8; 38%) were reported more frequently compared to the cohort average. Extrarenal manifestations included visual impairment (3/16; 19%) - mainly retinitis pigmentosa (n=2) -, obesity (n=2), congenital heart disease (n=1), oculomotor apraxia (n=1) and developmental delay (n=1).

NPHP4 (n=3)

Three patients with mutations in *NPHP4* presented with isolated NPH. Median reported age of symptom onset was 16 years (range 8-24 years). One patient already had ESRD when the diagnosis was made at age 8 years. The other two patients had not yet developed ESRD at age 19 and 41 years respectively. The renal phenotype was characterized by polydipsia and/or polyuria (n=2) and increased echogenicity (n=2), cysts (n=1) and abnormal corticomedullary differentiation (n=1) on renal ultrasound. There were no extrarenal features reported in patients with mutations in *NPHP4*.

WDR35 (n=3)

Three patients had biallelic mutations in *WDR35*; two patients (siblings) had cranioectodermal dysplasia (CED) and one patient had a ciliopathy phenotype that did not constitute a recognizable syndrome. The patients with CED did not yet develop ESRD at age 17 (CKD stage 3) and 12 years (CKD stage 1-2) respectively. Their phenotype was characterized by a narrow thorax and short limbs. The patient without a syndrome diagnosis developed ESRD at age 12 years. Extrarenal manifestations comprised retinitis pigmentosa, oculomotor abnormalities, autism spectrum disorder, liver cirrhosis, polydactyly and obesity.

BBS1 (n=2)

Biallelic mutations in *BBS1* were identified in two patients (siblings) with Bardet-Biedl syndrome and slowly progressive kidney disease. The patients had not yet developed ESRD at age 20 (CKD stage 1-2) and 16 years (CKD stage 2) respectively. Kidney cysts were present in the eldest patient. Both had visual impairment, developmental delay and obesity.

Other genes

Biallelic mutations in the ciliopathy-associated genes *AHI1*, *BBS10*, *IQCB1* and *OFD1* were identified in single patients. Renal and extrarenal findings associated with mutations in these genes are summarized in **Tables 1** and **2**.

when the signal is lost_marijn_8072018.indd 31 08/07/2018 10:50

2.4 DISCUSSION

We describe a cohort of 40 Dutch patients with NPH-RC included in the Nephronophthisis Registry over a period of three years (2014 to 2017). This study represents a comprehensive characterization of renal and extrarenal ciliopathy-associated features and associations with genetic findings in a well-defined population. Increased echogenicity was a more prevalent finding on renal ultrasound than kidney cysts (65% vs. 43%), especially in patients with mutations in *NPHP1* (70% vs. 33%). This finding is consistent with literature that describes increased echogenicity and a loss of corticomedullary differentiation on renal ultrasound in 78% of pediatric patients, and cystic lesions in only 51% [König et al., 2017]. Increased echogenicity is considered a sensitive marker for early stages of CKD in children, although it is not specific for NPH [Braun et al., 2016]. With the Nephronophthisis Registry, we aim to contribute to the growing understanding of NPH-RC phenotypes [König et al., 2017; Chaki et al., 2011; Soliman et al., 2012; Tory et al., 2009], which will in turn advance diagnostics and genetic counseling.

The median age of NPH symptom onset in the cohort presented here was 9 years (range 5-33 years), which is above the age of 6 years reported in the literature [Hildebrandt et al., 2009]. In addition, while the median age at which ESRD was reached (13 years) was consistent with literature [Hildebrandt et al., 1997, 2009; Soliman et al., 2012; Wolf, 2015], the age of ESRD onset varied from 5 to 47 years. Four patients with mutations in *NPHP1* developed ESRD at or after age 20 years. A recent report of *NPHP1*-associated adult onset NPH also supports a later onset of NPH than was previously assumed [Haghighi et al., 2016]. This is important because monitoring of renal function in syndromic ciliopathy patients is often discontinued if no kidney disease is present at age 18 years. Based on the range of reported age of onset in our cohort, presymptomatic monitoring of renal function should be performed annually in ciliopathy patients until at least age 30 years. If CKD is established, the monitoring frequency can be adjusted according to the rate of kidney function decline.

Individual patient reports demonstrated diagnostic delay in patients with isolated NPH. For example, a patient with Senior-Løken syndrome caused by *NPHP1* mutations (11:45) had secondary enuresis nocturna for at least one year prior to her diagnosis at age 13. Around the time of diagnosis, a renal biopsy showed chronic tubulointerstitial nephritis and glomerulosclerosis. While typical histologic findings, including tubulointerstitial fibrosis, thickened and disrupted tubular basement membrane, and sporadic corticomedullary cysts have been described in NPH [Zollinger et al., 1980; Hurd and Hildebrandt, 2011; Soliman et al., 2012], interstitial fibrosis, secondary glomerulosclerosis and tubular atrophy are hallmarks of ESRD of any etiology. Because NPH is typically first suspected in advanced stages of CKD when damage is extensive, histology is often inconclusive and of limited diagnostic value, while it is an invasive procedure for the patient that carries an even higher risk for complications in advanced stages of chronic kidney disease [Shidham et al., 2005]. Another patient with NPH (29:65) presented with polydipsia and polyuria at age seven, when the estimated glomerular filtration rate (eGFR) was normal. At

when the signal is lost_marijn_8072018.indd 32 08/07/2018 10:50

age 15, she presented with fatigue for several weeks and was diagnosed with renal failure. These examples illustrate that a potential treatment window exists if initial signs of NPH are recognized. In addition, early genetic testing and identification of biomarkers that are more sensitive than eGFR could benefit timely detection and adequate supportive treatment, including treatment of anemia and hypertension [Stokman et al., 2016a], in NPH-RC patients.

Persistent fatigue and muscle complaints were identified as new presenting symptoms of NPH that should prompt evaluation of kidney function. Muscle complaints could represent musculoskeletal pains, a uremic symptom which is highly prevalent in patients with CKD [Caravaca et al., 2016], or could result from electrolyte disturbances (for example low serum magnesium). Electrolyte data was not available for the respective patients at the time of symptoms onset. Hypertension was an initial sign in 21% of patients (n=5), including one patient who currently has CKD stage 2. This finding contradicts literature that suggests that hypertension is a late finding in NPH because of renal salt wasting [Niaudet, 2013]. However, because of the diagnostic delay in NPH, hypertension could be an initial sign indicating advanced CKD. Diagnostics of NPH can be challenging, even when a causal mutation in a ciliopathy-associated gene has been detected, because other kidney diseases can mimic the NPH phenotype [Braun et al., 2016]. We detected homozygous mutations in the ciliary gene *TTC21B* in four patients from one family with a renal ciliopathy phenotype comprising renal insufficiency and retinitis pigmentosa (**Supplementary Results S1**). However, early proteinuria indicated glomerular kidney disease, which has also been described in patients with *TTC21B* mutations [Bullich et al., 2017; Stokman et al., 2016b], instead of NPH. Consequently, knowledge of the NPH phenotype is critical, not only for early detection but also for proper distinction of NPH from phenocopies.

Eight out of 13 NPH-RC patients that were genetically tested in this study remained unsolved, consistent with the less than 50% mutation detection rate described in literature [Schueler et al., 2016; Braun et al., 2016]. We detected single heterozygous variants in ciliopathy-associated genes in two patients (15%). A patient with Joubert syndrome (3:36) carried heterozygous variants in *CEP290* and *KIF7*. Another patient with Joubert syndrome (2:35) carried a heterozygous predicted deleterious variant in *CEP164*. Sequencing and deletion/duplication analysis using YouMAQ did not reveal additional variants on the second allele. Single heterozygous mutations in ciliopathy-associated genes have been frequently reported in literature [Kroes et al., 2016; Schueler et al., 2016]. Possible explanations are that variants on the second allele were missed by the respective sequencing techniques, for example because of intronic localization, that detected heterozygous variants represent genetic modifiers, or that detected variants are unrelated to the phenotype. We also identified a heterozygous predicted deleterious variant in the previously described candidate ciliary gene *NINL* in a patient with isolated NPH (29:65). NINL, or ninein-like protein, colocalizes with CC2D2A at the base of the cilium. A heterozygous variant in *NINL* has been proposed to act as a genetic modifier in a patient with a severe form of Joubert syndrome caused by mutations in *CC2D2A* [Bachmann-Gagescu et al., 2015].

when the signal is lost_marijn_8072018.indd 33 08/07/2018 10:50

Further research is required to elucidate the role of *NINL* in NPH-RC.

We did not find statistically significant genotype-phenotype correlations as a result of the size and heterogeneity of our cohort. However, patterns can be discerned that support previously published gene-phenotype associations. Patients with biallelic *NPHP1* and *NPHP4* mutations exhibited isolated NPH more frequently (in 75% and 100%, respectively) compared to NPH patients with other gene defects, which is in line with previous literature [Soliman et al., 2012; Chaki et al., 2011; König et al., 2017]. Visual impairment was the most common extrarenal manifestation in patients with *NPHP1* mutations, present in 19%. Neurologic symptoms (oculomotor apraxia and developmental delay) were reported less frequently than in literature (n=1; 7%) [König et al., 2017; Soliman et al., 2012; Chaki et al., 2011]. Interestingly, we found an older median age of symptom onset of 16 years (range 8-24 years) and a lower rate of CKD progression in patients with *NPHP4* mutations compared to patients with other gene defects, corroborating the findings of König et al [König et al., 2017]. Larger, well-phenotyped cohorts of NPH-RC are required to strengthen genotype-phenotype correlations, which is essential for providing an accurate prognosis to patients. To this end, the Nephronophthisis Registry described here can be combined with other, international cohorts.

In conclusion, this study provides a comprehensive analysis of renal and extrarenal ciliopathy phenotypes in a cohort of 40 Dutch patients with NPH-RC. Persistent fatigue, polyuria, hypertension and muscle cramps were identified as initial signs and symptoms of NPH that should prompt timely evaluation of renal function. Symptom onset can occur in adulthood, which supports continuation of presymptomatic kidney function monitoring in patients with a syndromic ciliopathy until at least age 30 years. Our findings confirm that increased echogenicity is a more prevalent finding than cysts on renal ultrasound in NPH-RC patients and that mutations in *NPHP4* are associated with slower kidney disease progression and a lower prevalence of extrarenal manifestations than mutations in other NPH-associated genes. Ultimately, improving recognition of NPH and associated phenotypes will enable adequate surveillance and clinical care for patients with NPH-RC.

when the signal is lost_marijn_8072018.indd 34 08/07/2018 10:50

Acknowledgments

We thank the patients and their parents for participating in this research. We thank Jan Willem Deiman for designing the website www.kouncil.nl. We thank the following physicians for referring patients for inclusion into the Nephronophthisis Registry: M.G. Keijzer-Veen, M.J.H. van den Boogaard, A. van Zuilen, A.C. Abrahams, J.J. van Harssel, K.D. Lichtenbelt (UMC Utrecht), D.A. Hesselink, M.W.F van den Hoogen (EMC Rotterdam), J.M. Cobben (AMC Amsterdam, St. George's University Hospital London), M.H. Breuning, R.W.G. van Rooij (Leiden UMC), E. Levtchenko (KU Leuven), M.M. van Genderen (Bartimeus), J.B.G.M. Verheij, E. Zonneveld-Huijssoon, E.H. Gerkes (UMC Grongingen) and A. Eikelenboom (VUmc Amsterdam). The researchers received funding from the Dutch Kidney Foundation under grant agreements CP11.18 Kouncil (N.V.A.M.K., R.H.G., P.L.B., and H.H.A.), the European Community's Seventh Framework Programme (FP7/2009) under grant agreement 305608 EURenOmics (N.V.A.M.K.), 150KG18 (K.Y.R.) and the NIHR Great Ormond Street Hospital Biomedical Research Center (P.L.B.).

when the signal is lost_marijn_8072018.indd 35 08/07/2018 10:50

SUPPLEMENTARY MATERIAL

Supplementary Methods S1. *Deletion/duplication analysis*

For 9/13 patients without a molecular diagnosis at the time of inclusion (1:34, 3:36, 5:38, 6:39, 9:42, 9:43, 11:45, 24:60 and 29:65), deletion/duplication analysis of *NPHP1* was performed using multiplex ligation-dependent probe amplification (MLPA). MLPA analysis was performed in our EN ISO 15189:2012 accredited DNA diagnostics laboratory. The test was performed according to the manufacturer's protocol (MRC-Holland b.v.) and data were analyzed using the Genemarker program (software version 2.6.0, SoftGenetics LLC).

For one patient (10:44), deletion/duplication analysis was performed using the Flagged youMAQ kit (Multiplicom, Agilent Technologies, Niel, Belgium) according to the manufacturer's instructions. Data were analyzed using the Genemarker program (software version 2.6.0, SoftGenetics LLC). In addition, the Flagged youMAQ kit was used to assess copy number variations in ciliary genes in which we identified single heterozygous mutations.

when the signal is lost_marijn_8072018.indd 36 08/07/2018 10:50

Supplementary Methods S2. *Targeted next-generation sequencing*

S2.1 Gene panel sequencing

NGS-based NPH gene panel analysis for patient 10:44 was performed in our EN ISO 15189:2012 accredited DNA diagnostics laboratory. In brief: A custom SureSelectXT target enrichment assay (Agilent Technologies, elid# 0483791) was used to enrich for the protein coding and flanking intronic sequence of 15 genes known to be associated with NPH: *CEP164, CEP290, GLIS2, INVS, IQCB1, NEK8, NPHP1, NPHP3, NPHP4, RPGRIP1L, SDCCAG8, TMEM67, TTC21B, WDR19* and *ZNF423*. Sequencing was performed on a SOLiDTM 5500XL sequencer (50 basepair single read, Life Technologies/Applied Biosystems), with a minimal median coverage of 100X for the targeted bases. To reach a genotyping accuracy of >99%, a minimal vertical coverage of 15 unique reads per base was requested. To deliver a comprehensive analysis of the genes collected in the gene panel, an average horizontal coverage of at least 95% of targeted bases in the gene panel was requested. The horizontal coverage for our patient was 98.3%.

S2.2 Whole-exome sequencing

Fragment library preparation and exome target enrichment using the SureSelect 50 Mb (V4) All Exon Kit (Agilent Technologies, CA, USA) was performed as described previously [Harakalova et al., 2011]. Sequencing of the first seven barcoded samples (1:34, 2:35, 3:36, 4:37, 5:38, 9:42 and 9:43) was performed on the SOLiD 5500XL platform (Life technologies, Carlsbad, CA, USA). Average coverage of the exome was 75X. Reads were processed and aligned to the human reference genome (hg19). Variant calling and annotation were performed using our custom analysis pipeline as described previously [Nijman et al., 2010]. Variants were filtered based on coverage (>8 reads), percentage of the variant in exome reads (>70 for homozygous variants and >15 for heterozygous variants) and population allele frequency below 1% in publicly available genomic databases including Exome Variant Server [NHLBI GO Exome Sequencing Project, 2014], USCS Genome Browser [Kent et al., 2002] and the ExAC Browser [Lek et al., 2016], and prioritized based on predicted effect using Polyphen2 [Adzhubei et al., 2010], SIFT [Kumar et al., 2009] and MutationTaster2 [Schwarz et al., 2014], and relation to cilia based on our in-house database, CiliaCarta [Van Dam et al., 2017] and a Pubmed search.

For the latter four patient samples (10:44, 11:45, 23:58 and 29:65), exomes were enriched using the SureSelect XT Human All Exon V5 kit (Agilent) and sequenced in rapid run mode on the HiSeq2500 sequencing system (Illumina) at a mean target depth of 100X. The target was defined as all coding exons of UCSC and Ensembl +/- 20bp intron flanks. At this depth ~95% of the target was covered at least 15X. Reads were aligned to hg19 using BWA (BWA-MEM v0.7.5a) and variants were called using the GATK haplotype caller (v2.7-2). Detected variants were annotated, filtered and prioritized using the Bench NGS Lab platform (Cartagenia, Leuven, Belgium). For patient 23:58, trio analysis of patient and both parents was performed. Analysis was based upon a tiered analysis approach. The

when the signal is lost_marijn_8072018.indd 37 08/07/2018 10:50

first tier analyzed known intellectual disability genes. The second tier filtered for de novo variants and the last tier filtered for recessive variants. Variant confirmation and segregation analyses were performed using standard Sanger sequencing (primer sequences available upon request).

when the signal is lost_marijn_8072018.indd 38 08/07/2018 10:50

Supplementary Results S1. *Twelve patients with a renal ciliopathy phenotype*

Twelve out of 52 patients had a renal ciliopathy without sufficient evidence for NPH. Of these, six patients had a perinatally lethal phenotype, including four patients from one family with bilateral renal agenesis or renal hypoplasia due to homozygous mutations in *KIF14* [Filges et al., 2014], and two patients from two families with severe cystic kidney disease and anhydramnios sequence due to compound heterozygous mutations in *BBS10* and *BBS1,* respectively (**Supplementary Table S3**). Severe Meckel-Gruber syndrome-like phenotypes caused by mutations in Bardet-Biedl syndrome-associated genes, including *BBS1*, have been described previously [Ashkinadze et al., 2013; Karmous-Benailly et al., 2005]. Interestingly, a sibling of the patient with *BBS1* mutations, who had the same *BBS1* genotype, had mild developmental delay, polydactyly and no renal disease at age 3 years, demonstrating vast intrafamilial variability of phenotypes. Two other patients had a ciliopathy phenotype that included kidney cysts or unilateral kidney agenesis. Finally, four patients from one family had retinitis pigmentosa and renal insufficiency in combination with proteinuria due to mutations in *TTC21B*. Although mutations in *TTC21B* are known to cause nephronophthisis type 12, biallelic mutations in *TTC21B* have also been identified in patients with glomerulopathies [Bullich et al., 2017; Stokman et al., 2016b]. Because of the presence of proteinuria early in the disease course, we could not exclude glomerular kidney disease and our patients did not meet diagnostic criteria of nephronophthisis. These twelve patients highlight the spectrum of renal ciliopathy phenotypes and demonstrate that the distinction between NPH (especially infantile NPH, which can present with enlarged, cystic kidneys antenally) and other renal ciliopathy phenotypes can pose challenges [Salomon et al., 2009; Oud et al., 2014].

when the signal is lost_marijn_8072018.indd 39 08/07/2018 10:50

Supplementary Table S1. *Clinicical findings in cohort of 40 patients with nephronophthisis-related ciliopathies*

ID	M/F	Age	Gene	Zygosity	Renal phenotype	Visual impairment[1]	Oculomotor abnormalities	Developmental delay	Liver	Congenital heart defect	Narrow thorax	Poly-dactyly	Obesity	Additional information
39:79	M	25	*AHI1*	Comp het	NPH	+	+	+	-	-	-	-	-	Scoliosis
54:98	M	20	*BBS1*	Hom	NPH	+	NA	+	NA	NA	-	-	+	Benign hydrocephalus
54:99	F	16	*BBS1*	Hom	NPH	+	-	+	NA	NA	-	-	+	
18:52	M	13	*BBS10*	Hom	NPH	+	NA	+	-	-	-	+	+	Genital abnormality
48:91	M	29	*IQCB1*	Hom	NPH	+	+	-	NA	NA	-	-	-	Multinodular goiter
6:39	M	62	*NPHP1*	Hom	NPH	-	-	-	-	-	-	-	-	Hearing impairment
9:42	M	18	*NPHP1*	Comp het	NPH	-	-	-	NA	NA	NA	NA	+	
9:43	F	24	*NPHP1*	Comp het	NPH	-	-	-	-	-	-	-	-	
11:45	F	35[2]	*NPHP1*	Comp het	NPH	+	-	-	-	-	-	-	+	
12:46	F	34	*NPHP1*	Hom	NPH	-	-	-	-	-	-	-	-	
14:48	M	37	*NPHP1*	Hom	NPH	+[3]	-	-	-	-	-	-	-	
15:49	F	16	*NPHP1*	Comp het	NPH	-	-	-	NA	NA	-	-	-	
16:50	F	9	*NPHP1*	Hom	NPH	-	-	-	-	+[4]	-	-	-	
22:57	F	31	*NPHP1*	Hom	NPH	+	-	-	NA	-	-	-	-	Diaphragmatic hernia
24:60	M	32	*NPHP1*	Hom	NPH	-	-	-	-	-	-	-	-	
32:71	F	33	*NPHP1*	Comp het	NPH	-	NA	NA	-	-	NA	NA	-	

when the signal is lost_marijn_8072018.indd 40 08/07/2018 10:50

34:73	M	13	*NPHP1*	Hom	NPH	-	+	+	NA	-	-	-	-	Hypodontia
34:74	M	10	*NPHP1*	Hom	NPH	-	NA	NA	NA	NA	-	-	-	
38:78	F	12	*NPHP1*	Comp het	NPH	-	-	-	NA	-	-	-	-	
49:92	F	18	*NPHP1*	Hom	NPH	-	-	-	NA	-	-	-	-	
55:00	F	9	*NPHP1*	Hom	NPH	-	-	-	NA	-	-	-	-	
19:53	M	11	*NPHP4*	Hom	NPH	-	-	-	-	-	NA	-	-	
35:75	F	41	*NPHP4*	Comp het	NPH	-	-	-	NA	NA	NA	NA	-	Astma
53:97	F	19	*NPHP4*[5]	Comp het	NPH	-	-	-	NA	-	-	-	-	
41:81	M	12	*OFD1*	Hem	NPH	-	+	+	NA	-	-	-	-	
46:88	M	17	*WDR35*	Comp het	NPH	-	-	-	NA	-	+	-	-	Short limbs
46:89	F	12	*WDR35*	Comp het	NPH	-	-	-	-	-	+	-	-	
60:06	F	33	*WDR35*	Comp het	NPH	+	+	-	+	-	-	+	+	Pancreas cysts, ovarium cysts, neonatal teeth, bronchiectasis
1:34	M	17	-[6]	-	NPH	+	+	+	+	NA	NA	NA	-	Abnormal breathing pattern
2:35	F	16	-[6]	-	NPH	+	+	+	-	NA	-	+	+	Coloboma, tongue and mandible polyps, short limbs
3:36	M	24	-[6]	-	NPH	-	+	+	NA	NA	NA	+	-	Scoliosis
4:37	F	17	-[6]	-	NPH	+	+	+	+	NA	-	-	NA	Abnormal breathing pattern, coloboma

when the signal is lost_marijn_8072018.indd 41 08/07/2018 10:50

5:38	M	41	-[6]	-	NPH	+	+	+	+	NA	NA	NA	NA	Abnormal breathing pattern, coloboma
10:44	M	17	-[6]	-	NPH	-	-	-	-	NA	-	-	-	
23:58	F	15	-[6]	-	NPH	-	-	+	-	-	-	-	+	
27:63	F	19	-[7]	-	NPH	+	NA	+	+	+	NA	NA	+	
29:65	F	24	-[6]	-	NPH	-	-	-	-	-	-	-	-	
33:72	M	51	-[7]	-	NPH	+	NA	NA	NA	NA	NA	NA	-	
44:86	F	23	-[7]	-	NPH	-	-	-	-	-	-	-	-	
51:94	M	54	-[7]	-	NPH	+	NA	NA	NA	-	NA	NA	NA	Bilateral inguinal hernia

M: male, F: female, +: present, -: absent, NA: not available, Hom: homozygous, Comp het: compound heterozygous, Hem: hemizygous.

[1]Visual symptoms include night blindness, retinitis pigmentosa, constricted visual fields and ocular coloboma.

[2]Died from non-nephronophthisis-related cause.

[3]Abnormal electroretinography and constricted visual fields with normal findings on fundoscopy.

[4]Left-sided superior vena cava.

[5]Compound heterozygous known pathogenic variant and a variant of unknown significance in *NPHP4*.

[6]Findings from genetic testing described in Table 3.

[7]Genetic diagnosis not available and no consent for genetic testing within this study.

when the signal is lost_marijn_8072018.indd 42 08/07/2018 10:50

when the signal is lost_marijn_8072018.indd 43

***Supplementary Table S2**. Clinical findings in twelve patients with a renal ciliopathy*

ID	M/F	Age	Gene	Zygosity	Renal phenotype	Visual impairment[1]	Oculomotor abnormalities	Developmental delay	Liver	Congenital heart defect	Narrow thorax	Poly-dactyly	Obesity	Additional information
36:76	M	40	*BBS1*	Hom	Cysts	+	NA	+	NA	NA	-	+	+	
30:66	F	4	-	-	Unilateral agenesis	+	+	+	-	-	-	+	-	Hearing impairment
42:82	M	41	*TTC21B*	Hom	Renal insufficiency, proteinuria	+	NA	NA	NA	-	NA	NA	NA	Astma
42:83	F	33	*TTC21B*	Hom	Renal insufficiency, proteinuria	NA	NA	NA	NA	-	NA	NA	+	
42:84	F	43	*TTC21B*	Hom	Renal insufficiency, proteinuria	+	NA	NA	NA	+	NA	NA	NA	
42:96	F	35	*TTC21B*	Hom	Renal insufficiency, proteinuria	NA	NA	NA	NA	NA	NA	NA	NA	Astma
57:03	F	NA[1]	*BBS1*	Comp het	Polycystic kidneys	NA	NA	NA	NA	NA	NA	NA	NA	
59:05	M	NA[1]	*BBS10*	Comp het	Polycystic kidneys, dysplasia	NA	NA	NA	-	-	-	+	NA	Anhydramnios sequence
31:67	M	NA[1]	*KIF14*	Hom	Bilateral agenesis	NA	NA	NA	-	-	-	-	-	Anhydramnios sequence
31:68	F	NA[1]	*KIF14*	Hom	Cystic hypodysplasia	NA	NA	NA	-	-	-	-	-	Anhydramnios sequence

08/07/2018 10:50

31:69	M	NA[1]	*KIF14*	Hom	Cystic hypodysplasia	NA	NA	NA	-	+	-	-	-	Anhydramnios sequence
31:70	M	NA[1]	*KIF14*	Hom	Bilateral hypoplasia	NA	NA	NA	-	-	+	-	-	Anhydramnios sequence

M: male, F: female, +: present, -: absent, NA: not available, Hom: homozygous, Comp het: compound heterozygous.
[1]Termination of pregnancy.

when the signal is lost_marijn_8072018.indd 44 08/07/2018 10:50

when the signal is lost_marijn_8072018.indd 45

***Supplementary Table S3**. Renal phenotypes in 40 patients with NPH-RC*

ID Fam: case	Sex	Age (yrs)	Gene	Zygosity	Age symptom onset (yrs)	CKD stage/ Age ESRD (yrs)[1]	Polyuria	Polydipsia	Enuresis	First symptom	Renal ultrasound findings				
											Age	Cysts	Abnormal corticomedullary differentiation	Increased echogenicity	Other structural abnormalities
39:79	M	25	*AHI1*	Comp het	14	St. 3	-	-	-	Weight loss	23	-	-	-	-
54:98	M	20	*BBS1*	Hom	NA	St. 1-2	NA	NA	NA	NA	17	+	-	-	-
54:99	F	16	*BBS1*	Hom	NA	St. 2	-	-	-	NA	15	-	-	-	-
18:52	M	13	*BBS10*	Hom	NA	St. 1-2	+	+	-	NA	9	+	+	+	Enlarged kidneys antenatally
48:91	M	29	*IQCB1*	Hom	NA	10	NA	NA	NA	NA	NA	NA	NA	NA	-
6:39	M	62	*NPHP1*	Hom	26	28	+	NA	NA	Fatigue	27	+	NA	NA	-
9:42	M	18	*NPHP1*	Comp het	NA	14	NA	NA	NA	NA	14	-	NA	+	Small kidneys
9:43	F	24	*NPHP1*	Comp het	9	10	NA	-	-	Fatigue	10	-	NA	+	Small kidneys
11:45	F	35[2]	*NPHP1*	Comp het	12	20	+	+	+	Enuresis	13	+	-	+	-
12:46	F	34	*NPHP1*	Hom	13	14	+	+	-	Polydipsia and polyuria, fatigue	NA	NA	NA	NA	-
14:48	M	37	*NPHP1*	Hom	NA	26	NA	NA	NA	Fatigue, muscle cramps	NA	NA	NA	NA	-

08/07/2018 10:50

15:49	F	16	*NPHP1*	Comp het	7	12	-	-	+	Hypertension, enuresis	7	-	-	+	-
16:50	F	9	*NPHP1*	Hom	6	7	+	+	NA	NA	6	-	NA	+	-
22:57	F	31	*NPHP1*	Hom	NA	10	NA	NA	NA	NA	29	NA	NA	NA	Nephro-sclerosis
24:60	M	32	*NPHP1*	Hom	NA	15	+	+	-	NA	9	+	-	-	-
32:71	F	33	*NPHP1*	Comp het	15	22	NA	NA	-	Fatigue, dizziness	22	-	+	+	-
34:73	M	13	*NPHP1*	Hom	6	St. 3	+	+	+	Growth retardation	8	-	-	-	-
34:74	M	10	*NPHP1*	Hom	9	NA	+	+	NA	Polydipsia and polyuria	4	-	-	-	-
38:78	F	12	*NPHP1*	Comp het	7	7	+	+	-	Polydipsia and polyuria	7	+	+	NA	-
49:92	F	18	*NPHP1*	Hom	16	17	NA	NA	NA	Anaemia, fatigue	NA	NA	NA	NA	-
55:00	F	9	*NPHP1*	Hom	8	8	+	+	NA	Fatigue, uremic symptoms	8	-	+	+	Small, dysplastic kidneys
19:53	M	11	*NPHP4*	Hom	8	8	+	+	-	Growth retardation	8	NA	-	+	-
35:75	F	41	*NPHP4*	Comp het	24	St. 1-2	-	+	-	Red patches skin	24	+	NA	NA	-
53:97	F	19	*NPHP4*[3]	Comp het	16	St. 2	-	-	-	Hypertension, fatigue, muscle ruptures	17	-	+	+	-
41:81	M	12	*OFD1*	Hem	5	5	NA	NA	NA	Anaemia	5	-	-	+	-
46:88	M	17	*WDR35*	Comp het	NA	St. 3	+	+	-	Polydipsia and polyuria	15	-	+	+	-
46:89	F	12	*WDR35*	Comp het	NA	St. 1-2	-	-	-	NA	10	+	NA	+	-
60:06	F	33	*WDR35*	Comp het	9	12	+	NA	NA	Hypertension, polydipsia and polyuria	11	+	NA	NA	-

when the signal is lost_marijn_8072018.indd 46 08/07/2018 10:50

1:34	M	17	-[4]	-	NA	9	NA	+	NA	NA	NA	+	NA	NA	Enlarged kidneys, mild dysplasia
2:35	F	16	-[4]	-	NA	8	-	+	NA	NA	8	-	-	-	-
3:36	M	24	-[4]	-	NA	NA	+	+	NA	NA	NA	+	NA	NA	-
4:37	F	17	-[4]	-	NA	NA	NA	NA	NA	NA	12	-	-	-	-
5:38	M	41	-[4]	-	NA	27	NA	NA	NA	NA	18	NA	NA	+	-
10:44	M	17	-[4]	-	5	St. 3	-	+	+	Polydipsia and polyuria, fatigue	15	+	-	+	-
23:58	F	15	-[4]	Comp het	NA	St. 1-2	-	+	-	Polydipsia and polyuria	12	-	-	-	Unilateral renal agenesis
27:63	F	19	-[5]	-	NA	St. 1-2	NA	NA	NA	NA	6	NA	NA	NA	Small kidneys, unilateral dysplasia
29:65	F	24	-[4]	-	7	15	+	+	NA	Polydipsia and polyuria	15	+	+	+	Multicystic dysplastic kidneys
33:72	M	51	-[5]	-	NA	13	NA	NA	NA	NA	NA	NA	NA	NA	-
44:86	F	23	-[5]	-	19	St. 4	-	-	-	Hypertension,	20	-	-	+	-
51:94	M	54	-[5]	-	33	47	NA	NA	NA	Hypertension	NA	NA	NA	NA	-

M: male, F: female, +: present, -: absent, NA: not available, Hom: homozygous, Comp het: compound heterozygous, Hem: hemizygous.

[1]Last reported CKD stage is provided for patients who did not (yet) develop ESRD. Age at which ESRD was first reported is provided for patients with ESRD.

[2]Died from non-nephronophthisis-related cause.

[3]Compound heterozygous known pathogenic variant and a variant of unknown significance in *NPHP4.*

[4]Findings from genetic testing described in Table 3.

[5]Genetic diagnosis not available and no consent for genetic testing within this study.

when the signal is lost_marijn_8072018.indd 47 08/07/2018 10:50

when the signal is lost_marijn_8072018.indd 48

***Supplementary Table S4**. Genetic diagnoses in 23 patients*

ID Fam: case	Gene	Zygosity	Accession #	c.Position	p.Position	HGMD accession	Clinical diagnosis
39:79	AHI1	Comp het	NM_017651.4	c.910_911insA c.2057_2060delACAA	p.Thr304fs p.Asn686fs	CI061497 CD080787	JBTS
54:98	BBS1	Hom	NM_024649.4	c.1169T>G	p.Met390Arg	CM021489	BBS
54:99	BBS1	Hom	NM_024649.4	c.1169T>G	p.Met390Arg	CM021489	BBS
18:52	BBS10	Hom	NM_024685.3	c.271dupT	p.Cys91SerfsX5	CI064666	BBS
48:91	IQCB1	Hom	NM_001023570.3	c.897_900dupCTTG	p.Ile301fs	CI1211317	SLS
12:46	NPHP1	Hom	NM_000272.2	c.1-?_2202+?del	p.(?)	CG962922	NPH
14:48	NPHP1	Hom	NM_000272.2	c.320-?_522+?del (del exon 5), c.1698-?_1810+?del (del exon 17)	p.(?)	NA	NPH
15:49	NPHP1	Comp het	NM_000272.3 NM_001128178.1	c.1027G>A c.-29-?_1805+?del	p.Gly343Arg p.(?)	CM066932 CG962922	NPH
16:50	NPHP1	Hom	NM_000272.3	c.?_-94_*455_?del	p.(?)	NA	NPH
22:57	NPHP1	Hom	NA	deletion	NA	NA	SLS
32:71	NPHP1	Comp het	NM_000272.3	c.1027G>A c.1-?_2202+?del	p.Gly343Arg p.(?)	CM066932 CG962922	NPH
34:73	NPHP1	Hom	NM_000272.2	+/-150 kb deletion	NA	CG1511893	JBTS
34:74	NPHP1	Hom	NM_000272.2	+/-150 kb deletion	NA	CG1511893	JBTS
38:78	NPHP1	Comp het	NM_000272.2	c.1027G>A c.1-?_2202+?del	p.Gly343Arg p.(?)	CM066932 CG962922	NPH
49:92	NPHP1	Hom	NM_000272.2	c.?_-94_*455_?del	p.(?)	NA	NPH
55:00	NPHP1	Hom	NM_000272.2	c.1-?_2202+?del	p.(?)	CG962922	NPH
19:53	NPHP4	Hom	NM_015102.4	c.2932del	p.Glu978fs	NA	NPH
35:75	NPHP4	Comp het	NM_015102.4	c.148delG c.1892_1895delAGAA	p.Val79fs p.Gln631fs	CD051764 CD051765	NPH

08/07/2018 10:50

when the signal is lost_marijn_8072018.indd 49

53:97	NPHP4	Comp het	NM_015102.4	c.122C>T[1] c.271T>C	p.Pro41Leu p.Phe91Leu	NA CM051569	NPH
41:81	OFD1	Hem	NM_003611.2	c.872-877delAAGATA	p.Lys291_Asp292del	CD160579	Other[2]
46:88	WDR35	Comp het	NM_001006657.1	c.2891delT c.2623G>A	p.Pro964LeufsX15 p.Ala875Thr	CD105623 CM105621	CED
46:89	WDR35	Comp het	NM_001006657.1	c.2891delT c.2623G>A	p.P964LfsX15 p.Ala875Thr	CD105623 CM105621	CED
60:06	WDR35	Comp het	NM_001006657.1	c.932G>T c.3396-29_3396-18del[1]	p.Trp311Leu p.(?)	CM166931 NA	Other[3]

Hom: homozygous, Comp het: compound heterozygous, Hem: hemizygous, NA: not available, NPH: isolated nephronophthisis, JBTS: Joubert syndrome, BBS: Bardet-Biedl syndrome, SLS: Senior-Løken syndrome, CED: cranioectodermal dysplasia.

[1]Variant of unknown significance, predicted to be possibly pathogenic.

[2]Phenotype described as X-linked Joubert syndrome or oral-facial-digital syndrome type I.

[3]Phenotype consisting of nephronophthisis, retinitis pigmentosa, liver cirrhosis and autism spectrum disorder.

08/07/2018 10:50

Supplementary Table S5. *Reasons for suspected NPH in patients without a genetic diagnosis*

ID Fam: case	Sex	Age (yrs)	
1:34	M	17	Joubert syndrome, ESRD age 9, signs of a renal concentration defect, cysts on renal ultrasound, exclusion of other causes of renal failure
2:35	F	16	Joubert syndrome, ESRD age 8, signs of a renal concentration defect, exclusion of other causes of renal failure
3:36	M	24	Joubert syndrome, CKD (stage unknown), signs of a renal concentration defect, cysts on renal ultrasound, exclusion of other causes of chronic kidney disease
4:37	F	17	Joubert syndrome, CKD (stage unknown), exclusion of other causes of chronic kidney disease
5:38	M	41	Joubert syndrome, ESRD at age 27, increased echogenicity on renal ultrasound, exclusion of other causes of renal failure
10:44	M	17	CKD stage 3, signs of a renal concentration defect, renal ultrasound showing cysts and increased echogenicity, exclusion of other causes of chronic kidney disease
23.58	F	15	CKD stage 1-2, signs of renal concentration defect, exclusion of other causes of chronic kidney disease. Unilateral renal agenesis does not explain decline in renal function
27:63	F	19	Bardet-Biedl syndrome, CKD stage 1-2, unilateral kidney dysplasia on renal ultrasound, exclusion of other causes of chronic kidney disease
29:65	F	24	ESRD at age 15, signs of a renal concentration defect, renal ultrasound showing cysts, abnormal corticomedullary differentiation and increased echogenicity, exclusion of other causes of renal failure
33:72	M	51	Senior-Løken syndrome, ESRD at age 13 and exclusion of other causes of renal failure
44:86	F	23	CKD stage 4, increased echogenicity on renal ultrasound and exclusion of other causes of chronic kidney disease
51:94	M	54	Bardet-Biedl syndrome, ESRD at age 47 and exclusion of other causes of renal failure

ESRD: end-stage renal disease, CKD: chronic kidney disease.

when the signal is lost_marijn_8072018.indd 50

08/07/2018 10:50

when the signal is lost_marijn_8072018.indd 51 08/07/2018 10:50

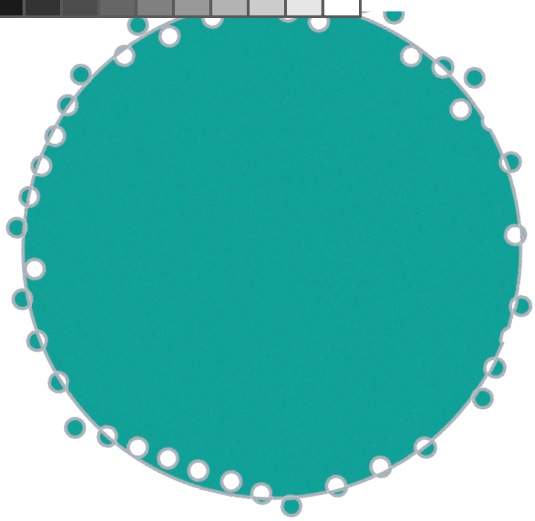

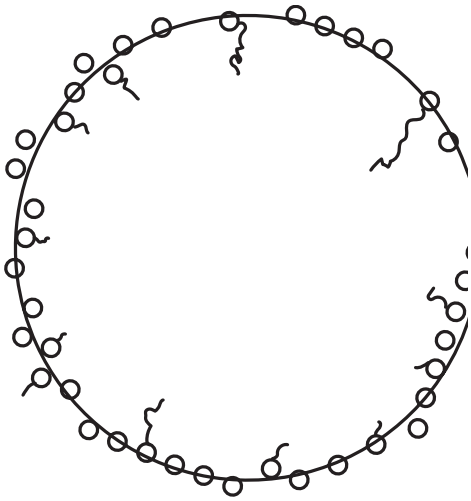

CHAPTER 3

De novo 14q24.2q24.3 microdeletion including *IFT43* is associated with intellectual disability, skeletal anomalies, cardiac anomalies and myopia

Stokman MF, Oud MM, Van Binsbergen E, Slaats GG, Nicolaou N, Renkema KY, Nijman IJ, Roepman R, Giles RH, Arts HH, Knoers NVAM, Van Haelst MM

2016. Am. J. Med. Genet. A. 170: 1566-1569
DOI:10.1002/ajmg.a.37598

ABSTRACT

We report an eleven-year-old girl with mild intellectual disability, skeletal anomalies, congenital heart defect, myopia and facial dysmorphisms including an extra incisor, cup-shaped ears and a preauricular skin tag. Array comparative genomic hybridization analysis identified a de novo 4.5-Mb microdeletion on chromosome 14q24.2q24.3. The deleted region and phenotype partially overlap with previously reported patients. Here, we provide an overview of the literature on 14q24 microdeletions and further delineate the associated phenotype. We performed exome sequencing to examine other causes for the phenotype and queried genes present in the 14q24.2q24.3 microdeletion that are associated with recessive disease for variants in the non-deleted allele. The deleted region contains 65 protein-coding genes, including the ciliary gene *IFT43*. Although Sanger and exome sequencing did not identify variants in the second *IFT43* allele or in other IFT complex A-protein-encoding genes, immunocytochemistry showed increased accumulation of IFT-B proteins at the ciliary tip in patient-derived fibroblasts compared to control cells, demonstrating defective retrograde ciliary transport. This could suggest a ciliary defect in the pathogenesis of this disorder.

when the signal is lost_marijn_8072018.indd 54 08/07/2018 10:50

3.1 INTRODUCTION

Interstitial deletions encompassing the 14q24.2q24.3 region are rare and associated with intellectual deficit in the majority of patients. Defining a consistent clinical phenotype and determining the causal genes within the deletion remains a challenge. Recently, two patients with overlapping 14q24 deletion were reported: one with a 5.4-Mb deletion and mild intellectual disability (ID), atrial septal defect (ASD), small thumbs and facial dysmorphisms [Oehl-Jaschkowitz et al., 2014] and one with a 5.3-Mb deletion and mild psychomotor delay, ASD, short digits, facial dysmorphisms and focal epilepsy [Tassano et al., 2014]. The DECIPHER database reports thirteen patients with overlapping copy number loss in the 14q24 region, and clinical features that include ID in seven patients, heart defect in one patient and preauricular skin tag in one patient [Firth et al., 2009] (**Supplementary Table S1**).

Here, we report a patient with a de novo 4.5-Mb 14q24.2q24.3 microdeletion with clinical features as previously reported in patients with overlapping 14q24 deletions: mild ID, skeletal anomalies including small thumb, ASD and facial dysmorphisms including cup-shaped ears and preauricular skin tag. We explored genetic and environmental factors that could have contributed to the phenotype and further characterized the phenotypic spectrum associated with 14q24 microdeletions. Finally, we investigated whether the distinctive skeletal, ocular and ectodermal abnormalities in the index patient could reflect a ciliary defect associated with deletion of the gene encoding intraflagellar transport protein 43 (*IFT43*) (MIM# 614099), one of the 65 protein-coding genes located within the 14q24.2q24.3 microdeletion.

3.2 CLINICAL REPORT

The index patient is the second child of non-consanguineous Caucasian parents; she has a healthy older brother. Mother of the patient has a history of insulin-dependent diabetes type I. The patient was born after a full-term pregnancy, with birth length: 51 cm (0 SD), weight: 3505 grams (0 SD) and OFC: 32.5 cm (-1.2 SD). At 11 years of age, she presented at the genetics clinic with mild ID (TIQ 66 measured with WISC-III, VIQ 71, PIQ 66) and multiple congenital malformations. Her height was 141.5 cm (-0.4 SD), weight: 35.6 kg (+0.5 SD) and OFC: 52 cm (-0.4 SD). She had a wide nasal bridge, cup-shaped ears, long limbs (sitting-height/length ratio 0.49 (-1.8 SD), arm span 157.2 cm (+2 SD)) and digits, and a short, broad thorax (**Figure 1**). Previous medical history mentioned hip dysplasia, deviation of the sacrum with dysplastic corpora and lipomas around the conus and proximal filum terminale. On the right hand she had a small thumb for which she underwent pollicization of the index finger, contracture of the proximal interphalangeal joint of the third finger and flexion contracture of the wrist. Her preauricular skin tag and extra central incisor had been surgically removed. In addition, she had a ventricular septal defect that had closed without intervention and a large ASD that required surgical closure. Ultrasound of the abdomen showed normal kidneys. She had astigmatism and myopia (-5 and -8 ODS). Retinal examination was normal.

when the signal is lost_marijn_8072018.indd 55 08/07/2018 10:50

Figure 1. Phenotype index patient. **A.** Physical characteristics of index patient during infancy: preauricular skin tag (i) and small right thumb (ii). **B.** Patient at age ten. Cup-shaped ears with preauricular scar from surgical removal of skin tag (iii). Long upper and lower limbs and short, broad thorax (iv). Long, slender digits on feet (v) and hands (vi) with right hand showing pollicization of index finger.

when the signal is lost_marijn_8072018.indd 56 08/07/2018 10:50

3.3 METHODS

3.3.1 Genome-wide array comparative genomic hybridization analysis

Array-CGH microarray analysis was performed using 180K (Amadid 023363, hg19) microarray slides from Agilent Technologies (Santa Clara, CA, USA) following manufacturer's protocols and a mixed pool of 50 healthy controls as reference. Scanned images were analyzed by Feature Extraction software (Agilent Technologies). CNV analysis was performed with Nexus software (version 7). Parentage was confirmed by DNA fingerprinting. The deletion has been submitted to ClinVar database, accession number SCV000245406 (www.ncbi.nlm.nih.gov/clinvar).

3.3.2 Exome sequencing

Exome sequencing was performed on the patient to exclude other causes, to query genes present in the 14q24 microdeletion that are associated with recessive diseases for variants on the non-deleted allele and to query ciliopathy-associated genes for variants that could complement the *IFT43* deletion resulting in possible oligogenic inheritance. Fragment library preparation and exome target enrichment using the SureSelect 50 Mb (V4) All Exon Kit (Agilent Technologies, CA, USA) was performed as described previously [Harakalova et al., 2011] (**Supplementary Methods S1**) and sequencing of barcoded samples was performed on the SOLiD 5500XL platform (Life technologies, Carlsbad, CA, USA). Sanger sequencing (ABI 3730 DNA Analyzer, Life Technologies, Forster City, CA, USA) of the coding regions and intron-exon boundaries of *IFT43* was performed. Primer sequences are available upon request.

3.3.3 Immunocytochemistry of IFT43 and IFT88

As chromosome 14 contains numerous imprinted regions, we assessed expression of IFT43 using immunofluorescence in patient-derived fibroblasts to exclude imprinting of the non-deleted allele (**Supplementary Methods S2**). In addition, we assessed primary cilia length and morphology in control- and patient-derived fibroblasts as previously described [Arts et al., 2011]. For a list of antibodies used, see **Supplementary Methods S3**.

3.4 RESULTS

3.4.1 Genetic analysis identifies a de novo 4.5-Mb microdeletion on chromosome 14q24

Array-CGH analysis identified a *de novo* 4.5-Mb microdeletion on chromosome 14q24.2q24.3 (73,152,115 – 77,698,582; GRCh 37/hg19) in the patient. No CNVs were detected in the parents. The deleted region contained 65 protein-coding genes listed in Online Mendelian Inheritance in Man (OMIM). **Supplementary Figure S1** shows an overview of the genes and overlapping deletions in DECIPHER. Exome sequencing did not identify variants in genes present in the 14q24 microdeletion that are associated with recessive diseases and there were no other

when the signal is lost_marijn_8072018.indd 57 08/07/2018 10:50

variants that could likely explain the phenotype (**Supplementary Table S2**). We did not detect mutations in the non-deleted *IFT43* allele or in other ciliopathy-associated genes.

3.4.2 IFT43 is expressed along the ciliary axoneme in patient-derived fibroblasts
IFT43 expression was detected in the cytoskeleton and along the primary cilium axoneme in control- and patient-derived fibroblasts (**Supplementary Figure S2**), excluding methylation of the non-deleted *IFT43* allele.

3.4.3 Accumulation of IFT88 at the ciliary tip in patient-derived fibroblasts
Primary cilia morphology was evaluated in skin fibroblasts derived from the index patient. **Supplementary Figure S3** illustrates the cilia phenotype in detail and **Supplementary Figure S4** shows a whole-field image of the cells. Patient-derived fibroblasts showed a statistically significant increase in cells with substantial accumulation of IFT88 in the ciliary tip compared to control fibroblasts (P equals 0.0002). There was no statistically significant difference in primary cilia length or number between patient- and control cells (data not shown).

3.5 DISCUSSION

We describe a patient with mild ID, ASD, skeletal anomalies and facial dysmorphisms who carries a de novo 14q24.2q24.3 microdeletion encompassing 65 protein-coding genes. Mild ID and congenital heart defect have been reported in all four previously reported patients with a 14q24 deletion [Oehl-Jaschkowitz et al., 2014; Tassano et al., 2014] and small or proximally-set thumb in two. However, the deletion in the index patient does not overlap with the smallest region of overlap of the previously reported patients (**Supplementary Figure S5**), suggesting the effect of multiple loci on 14q24 or elsewhere in the genome associated with these features. Haploinsufficiency of genes located within the deletion could contribute to the phenotype. Heterozygous mutation in *TGFB3* (MIM# 190230) has been reported in patient with arachnodactyly and marked contractures of the proximal interphalangeal joints that were also observed in the index patient [Rienhoff et al., 2013] and in four other patients with Marfan and Loeys-Dietz-like phenotypes [Matyas et al., 2014; Kuechler et al., 2015], suggesting that this gene could be involved in skeletal features. The mouse homologue of *VSX2* (MIM# 142993) was demonstrated to be a regulator of formation of the lumbosacral region, possibly accounting for sacral hypoplasia [Wellik and Capecchi, 2003]. Previously, *C14of169* (MIM# 611919), *NUMB* (MIM# 603728) and *PSEN1* (MIM# 104311) have been proposed to contribute to skeletal, cardiac and neurological anomalies [Tassano et al., 2014]. Maternal diabetes mellitus, a risk factor for sacral hypoplasia and congenital heart defect, could also have contributed to the phenotype [Al Kaissi et al., 2008; Liu et al., 2013].

Because of the combination of skeletal, ectodermal and ocular features in the index patient, we investigated a ciliary defect on the cellular level and

when the signal is lost_marijn_8072018.indd 58 08/07/2018 10:50

found excess accumulation of IFT88 in ciliary tips of patient-derived fibroblasts. Accumulation of IFT-B proteins (marked by IFT88) in ciliary tips indicates impaired retrograde ciliary transport [Arts et al., 2011; Cole et al., 2003], characteristic of cranioectodermal dysplasia (CED) (MIM# 614099) [Arts et al., 2011;Lin et al., 2013]. Biallelic mutations in *IFT43* have been identified in a family with CED [Arts et al., 2011]. Deletion of *IFT43* could therefore be a modifier of the 14q24 microdeletion syndrome phenotype. However, there are differences between the phenotype of the index patient and CED (long fingers and limbs instead of short fingers and limbs, a short, broad thorax instead of a narrow thorax and an extra central incisor instead of hypodontia) and we did not detect mutations in or imprinting of the non-deleted *IFT43* allele. Exome sequencing was used to examine oligogenic inheritance and modifier genes, which have been reported in ciliopathies [Katsanis, 2001]. Although we did not identify variants in other ciliopathy-associated genes, we cannot exclude variants in genes encoding unknown regulators of IFT-A or regulatory elements of ciliopathy-associated genes.

In conclusion, we report a patient with mild ID, skeletal anomalies, congenital heart defect, myopia and facial dysmorphisms caused by a de novo 14q24.2q24.3 microdeletion. The deletion encompasses 65 genes and shows partial overlap with previously reported 14q24 microdeletions. Patient cells showed defective retrograde ciliary transport. This could be associated with haploinsufficiency of *IFT43*; however, additional variants in ciliary genes or gene regulatory elements are required to support the role of a ciliary defect in the pathogenesis of skeletal, ocular and ectodermal features. Further patients with overlapping deletions are needed to confirm the pathophysiological mechanisms underlying this phenotype.

Acknowledgments

We thank the patient and her parents, M. Van Roosmalen for his assistance in making the figures, and the Cell Microscopy Core at the Department of Cell Biology, Center for Molecular Medicine, UMC Utrecht for use of the confocal laser microscope. We used DECIPHER Consortium data (http://decipher.sanger.ac.uk). This project was financed by grants from the Dutch Kidney Foundation (KOUNCIL consortium: CP11.18 to N.V.A.M.K., R.H.G. and H.H.A.), the Netherlands Organization for Health Research and Development (ZonMW Veni-91613008 to H.H.A.), the Netherlands Organization for Scientific research (NWO Vici-865.12.005 to R.R.) and the European Community's Seventh Framework Programmes FP7/2009 (SYSCILIA grant agreement no. 241955 to R.R. and R.H.G.).

when the signal is lost_marijn_8072018.indd 59 08/07/2018 10:50

SUPPLEMENTARY MATERIAL

Supplementary Methods S1. *Whole-exome sequencing*

Purified genomic DNA (Qiagen, Hilden, Germany) was fragmented using sonication (Covaris, Woburn, MA, USA), blunt-ended and 5'-phosphorylated. Shortened double-stranded adaptors complementary with the SOLiD next-generation sequencing platform were ligated to the ends. Fragments were amplified using primers with sequencing barcodes to enable multiplexing with three additional samples. An enrichment reaction was performed at 65°C for 24 hours and sequencing of barcoded samples was performed on the SOLiD 5500XL platform (Life technologies, Carlsbad, CA, USA). Average coverage of the exome for the index patient was 86-fold. Reads were processed and aligned to the human reference genome (hg19). Subsequent calling of single-nucleotide variants and small indels and variant annotation were performed using our custom analysis pipeline as described previously [Nijman et al., 2010]. Variants were filtered based on coverage (>8 reads), percentage of the variant in exome reads (≥20) and population allele frequency below 1% based on publically available databases including 1000 Genomes Project, NHLBI Exome Sequencing Project Exome Variant Server and our in-house database [The 1000 Genomes Project Consortium, 2010; NHLBI GO Exome Sequencing Project (ESP), 2014].

when the signal is lost_marijn_8072018.indd 60 08/07/2018 10:50

Supplementary Methods S2. *Immunocytochemistry IFT43*

Control- and patient-derived fibroblasts were cultured on glass slides under standard cell culture conditions in DMEM containing 10% FCS. Formation of primary cilia was stimulated using serum-depleted medium (DMEM containing 0% FCS) for 24 hours prior to fixation in 4% PFA in PBS and permeabilization with 0.1% Triton-X-100 in PBS. Cells were blocked with 3% bovine serum albumin (BSA) in PBS to minimize non-specific binding. Primary antibody incubations were performed overnight at 4 °C with anti-IFT43 (rabbit polyclonal, 1:50; Novus NBP1-92019, Cambridge, UK) and anti-acetylated α-tubulin (mouse monoclonal, 1:20,000; Sigma T6793). Specificity of the antibody against IFT43 was confirmed by the manufacturer on a protein array containing IFT43 protein plus 383 other non-specific proteins and in a study that demonstrated a statistically significant reduction in antibody signal intensity after siRNA knockdown of *IFT43* [Stadler et al., 2012]. Secondary antibodies (Life Technologies, Forster City, CA, USA) anti-mouse IgG Alexa Fluor 488 (1:500) and anti-rabbit IgG Alexa Fluor 568 (1:500) and Hoechst (1:5000; Invitrogen, H3570) were used. Coverslips were washed with PBS and mounted in Fluormount G (Cell Lab, Beckman Coulter). Confocal imaging was performed using Zeiss Confocal laser microscope LSM700 and images were processed with ZEN 2011 software.

when the signal is lost_marijn_8072018.indd 61 08/07/2018 10:50

Supplementary Methods S3. *Immunocytochemistry IFT88*

Control- and patient-derived fibroblasts were cultured on glass slides under standard cell culture conditions in Dulbecco's Modified Eagle's Medium (DMEM) containing 20% Fetal Calf Serum (FCS). The formation of primary cilia was stimulated using serum-depleted medium (DMEM containing 0.2% FCS) for 48 hours prior to immunostaining. The cells were then fixed in 2% paraformaldehyde (PFA) in Phosphate Buffered Saline (PBS), and permeabilized with 1% Triton-X-100 in PBS. Subsequently, the cells were blocked with 2% bovine serum albumin (BSA) in PBS minimizing non-specific binding, followed by a one-hour incubation with the primary antibody at room temperature. The following primary antibodies were used: anti-IFT88 (rabbit polyclonal, 1:00; Proteintech, Chicago, IL, USA), anti-RPGRIP1L (guinea pig polyclonal, 1:500; SNC040) [Arts et al., 2007], and anti-acetylated α-tubulin (mouse monoclonal, 1:1,000; Life Technologies, Foster City, CA, USA). Cells were washed with PBS prior to a one-hour incubation with the secondary antibody at room temperature. The following secondary antibodies (Life Technologies, Forster City, CA, USA) were used: anti-mouse IgG Alexa Fluor 488 (1:300), anti-rabbit IgG Alexa Fluor 568 (1:300), and anti-guinea pig IgG Alexa Fluor 647 (1:300). The cover slides were embedded in Vectashield containing DAPI (Vector Laboratories, Burlingame, CA, USA) on a microscopic glass slide. Microscopic analysis was performed on an Axio Imager ZI fluorescence microscope (Zeiss, Sliedrecht, The Netherlands) with an ApoTome slider. Images were processed using AxioVision (Zeiss) and Photoshop CS4 (Adobe Systems, San Jose, CA, USA) software.

when the signal is lost_marijn_8072018.indd 62 08/07/2018 10:50

when the signal is lost_marijn_8072018.indd 63

Supplementary Table S1. *Patients with overlapping 14q24 deletions and associated clinical findings*

Clinical feature	Present case	Oehl-Jaschkowitz et al. (2014)	Tassano et al. (2014)	DECIPHER 292616	DECIPHER 261280	DECIPHER 254258	DECIPHER 249722	DECIPHER 255084	DECIPHER 250761
Position (hg19)	14:73,152,115 -77,698,582	14:69,379,727-74,826,674	14:69,500,246 -74,845,355	14:75746308-76061709	14:75,059,408-77,069,618	14:74,507,706 -74,574,163	14:74,212,730 - 76,281,643	14:74,053,744-74,062,912	14:74,001,123 - 74,029,907
Size of deletion	4.5 Mb	5.4 Mb	5.3 Mb	0.32 Mb	2.01 Mb	0.07 Mb	2.07 Mb	0.01 Mb	0.03 Mb
IFT43 deleted	+	-	-	-	+	-	-	-	-
Additional CNV	-	-	-	-	-	-	-	+	+
Sex	Female	Male	Male	Male	Male	Male	NA	Female	Male
Intellectual disability	Mild	Mild	Mild	NA	NA	+	+	+	+
Congenital heart disease	ASD, VSD	ASD	ASD	VSD	NA	NA	NA	NA	NA
Hypoplastic thumbs	+	+	-	NA	NA	NA	NA	NA	NA
Brachydactyly	-	+	+	NA	NA	NA	NA	+	NA
Dysmorphic ears	Cup-shaped	NA	Prominent (anti)helix, large lobes	NA	Abnormality of antihelix	Prominent ears	NA	NA	Prominent ears
Preauricular skin tag	+	NA	NA	NA	NA	NA	+	NA	NA
Dysmorphic features	Wide nasal bridge, extra incisor, long fingers	Hypertelorism, high nasal bridge, flat philtrum, thin upper lip	Wide nasal bridge, long philtrum, thin upper lip	NA	Hypertelorism, malar flattening	NA	Proportionate short stature	Hypertelorism, malar flattening, proportionate short stature	Broad nasal tip, thin upper lip, thick lower lip

08/07/2018 10:50

Additional findings	Myopia, astigmatism Broad thorax	Limited elbow extension and supination	Pextus excavatum, joint hyperlaxity, focal epilepsy	Horseshoe kidney	NA	NA	Psychiatric/ behavioral abnormality	NA	NA

+, present; -, absent; NA, not reported/not applicable.

For patients with DECIPHER ID 253894, 265207, 277160, 282030, 289298, 290148 and 292650 and overlapping 14q24 microdeletions, phenotypic information was limited. Note that *IFT43* is deleted in patient with DECIPHER ID 261280.

when the signal is lost_marijn_8072018.indd 64 08/07/2018 10:50

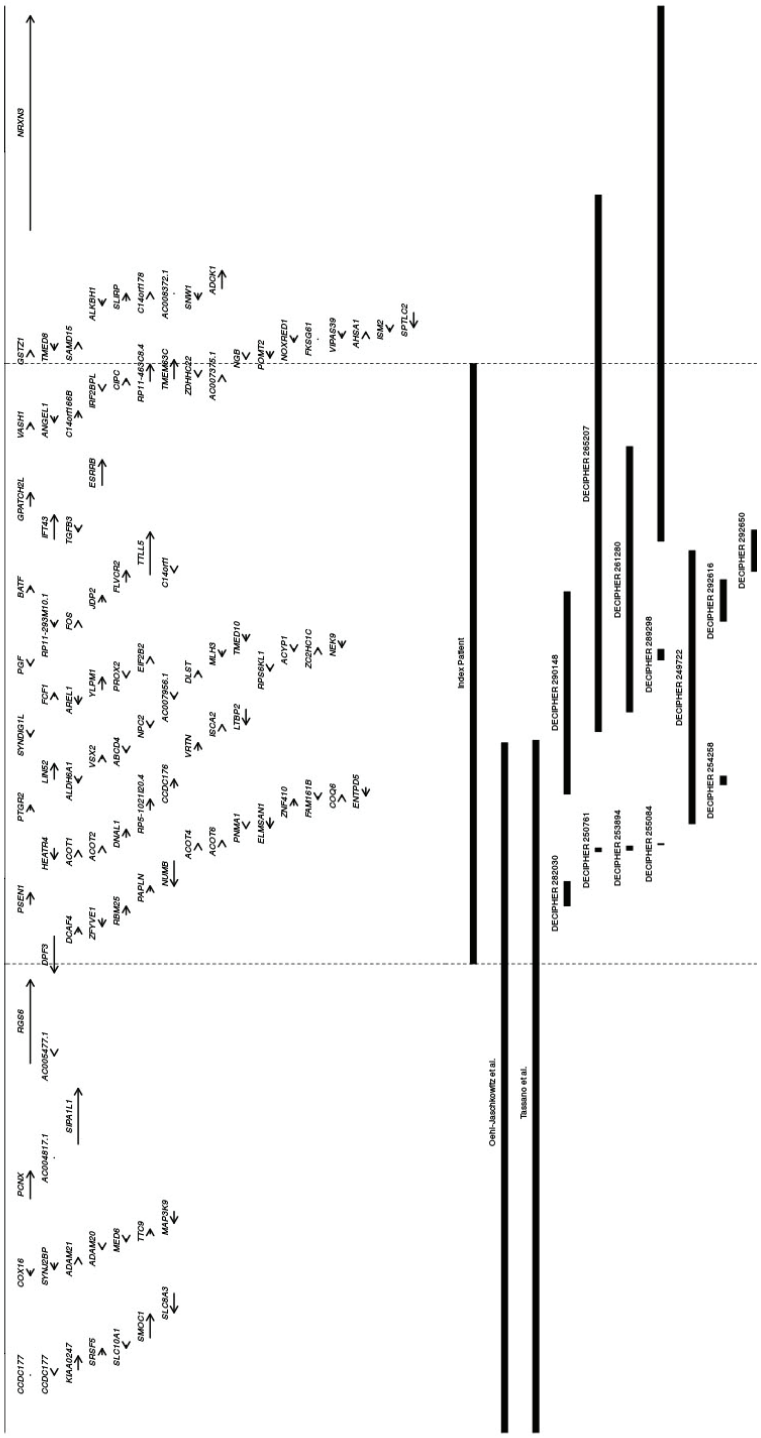

Supplementary Figure S1. Schematic overview gene content of the 14q24.2q24.3 region according to UCSC Genome Browser (GRCh37/hg19 assembly; http://genome.ucsc.edu) and of previously reported patients with overlapping deletions.

when the signal is lost_marijn_8072018.indd 65 08/07/2018 10:50

***Supplementary Table S2**. Ciliopathy-associated genes and genes within deletion queried in exome data*

Ciliopathy-associated genes				**Genes in 14q24.2q24.3 microdeletion**		
NPHP1	*B9D1*	*IFT88*	*AIPL1*	*DPF3*	*CCDC176*	*NEK9*
INVS	*MKS3*	*IFT72*	*LCA5*	*DCAF4*	*ALDH6A1*	*HIF1AP1*
NPHP3 H485Q	*TMEM216* indel	*IFT27*	*CRX*	*ZFYVE1*	*LIN52*	*TMED10*
NPHP4	*TCTN3*	*IFT46*	*CRB1*	*RBM25*	*VSX2*	*FOS*
IQCB1	*TMEM237*	*IFT70*	*IMPD1*	*PSEN1*	*ABCD4*	*JDP2*
CEP290	*C5ORF42*	*IFT81*	*RD3*	*PAPLN*	*VRTN*	*BATF*
GLIS2	*CEP41*	*IFT25*	*RDH12*	*NUMB*	*SUB1P2*	*FLVCR2*
RPGRIP1L	*KIF7*	*IFT22*	*BBS1*	*HEATR4*	*RPS2P2*	*RNA5SP38*
NEK8	*WDR19*	*IFT74*	*BBS2*	*C14orf169*	*SYNDIG1L*	*TTLL5*
SDCCAG8	*IFT144*	*IFT57*	*ARL6*	*ACOT1*	*NPC2*	*C14orf1*
TMEM67	*IFT140*	*IFT20*	*BBS4*	*NT5CP2*	*MIR4709*	*IFT43*
TTC21B	*THM1*	*IFT54*	*BBS5*	*ACOT2*	*RAP1AP*	*TGFB3*
WDR19	*TTC21B*	*TULP3*	*MKKS*	*NT5CP1*	*ISCA2*	*GPATCH2L*
ZNF423	*IFT139*	*CEP120* E560K	*BBS7*	*ACOT4*	*LTBP2*	*ESRRB*
CEP164	*WDR10*	*CEP83*	*TTC8*	*ACOT6*	*KIAA0317*	*VASH1*
ANKS6	*IFT122*	*CSPP1*	*BBS9*	*NDUFB8P*	*FCF1*	*ANGEL1*
B9D2	*WDR35*	*DCDC2*	*BBS10*	*DNAL1*	*YLPM1*	*C14orf166*
TCTN1	*IFT121*	*INPP5E*	*TRIM32*	*PNMA1*	*PROX2*	*IRF2BPL* Q110K
TCTN2	*IFT43*	*ARL13B*	*BBS12*	*ELMSAN1*	*DLST*	*KIAA1737*
MKS1	*WDR34*	*OFD1* E906K	*WDPCP*	*MIR4505*	*RPS6KL1*	*TMEM63C*
AHI1	*DYNC2H1*	*CXORF5*	*LZTFL1*	*PTGR2*	*PGF*	*ZDHHC22*
CC2D2A	*DHC1B*	*TMEM138*	*BBIP1*	*ZNF410*	*EIF2B2*	
TMEM231	*IFT172*	*GUCY2D*	*ALMS1*	*FAM161B*	*MLH3*	
TMEM17	*IFT80*	*RPE65*	*EVC1*	*COQ6*	*ACYP1*	
KCTD10	*IFT52*	*SPATA7*	*EVC2*	*ENTPD5*	*ZC2HC1C*	

Presence of variants in ciliopathy-associated genes including IFT-complex genes and their synonyms, and all genes contained within the deletion, was investigated in whole-exome sequencing data. All variants in ciliopathy-associated genes were present in heterozygous form. Variants in *TMEM216* and *CEP120* were filtered out because of population frequency >1%. Because there is no direct interaction between *NPHP3* and IFT-A complex proteins, digenic inheritance involving heterozygous variants in these genes is unlikely. The variant in *OFD1* is a 'variant of unknown significance' (VUS) and was discarded because the phenotype in the index patient does not match criteria for Oral-facial-digital syndrome type I. *IRF2BPL* is not associated with recessive disease.

when the signal is lost_marijn_8072018.indd 66 08/07/2018 10:50

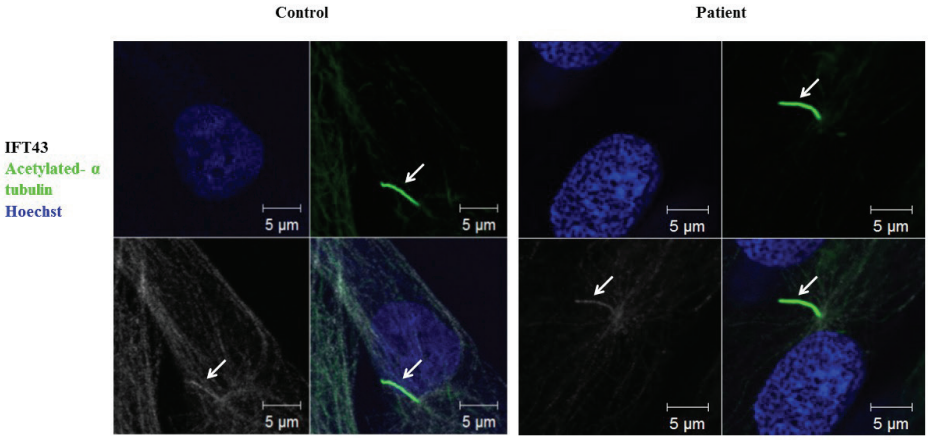

Supplementary Figure S2. IFT43 is expressed along the ciliary axoneme in control- and patient-derived fibroblasts. Patient-derived skin fibroblasts were used to qualitatively assess IFT43 protein expression in the primary cilium compared to control fibroblasts. IFT43 expression was observed in the cytoskeleton and along the ciliary axoneme (indicated by arrows) in both control- and patient-derived fibroblasts. The ciliary axoneme is shown in green (acetylated-α-tubulin) and IFT43 is shown in white. The scale bar represents 5 µm.

when the signal is lost_marijn_8072018.indd 67 08/07/2018 10:50

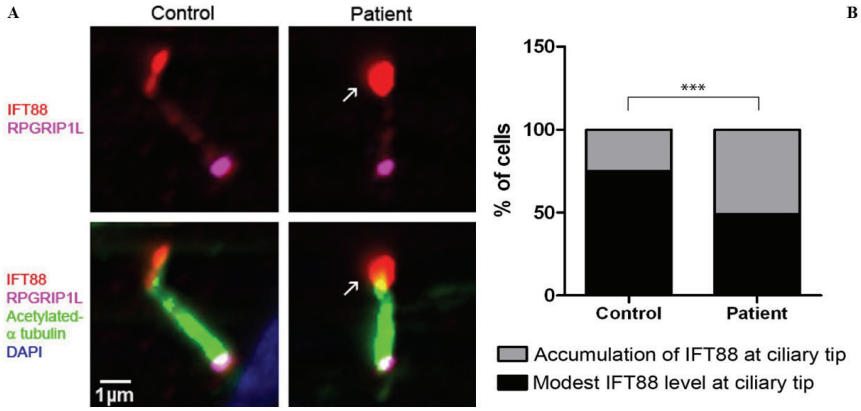

Supplementary Figure S3. IFT88 accumulates in ciliary tips in patient-derived cells. Patient-derived skin fibroblasts were used to evaluate the localization of IFT88 in the primary cilium in comparison to fibroblasts from a healthy control. **A.** Cilium from a control individual with modest IFT88 levels (red) in the ciliary tip and a cilium in a cell from the index patient with substantial IFT88 accumulation in the ciliary tip (arrows). The ciliary axoneme is shown in green (acetylated-α-tubulin), the transition zone that marks the proximal cilium is indicated in pink (RPGRIP1L), and IFT88 is shown in red. The scale bar represents 1 µm. **B.** An accumulation of IFT88 at the tip of the ciliary axoneme was seen in 51% of cilia in patient- derived fibroblasts, whereas such accumulations were only seen in 25% of cilia in control fibroblasts (>50 cells analyzed). The asterisks indicate that this is a statistically significant difference (two-tailed P-value equals 0.0002, calculated using the Fisher's exact test).

when the signal is lost_marijn_8072018.indd 68 08/07/2018 10:50

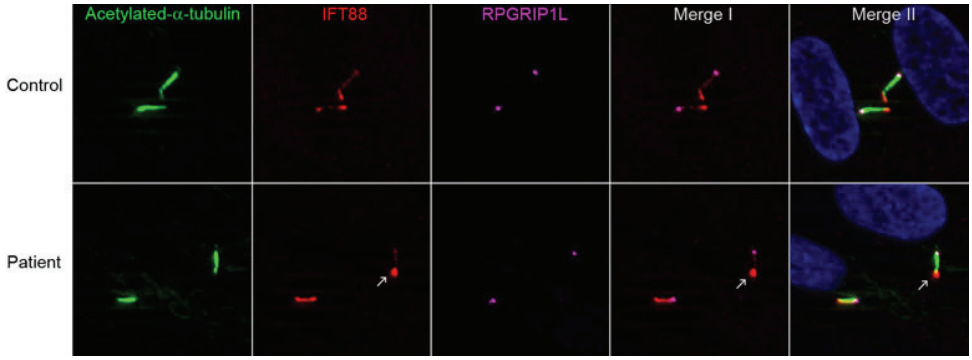

Supplementary Figure S4. IFT88 protein localization in cilia from patient- and control cells. The ciliary axoneme is marked by acetylated-α-tubulin (green), the transition zone that marks the proximal cilium is marked by RPGRIP1L (pink), and IFT88 is shown in red. The arrow points at an accumulation of IFT88 in the ciliary tip in one of the patient-derived cells (lower panel).

when the signal is lost_marijn_8072018.indd 69 08/07/2018 10:50

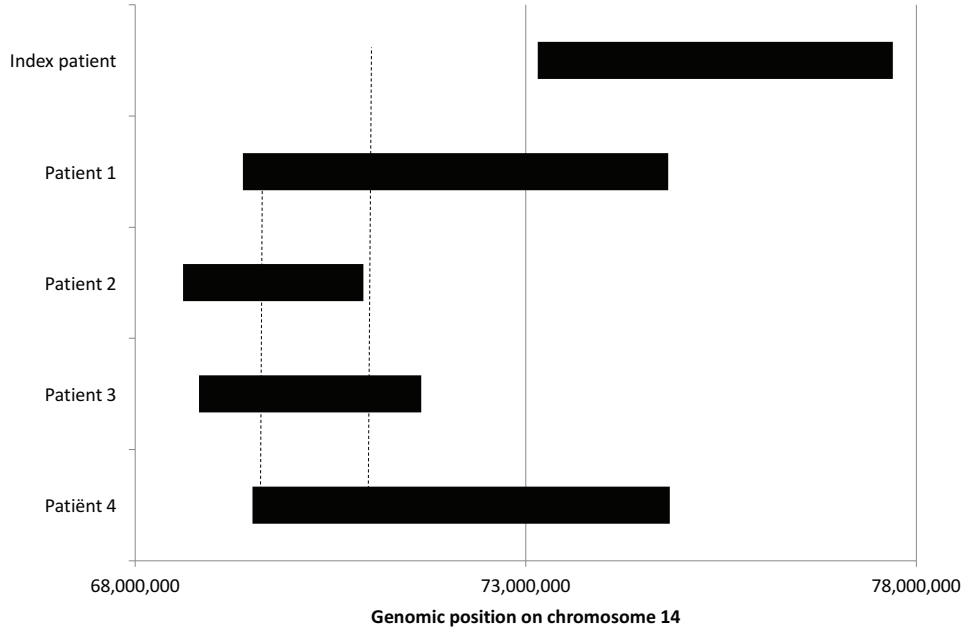

Supplementary Figure S5. Schematic overview of 14q24 deletions in index patient and patients reported in literature with similar phenotype. Phenotype of patients 1 to 3 reported by Oehl-Jaschkowitz et al. and patient 4 reported by Tassano et al. overlaps with phenotype observed in index patient [Oehl-Jaschkowitz et al., 2014; Tassano et al., 2014]. Dashed lines represent smallest region of overlap between these patients. Deletion found in index patient does not overlap with this region.

when the signal is lost_marijn_8072018.indd 70 08/07/2018 10:50

when the signal is lost_marijn_8072018.indd 71 08/07/2018 10:50

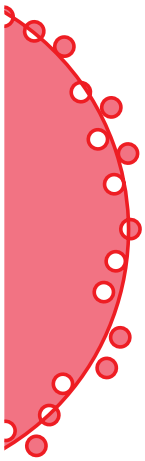

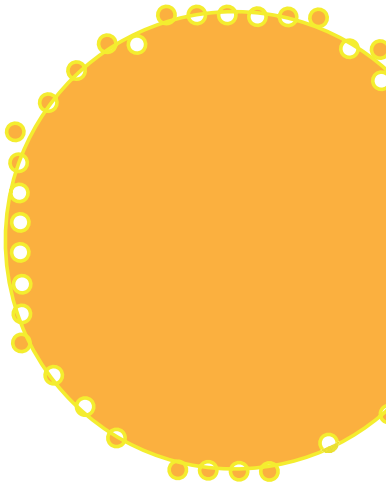

CHAPTER 4

Compound heterozygous *NEK1* variants in two sibs with oral-facial-digital syndrome II (Mohr syndrome)

Monroe GR*, Kappen IF*, Stokman MF*, Terhal PA, Van den Boogaard MH, Savelberg SM, Van der Veken LT, Van Es RJ, Lens SM, Hengeveld RC, Creton MA, Janssen NG, Mink van der Molen AB, Ebbeling MB, Giles RH, Knoers NVAM, Van Haaften G

* These authors contributed equally

2016. Eur. J. Hum. Genet. 24: 1752-1760
DOI:10.1038/ejhg.2016.103

when the signal is lost_marijn_8072018.indd 73 08/07/2018 10:50

ABSTRACT

The oral-facial-digital (OFD) syndromes comprise a group of related disorders with a combination of oral, facial and digital anomalies. Variants in several ciliary genes have been associated with subtypes of OFD syndrome, yet in most OFD patients the underlying cause remains unknown. We investigated the molecular basis of disease in two brothers with OFD type II, Mohr syndrome, by performing single nucleotide polymorphism (SNP)-array analysis on the brothers and their healthy parents to identify homozygous regions and candidate genes. Subsequently, we performed whole-exome sequencing (WES) on the family. Using WES we identified compound heterozygous variants c.[464G>C;1226G>A] in NIMA (Never in Mitosis Gene A) - Related Kinase 1 (*NEK1*). The novel variant c.464G>C disturbs normal splicing in an essential region of the kinase domain. The nonsense variant c.1226G>A, p.(Trp409*), results in nonsense-associated alternative splicing, removing the first coiled-coil domain of NEK1. Candidate variants were confirmed with Sanger sequencing and alternative splicing assessed with cDNA analysis. Immunocytochemistry was used to assess cilia number and length. Patient-derived fibroblasts showed severely reduced ciliation compared to control fibroblasts (18.0% vs. 48.9%, P<0.0001) but showed no significant difference in cilia length. In conclusion, we identified compound heterozygous deleterious variants in *NEK1* in two brothers with Mohr syndrome. Ciliation in patient fibroblasts is drastically reduced, consistent with a ciliary defect pathogenesis. Our results establish *NEK1* variants involved in the etiology of a subset of patients with OFD syndrome type II and support the consideration of including (routine) *NEK1* analysis in patients suspected of OFD.

when the signal is lost_marijn_8072018.indd 74 08/07/2018 10:50

4.1 Introduction

The oral-facial-digital (OFD) syndromes comprise a group of related disorders with a specific combination of oral, facial and digital anomalies. To date, fourteen phenotypically different subtypes have been reported, of which nine have been well-characterized [Gurrieri et al., 2007; Toriello et al., 2016]. These subtypes show an autosomal recessive inheritance pattern, except for OFD type I, type VII and type VIII, which are X-linked forms of OFD [Gurrieri et al., 2007; Toriello et al., 2016]. Common characteristic findings associated with these syndromes include: hamartomas of the tongue and a lobulated tongue, midline cleft of the upper lip and/or palate, gingival frenulae, dental anomalies, brachydactyly, syndactyly, pre- or post-axial polydactyly and cystic renal disease [Gurrieri et al., 2007; Toriello et al., 2016].

In 2001, the causative gene for OFD type 1 (OMIM 300170), *OFD1*, was identified [Ferrante et al., 2001]. Functional studies have shown that the encoded protein has an important role in the formation of primary cilia [Macca and Franco, 2009; Romio, 2004]. Because cilia play an essential role in the morphogenesis and tissue homeostasis of multiple organ systems, gene variants interrupting cilia function manifest systemically and result in a diverse phenotypic picture [Fry et al., 2014; Powles-Glover, 2014; Satir et al., 2010]. In the following years, variants in several other genes involved in ciliogenesis or ciliary signaling have been implicated in specific subtypes of OFD, namely *TCTN3* for OFD type IV (OMIM 258860), *TMEM216* and *C5orf42* for OFD VI (OMIM 277170), *DDX59* for an unclassified autosomal recessive form of OFD with intellectual disability, *TBC1D32/C6orf170* or *SCLT1* for OFD IX (OMIM 258865) and *C2CD3* for an atypical type of OFD with severe microcephaly and cerebral malformations [Adly et al., 2014; Lopez et al., 2014; Shamseldin et al., 2013; Thauvin-Robinet et al., 2014; Thomas et al., 2012]. Variants in two of these genes, *TCTN3* and *TMEM216*, are also found in other ciliopathies such as Joubert syndrome and Meckel-Gruber syndrome [Thomas et al., 2012; Valente et al., 2010]. These findings indicate that multiple OFD subtypes can be classified as ciliopathies. However, in the majority of patients with an autosomal recessive form of OFD the underlying genetic cause remains to be identified.

In the present study we performed genetic analysis on two brothers from consanguineous parents who have features compatible with OFD type II (Mohr syndrome, OMIM 252100). As several other OFD subtypes have been shown to be ciliary diseases, we presumed that the brothers would also have a ciliopathy. The extreme genetic heterogeneity of ciliopathies and the large number of genes involved in ciliary pathways, as well as the large potential number of yet unknown ciliary proteins, prompted us to perform whole-exome sequencing (WES) to identify the disease related gene in the family [Huber and Cormier-Daire, 2012; Sun et al., 2015].

when the signal is lost_marijn_8072018.indd 75 08/07/2018 10:50

4.2 METHODS

4.2.1 Patient material collection and consent

Blood was obtained from both brothers and their parents after informed consent. Skin fibroblasts of the eldest brother were obtained during a scheduled knee operation. Informed consent was obtained for whole genome SNP-array analysis and WES in the diagnostics laboratory. The medical ethical committee of the University Medical Center Utrecht (UMCU) approved the WES patient information and informed consent form.

4.2.2. SNP-array analysis

Genomic DNA was extracted from peripheral leukocytes according to standard protocols. SNP-array copy number profiling and analysis of regions of homozygosity were performed according to standard procedures using the Infinium Human Omni Express Exome BeadChip (Illumina, San Diego, CA, USA). Subsequently, visualizations of SNP-array results and data analysis were performed using Nexus 7.5 software (BioDiscovery, Los Angeles, CA, USA). Human genome build Feb. 2009 GRCh37/hg19 was used. Results were classified with Cartagenia BENCH software (Cartagenia, Leuven, Belgium).

4.2.3 Whole-exome sequencing

Fragment libraries of the DNA samples of the two brothers and their parents were prepared (Kapa Biosystems, Wilmington, MA, USA), enriched using Agilent Sureselect V5 (Agilent, Santa Clara, CA, USA) and sequenced as a Rapid Run on the Illumina HiSeq 2500 Sequencer (Illumina, San Diego, CA, USA) at the Utrecht Sequencing Facility (Utrecht, Netherlands). A phased vcf was created and imported into Cartagenia BENCHlab NGS module (Cartagenia, Leuven, Belgium) for variant interpretation. Due to the consanguineous nature of the parents, homozygous variants were initially investigated, and subsequently compound heterozygote and X-chromosome variants were also examined (**Supplementary Methods S1**). Candidate variants for both brothers were examined to detect the variant(s) that both brothers shared (**Supplementary Table S1**). Variants that cosegregated in both brothers were confirmed by Sanger sequencing (primer sequences available on request). Subsequently a literature search on the relevant variants was performed. Variants have been submitted to the Leiden Open Variation Database (LOVD) at http://databases.lovd.nl/shared/genes/NEK1 (LOVD DB-IDs NEK1_000002 and NEK1_000003).

4.2.4 Fibroblast RNA isolation and cDNA conversion

Patient and control fibroblasts were cultured with Dulbecco's Modified Eagle's Medium (DMEM) containing 10% Fetal Calf Serum (FCS) in standard cell culture conditions. Cells were washed with Phosphate Buffered Saline (PBS), harvested, and RNA extracted (RNeasy Mini, Qiagen, Germany). RNA was converted to cDNA using the iScript cDNA Synthesis Kit (Bio-Rad, Hercules, CA, USA).

when the signal is lost_marijn_8072018.indd 76 08/07/2018 10:50

4.2.5 Variant screening of NEK1 in an OFD type II cohort

To evaluate if *NEK1* variants were causal for OFD type II, *NEK1* was screened in a cohort of four patients suspected of having OFD and showing overlapping features with the presently described brothers (**Supplementary Table S2**). The full coding regions and exon-intron boundaries were analyzed by Sanger sequencing. Primer sequences are listed in **Supplementary Table S3**.

4.2.6 Immunocytochemistry

To assess primary cilia length and morphology, control- and patient-derived fibroblasts were cultured on glass slides under standard cell culture conditions in DMEM containing 10% FCS. The formation of primary cilia was stimulated using serum-depleted medium (DMEM containing 0% FCS) for 24 hours prior to immunostaining. Cells were put on ice for 5 minutes before fixation with 4% paraformaldehyde (PFA) in PBS, and permeabilization with 0.1% Triton-X-100 in PBS. Cells were blocked with 3% bovine serum albumin (BSA) in PBS minimizing non-specific binding, followed by a 2.5-hour incubation with primary antibodies and 1-hour incubation with secondary antibodies at room temperature. For a full list of antibodies used, see **Supplementary Methods S2**. Coverslips were washed with PBS and mounted in Fluormount G (Cell Lab, Beckman Coulter, Brea, CA, US). Confocal imaging was performed using Zeiss Confocal laser microscope LSM700 (Carl Zeiss AG, Oberkochen, Germany) and images were processed with ZEN 2011 software (Carl Zeiss AG, Oberkochen, Germany) and Volocity 6.3 software (PerkinElmer, Coventry, UK).

4.3 RESULTS

4.3.1 Patient description

The brothers showed similar features, summarized in **Table 1** and **Figure 1(A-H)**. They are the only children of healthy, consanguineous parents (4th degree relatives), as is depicted in **Figure 1(I)**. The elder brother (LOVD individual id 00064295) was born after a gestation of 39 weeks with a birth weight of 3540 gram (0.03 SD), a birth length of 49 cm (-1.44 SD) and head circumference of 37.5 cm (+1.37 SD). The CT scan of the brain shortly after birth did not show any abnormalities. Histopathological examination of the tongue hamartomas showed polyp-like non-keratinizing stratified squamous epithelium. The underlying stroma contained mucoserous acini, fat and muscle cells and the tissue had a benign aspect. At the age of 21 years he had progressive, mainly conductive hearing loss, his right ear being more severely affected than his left one. A CT scan of the mastoid showed bilateral plump vestibulae and lateral semicircular canals.

when the signal is lost_marijn_8072018.indd 77 08/07/2018 10:50

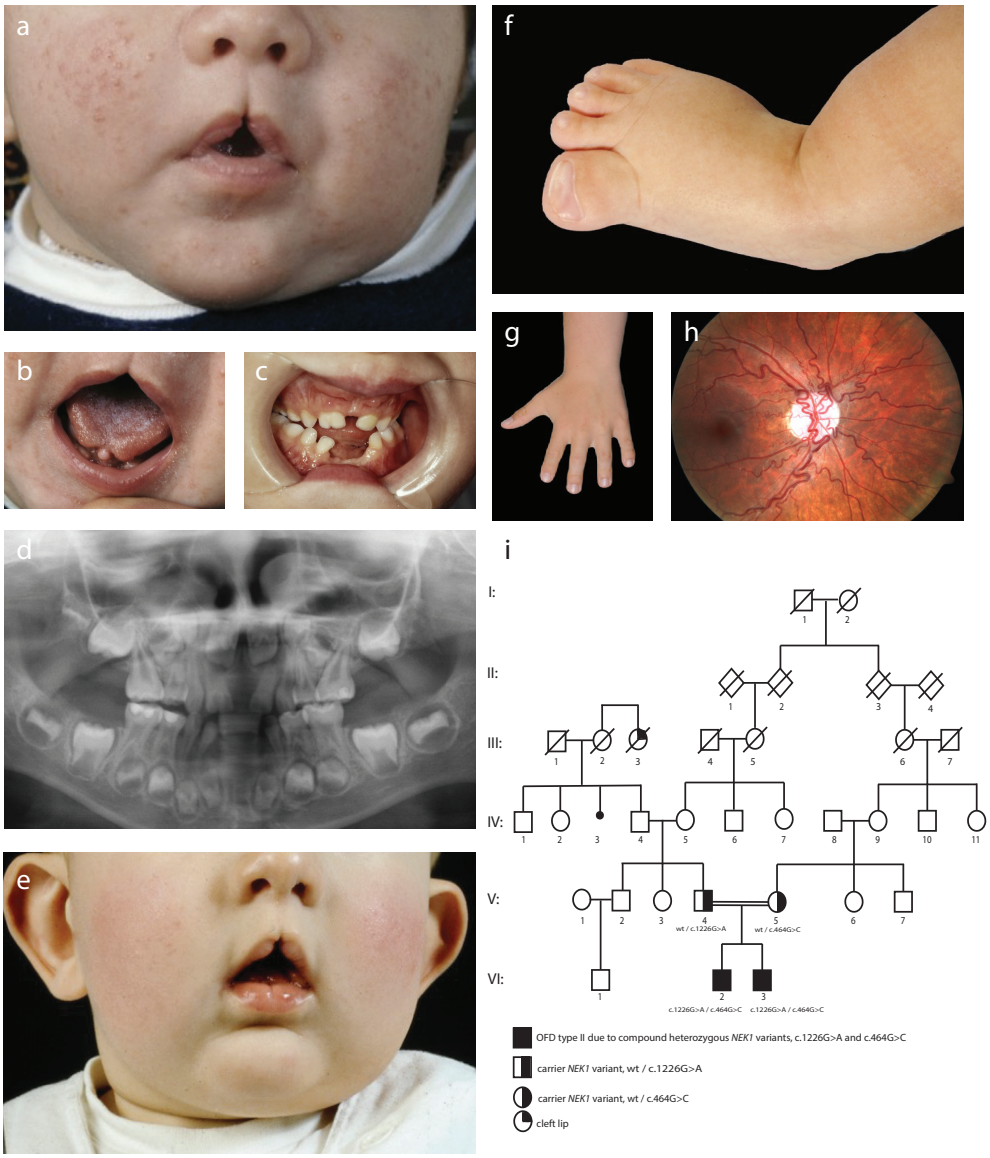

when the signal is lost_marijn_8072018.indd 78 08/07/2018 10:50

Figure 1. Clinical features of both brothers* and pedigree of the family. **A.** Partial midline cheilognathoschisis present in the younger brother at the age of 1 month. **B.** Bilobulated tongue with tongue hamartoma and short frenulum of the younger brother at the age of 1 month. **C.** The intraoral situation of the younger brother (age 3.5 years old), shows a fusion of the two deciduous incisors 5.1 and 5.2. Also, the deciduous upper left lateral incisor (6.2) is congenitally missing. Furthermore, the typical hyperplastic frenula can be seen in the upper jaw. **D.** The orthopantomogram of the younger brother at the age of 5, shows that the permanent and deciduous central incisors of the lower jaw (3.1, 4.1, 7.1 and 8.1) are missing. The molar roots are conical and seem to be fused, while the pulp chambers are taurodontic. **E.** Incomplete midline cheilognathoschisis and mild protruding ears of the elder brother at the age of 8 months. **F.** Broad right hallux of the elder brother at the age of 8 months. **G.** Brachydactyly with partial cutaneous syndactyly present in the younger brother. Picture was taken at the age of 9.5 years. **H.** Tortuosity of the retinal veins of younger brother at the age of 16 years. **I.** Pedigree of the family. Circles represent females and squares represent males. Solid symbols indicate compound heterozygosity for the c.[464G>C;1226G>A] variants and half solid symbols indicate heterozygosity. Carriership was confirmed in both parents. * *We obtained informed consent and approval of both parents and patients to include the present pictures.*

The younger brother (LOVD individual id 00064296) was born after a gestation of 39 weeks with a birth weight of 3390 gram (-0.37 SD), a birth length of 44 cm (-3.59 SD) and a head circumference of 37.5 (+1.37 SD). A CT scan of the brain that was performed shortly after birth did not show abnormalities. The tongue hamartomas were resected shortly after birth and histopathological examination showed non-keratinizing stratified squamous epithelium, with the underlying stroma containing a mucoserous acinus and fat cells. At the age of 9.5 years a mild bilateral conductive hearing loss of 15-20 dB was detected. Both brothers had a normal psychomotor development and normal intelligence. An ultrasound of the kidneys was performed at 20 years in the elder brother and at 16 years in the younger brother; these did not show abnormalities. The elder brother had normal serum creatinine level when he was tested at age 11 years and both brothers do not have polyuria. Ophthalmological examination was also performed at the age of 20 in the eldest brother and 16 in the younger. Both brothers had bilateral tortuosity of the retinal veins. There were no signs of retinopathy. X-rays of the thorax, humerus, femur, ankle, and feet were made at different ages and showed mild shortening of the tibia and broad halluces in both brothers, with a bony duplication of the right hallux in the elder patient. Several dental panoramic x-rays were performed and showed the anomalies described in **Table 1**. Both brothers had orthodontic treatment before a surgically assisted prosthodontic rehabilitation. Both brothers developed velopharyngeal insufficiency for which they underwent a pharyngoplasty.

Based on the clinical features, specifically the congenital malformations in combination with the recessive inheritance pattern and the absence of cerebral malformations, intellectual disability, and severe tibia defects, OFD type II (Mohr syndrome) was diagnosed by two clinical geneticists (M.H.B., P.A.T.).

when the signal is lost_marijn_8072018.indd 79 08/07/2018 10:50

4.3.2 SNP-array analysis

SNP-array analysis showed a normal male karyotype in both brothers and several homozygous regions indicative of distant consanguinity of the parents.

4.3.3 WES identifies biallelic variants in NEK1

Subsequently, the WES data of the parents and the two affected brothers were investigated. The genes implicated in the various OFD types were initially analyzed (*OFD1, TCTN3, TMEM216, C5orf42, DDX59, TBC1D32/C6orf170, SCLT1, C2CD3*) but no variants that could be considered causal were detected. Subsequently, the consanguineous relationship prompted us to investigate the shared homozygous regions in both boys for candidate homozygous variants but no plausible candidate genes were identified. After expanding our search in the whole exome and filtering for autosomal recessive and X-linked inheritance models, several gene variants were identified in candidate genes (**Supplementary Table S1**). Based on population frequency, predicted effect of the variant on gene function and previous literature, variants in *NEK1* were the most likely candidates. Both brothers share the same novel compound heterozygous variants in *NEK1*, comprising an exonic transversion NM_012224.2:c.464G>C at the last base of exon 6 inherited from the mother and a transition variant NM_012224.2:c.1226G>A inherited from the father, c.[464G>C;1226G>A] (**Figure 2**; exons are numbered similarly as in Thiel et al. 2011) [Thiel et al., 2011]. Variants were validated and segregation was confirmed by Sanger sequencing. Both variants were novel and not present in the population frequency reference datasets of NCBI dbSNP Build 137 for Human, the Exome Variant Server (EVS), the 1000Genomes, the Genome of the Netherlands (GoNL) or our in-house dataset. The variant c.1226G>A results in a nonsense variant p.(Trp409*) in exon 15 and the resulting shortened mRNA transcript includes the full coding sequence for a functional kinase domain but lacks part of the coiled-coil domain. The effect of the exonic variant c.464G>C appeared to be a nonsynonymous coding change from serine to threonine, but we postulated that alternative splicing may also occur due to the position of this base so near to the canonical splice site. This position is conserved and classified as disease-causing by Alamut Visual (Alamut Interactive Biosoftware, Rouen, France) and predicted to result in abnormal splicing. Further Sanger sequencing of *NEK1* in four other patients with OFD type II did not reveal any additional variants in *NEK1* that could be considered causal.

when the signal is lost_marijn_8072018.indd 80 08/07/2018 10:50

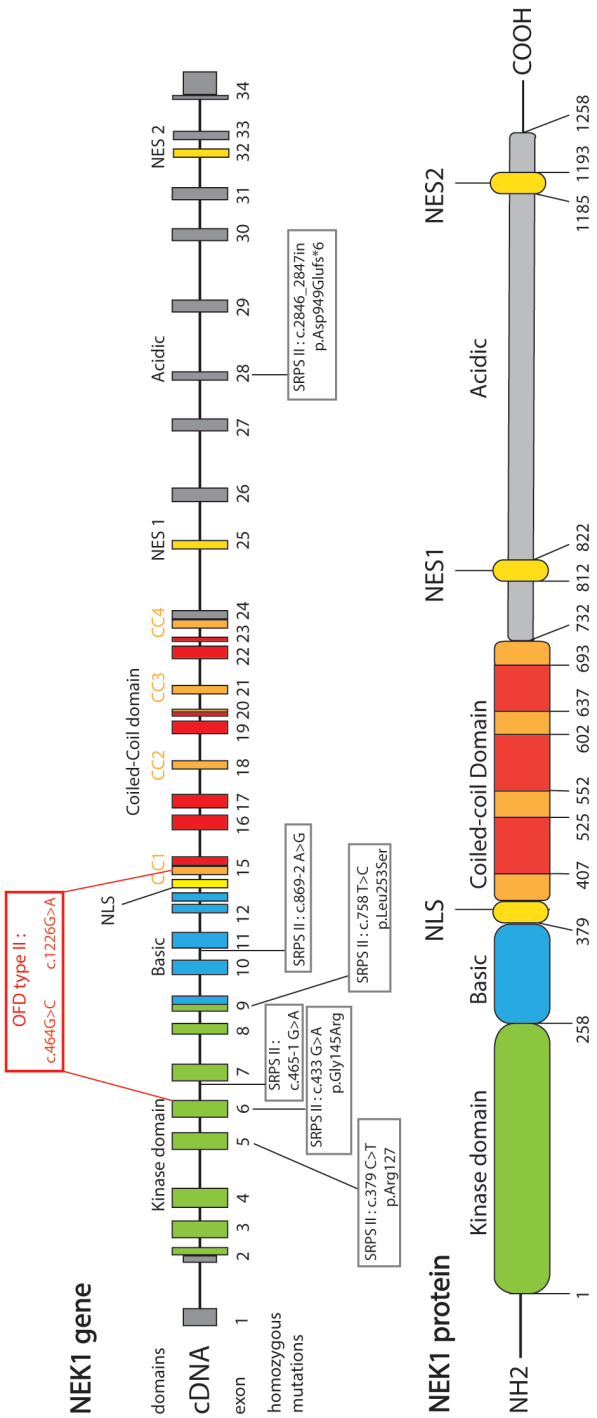

Figure 2. *NEK1* genomic and protein structure. **A.** *NEK1* genomic structure including the kinase domain, basic domain, coiled-coil domains (cc1-cc4), nuclear localization signal (NLS) and nuclear exportation signal (NES1-2). Variants found in the patients presented in this study with OFD type II are indicated above, namely c.464G>C in the kinase domain (exon 6) and c.1226G>A in the coiled-coil domain 1 (CCD1, exon 15). NCBI reference transcript NM_012224.2 is used. **B.** NEK1 protein structure including the kinase, basic and coiled-coil domains, the nuclear localization signal (NLS) and nuclear exportation signal (NES).

when the signal is lost_marijn_8072018.indd 81 08/07/2018 10:50

4.3.4 cDNA sequencing confirms that both variants result in alternative splicing

To assess the splicing impact of the variant c.464G>C, we designed primers covering several exons upstream and downstream of the variant in the cDNA of the elder brother (**Supplementary Methods S3**). Analysis of the resulting PCR products on 1% agarose gel identified a smaller product in addition to the expected product size, indicating an alternatively spliced product. Subsequent Sanger sequencing of the smaller product confirmed that the variant c.464G>C resulted in alternative splicing and exon skipping of exon 6 (**Figure 3, A-D**). The removal of exon 6 results in shift of the reading frame and introduces an early stop codon. The resulting transcript, r.397_464del, lacking exon 6, most likely undergoes nonsense-mediated decay due to the position of the premature stop codon. We observed that the correctly spliced product including exon 6 has no visible alternative allele C at position 464, demonstrating that this variant has no or minimal effect on coding changes from serine to threonine at this position. Additionally, any transcripts escaping nonsense mediated decay would lack exon 6 and the critical DFG motif (comprising the amino acids Asp-Phe-Gly) essential for the correct conformation of the ATP-binding site of the kinase domain NEK1 (**Figure 3C**) [Ung and Schlessinger, 2015].

To assess the effect of nonsense variant c.1226G>A in the same cDNA, we designed primers covering several exons upstream and downstream of exon 15 (**Supplementary Methods S4**). We selected the allele containing the c.1226G>A variant using a primer in exon 6, which was confirmed by the absence of the c.464G>C variant. Sanger sequencing of this region showed that exon 15 is skipped in frame in nearly all transcripts (**Figure 3, E-H**). The resulting transcripts, r.1192_1266del, are near-full length. The loss of exon 15 removes the first coiled-coil domain of NEK1. The region containing coiled-coil domains 1 and 2 has been shown to interact strongly with ATRX and weakly with MRE11 and 53BP1 that are involved in dsDNA break repair and homologous recombination [Surpili et al., 2003]. The coiled-coil domains 1 and 2 are also required for localization to the primary cilium, although the ciliary signal is strongest in transcripts containing coiled-coil domain 2 [White and Quarmby, 2008].

when the signal is lost_marijn_8072018.indd 82 08/07/2018 10:50

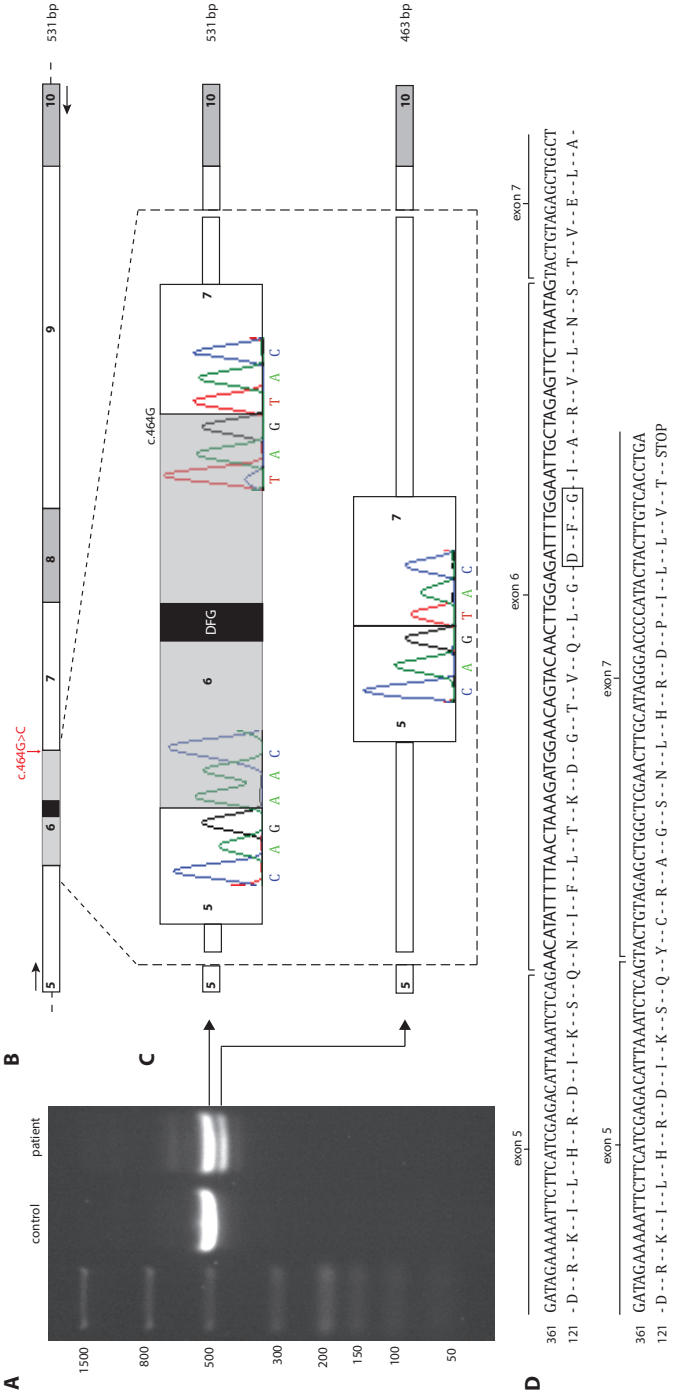

when the signal is lost_marijn_8072018.indd 83 08/07/2018 10:50

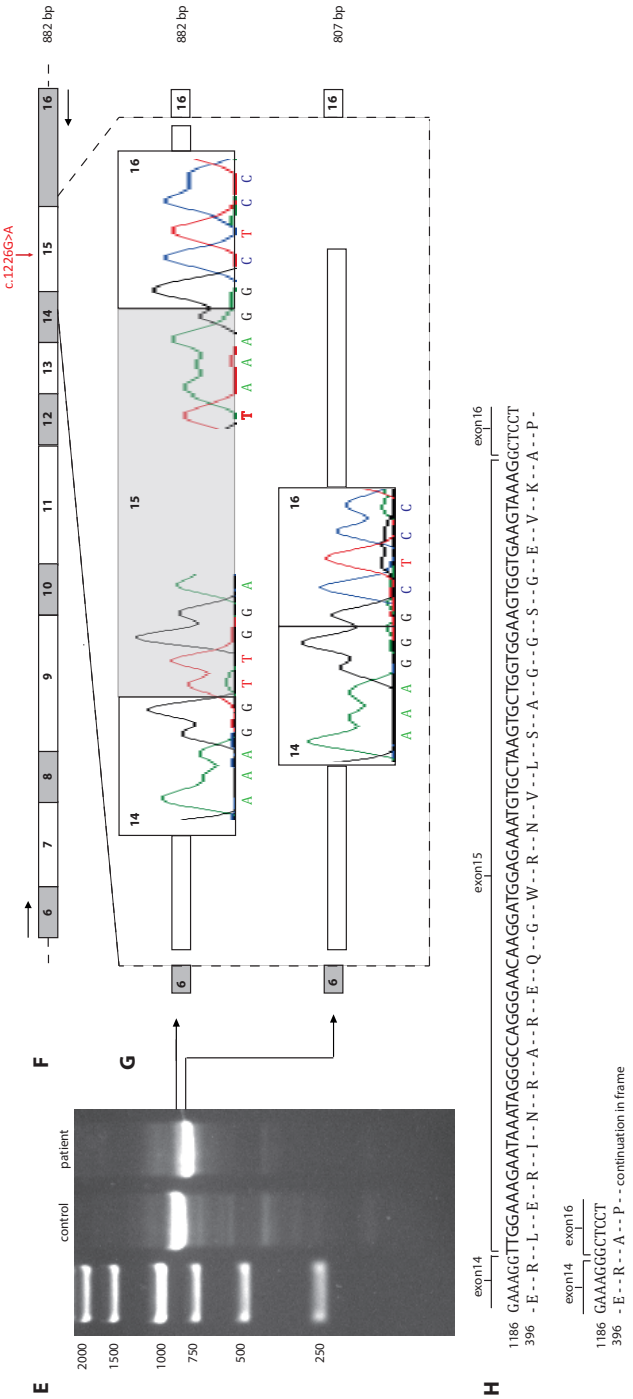

when the signal is lost_marijn_8072018.indd 84 08/07/2018 10:50

Figure 3. *NEK1* cDNA analysis of variant c.464G>C (A-D) and nonsense variant c.1226G>A, p.(Trp409*) (E-H). **A.** Primers flanking the patient variant c.464G>C were used for PCR on patient and control cDNA isolated from fibroblast mRNA. Following PCR amplification, the patient cDNA contained an extra product at 463 bp, indicating differential splicing. **B.** Visualization of the cDNA region amplified by PCR. Locations of the forward and reverse PCR primers are indicated with arrows. The position in exon 6 of the coding region for the DFG motif is indicated by a black box. The variant is located on the last base of exon 6. The expected full length PCR product is 531 bp. **C.** Zoom in view of the splicing effect of c.464G>C. The wild type allele G at position 464 of the cDNA (top) results in normal splicing, retaining exon 6, as seen in control cDNA and one allele of the patient cDNA. Sanger sequencing of splice junctions are shown. The product due to alternative splicing caused by variant c.464G>C (bottom) lacks exon 6, including the coding region for the DFG motif, and as a result is only 463 bp. **D.** Alternative splicing results in a frameshift and introduction of a premature stop codon. The wild type allele G (top) results in correct splicing and translation. The splicing variant C (bottom) results in a frameshift due to the loss of exon 6 and introduces a premature stop codon eighteen amino acids after the frameshift, presumably resulting in nonsense-mediated decay. **E.** Primers flanking the variant c.1226G>A were used for PCR on cDNA from mRNA isolated from patient and control-derived fibroblasts. Analysis of the PCR product on 1% Agarose gel showed that the patient cDNA transcript was 75 bp shorter than the control cDNA transcript (882 bp). **F.** Representation of the amplified cDNA region. Location of the forward and reverse PCR primers are indicated by arrows. The expected full-length PCR product is 882 bp. **G.** Detailed view of Sanger sequences surrounding the splice junctions caused by the nonsense variant in exon 15. Nonsense-associated alternative splicing causes skipping of exon 15 (75 bp) in the patient. **H.** Skipping of mutated exon 15 in the patient results in a continuation in the same reading frame. The nucleotide sequence containing the wild type allele G results in correct splicing and translation (top). The nonsense variant c.1226G>A removes exon 15 (75 bp) from the transcript which continues in frame (bottom) resulting in a near-full length transcript.

4.3.5 Cilia number is reduced in patient-derived fibroblasts compared to controls

To determine the cellular effects of *NEK1* variants in the patients, we examined cilia number and length in primary skin fibroblasts from the elder brother and a healthy control using anti-acetylated α-tubulin and anti-ARL13B antibodies to mark the ciliary axoneme and anti-RPGRIP1L antibody to mark the basal body at the base of the cilium (**Figure 4**). Patient-derived fibroblasts showed a statistically significant reduction in cilia number compared to control fibroblasts (18.0% vs. 48.9%, $P<0.0001$). In addition, patient-derived fibroblasts showed a marked increase in cytoplasmic acetylated α-tubulin compared to control fibroblasts (12.3 vs. 3.8 gray units, $P=0.002$). There was no significant difference in mean cilia length (3.7 vs. 3.5 μm, $P=0.09$). Reconstitution of the cilia phenotype by transfecting fibroblasts with a full-length wild type *NEK1* construct was attempted; however, robust results were not obtainable (data not shown).

when the signal is lost_marijn_8072018.indd 85 08/07/2018 10:50

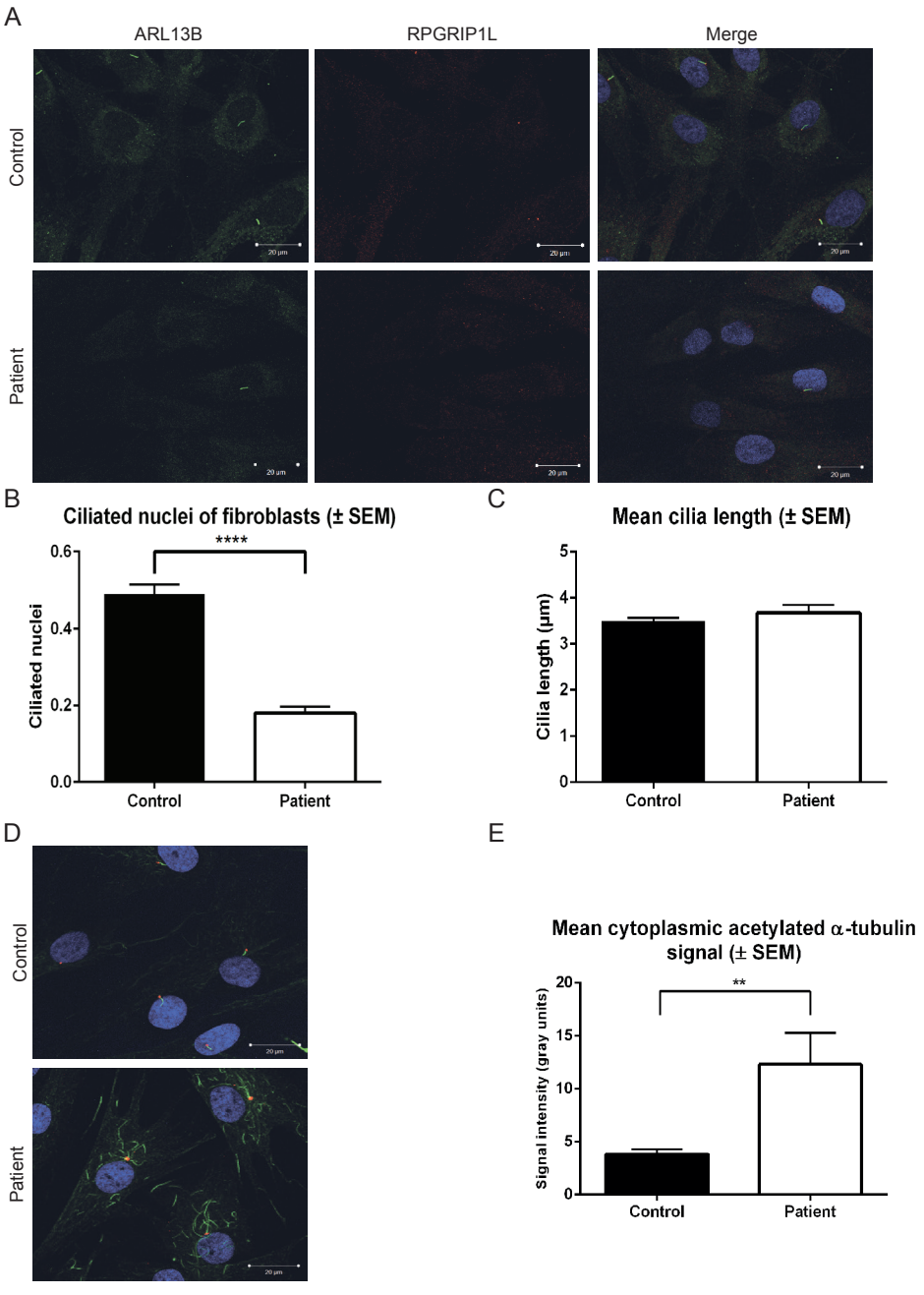

when the signal is lost_marijn_8072018.indd 86 08/07/2018 10:50

Figure 4. Patient-derived fibroblasts show a severe ciliation defect. **A.** Immunofluorescence of ciliary axoneme (ARL13B, green), basal body (RPGRIP1L, red) and nucleus (Hoechst, blue) shows a severe reduction in cilia number but not in cilia length in patient- compared to control-derived fibroblasts. Scale bars represent 20 µm. **B.** An average of 48.9% of control-derived fibroblasts are ciliated compared to 18.0% of patient-derived fibroblasts (>800 cells analyzed). This difference is statistically significant (**** indicates two-tailed P value <0.0001, calculated using Mann-Whitney test). **C.** Mean cilia length in control-derived fibroblasts was 3.5 ± 0.1 µm and in patient-derived fibroblasts 3.7 ± 0.2 µm (± 200 and 50 cilia analyzed for control and patient respectively). This difference is not statistically significant (two-tailed P value equals 0.09, calculated using Mann-Whitney test). **D.** Immunofluorescence of acetylated α-tubulin (green), pericentrin (red) and Hoechst (blue) shows a marked increase in cytoplasmic acetylated α-tubulin in patient- compared to control-derived fibroblasts. Scale bars represent 20 µm. **E.** Comparison of the intensity of cytoplasmic acetylated α-tubulin signal in control- and patient-derived fibroblasts (3.8 vs. 12.3 gray units, ** indicates P=0.002, calculated using Mann-Whitney test).

4.4 DISCUSSION

In this study we identified compound heterozygous variants in *NEK1* in two brothers with OFD syndrome type II, Mohr syndrome. Homozygous variants in *NEK1* are associated with short-rib polydactyly syndrome (SRPS) Majewski type (OMIM 263520) [Thiel et al., 2011; El Hokayem et al., 2012], which in the past has been considered allelic to OFD (Mohr syndrome) [Franceschini et al., 1995; Silengo et al., 1987]. Our results confirm that these syndromes may be part of the same phenotypic spectrum.

NEK1 is a known ciliary gene comprising a kinase domain in addition to a basic and coiled-coil domain for localization and protein interaction (**Figure 2**) [White and Quarmby, 2008; Shalom et al., 2008; Meirelles et al., 2014]. NEK1 kinase is a member of the NIMA-related kinase family and is localized at the cilium's basal body [Shalom et al., 2008]. This kinase family is considered to play a role in cell cycle regulation and DNA damage repair, with some kinases having an additional role in the formation of the primary cilium [White and Quarmby, 2008; Shalom et al., 2008; Fry et al., 2012].

Immunocytochemistry in patient-derived fibroblasts demonstrated severely reduced ciliation and an increase in cytoplasmic acetylated α-tubulin signal compared to control-derived fibroblasts. Our findings are consistent with the reduced number of normal cilia and the expression of long, thick microtubular extensions marked by acetylated α-tubulin in fibroblasts of a fetus with SRPS Majewski type resulting from *NEK1* variants [Thiel et al., 2011]. This increase in cytoplasmic acetylated α-tubulin may be due to the inability of variant NEK1 to phosphorylate VHL, which stabilizes microtubules [Patil et al., 2013]. A reduction in ciliated cells was also noted in embryonic fibroblasts of kat2J mice homozygous for a frameshift variant in the kinase domain [Shalom et al., 2008]. Contrary to previous reports, we did not detect a difference in mean cilia length [Thiel et al., 2011]. This could be related to using the anti-ARL13B antibody to visualize the ciliary axoneme instead of the anti-acetylated α-tubulin antibody, as increased

when the signal is lost_marijn_8072018.indd 87 08/07/2018 10:50

microtubule staining prevented reliable measurements of cilia.

Decreased ciliation could negatively affect adequate signal transduction during morphogenesis and craniofacial development since cilia are involved in multiple signaling pathways such as Hedgehog and Wingless (Wnt) signaling [Satir et al., 2010; Zaghloul and Brugmann, 2011; Veland et al., 2009]. For example, variants in the NEK1 interaction partner KIF3A, a component of the intraflagellar transport system, lead to cilia defects resulting in an inappropriate increase in canonical Wnt signaling [Corbit et al., 2008]. Although homozygous *Kif3a* null variants are lethal in mice [Marszalek et al., 1999], mice with conditional *Kif3a* deletions in cranial neural crest cells are characterized by impaired skeletogenesis and proliferation defects in the facial midline, similar to the anomalies detected in our patients [Liu et al., 2014]. Additionally, inactivation of *OFD1* is also associated with defective ciliation and subsequent disturbed Hedgehog and canonical Wingless signaling, showing overlap in the pathogenic disease mechanism [Romio, 2004; Ferrante et al., 2009, 2006; Bimonte et al., 2011]. This might therefore explain the considerable overlap in phenotype between patients with OFD type I and our patients [Thauvin-Robinet, 2006].

In addition to localizing to the basal body of the cilium, NEK1 resides in the cilium, the cytoplasm and the nucleus [Shalom et al., 2008; Hilton et al., 2009; Mahjoub, 2005]. There is a canonical nuclear localization signal in residues 355-378 within the coiled-coil domain of NEK1, and a cryptic nuclear localization signal within residues 258-321 of the basic domain (**Figure 2**) [Hilton et al., 2009]. The coiled-coils 1 and 2 are essential for localization to the primary cilium [White and Quarmby, 2008]. However, in a study investigating the role of Nek1 in murine IMCD3 cells, a tagged-Nek1 construct was only retained in the ciliary compartment long enough to be visualized if the kinase domain (which normally targets the protein to the cytoplasm) was non-functional, and endogenous mNek1 could not be visualized in the primary cilium [White and Quarmby, 2008]. Cycling of NEK1 through the ciliary, cytoplasmic and nuclear compartments can partly explain why reconstitution assays yielded no robust results [White and Quarmby, 2008]. Transient expression of NEK1 at the basal body prevented assessment of transfected cells only, and therefore the rescue of the cilia phenotype could not be quantified. Moreover, rescue of the cilia phenotype was limited because NEK1 overexpression also inhibits ciliogenesis [White and Quarmby, 2008; Shalom et al., 2008]. Similar to other ciliary proteins with a dual role in the nucleus, NEK1 is involved in DNA damage response and cell-cycle control [Chaki et al., 2012; Chen et al., 2011b]. Expression and kinase activity of NEK1 are upregulated in irradiated cells and *NEK1*-null cells are hypersensitive to DNA damage by ionizing radiation [Chen et al., 2011b; Polci et al., 2004]. A portion of NEK1 can redistribute to form discrete nuclear foci at sites of DNA damage [Chen et al., 2011b; Polci et al., 2004]. The mechanism for this DNA damage response has not yet been fully established, but OFD1 has been linked to DNA repair through its interaction with the chromatin-remodeling complex TIP60 [Giorgio et al., 2007]. NEK1-deficient primary renal tubular epithelial (RTE) cells of kat2J mice showed increased chromosome missegregation events and aneuploidy after mitosis [Chen et al.,

when the signal is lost_marijn_8072018.indd 88 08/07/2018 10:50

2011b]. The DNA damage response of these ciliary proteins likely also has a role during morphogenesis when progenitor cells are under increased replication stress. Impairment of this response would therefore possibly result in tissue dysplasia [Chaki et al., 2012]. Secondly, the impaired DNA damage response can underlie degenerative instead of developmental phenotypes in ciliopathies, e.g. nephronophthisis [Chaki et al., 2012; Slaats et al., 2015]. Renal cysts were present in five out of eight reported lethal *NEK1*-related SRPS type Majewski patients [Thiel et al., 2011; El Hokayem et al., 2012] and *NEK1* deficient kat and kat2J mice display slowly progressive polycystic kidney disease [Upadhya et al., 2000, 1999]. Although our patients had a normal renal ultrasound at age 20 and 16 years respectively, we cannot exclude that a renal phenotype may develop at an older age.

The phenotype in our patients is mild compared to the previously described lethal cases with *NEK1* variants. This could reflect the extreme clinical heterogeneity associated with variants in ciliary genes; for example, in the ciliary gene *MKS1* biallelic null variants cause the embryonically lethal Meckel-Gruber syndrome while missense variants cause Joubert syndrome [Romani et al., 2014]. In *NEK1*, missense, splice-site, nonsense and frameshift variants have been reported in the patients with SRPS (**Supplementary Table S4**) [Thiel et al., 2011; El Hokayem et al., 2012; Chen et al., 2012].

Most variants were identified in the kinase domain of *NEK1*. In addition, one patient showed a homozygous frameshift variant in the C-terminal domain of *NEK1* and in another patient digenic inheritance with *DYNC2H1* plays a role [Thiel et al., 2011; El Hokayem et al., 2012; Chen et al., 2012] (**Figure 2**). The splice variant c.464G>C identified in the present study is predicted to result in nonsense mediated decay of the mRNA transcript due to the premature stop codon and thus no protein translation. The nonsense variant p.(Trp409*) removes the first coiled-coil domain. A possible explanation for the milder phenotype in our patients compared to previously published patients is basal exon skipping of exon 15 that contains the premature stop codon. Basal exon skipping is a mechanism whereby detrimentally mutated exons that begin and end in the same reading frame can be selectively spliced out of the final gene transcript [Drivas et al., 2015]. This mechanism has been described in other ciliopathies [Drivas et al., 2015; Littink et al., 2010]. Nonsense-associated alternative splicing results in a detectable level of near-full length *NEK1* transcript that contains the complete kinase domain and is expected to escape nonsense-mediated decay. The resulting protein likely has some residual kinase function. As the N-terminal kinase domain is required for cilia formation [Thiel et al., 2011; White and Quarmby, 2008], the remaining 18% ciliation in patient-derived fibroblasts could suggest that some functioning kinase domain is (partly) preserved. Moreover, variants in modifier genes could play a role in the milder phenotype seen in our patients.

Similar to other ciliopathies, OFD type II is probably a genetically heterogeneous condition. Further studies in a cohort of patients with autosomal recessive types of OFD for variants in *NEK1* and genes coding for proteins interacting with NEK1, such as *KIF3A*, might reveal more insight into the underlying

when the signal is lost_marijn_8072018.indd 89 08/07/2018 10:50

pathogenic mechanisms (NEK1 interacting proteins reviewed in [Surpili et al., 2003]). The fact that we found compound heterozygous variants in a gene outside homozygous regions illustrates that consanguinity can be misleading and that WES or whole-genome sequencing can provide more information in cases in which homozygosity mapping does not lead to the causative variants.

In this study, we provide the first genetic and functional evidence that variants in *NEK1* can be involved in the etiology of OFD type II. Similar to the cellular phenotype seen in SRPS type Majewski, fibroblasts derived from our patient with OFD type II show a severe defect in cilia formation and an increase in cytoplasmic acetylated α-tubulin. Analysis of *NEK1* should be considered in patients with autosomal recessive OFD.

Acknowledgments

We would like to thank the patients and their parents for their participation in this study. We wish to thank the Utrecht Sequencing Facility, UMC Utrecht, for WES using the Illumina HiSeq 2500 and further data processing with the bioinformatics pipeline. We thank the Cell Microscopy Core at the Department of Cell Biology, Center for Molecular Medicine, UMC Utrecht for use of the Zeiss Confocal laser microscope LSM700 and Corlinda ten Brink for help with the Volocity 6.3 software. We thank Dr. R. Roepman and Dr. H. Arts for providing us with the anti-RPGRIP1L antibody and J. Hoogeboom (Department of Clinical Genetics, Erasmus Medical Center, Rotterdam, the Netherlands) for providing us with clinical data on patients in the OFD type II cohort.

when the signal is lost_marijn_8072018.indd 90 08/07/2018 10:50

SUPPLEMENTARY MATERIAL

Supplementary Methods S1. *Whole-exome sequencing*

Parent-patients quatro WES was performed with an emphasis on autosomal recessive variant detection analysis for the causal variants. DNA libraries of the two patients and their parents were prepared using Kapa Biosystems reagents and enriched using Agilent Sureselect All exon V5 and a custom pooling protocol. Briefly, 1 ug of purified gDNA (Qiagen, Hilden, Germany) was sheared into 100-500 bp fragments with a Covaris S2 sonicator (Covaris, Woburn, MA, USA), blunt-ended, 5'phosphorylated, and A-tailed using Kapa Biosystems reagents (Kapa Biosystems, Wilmington, MA, USA). Adaptors containing the Illumina barcode sequences were ligated to each sample and amplified with 7 PCR cycles. Samples were finally quantified and were equimolarly combined into one pooled batch containing three samples. The fourth member of the quarto was enriched with two unrelated samples for a different project. Barcode blockers for the Illumina adaptor sequences and barcodes were added (sequences available upon request), and the pools were enriched according to the Agilent Sureselect V5 exome protocol (Agilent, Santa Clara, CA, USA), and finally PCR amplified 8 times. Two pools of three samples were then combined into a batch of six samples together and sequenced on a full flow cell as a Rapid Run on the Illumina HiSeq 2500 at the Utrecht Sequencing Facility (Utrecht, Netherlands).

Sequencing reads were aligned using BWA and data was processed with GATK v3.1.1, according to best practice guidelines [Van der Auwera et al., 2014; McKenna et al., 2010] but skipping BQSR and applying the hard filters instead of VQSR. Samples had mean bait coverage of 104X and 93% of the target bases were over 20X.

A phased vcf was created and imported into Cartagenia BENCHlab NGS module (Cartagenia, Leuven, Belgium) for variant interpretation. Homozygous variants, compound heterozygous variants, and X chromosome variants were investigated. Variants were filtered out by presence above the minor allele frequency greater than 1.5% in the public population frequency databases of the NCBI dbSNP Build 137 for Human (https://www.ncbi.nlm.nih.gov/SNP), the Exome Variant Server (EVS) (http://evs.gs.washington.edu/EVS), the 1000 Genomes Project (http://www.1000genomes.org), the Genome of the Netherlands (GoNL) (http://www.nlgenome.nl), or our in-house dataset, as well as in the clinical variant database Human Gene Mutation Database (HGMD) (http://www.hgmd.cf.ac.uk/ac/index.php). Variants were further prioritized by amino acid change or splicing effect, conservation score (GERP) [Cooper et al., 2005], and predicted effect on protein function using prediction algorithms (Polyphen2, SIFT) [Adzhubei et al., 2010; Kumar et al., 2009].

when the signal is lost_marijn_8072018.indd 91 08/07/2018 10:50

Supplementary Table S1. *Homozygous and compound heterozygous candidate variants identified from whole-exome sequencing*

Gene	Zygosity	Chr:Pos	dbSNP	Ref	Alt	HGVS nucleotide	HGVS amino acid	Coding effect	MAF* (ExAc)	Sift	Polyphen	Gene function	Interpretation
NPRL3	Homozygous	16:138725	rs202015937	T	A	NM_001077350.2:c.1516A>T	p.(Asn506Tyr)	missense	0.0007	deleterious	probably damaging	Nitrogen permease regulator-like 3. Component of the GATOR1 complex, an inhibitor of mTORC1 signaling. GTPase activator. Required for normal cardiovascular development. Highly conserved.	Known gene function cannot be linked to phenotype
PRR35	Heterozygous	16:613344	rs116903998	G	A	NM_145270.2:c.50G>A	p.(Arg17Gln)	missense	0.0038	deleterious	probably damaging	Proline Rich 35; very little known.	rs74459225 not predicted to be deleterious; gene variants are probably not causal.
PRR35	Heterozygous	16:615095	rs74459225	G	A	NM_145270.2:c.1504G>A	p.(Gly502Ser)	missense	0.0403	tolerated	benign		
TPTE	Heterozygous	21:10941966	rs149843545	A	G	NM_199259.3:c.683T>C	p.(Ile228Thr)	missense	0.0050	deleterious	probably damaging	Transmembrane Phosphatase With Tensin Homology; signal transduction pathways of endocrine of spermatogenic function of testis.	Expression solely in the testes; not likely candidate
TPTE	Heterozygous	21:10944668	rs138088406	C	T	NM_199259.3:c.512G>A	p.(Arg171Lys)	missense	0.0023	deleterious	probably damaging		

*MAF has been updated with newly available frequency information from ExAC via dbSNP (accessed May 10, 2016).

when the signal is lost_marijn_8072018.indd 92

08/07/2018 10:50

when the signal is lost_marijn_8072018.indd 93

Supplementary Table S2. *Clinical phenotype and genetic tests OFD type II cohort*

	Patient 1	Patient 2	Patient 3	Patient 4
Age	17	17	28	28
Oral anomalies	Frenulae from lip to gingiva Minimal median notch upper lip Notches gingiva Supernumerary incisor	Notches gingiva Lobulated tongue	Hyperplastic frenula Cleft tongue	Cleft lip, palate and uvula Palatal fibromas Ectopic tongue tissue Ankyloglossia
Facial anomalies		Broad nasal bridge Milae	Micrognathia	
Limb anomalies	Abnormal proximal phalanx and broad distal phalanx digitus 1 right hand Short middle phalanx digitus 5 right hand	Brachydactyly Syndactyly digiti 4 and 5 right hand Partial syndactyly digiti 2 and 3 left hand Broad digitus 1 left hand Bilateral syndactyly 2nd and 3rd toe	Unilateral preaxial polydactyly Bifid toes	Tarsal coalition left foot Pes planovalgus
Other features		Developmental delay (IQ 49) Left frontal interhemispheral cyst Corpus callosum agenesis	Developmental delay (IQ 74) Epilepsy Coarctatio aortae Bicuspid aortic valve Genital anomaly	Developmental delay Speech delay Hearing loss
Genetic findings	Normal female karyotype	Analysis of *OFD1*, *TCTN3* and other ciliopathy-associated genes[1] was normal	No information available	No information available

[1] Investigated ciliopathy-associated genes are: *AHI1*, *C5orf42*, *CC2D2A*, *CEP290*, *CEP41*, *INPP5E*, *KIF7*, *MKS1*, *NPHP1*, *RPGRIP1L*, *TCTN1*, *TMEM138*, *TMEM216*, *TMEM231*, *TMEM237*, *TMEM67*, *TTC21B* and *ZNF423*.

08/07/2018 10:50

Supplementary Table S3. *Primers used for NEK1 variant screening*

	Forward	Reverse
Amplicon 1	5' GTTTCCTATGCTTTGGTTGG 3'	5' TTTACAGTGATCACCCATGC 3'
Amplicon 2	5' AAATTAAAAATATGGACTTAAAGGAC 3'	5' GTGAATGTGAATGCGATAGTG 3'
Amplicon 3	5' TCTTCATCTTCATGAATAGCC 3'	5' AGCAAAACATGGAGGTGTG 3'
Amplicon 4	5' AAAGGGGAGAGACCCAGAG 3'	5' TGTATTCATCCTCAATTTACCG 3'
Amplicon 5	5' TCCAGCTAGGTGACAGAGTG 3'	5' AGACTGAGCTGAAATTCAAGAG 3'
Amplicon 6	5' TTGTTGGATGTGTGTTTGTG 3'	5' TTATTCAGAAGGTAATATACTGACAC 3'
Amplicon 7	5' AAACTTTCACTGCCATGTTG 3'	5' ATTCACAGGTCAAGGGTGAG 3'
Amplicon 8	5' GGTGTGAGCCACTGTGC 3'	5' TTGAAGAGAAAATTTTACATAATGG 3'
Amplicon 9	5' TTTTGGGGTGACTTGTTAGG 3'	5' AAACCATTTTGACCACCATAG 3'
Amplicon 10	5' CCATCCAGGTCTATCAGGTC 3'	5' GCATTTCAGATAAGAGATACTCAGTC 3'
Amplicon 11	5' AGGGAGGCACTTCTATTCG 3'	5' TCTCTTCCTCTGTATCTATCTGC 3'
Amplicon 12	5' TTTCATGCTCTTTGGCATC 3'	5' GAGTATATGAATTTTCCTCTAATTTC 3'
Amplicon 13	5' CTTATAAACAATGAGGCTCCAG 3'	5' GATTAACAAAATCTTACACTTGAATC 3'
Amplicon 14	5' CCCAAATAACTTCCACATTG 3'	5' GAAGGCAAATGAAGTCTGTG 3'
Amplicon 15	5' TGCCATGGTTTTATCTATTTTC 3'	5' ACTGATGACGACAGTGGAAG 3'
Amplicon 16	5' GAATTTCTCTGGAACAAATGG 3'	5' GAAGATTTTGTAGGTCTGTAGGG 3'
Amplicon 17	5' TCAAAAGAAAAGAAACTGAAATC 3'	5' GGGTTTAACCTCCAAAGCAG 3'
Amplicon 18	5' TCCCAATTAACCAAAGCAAC 3'	5' CAGATTCTTCCGTAATTAAGTGTATC 3'
Amplicon 19	5' AATCAGGCTGAACTGGAAAG 3'	5' GTGAGAGCTCTTTGTTTAATCC 3'
Amplicon 20	5' CTTGTTTAGACACCGCCTTC 3'	5' TGTTTGTCACATTATGCTTTATTATC 3'
Amplicon 21	5' GAGTATAGTCACATAACAGCAACAC 3'	5' AAGCAGCAAGAAAGAGAAGG 3'
Amplicon 22	5' TGCCTACCTTTACTTCACCAC 3'	5' CATCTGTCTGGTTATTTTAAAGC 3'
Amplicon 23	5' GGGAAAAGAAATAAACAAAACAC 3'	5' TTGGGATTTTCAAATAAGTGC 3'
Amplicon 24	5' TTCTCTTTCTTGCTGCTTCC 3'	5' GACCCTAAATTTTTAATCTTGTTTG 3'
Amplicon 25	5' TGACTCCTGTAAGGCTTCTC 3'	5' GATACGTGCAACCATCACTC 3'
Amplicon 26	5' CAGCTAGGCATTTGATAAAGAC 3'	5' GAGGGAGTAAGCATGAGAGG 3'
Amplicon 27	5' AGACCATGGAAAGGAAAGTG 3'	5' CGTTTATTTAATACATCCCATC 3'
Amplicon 28	5' TCTGTCATTAGAAATAATTTTCTGG 3'	5' AGCTGTTGCAAATTTCTTAATAC 3'
Amplicon 29	5' TCTTTCTGCTGTTCTTCCAG 3'	5' TGGAAGTTGCTTTCTGTGAG 3'
Amplicon 30	5' ATACAGCCTGCCTGTGTAGC 3'	5' CTTGATGGTGTCCTTTGATG 3'
Amplicon 31	5' TCAGAGACTGGGAAGGAAAG 3'	5' CCCTATCCCTAAAGAAGTGG 3'
Amplicon 32	5' ATAAATGAGATGGGCAACTG 3'	5' TGAATGAAATCAAGTATGTCTGC 3'
Amplicon 33	5' GAGGCAGAGGTTGGAGTAAG 3'	5' CTCCTTTATTCCCGCTAATATC 3'
Amplicon 34	5' GATTAGGTTACAGAACAGCAAG 3'	5' TATGCAGTATTTGGCTTTCC 3'

when the signal is lost_marijn_8072018.indd 94 08/07/2018 10:50

Supplementary Methods S2. *Immunocytochemistry and statistical analysis*

Immunocytochemistry

The following primary antibodies were used to prepare coverslips for measurement of cilia number: anti-acetylated α-tubulin (mouse monoclonal, 1:10,000; Sigma T6793) and anti-ARL13B (rabbit polyclonal, 1:1,000; ProteinTech 17711-1-AP) (**Supplementary Figure S1**). Anti-ARL13B (rabbit polyclonal, 1:1,000; ProteinTech 17711-1-AP) and anti-RPGRIP1L (guinea pig, 1:1,000; Eurogentec SNC039) were used to prepare coverslips to measure cilia length as hyper-stabilized acetylated α-tubulin prevented accurate measurement using anti-acetylated α-tubulin. Cells were washed with PBS prior to 1-hour incubation with the secondary antibody and Hoechst (1:5000; Invitrogen, H3570) at room temperature. The following secondary antibodies (Life Technologies, Forster City, CA, USA) were used: anti-mouse IgG Alexa Fluor 488 (1:500), anti-rabbit IgG Alexa Fluor 568 (1:500) and anti-guinea pig IgG Alexa Fluor 488 (1:500).

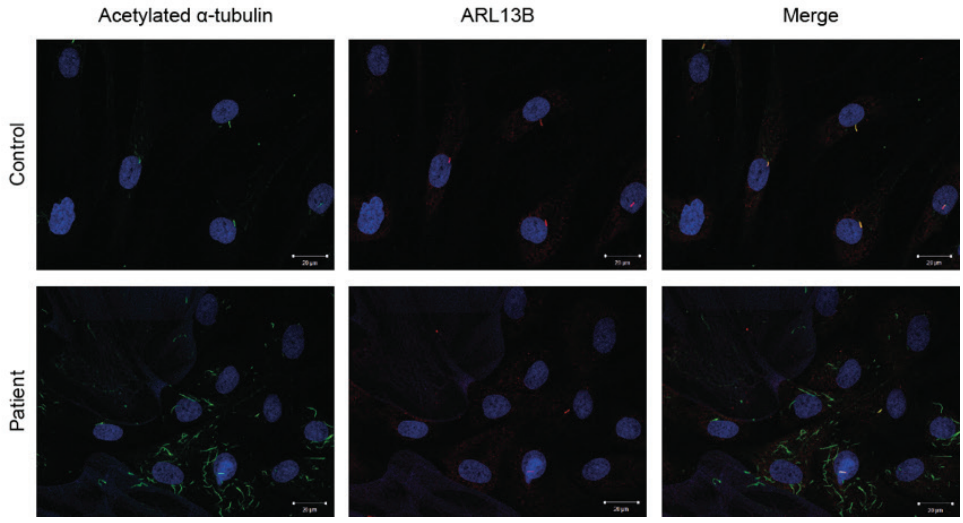

Supplementary Figure S1. Costaining of acetylated α-tubulin and ARL13B. Immunofluorescence of acetylated α-tubulin (green), ARL13B (red) and Hoechst (blue). ARL13B signal corresponds to ciliary but not cytoskeletal acetylated α-tubulin. Scale bars represent 20 μm.

Statistical analysis

GraphPad prism 6.0 was used for cilia statistical analysis (©2015 GraphPad Software, La Jolla, California, USA). Equal nuclei density between patients and control cells was confirmed using the Mann-Whitney test. Outliers in nuclei density were removed using the modified Thompson tau test. To compare cilia number, approximately 800 nuclei were scored for patient- and control-derived fibroblasts

when the signal is lost_marijn_8072018.indd 95 08/07/2018 10:50

in two technical replicates. GraphPad Prism 6.0 was used to perform Fisher's exact test and the Mann-Whitney test for non-parametric data.

Cilia length was measured using Image J. Approximately 50 cilia were measured in the patient-derived fibroblasts and 200 in the control. Outliers were removed using the ROUT method (Q=1%) in GraphPad Prism 6.0, and cilia length was analyzed using the Mann-Whitney test for non-parametric data.

Signal intensity cytoplasmic acetylated α-tubulin

To quantify the observed difference in cytoplasmic acetylated α-tubulin signal, ten 8-bit images of 10 x 10 µm (1024 x 1024 pixels) of the cytoplasm were taken using the same settings for control- and patient-derived fibroblasts. We measured signal intensity of acetylated α-tubulin for each image using Volocity 6.3 software. To control for acetylated α-tubulin background signal, we took ten 8-bit images of 10 x 10 µm of the intercellular space for each condition and subtracted the mean intensity of the background acetylated α-tubulin signal from the cytoplasmic acetylated α-tubulin signal. Relative intensities were analyzed in GraphPad prism 6.0. Outliers were removed using the ROUT method (Q=1%). Cytoplasmic acetylated α-tubulin signal intensity was analyzed using the Mann-Whitney test for non-parametric data.

Signal intensity ciliary ARL13B

We measured ARL13B signal intensity to exclude an effect of the NEK1 mutation on ARL13B signal intensity inside the cilium, which could influence cilia count and measurements. We took 16-bit z-stacks of 21 x 21 µm (1024 x 1024 pixels) of nuclei and cilia, using the optimal interval and the same settings for control- and patient-derived fibroblasts (8 and 12 z-stacks respectively). We measured signal intensity of ARL13B inside the cilium for each composite image using Volocity 6.3 software. A region of interest (ROI) was defined around the cilium using the same intensity threshold for all images. Background signal was excluded. Intensity measurements were analyzed in GraphPad prism 6.0. Outliers were removed using the ROUT method (Q=1%).

There was no significant difference in ciliary ARL13B signal intensity between control- and patient-derived fibroblasts (15,456 vs. 14,371 gray units; two-tailed P-value =0.25, calculated using unpaired t-test) (**Supplementary Figure S2**).

when the signal is lost_marijn_8072018.indd 96 08/07/2018 10:50

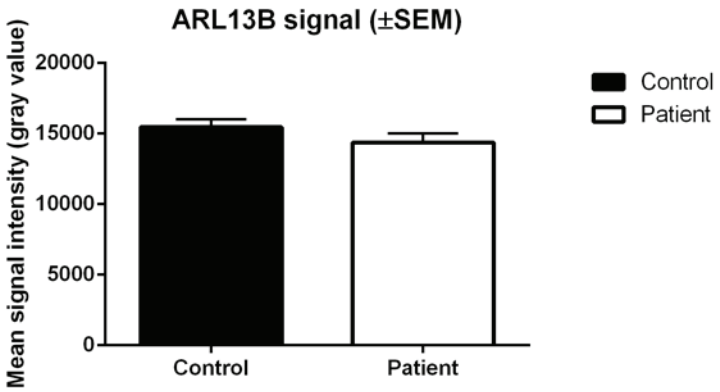

Supplementary Figure S2. Mean signal intensity ciliary ARL13B in control- and patient-derived fibroblasts.

when the signal is lost_marijn_8072018.indd 97 08/07/2018 10:50

Supplementary Methods S3. *Splicing assessment of c.464G>C variant*

To evaluate the splicing effect of the variant c.464G>C on the last base of exon 6, we designed primers upstream (exon 5) and downstream (exon 10) of the variant. Primers used were 5′ CAGATATGTTTGGCCCTGAAA 3′ and 5′ AGGCTGTGATCCAAACTTCG 3′. RNA was isolated from patient and control fibroblasts and cDNA created as described. The following touchdown PCR program was used: 7′ at 94°C, (30″ at 94°C, 30″ at 65-58°C in 0.5°C decreasing increments, 1′ at 72°C) X 15, (30″ at 94°C, 30″ at 58°C, 1′ at 72°C) X 27, 4′ at 72°C, 8°C. Patient and control PCR products were run on a 1% agarose gel for 1 hour at 120 volts with a Lonza FlashGel DNA 50-1.5 kb marker. Sequencing of the PCR product was performed using standard Sanger sequencing.

when the signal is lost_marijn_8072018.indd 98 08/07/2018 10:50

Supplementary Methods S4. *Splicing assessment of c.1226G>A variant*

To evaluate the splicing effect of the variant c.1226G>A in exon 15, we designed primers upstream (exon 6) and downstream (exon 16) of the variant. Primers used were 5′ TGGAACAGTACAACTTGGAGAT 3′ and 5′ GCTATAGTCCCTCCACTGCC 3′. RNA was isolated from patient and control fibroblasts and cDNA created as described. The following touchdown PCR program was used: 7′ at 94°C, (30″ at 94°C, 30″ at 65-58°C in 0.5°C decreasing increments, 1′ at 72°C) X 15, (30″ at 94°C, 30″ at 58°C, 1′ at 72°C) X 27, 4′ at 72°C, 8°C. Patient and control PCR products were run on a 1% agarose gel for 1 hour at 120 volts with a GeneRuler DNA 1 kb marker. Sequencing of the PCR product was performed using standard Sanger sequencing. The forward primer 5′ TTCTCTCTCCTCAGC 3′ was used to sequence the variant in exon 15 while the reverse primer 5′ CATGCTTTTGAAGCTG 3′ was used to confirm the absence of the c.464G>C mutation in exon 6.

when the signal is lost_marijn_8072018.indd 99 08/07/2018 10:50

Supplementary Table S4. *Previously reported variants in NEK1*

Author	Diagnosis	Zygosity	Nucleotide change	Exon/ intron	Type of variant	Amino Acid Change	Domain
[El Hokayem et al., 2012] (case 1)	SRPS type II	hom	c.433G>A	Ex 6	missense	p.(Gly145Arg)	kinase
[El Hokayem et al., 2012] (case 2)	SRPS type II	hom	c.758T>C	Ex 9	missense	p.(Leu253Ser)	kinase
[El Hokayem et al., 2012] (case 3)	SRPS type II	hom	c.2847delinsGG[§]	Ex 28	frameshift	p.(Asp949Glufs*11) [§]	C terminal
[El Hokayem et al., 2012] (case 4)	SRPS type II	hom	c.379C>T	Ex 5	nonsense	p.(Arg127*)	kinase
[El Hokayem et al., 2012] (case 9); [Thiel et al., 2011]	SRPS type II	hom	c.379C>T	Ex 5	nonsense	p.(Arg127*)	kinase
[El Hokayem et al., 2012] (case 10) ; [Thiel et al., 2011]	SRPS type II	hom	c.869-2A>G	In 10	splice	-	basic
[El Hokayem et al., 2012] (case 11) ; [Thiel et al., 2011]	SRPS type II	digenic	NEK1: c.1640dup DYNC2H1: c.11747G>A	Ex 18 Ex 82	frameshift missense	p.(Asn547Lysfs*2) p.(Gly3916Asp)	coiled- coil C terminal
[Chen et al., 2012]	SRPS type II	het	c.465-1G>A	In 7	splice	-	kinase
Present study	OFD type II	comp het	c.1226G>A c.464G>C	Ex 15 Ex 6	nonsense splice site	p.(Trp409*) -	coiled-coil kinase

Hom: homozygous; het: heterozygous; comp het: compound heterozygous; Ex: exon; In: Intron. *NEK1* NCBI reference sequence: NM_012224.2. *DYNC2H1* NCBI reference sequence: NM_001080463.1.

[§] El Hokayem *et al.* original nomenclature is c.2846_2847insGG2847delT,p.(Asp949Glufs*6) [El Hokayem et al., 2012]; notation in this manuscript corresponds to current HGVS standards.

when the signal is lost_marijn_8072018.indd 100 08/07/2018 10:50

when the signal is lost_marijn_8072018.indd 101 08/07/2018 10:50

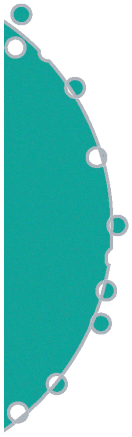

CHAPTER 5

Mutations in *KIF14* cause Meckel-Gruber syndrome and cytokinesis defects

Stokman MF, Van Harssel JJ, Peters EDJ, Verduijn JM, Nguyen TQ, Castigliego D, Den Ouden K, Van Gassen KL, Van der Veken LT, Renkema KY, Lilien MR, Bongers EMHF, Knoers NVAM, Filges I, Benmerah A, Giles RH

Manuscript in preparation

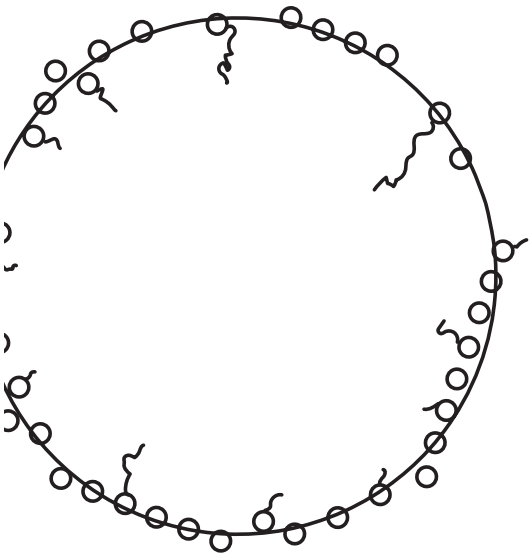

ABSTRACT

Meckel-Gruber syndrome is a lethal developmental disorder caused by defects in the primary cilia during embryogenesis. Pathogenic mutations have been identified in twelve genes. We performed trio whole-exome sequencing on one of four fetuses with Meckel-Gruber syndrome from a single family and the healthy parents. Sanger sequencing was used to confirm the detected mutation in two other fetuses from whom DNA was available. A homozygous c.[1792C>T] p.[(Arg598*)] truncating mutation in Kinesin family member 14 (*KIF14*) was identified that segregated with the Meckel-Gruber syndrome phenotype. The mutation was located in the kinesin motor domain, in which mutations have been previously described in patients with a prenatally lethal ciliopathy. Immunohistochemistry demonstrated KIF14 to be localized in the cilia of control fetal kidney tissue; however, in patient-derived kidney tissue both cilia and KIF14 were largely absent. Further functional experiments showed that disruption of *KIF14* resulted in an increased number of mitotic cells which could suggest cytokinesis defects in patient-derived fibroblasts. In conclusion, we provide additional evidence for the role of *KIF14* in Meckel-Gruber syndrome and demonstrate that mutations in *KIF14* could disrupt cytokinesis, which may play a central role in the pathogenesis of this severe ciliopathy.

when the signal is lost_marijn_8072018.indd 104 08/07/2018 10:50

5.1 INTRODUCTION

Meckel-Gruber syndrome is a rare ciliopathy that is prenatally or perinatally lethal. The phenotype is characterized by cystic kidney disease, central nervous system abnormalities and liver abnormalities including hepatic fibrosis and bile duct proliferation [Logan et al., 2011]. Mutations in thirteen genes have been identified to cause Meckel-Gruber syndrome to date. Mutations in ten of these genes, namely *MKS1, TMEM216, TMEM67, CEP290, RPGRIP1L, CC2D2A, TCTN2, B9D1, TMEM231* and *TMEM107* have also been identified in patients with a less severe ciliopathy called Joubert syndrome [Romani et al., 2014; Valente et al., 2010; Baala et al., 2007b; Sayer et al., 2006; Delous et al., 2007; Gorden et al., 2008; Huppke et al., 2015; Srour et al., 2012; Lambacher et al., 2016], demonstrating that Meckel-Gruber syndrome and Joubert syndrome represent two ends of a phenotypic spectrum.

Ciliopathies are a group of diseases characterized by defects in the primary cilia. Primary cilia are sensory organelles that coordinate various signal transduction pathways with a major role in embryonic development, including Wnt signaling and Hedgehog signaling, which are involved in neurodevelopment [Logan et al., 2011]. In addition, ciliary proteins have been implicated in DNA damage response signaling and cell cycle checkpoint control [Chaki et al., 2012]. Impaired DNA damage response signaling during tissue development, when cells are highly proliferative, could cause lack of progenitor cells leading to tissue dysplasia. As a result of both mechanisms, ciliopathies can be prenatally or perinatally lethal or present with severe congenital malformations. Examples include Meckel-Gruber syndrome, severe forms of Bardet-Biedl syndrome [Karmous-Benailly et al., 2005] and Jeune asphyxiating thoracic dystrophy.

Mutations in the gene *KIF14* have been identified in two fetuses with a lethal ciliopathy comprising intrauterine growth restriction, complex brain malformations and renal cystic dysplasia/agenesis [Filges et al., 2014]. Immunohistochemistry of patient-derived brain and kidney tissue demonstrated an increased number of bi-nucleated cells compared to tissue from age-matched controls [Filges et al., 2014]. This finding is consistent with the report that siRNA-mediated silencing of *KIF14* induced cytokinesis failure in HeLa cells and resulted in multinucleated cells [Carleton et al., 2006]. In addition, siRNA-mediated knockdown of *KIF14* in RPE-hTERT cells resulted in reduced cilia frequency [Basten, 2013], suggesting that *KIF14* is required for ciliogenesis. However, additional evidence for a causal role of *KIF14* in this prenatally lethal ciliopathy was lacking.

Here, we describe a second family with four affected fetuses with Meckel-Gruber syndrome caused by a novel homozygous truncating mutation in *KIF14*. We examine ciliogenesis, cell cycle progression, and cytokinesis in patient-derived kidney tissue and fibroblasts. In summary, we provide additional evidence for a causal role of mutations in *KIF14* in the pathogenesis of Meckel-Gruber syndrome.

when the signal is lost_marijn_8072018.indd 105 08/07/2018 10:50

5.2 PATIENTS AND METHODS

5.2.1 Ethics statement

Patients were included via the AGORA (Aetiologic Research into Genetic and Occupational/environmental Risk factors for Anomalies in children) biobank project. The study protocol was approved by the regional Committee on Research involving Human Subjects (CMO Arnhem/Nijmegen 2006/048). DNA from fibroblasts and (umbilical cord) blood was obtained from fetus 1, 2 and 4 and from blood from both parents. Written informed consent was obtained from both parents for whole genome SNP-array analysis and whole-exome sequencing of DNA from fetus 4 and analysis of skin fibroblasts obtained from fetus 1.

5.2.2 SNP-array analysis

Because parents were consanguineous and autosomal recessive inheritance was suspected based on the phenotype, single nucleotide polymorphism (SNP)-array analysis was performed to investigate genes located inside regions of homozygosity. Genomic DNA was extracted from fibroblasts obtained from a skin biopsy from fetus 4 according to standard protocols. Analysis of regions of homozygosity and copy number profiling were performed using the CytoSNP-850K BeadChip SNP-array (Illumina, San Diego, CA, USA) according to standard procedures. SNP-array results were visualized and data analysis was performed using Nexus software version 7 (BioDiscovery, Los Angeles, CA, USA) and the reference Human genome build Feb. 2009 GRCh37/hg19. Results were classified with Cartagenia BENCH software (Cartagenia, Leuven, Belgium).

5.2.3 Whole-exome sequencing

Whole-exome sequencing (WES) was performed on DNA from fetus 4. Protein coding genes and flanking (splice-site consensus) sequences were captured and enriched using the SureSelectXT Human All Exon V5 capture library (Agilent, Santa Clara, CA, USA) and sequenced in rapid run mode on the HiSeq 2500 Sequencing system (Illumina, San Diego, CA, USA) at a mean target depth of 100X. The target is defined as all coding exons of UCSC [Kent et al., 2002] and Ensembl [Aken et al., 2017] +/- 20bp intron flanks. At this depth ~95% of the target is covered at least 15X. Reads were aligned to the reference Human genome build Feb. 2009 GRCh37/hg19 using BWA (BWA-MEM v0.7.5a) and variants were called using the GATK haplotype caller (v2.7-2). Results were imported into Cartagenia BENCH Lab NGS Module (Cartagenia, Leuven, Belgium) for variant annotation, filtering and prioritization. Filtering was performed for variants in genes associated with neurodevelopmental abnormalities (for a full list of genes, see **Supplementary Methods S1**). Identified variants were validated and segregation analysis was performed using standard Sanger sequencing.

5.2.4 Immunohistochemistry

To assess the effect of mutations in *KIF14* on cilia formation and ciliary localization of KIF14 in the kidney, paraffin embedded fetal kidney tissue was obtained from a

when the signal is lost_marijn_8072018.indd 106 08/07/2018 10:50

control and from patient 2 reported by Filges et al. [Filges et al., 2014]. Fetal control fibroblasts (gestational age 18-20 weeks) were cultured in Dulbecco's Modified Eagle's Medium (DMEM) containing 10% FCS, suspended in formaldehyde and fixed in paraffin as a positive control. Kidney sections were cut at a thickness of 4 µm, put on positively charged glass slides and stained using the VENTANA BenchMark ULTRA automated slide stainer (Ventana Medical Systems, Inc.). Briefly, deparaffinization, rehydration, and antigen retrieval were performed by CC1 (prediluted; pH 8.0) antigen retrieval solution. Slides were incubated with anti-KIF14 antibody (rabbit polyclonal, 1:50; Abcam ab3746), followed by visualization with the OptiView DAB Detection Kit. Next, slides were incubated with anti-acetylated α-tubulin antibody (mouse monoclonal, 1:15,000; Sigma T6793), followed by visualization with the UltraView Universal AP Red Detection Kit. Slides were then counterstained with haematoxylin II and bluing reagent and coverslipped.

5.2.5 Immunocytochemistry

To assess primary cilia morphology and length, fetal control- and patient-derived fibroblasts were cultured on glass slides under standard cell culture conditions in DMEM containing 10% FCS. The formation of primary cilia was stimulated using serum-depleted medium (DMEM containing 0% FCS) for 48 hours prior to immunostaining. Cells were put on ice for 5 minutes before fixation with 4% paraformaldehyde (PFA) in Phosphate Buffered Saline (PBS), and permeabilization with 0.1% Triton-X-100 in PBS. Cells were blocked with 3% bovine serum albumin (BSA) in PBS minimizing non-specific binding, followed by a 2.5-hour incubation with primary antibodies and 1-hour incubation with secondary antibodies and Hoechst (1:5000; Invitrogen, H3570) at room temperature. The following primary antibodies were used: anti-acetylated α-tubulin (mouse monoclonal, 1:10,000; Sigma T6793) and anti-ARL13B (rabbit polyclonal, 1:1,000; ProteinTech 17711-1-AP). We used secondary antibodies anti-mouse IgG Alexa Fluor 488 (1:500) and anti-rabbit IgG Alexa Fluor 568 (1:500) (Life Technologies, Forster City, CA, USA).

To assess the effect of *KIF14* mutations on cytokinesis, fetal control- and patient-derived fibroblasts were cultured on glass slides as described above. Cells were cultured in serum-depleted medium for 24 hours. Subsequently, synchronized cell division was stimulated using DMEM containing 10% FCS for 12 hours. Fixation, permeabilization, blocking and immunostaining were performed as described above. We used the following primary antibodies: anti-acetylated α-tubulin (mouse monoclonal, 1:10,000; Sigma T6793) and anti-KIF14 (rabbit polyclonal, 1:1,000; Abcam ab3746). Secondary antibodies anti-mouse IgG Alexa Fluor 488 (1:500) and anti-rabbit IgG Alexa Fluor 568 (1:500) (Life Technologies, Forster City, CA, USA) and Hoechst (1:5000; Invitrogen H3570) were used.

Coverslips were washed with PBS and mounted in Fluormount G (Cell Lab, Beckman Coulter, Brea, CA, US). Confocal imaging was performed using Zeiss Confocal laser microscope LSM700 and images were processed with ZEN 2011 software.

when the signal is lost_marijn_8072018.indd 107 08/07/2018 10:50

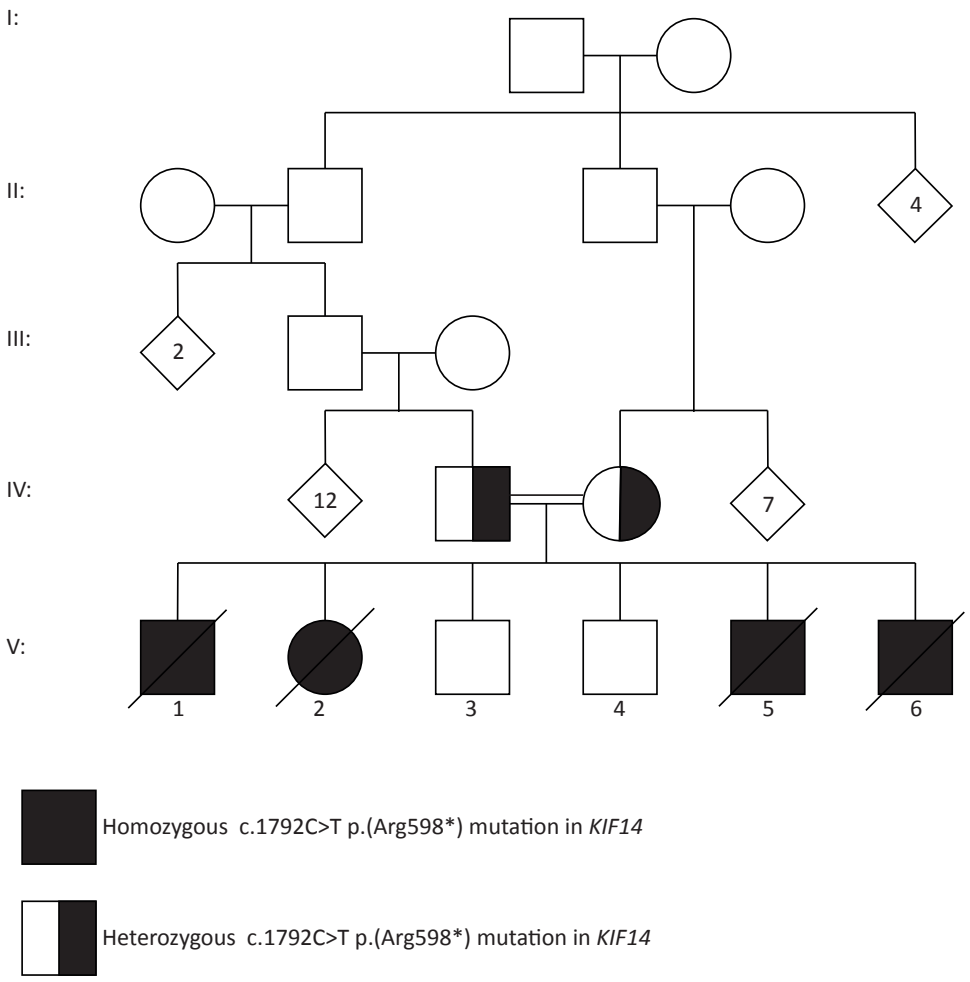

Figure 1. Pedigree of family

when the signal is lost_marijn_8072018.indd 108 08/07/2018 10:50

5.3 RESULTS

5.3.1 Patient description

The family came to our attention via the Gynaecology Department of the University Medical Center Utrecht. Severe malformations on second trimester ultrasound resulted in four terminations of pregnancy (phenotypes are summarized in **Table 1**). Parents were healthy and consanguineous (5th degree relatives). They had two healthy sons (**Figure 1**). The first pregnancy was terminated at gestational age (GA) 27 + 4/7 weeks because of bilateral renal agenesis, anyhdramnios and growth restriction on second trimester ultrasound examination. Autopsy of the male fetus revealed a weight of 550 grams, occipital sacral length (OSL) 19 cm and occipital frontal circumference (OFC) 19 cm (all <5th centile). There was bilateral agenesis of the kidneys and ureters. The fetus had lung hypoplasia, contractures of knees and hips, clubfeet and facial dysmorphisms secondary to anhydramnios. Autopsy of the brain showed microlissencephaly, a small brain stem and loss of neurons with diffuse gliosis in cortex and cerebellum, and absent corticospinal tracts. X-ray showed an abnormal position of the cranial bones with onset of craniosynostosis.

The second pregnancy was terminated at GA 17 + 4/7 weeks. The female fetus had a weight of 100 grams, OSL 11 cm and OFC 11.5 cm (all <5th centile). Autopsy showed two small cystic renal structures with absent ureters and bladder, and anal agenesis. The brain showed micrencephaly and microscopic structural anomalies.

The third pregnancy of a male fetus was terminated at GA 21 + 2/7 weeks. Weight was 200 grams, OSL 14 cm and OFC 15 cm (all <5th centile). Dysmorphisms included microcephaly, single palmar crease of the right hand and features caused by anhydramnios. The fetus had a bicuspid aortic valve, tubular hypoplasia of the aortic arch (type B), right and left ventricle hypertrophy, single-lobed lungs and splenomegaly with fibrosis. He had severe hypoplastic and dysplastic cystic kidneys without ureters. Microscopy revealed no clear nephrogenic zone, maldeveloped glomeruli and cysts. Autopsy of the brain showed hypoplastic frontal lobes and cerebellum, lissencephaly and leptomeningeal glioneuronal heterotopia.

The fourth pregnancy was terminated at a GA 23 weeks. The male fetus had a weight of 173 grams, OSL 15 cm, OFC 14 (all <5th centile), a narrow thorax and cervical ribs. Kidneys were hypoplastic with loss of glomeruli, fibrotic aspect of the medulla and absent ureters. Autopsy of the brain showed micrencephaly and white matter calcifications.

when the signal is lost_marijn_8072018.indd 109 08/07/2018 10:50

Table 1. Phenotypes of patients with KIF14 mutations

Phenotype	Fetus 1	Fetus 2	Fetus 3	Fetus 4	Fetus 1 (Filges et al 2014)	Fetus 2 (Filges et al 2014)
AD (weeks)	27 + 4	17 + 4	21 + 2	23	21 + 4	18 + 5
Gender	Male	Female	Male	Male	Female	Female
IUGR	550 g (<5th Centile)	100 g (<5th Centile)	200 g (<5th Centile)	173 g (<5th Centile)	<5th Centile	<5th Centile
Kidney/urogenital						
Kidney	Bilateral agenesis	Bilateral cystic hypodysplasia	Bilateral cystic hypodysplasia Absent nephrogenic zone Malformed glomeruli	Bilateral hypoplasia Loss of glomeruli Fibrosis medulla	Bilateral agenesis	Bilateral hypoplasia Cystic dysplasia
Urinary	Ureteral agenesis	Ureteral agenesis Absent bladder	Ureteral agenesis	Ureteral agenesis	Ureteral agenesis	Ureteral hypoplasia
Other					Uterine hypoplasia	Uterine hypoplasia Vaginal atresia
Brain						
OFC	19 cm (<5th Centile)	11.5 cm (<5th Centile)	15 cm (<5th Centile)	14 cm (<5th Centile)	<5th Centile	<5th Centile
Cerebrum	Microlissencephaly Loss of neurons Diffuse gliosis	Micrencephaly Microscopic structural anomalies	Lissencephaly Hypoplasia frontal lobes	Micrencephaly White matter calcifications	Hypoplasia Flat forehead	Hypoplasia
Cerebellum	Diffuse gliosis		Hypoplasia	Hypoplasia	Hypoplasia Vermis agenesis	Hypoplasia Partial vermis agenesis
Other	Small brain stem Absent corticospinal tracts		Leptomeningeal glioneural heterotopia		Agenesis occipital lobes	Holoprocencephaly Corpus callosum agenesis
Skeletal	Contractures lower limbs Clubfeet Abnormal cranial bones	Contractures Clubfeet	Contractures Clubfeet	Narrow thorax and cervical ribs	Flexion contractures Rocker bottom feet Fusion 3rd/4th vertebrae	Flexion contractures Bilateral cubital pterygia Prominent heels Absent ossification 12th rib
Craniofacial	Dysmorphisms	Dysmorphisms	Hypertelorism		Bifid uvula	Anteverted nose

when the signal is lost_marijn_8072018.indd 110 08/07/2018 10:50

when the signal is lost_marijn_8072018.indd 111

	secondary to anhydramnios	secondary to oligohydramnios	Low-set left ear Single palmar crease Dysmorphisms secondary to oligohydramnios		Broad nasal root secondary to oligohydramnios	Low-set ears Discrete micrognathia
Other	Lung hypoplasia secondary to anhydramnios	Anal agenesis Mild lung hypoplasia secondary to oligohydramnios	Lung hypoplasia Cardiac hypertrophy Enlarged fibrotic spleen secondary to oligohydramnios	Mild lung hypoplasia secondary to oligohydramnios Echodense intestines		

GA: gestational age; IUGR: intrauterine growth retardation; OFC: occipital frontal circumference

08/07/2018 10:50

5.3.2 SNP-array

SNP-array performed in the fourth fetus showed a normal male pattern and multiple homozygous regions consistent with consanguinity. Analysis of regions >1Mb did not reveal genes associated with recessive disease that could explain the phenotype (full list of genes contained within homozygous regions provided in **Supplementary Table S1**). *KIF14* was not contained within these regions.

5.3.3 Exome sequencing detects a homozygous truncating mutation in KIF14

By filtering for variants that fit an autosomal recessive inheritance model, a novel homozygous truncating mutation was identified in *KIF14*. The mutation NM_014875.2: c.[1792C>T] p.[(Arg598*)] results in a premature stop codon in exon 9, which is expected to result in nonsense-mediated decay of the shortened transcript. Exon 9 is located in the kinesin motor domain of *KIF14* (**Figure 2**), which exhibits microtubule-dependent ATPase activity [Carleton et al., 2006]. Consequently, any transcripts escaping nonsense-mediated decay would lack microtubule motor function. The mutation was not present in the Exome Aggregation Consortium (ExAC) database [Lek et al., 2016]. We considered the mutation to be causal because the phenotype of the patients presented here matched the phenotype of previously published patients with compound heterozygous mutation in exon 9 of *KIF14* [Filges et al., 2014]. Homozygous mutations were confirmed in fetus 4, 1 and 2 using Sanger sequencing. Carriership was confirmed in both parents and not tested in two healthy siblings.

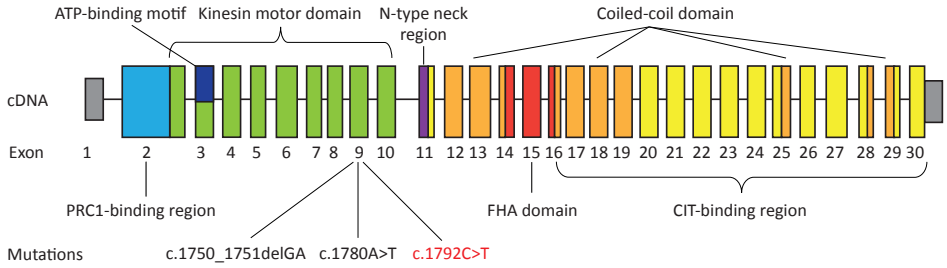

Figure 2. *KIF14* genomic structure and localization of mutations. The homozygous c.[1792C>T] p.[(Arg598*)] mutation in the kinesin motor domain (exon 9) identified in the index patient is indicated in red. The compound heterozygous mutations previously detected in the patients described by Filges et al. are indicated in black [Filges et al., 2014].

5.3.4 Mutations in KIF14 cause a tissue-specific cilia defect

Ciliogenesis and localization of KIF14 was examined in fetal control- and patient-derived kidney tissue. Fetal control kidney showed ciliated proximal tubular epithelial cells (**Figure 3A**). KIF14 colocalized with cilia in proximal tubules. In addition, KIF14 staining was positive in distal tubular and parietal epithelial cells, minimally present in endothelial cells and absent from the interstitium. This is

when the signal is lost_marijn_8072018.indd 112 08/07/2018 10:50

the first visualization of the ciliary localization of endogenous KIF14. In contrast, patient-derived kidney tissue showed tubular microcyst formation with absence of cilia and KIF14 protein.

To assess the effect of the homozygous truncating *KIF14* mutation on ciliogenesis in cells, we examined cilia formation and length in fetal control- and patient-derived fibroblasts. Patient-derived fibroblasts demonstrated normal cilia formation and length (average number of ciliated cells 65.9% ± 15.8) (**Figure 3B**). Together with the finding of reduced cilia formation in patient-derived kidney tissue, this suggests a tissue specific effect of the *KIF14* mutation on ciliogenesis. However, a comparison between control-and patient-derived fibroblasts was not possible because of aberrant proliferation and cilia formation in fetal control-derived fibroblasts.

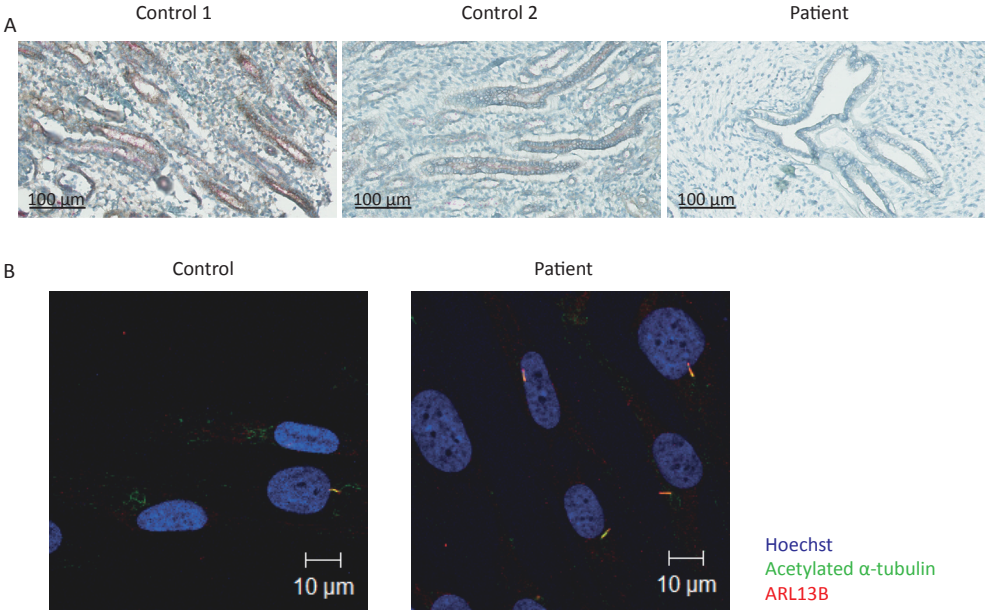

Figure 3. Patient with *KIF14* mutations show a tissue-specific defect in cilia formation. **A.** Fetal kidney tissue from two controls at gestational age 18 to 20 weeks showed ciliary colocalization of acetylated α-tubulin (red) and KIF14 (brown). Fetal kidney tissue from patient at gestational age 18+5 weeks showed tubular microcyst formation and absence of cilia (acetylated α-tubulin, red) and KIF14 staining (brown). Scale bars represent 100 µm. **B.** Immunofluorescence of microtubules (acetylated α-tubulin, green), ciliary axoneme (ARL13B, red) and nucleus (Hoechst, blue) shows normal cilia formation in control- and patient-derived fibroblasts. Scale bars represent 10 µm.

5.3.5 Patient-derived fibroblasts show increased cells in mitosis

Because multinucleated cells and impairment of cytokinesis were previously reported in *KIF14* deficient cells [Carleton et al., 2006; Filges et al., 2014], we determined the number of mitotic cells in fetal control- and patient-derived

when the signal is lost_marijn_8072018.indd 113 08/07/2018 10:50

fibroblasts. Patient-derived fibroblasts showed an increased number of mitotic cells compared to fetal control fibroblasts (10% vs. 0%; 110 and 118 cells analyzed respectively), which could suggest impaired cytokinesis (**Figure 4**). This difference was statistically significant (two-tailed P-value = 0.002, calculated using Mann-Whitney test). In addition, KIF14 was lacking from the midbody in patient-derived cells.

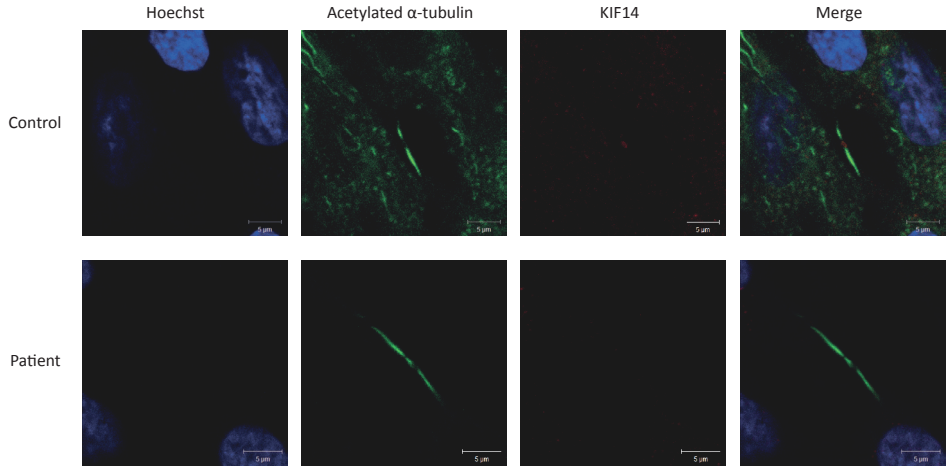

Figure 4. Patient-derived derived fibroblasts show impaired cytokinesis. Immunofluorescence of spindle microtubules (acetylated α-tubulin, green), KIF14 (red) and nucleus (Hoechst, blue) shows the presence of KIF14 at the midbody in control-derived fibroblasts and the absence of KIF14 at the midbody in patient-derived fibroblasts. Ten percent of patient-derived fibroblasts were in a mitotic phase compared to 0% of control-derived fibroblasts (>100 cells analyzed). Scale bars represent 5 µm.

5.4 DISCUSSION

We describe the second family with Meckel-Gruber syndrome caused by mutations in the ciliary gene *KIF14*, encoding a kinesin motor protein. The phenotype of affected fetuses is characterized by severe intrauterine growth restriction, renal cystic dysplasia or agenesis and complex brain malformations. Similar to previously reported compound heterozygous mutations, the identified c.[1792C>T] p.[(Arg598*)] mutation is located in exon 9 of the kinesin motor domain of *KIF14*. The *KIF14* motor domain contains a neck sequence with plus-end-directed determinants and is essential for KIF14 function [Carleton et al., 2006; Vale and Fletterick, 1997]. The identified truncating mutations are expected

when the signal is lost_marijn_8072018.indd 114 08/07/2018 10:50

to result in nonsense-mediated decay of the transcript and loss of KIF14.

Accordingly, KIF14 immunohistochemical staining was absent from patient-derived kidney tissue. We showed localization of KIF14 in the primary cilia in fetal control kidney tissue, confirming that *KIF14* is a ciliary gene. In addition, a ciliogenesis defect was observed in patient-derived kidney tissue, suggesting that *KIF14* is required for ciliogenesis. In contrast, we found normal ciliogenesis in patient-derived fibroblasts, indicating a tissue-specific effect of *KIF14* mutations on cilia formation. Endogenous KIF14 was not visualized at the cilium in patient- and fetal control-derived fibroblasts (data not shown). This is consistent with previous reports that exogenously expressed KIF14-EGFP localized to the cytoplasm in interphase HEK 293T cells and redistributed to the nucleus during mitosis [Carleton et al., 2006].

Patient-derived fibroblasts showed an increased number of mitotic cells compared to fetal-control derived fibroblasts, and an absence of concentration of KIF14 at the midbody. Previous studies showed that KIF14 colocalizes with midbody proteins including citron kinase at the contractile ring in cells about to undergo abscission [Carleton et al., 2006; Gruneberg et al., 2006]. SiRNA-mediated silencing of *KIF14* in HeLa cells resulted in an inability to complete cytokinesis, inducing several rounds of endoreduplication, accumulation of multinucleated cells and subsequent apoptosis [Carleton et al., 2006]. Similarly, binucleated cells were reported in kidney and brain tissue of patients with *KIF14* mutations [Filges et al., 2014]. Through regulation of cell division and apoptosis, Kif14 has been proposed to regulate cerebral and cerebellar cortex development in a *Kif14* mutant mouse model [Yunus et al., 2014]. Loss of KIF14 can therefore result in the complex brain malformation phenotypes observed in our patients and patients reported by Filges et al [Filges et al., 2014]. Although loss of KIF14 has been associated with aneuploid DNA content *in vitro*, it is not associated with an increased tumor risk. Rather, siRNA mediated downregulation of KIF14 suppressed proliferation and induced apoptosis in medulloblastoma and glioblastoma cell lines while KIF14 overexpression has been reported in breast cancer, prostate cancer and medulloblastoma tumor samples [Huang et al., 2015; Li et al., 2017; Zhang et al., 2017; Brynychova et al., 2016]. Because loss of KIF14 suppresses tumor cell proliferation, possibly through cytokinesis failure and inactivation of the Protein Kinase B (PKB/Akt) signaling pathway [Huang et al., 2015], several groups have studied KIF14 as a therapeutic target in cancer [Yang et al., 2013a; Basavarajappa and Corson, 2012].

Until recently, only loss-of-function mutations in *KIF14* had been reported in patients with a lethal fetal ciliopathy phenotype. Ciliopathies are characterized by phenotypic variability that can be associated with the severity of the causal mutation. For example, biallelic deleterious mutations in *MKS1* cause Meckel-Gruber syndrome, while missense mutations cause Joubert syndrome, which is characterized by a combination of developmental and degenerative phenotypes [Romani et al., 2014; Slaats et al., 2016a]. Similarly, hypomorphic mutations in *KIF14* have been predicted to cause viable developmental and degenerative phenotypes including nephronophthisis [Filges et al., 2014]. Indeed, milder

when the signal is lost_marijn_8072018.indd 115 08/07/2018 10:50

mutations in *KIF14* have recently been described in four families with autosomal recessive primary microcephaly [Moawia et al., 2017]. An affected 3-year-old male had a reduced glomerular filtration rate and showed small kidneys with increased echogenicity on renal ultrasound [Moawia et al., 2017], which is suggestive of nephronophthisis. These findings warrant analysis of *KIF14* in patients suspected of a ciliopathy.

In conclusion, our findings in a family with four fetuses with a lethal ciliopathy provide additional proof for a causal role of mutations in *KIF14* in Meckel-Gruber syndrome. Disruption of cell cycle progression and increased apoptosis could be mechanism behind central nervous system and kidney dysplasia observed in patients with *KIF14* mutations.

Acknowledgments

We thank the patients and their parents for participating in this research. We thank Dr. I. Filges for providing us with kidney tissue from an affected fetus and Dr. P. Nikkels for providing us with fetal control kidney tissue. We thank Dr. E. Luna (University of Massachusetts Medical School) and Dr. A. Benmerah (Institut Imagine, Université Paris Descartes) for providing us with the eGFP-KIF14 construct. The researchers received funding from the Dutch Kidney Foundation under grant agreements CP11.18 Kouncil (N.V.A.M.K. and R.H.G.) and the European Community's Seventh Framework Programme (FP7/2009) under grant agreement 305608 EURenOmics (N.V.A.M.K.).

when the signal is lost_marijn_8072018.indd 116 08/07/2018 10:50

SUPPLEMENTARY MATERIAL

Supplementary Methods S1. *Full list of genes included in neurodevelopmental abnormalities gene panel*

ABAT; ABCC9; ABCD1; ABCD4; ABHD5; ACAD9; ACADSB; ACAT1; ACO2; ACOX1; ACSF3; ACSL4; ACTB; ACTG1; ACVR1; ACY1; ADAR; ADCK3; ADSL; AFF2; AGA; AGPAT2; AHCY; AHI1; AIFM1; AIMP1; AK1; AKT3; ALDH18A1; ALDH1A3; ALDH3A2; ALDH4A1; ALDH5A1; ALG1; ALG11; ALG12; ALG2; ALG3; ALG6; ALG9; ALMS1; AMT; ANKH; ANKRD11; ANO10; AP1S1; AP1S2; AP3B1; AP4B1; AP4E1; AP4M1; AP4S1; APTX; AQP2; ARFGEF2; ARG1; ARHGEF9; ARID1A; ARID1B; ARL13B; ARL6; ARX; ASL; ASNS; ASPA; ASPM; ASXL1; ATCAY; ATIC; ATP1A2; ATP2A2; ATP5E; ATP6AP2; ATP6V0A2; ATP7A; ATPAF2; ATR; ATRX; AUH; B3GALNT2; B3GALTL; B3GNT1; B4GALT1; B4GALT7; BBS1; BBS10; BBS12; BBS2; BBS4; BBS5; BBS7; BBS9; BCAP31; BCKDHA; BCKDHB; BCKDK; BCOR; BCS1L; BLM; BRAF; BRAT1; BRWD3; BSCL2; BTD; BUB1B; C10orf2; C12orf65; C5orf42; CA2; CA8; CACNA1C; CACNG2; CAMTA1; CANT1; CASC5; CASK; CBS; CC2D1A; CC2D2A; CCBE1; CCDC78; CDC6; CDH15; CDK5RAP2; CDK6; CDKL5; CDKN1C; CDON; CENPJ; CEP135; CEP152; CEP290; CEP41; CEP57; CEP63; CHD2; CHD7; CHKB; CHKB-CPT1B; CHSY1; CIC; CLIC2; CLN5; CLN8; CNTNAP2; COA5; COG1; COG4; COG5; COG6; COG7; COG8; COL4A1; COL4A2; COLEC11; COQ2; COQ9; COX10; COX15; COX6B1; CPS1; CRADD; CRBN; CREBBP; CSPP1; CTCF; CTDP1; CTNNB1; CTSA; CUL4B; CYB5R3; D2HGDH; DAG1; DARS2; DBT; DCAF17; DCHS1; DCX; DDC; DDHD2; DDOST; DDX11; DHCR24; DHCR7; DHFR; DHTKD1; DIP2B; DKC1; DLD; DLG3; DMD; DMPK; DNAJC19; DNMT3B; DPAGT1; DPM1; DPP6; DPYD; DYM; DYNC1H1; DYRK1A; EFTUD2; EGF; EHMT1; EIF2AK3; EIF4A3; ELOVL4; EMX2; EP300; EPB41L1; ERCC2; ERCC3; ERCC5; ERCC6; ERCC8; ERLIN2; ESCO2; ETHE1; EXOSC3; EZH2; FANCD2; FAT4; FBLN1; FBN1; FBXL4; FGD1; FGFR1; FGFR2; FGFR3; FH; FKRP; FKTN; FLNA; FMN2; FMR1; FOXG1; FOXP1; FRAS1; FREM1; FREM2; FTCD; FTO; FTSJ1; FUCA1; GABRG2; GAD1; GALE; GALT; GAMT; GATAD2B; GATM; GBA; GCH1; GCSH; GDI1; GFAP; GJC2; GK; GLDC; GLI2; GLI3; GLYCTK; GMPPA; GNAO1; GNAS; GNPAT; GNPTAB; GNS; GPC3; GPHN; GPR56; GRIA3; GRIK2; GRIN1; GRIN2A; GRIN2B; GRIP1; GRM1; GSS; GTDC2; GTF2H5; GUSB; HAX1; HCCS; HCFC1; HDAC4; HDAC8; HEPACAM; HESX1; HLCS; HOXA1; HPD; HPRT1; HRAS; HSD17B10; HSD17B4; HSPD1; HUWE1; IDS; IDUA; IER3IP1; IFT172; IGF1; IGF1R; IKBKG; IL1RAPL1; INF2; INPP5E; IQSEC2; ISPD; IVD; JAM3; KANK1; KANSL1; KAT6B; KCNJ10; KCNJ11; KCNK9; KCNQ2; KCNT1; KCTD7; KDM5C; KDM6A; KIAA1279; KIAA2022; KIF11; KIF14; KIF1A; KIF22; KIF2A; KIF5C; KIF7; KIRREL3; KMT2A; KMT2D; KPNA7; KPTN; KRAS; L1CAM; L2HGDH; LAMA2; LAMC3; LAMP2; LARGE; LARP7; LIAS; LIG4; LRP2; LRPPRC; MAGEL2; MAN1B1; MAN2B1; MANBA; MAOA; MAP2K1; MAP2K2; MAT1A; MBD5; MBTPS2; MCCC1; MCCC2; MCOLN1; MCPH1; MECP2; MED12; MED17; MED23; MEF2C; MGAT2; MICU1; MID1; MID2; MKKS; MLC1; MLL2; MLYCD; MMAA; MMACHC; MMADHC; MOCS1; MOCS2; MPDU1; MPLKIP; MRPL3; MRPS22; MTHFR; MTR; MTRR; MUT; MVK; MYCN; MYO5A; NAA10; NAA10; NAGA; NAGLU; NALCN; NBN; NDE1; NDP; NDUFA1; NDUFA11; NDUFA12; NDUFAF5; NDUFS1; NDUFS2; NDUFS3; NDUFS4; NDUFS7; NDUFS8; NDUFV1; NEU1; NF1; NFIX; NHEJ1; NHS; NIN; NIPBL; NKX2-1; NLGN4X; NLRP3; NPHP1; NR2F1; NRXN1; NSD1; NSDHL; NSUN2; NTRK1; NUP62; OCLN; OCRL; OFD1; OPHN1; ORC1; OTC; PACS1; PAFAH1B1; PAH; PAK3; PANK2; PAX6; PC; PCCA; PCCB; PCDH19; PCNT; PDHA1; PDSS1; PDSS2; PEPD; PEX1; PEX10; PEX11B; PEX12; PEX13; PEX14; PEX16; PEX19; PEX2; PEX26; PEX3; PEX5; PEX6; PEX7; PGAP2; PGK1; PHF6; PHF8; PHGDH; PIGA; PIGL; PIGN; PIGO; PIGV; PIGW; PIK3R2; PLA2G6; PLCB1; PLP1; PLXNA3; PMM2; PNKP; PNP; POC1A; POLR3A; POLR3B; POMGNT1; POMT1; POMT2; PORCN; PPOX; PPT1; PQBP1; PRODH; PRPS1; PRSS12; PSAT1; PTCH1; PTCHD1; PTDSS1; PTEN; PTPN11; PTS; PUS1; PVRL1; PYCR1; QDPR; RAB18; RAB27A; RAB39B; RAB3GAP1; RAB3GAP2; RAB40AL; RAD21; RAD50; RAF1; RAI1; RARS2; RBBP8; RBM28; RECQL4; RELN; RFT1; RIT1; RMND1; RMRP; RNASEH2A; RNASEH2B; RNASEH2C; ROGDI; RPGRIP1L; RPS19; RPS6KA3; SALL1; SAMHD1; SATB2; SC5D; SCN1A; SCN2A; SCN8A; SCO2; SDHA; SEPSECS; SERAC1;

when the signal is lost_marijn_8072018.indd 117 08/07/2018 10:50

SETBP1; SHANK3; SHH; SHOC2; SHROOM4; SIL1; SIX3; SKI; SLC12A6; SLC16A2; SLC17A5; SLC25A12; SLC25A15; SLC25A22; SLC2A1; SLC33A1; SLC35A2; SLC35C1; SLC46A1; SLC4A4; SLC6A8; SLC9A6; SMAD4; SMARCA2; SMARCA4; SMARCB1; SMC1A; SMC3; SMOC1; SMPD1; SMS; SNAP29; SNIP1; SOBP; SOS1; SOX10; SOX2; SOX3; SPAST; SPR; SPRED1; SPTAN1; SRCAP; SRD5A3; ST3GAL3; ST3GAL5; STAMBP; STIL; STRA6; STXBP1; SUCLG1; SUOX; SURF1; SYN1; SYNGAP1; SYP; SYT14; SZT2; TAF2; TAT; TBC1D20; TBC1D24; TBCE; TBX1; TCF4; TCN2; TCTN3; TECR; TFAP2A; TGFBR1; TGFBR2; TGIF1; TH; THRB; TIMM8A; TINF2; TMCO1; TMEM165; TMEM231; TMEM237; TMEM67; TMEM70; TPI1; TRAPPC11; TRAPPC9; TREX1; TRIM32; TSC1; TSC2; TSPAN7; TTC19; TTC21B; TTC37; TTC8; TTI2; TUBA1A; TUBB2B; TUBB3; TUBG1; TUSC3; TWIST1; UBE2A; UBE3A; UBR1; UPB1; UPF3B; UQCRQ; UROC1; VLDLR; VPS13B; VPS37A; WDR45; WDR62; WDR81; WWOX; XPA; ZBTB16; ZBTB18; ZBTB24; ZDHHC15; ZDHHC9; ZEB2; ZFYVE26; ZIC2; ZNF592; ZNF674; ZNF711; ZNF81

when the signal is lost_marijn_8072018.indd 118 08/07/2018 10:50

Supplementary Table S1. *Genes associated with recessive disease located within regions of homozygosity >1Mb*

Ensembl ID	Gene symbol	Gene MIM#	Phenotype MIM#	Location
ENSG00000135821	GLUL	138290	610015	1:182,350,839-182,361,341
ENSG00000058085	LAMC2	150292	226700	1:183,155,373-183,214,035
ENSG00000116701	NCF2	608515	233710	1:183,524,698-183,560,011
ENSG00000116690	PRG4	604283	208250	1:186,265,405-186,283,694
ENSG00000000971	CFH	134370	610698	1:196,621,008-196,716,634
ENSG00000116785	CFHR3	605336		1:196,743,925-196,763,203
ENSG00000244414	CFHR1	134371		1:196,788,887-196,801,319
ENSG00000143278	F13B	134580	613235	1:197,008,321-197,036,397
ENSG00000066279	ASPM	605481	608716	1:197,053,258-197,115,824
ENSG00000134376	CRB1	604210	613835	1:197,170,592-197,447,585
ENSG00000081237	PTPRC	151460	608971	1:198,607,801-198,726,545
ENSG00000049860	HEXB	606873	268800	5:73,935,848-74,018,472
ENSG00000132842	AP3B1	603401	608233	5:77,296,349-77,590,579
ENSG00000113273	ARSB	611542	272200	5:78,073,032-78,281,910
ENSG00000132837	DMGDH	605849	605850	5:78,293,438-78,531,861
ENSG00000228716	DHFR	126060	613839	5:79,922,047-79,950,802
ENSG00000164199	GPR98	602851	605472	5:89,825,161-90,460,038
ENSG00000112294	ALDH5A1	610045	271980	6:24,495,080-24,537,435
ENSG00000124564	SLC17A3	611034	612671	6:25,833,294-25,882,514
ENSG00000010704	HFE	613609	614193	6:26,087,509-26,098,571
ENSG00000096433	ITPR3	147267		6:33,588,142-33,664,351
ENSG00000124713	GNMT	606628	606664	6:42,928,496-42,931,618
ENSG00000044090	CUL7	609577	273750	6:43,005,355-43,021,683
ENSG00000171453	POLR1C	610060	248390	6:43,477,440-43,497,323
ENSG00000124608	AARS2	612035	614096	6:44,267,391-44,281,063
ENSG00000146085	MUT	609058	251000	6:49,398,073-49,430,904
ENSG00000112077	RHAG	180297	268150	6:49,572,871-49,604,552
ENSG00000170927	PKHD1	606702	263200	6:51,480,098-51,952,423
ENSG00000112144	ICK	612325	612651	6:52,866,077-52,926,600
ENSG00000001084	GCLC	606857	230450	6:53,362,139-53,481,768
ENSG00000112210	RAB23	606144	201000	6:57,053,607-57,087,078
ENSG00000185002	RFX6	612659	601346	6:117,198,375-117,253,326
ENSG00000152661	GJA1	121014	600309	6:121,756,838-121,770,873
ENSG00000196569	LAMA2	156225	607855	6:129,204,342-129,837,714
ENSG00000118520	ARG1	608313	207800	6:131,894,284-131,905,472
ENSG00000197594	ENPP1	173335	613312	6:132,129,156-132,216,295
ENSG00000135541	AHI1	608894	608629	6:135,604,670-135,818,914
ENSG00000112357	PEX7	601757	614879	6:137,143,717-137,235,075
ENSG00000027697	IFNGR1	107470	600263	6:137,518,621-137,540,586
ENSG00000034693	PEX3	603164	614882	6:143,771,944-143,811,147
ENSG00000112425	EPM2A	607566	254780	6:145,822,719-146,057,160
ENSG00000104687	GSR	138300	138300	8:30,535,583-30,585,443
ENSG00000165392	WRN	604611	277700	8:30,891,317-31,031,285
ENSG00000147475	ERLIN2	611605	611225	8:37,594,117-37,616,619
ENSG00000147465	STAR	600617	201710	8:38,001,167-38,008,783

when the signal is lost_marijn_8072018.indd 119 08/07/2018 10:50

ENSG00000165102	HGSNAT	610453	252930	8:42,995,556-43,057,998
ENSG00000019549	SNAI2	602150	608890	8:49,830,249-49,834,299
ENSG00000104331	IMPAD1	614010	614078	8:57,870,492-57,906,403
ENSG00000178538	CA8	114815	613227	8:61,099,906-61,193,971
ENSG00000137561	TTPA	600415	277460	8:63,961,112-63,998,612
ENSG00000172817	CYP7B1	603711	613812	8:65,500,320-65,711,318
ENSG00000165078	CPA6	609562	614418	8:68,334,360-68,658,620
ENSG00000175606	TMEM70	612418	614052	8:74,884,672-74,895,018
ENSG00000104381	GDAP1	606598	608340	8:75,233,365-75,401,107
ENSG00000164751	PEX2	170993	614867	8:77,892,494-77,913,280
ENSG00000104267	CA2	611492	259730	8:86,376,081-86,393,722
ENSG00000170289	CNGB3	605080	262300	8:87,566,205-87,755,903
ENSG00000104320	NBN	602667	609135	8:90,945,564-91,015,456
ENSG00000104325	DECR1	222745	222745	8:91,013,633-91,064,320
ENSG00000164953	TMEM67	609884	613550	8:94,767,072-94,831,462
ENSG00000164951	PDP1	605993	608782	8:94,870,035-94,938,294
ENSG00000156170	NDUFAF6	612392	252010	8:95,907,995-96,128,683
ENSG00000156172	C8orf37	614477	614500	8:96,257,147-96,281,429
ENSG00000156467	UQCRB	191330	615158	8:97,238,148-97,247,862
ENSG00000132549	VPS13B	607817	216550	8:100,025,494-100,889,808
ENSG00000164930	FZD6	603409	614157	8:104,310,661-104,345,094
ENSG00000147647	DPYS	613326	222748	8:105,342,552-105,479,281
ENSG00000197969	VPS13A	605978	200150	9:79,792,269-80,036,457
ENSG00000135069	PSAT1	610936	610992	9:80,912,059-80,945,009
ENSG00000102575	ACP5	171640	607944	19:11,685,475-11,689,823
ENSG00000104774	MAN2B1	609458	248500	19:12,757,325-12,777,556
ENSG00000105607	GCDH	608801	231670	19:13,001,840-13,025,021
ENSG00000132024	CC2D1A	610055	608443	19:14,017,014-14,041,692
ENSG00000248099	INSL3	146738	219050	19:17,927,321-17,932,383
ENSG00000105641	SLC5A5	601843	274400	19:17,982,782-18,005,983
ENSG00000096996	IL12RB1	601604	209950	19:18,169,805-18,209,754
ENSG00000006016	CRLF1	604237	272430	19:18,683,030-18,718,551
ENSG00000130283	GDF1	602880	613854	19:18,979,361-19,006,905
ENSG00000117593	DARS2	610956	611105	1:173,793,641-173,827,684
ENSG00000117601	SERPINC1	107300	613118	1:173,872,947-173,886,516
ENSG00000116096	SPR	182125	612716	2:73,114,489-73,119,287
ENSG00000116127	ALMS1	606844	203800	2:73,612,886-73,837,920
ENSG00000160796	NBEAL2	614169	139090	3:47,021,173-47,051,193
ENSG00000213689	TREX1	606609	610448	3:48,506,445-48,509,044
ENSG00000114270	COL7A1	120120	607523	3:48,601,506-48,632,700
ENSG00000124491	F13A1	134570	613225	6:6,144,318-6,321,246
ENSG00000164494	PDSS2	610564	614652	6:107,473,761-107,780,768
ENSG00000156110	ADK	102750	614300	10:75,910,960-76,469,061
ENSG00000156650	KAT6B	605880	606170	10:76,585,340-76,792,380
ENSG00000187486	KCNJ11	600937	610582	11:17,407,406-17,410,878
ENSG00000006071	ABCC8	600509	610374	11:17,414,432-17,498,449

when the signal is lost_marijn_8072018.indd 120 08/07/2018 10:50

ENSG00000006611	USH1C	605242	602092	11:17,515,442-17,565,963
ENSG00000134333	LDHA	150000	612933	11:18,415,935-18,429,972
ENSG00000134569	LRP4	604270	614305	11:46,878,419-46,940,193
ENSG00000134574	DDB2	600811	278740	11:47,236,493-47,260,767
ENSG00000134575	ACP2	171650	200950	11:47,260,853-47,270,457
ENSG00000165915	SLC39A13	608735	612350	11:47,428,683-47,438,047
ENSG00000165917	RAPSN	601592	608931	11:47,459,308-47,470,730
ENSG00000213619	NDUFS3	603846		11:47,586,888-47,606,114
ENSG00000139531	SUOX	606887	272300	12:56,390,964-56,400,425
ENSG00000065361	ERBB3	190151	607598	12:56,473,641-56,497,289
ENSG00000171723	GPHN	603930	252150	14:66,974,125-67,648,520
ENSG00000167972	ABCA3	601615	610921	16:2,325,882-2,390,747
ENSG00000162065	TBC1D24	613577	615338	16:2,525,147-2,555,735
ENSG00000103313	MEFV	608107	249100	16:3,292,028-3,306,627
ENSG00000188827	SLX4	613278	613951	16:3,631,182-3,661,599
ENSG00000033011	ALG1	605907	608540	16:5,083,703-5,137,380
ENSG00000102893	PHKB	172490	261750	16:47,495,034-47,735,434
ENSG00000259384	GH1	139250	612781	17:61,994,560-61,996,179
ENSG00000007312	CD79B	147245	612692	17:62,006,100-62,009,714
ENSG00000115286	NDUFS7	601825	256000	19:1,383,526-1,395,583
ENSG00000130005	GAMT	601240	612736	19:1,397,091-1,401,569
ENSG00000171105	INSR	147670	610549	19:7,112,266-7,294,045
ENSG00000090674	MCOLN1	605248	252650	19:7,587,512-7,598,895
ENSG00000100997	ABHD12	613599	612674	20:25,275,379-25,371,619
ENSG00000101444	AHCY	180960	613752	20:32,868,074-32,899,608
ENSG00000078747	ITCH	606409	613385	20:32,951,041-33,099,198
ENSG00000100983	GSS	601002	266130	20:33,516,236-33,543,620

when the signal is lost_marijn_8072018.indd 121 08/07/2018 10:50

when the signal is lost_marijn_8072018.indd 122 08/07/2018 10:50

PART 2

NOVEL APPROACHES TO KIDNEY DISEASE DIAGNOSTICS

when the signal is lost_marijn_8072018.indd 123 08/07/2018 10:50

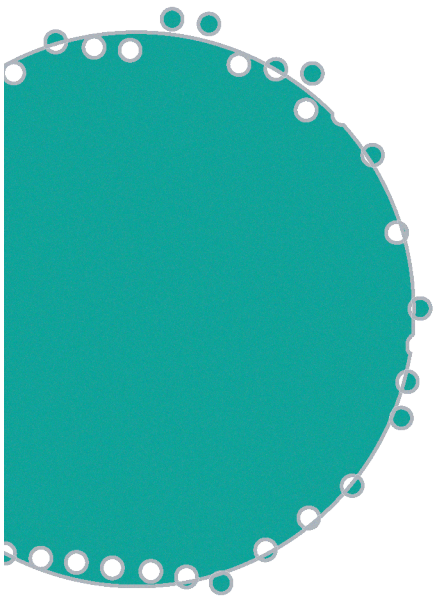

when the signal is lost_marijn_8072018.indd 124 08/07/2018 10:50

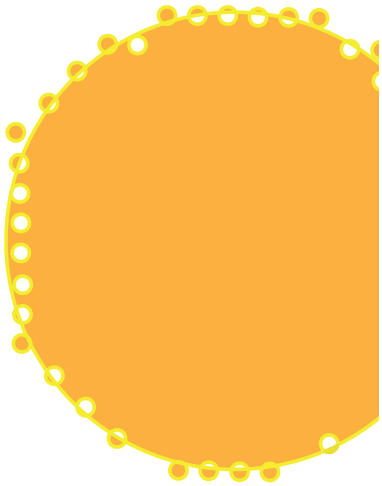

CHAPTER 6

Changes in the urinary extracellular vesicle proteome are associated with nephronophthisis-related ciliopathies

Stokman MF, Bijnsdorp IV, Schelfhorst T, Peters EDJ, Pham TV, Piersma SR, Knol JC, Giles RH, Bongers EMHF, Knoers NVAM, Lilien MR, Jimenez CR*, Renkema KY*

*These authors contributed equally

Manuscript submitted

ABSTRACT

Nephronophthisis is one of the leading genetic causes of end-stage renal disease in childhood. Early diagnostics and prognostics for nephronophthisis are currently limited. We aimed to identify non-invasive protein biomarkers for nephronophthisis in urinary extracellular vesicles. Extracellular vesicles were isolated from urine of 12 patients with a nephronophthisis-related ciliopathy and 12 age- and gender-matched controls, followed by in-depth label-free LC-MS/MS proteomics analysis of gel fractionated extracellular vesicles proteins. Supervised cluster analysis of proteomic profiles separated patients from controls. We identified 156 differentially expressed proteins with fold change ≥4 in patients compared to controls ($P<0.05$). Importantly, expression levels of discriminating proteins were correlated with chronic kidney disease stage, suggesting possible applications for urinary extracellular vesicle biomarkers in prognostics for nephronophthisis. Enrichment analysis of gene ontology terms revealed GO terms including signaling, actin cytoskeleton and endocytosis among the downregulated proteins in patients, whereas terms related to response to wounding and extracellular matrix organization were enriched among upregulated proteins. Our findings represent the first step towards a non-invasive diagnostic test for nephronophthisis. Further research is needed to determine specificity of the candidate biomarkers. In conclusion, proteomic profiles of urinary extracellular vesicles differentiate nephronophthisis-related ciliopathy patients from healthy controls.

when the signal is lost_marijn_8072018.indd 126 08/07/2018 10:50

6.1 Introduction

Nephronophthisis is an important genetic cause of end-stage renal disease (ESRD) in children and young adults, accounting for 2.4% to 15% of pediatric ESRD cases [Hildebrandt et al., 1993; Hamiwka et al., 2008; Hildebrandt et al., 2009]. Nephronophthisis is known to result from defective ciliary signaling and has been classified as a renal ciliopathy. It is characterized by chronic tubulointerstitial nephritis leading to loss of renal function and a reduced concentrating ability of the kidney. The diagnosis of nephronophthisis is currently based on clinical symptoms including polydipsia, polyuria, growth retardation and refractory anemia, chronic kidney disease (CKD) and a family history consistent with autosomal recessive disease [Hildebrandt et al., 2009; Simms et al., 2011]. Renal ultrasound findings include hyperechogenic kidneys and corticomedullary cysts in approximately 50% of patients [Hildebrandt and Zhou, 2007; Hurd and Hildebrandt, 2011; Soliman et al., 2012].

As a result of the variable and non-specific presenting symptoms, nephronophthisis is diagnosed on average 3.5 years after symptom onset, often in advanced stages of CKD when kidney damage is irreversible [Soliman et al., 2012]. This diagnostic delay occurs especially in nephronophthisis patients without extra-renal manifestations (e.g. retinitis pigmentosa or neurological signs) that could be indicative of a ciliopathy and would usually prompt monitoring of renal function. In addition, DNA testing currently confirms the diagnosis in only 40-50% of nephronophthisis patients and genetic confirmation does not enable accurate prognostics yet, hindering disease management and genetic counseling [Otto et al., 2010; Halbritter et al., 2013; Braun et al., 2016]. Therefore, the discovery of early biomarkers for nephronophthisis-related ciliopathies (NPH-RC) is essential to permit early diagnostics and monitoring of disease progression. Early diagnostics will permit 'reverse phenotyping', i.e. the monitoring of other ciliopathy-related features such as retinal degeneration and liver fibrosis in apparently isolated nephronophthisis. Furthermore, early diagnostics will pave the way for timely supportive treatment, aimed at slowing down disease progression towards ESRD, and preparation for pre-emptive renal transplantation. Additionally, early detection of nephronophthisis may be indispensable for the success of future targeted therapies.

Biofluids contain extracellular vesicles (EVs) including exosomes that have emerged as a treasure trove of molecular markers [Pomatto et al., 2017]. Exosomes originate from 50-130 nm intraluminal vesicles of multivesicular bodies that are secreted into extracellular fluids [Raposo et al., 1996]. Exosomes are important mediators of intercellular communication [Mathivanan et al., 2010]. The content of exosomes has been shown to reflect the physiological state of the cells of origin, in the case of urine the cells lining the kidney and urinary tract [de Jong et al., 2012]. Previous studies have shown that proteomic analysis of urinary exosomes offers unique insights into pathophysiological mechanisms that underlie kidney disease [Zubiri et al., 2015]. Thus, urinary exosomes are an excellent non-invasive source of biomarkers for kidney diseases [Conde-Vancells and Falcon-Perez, 2012].

when the signal is lost_marijn_8072018.indd 127 08/07/2018 10:50

Here, we present the first study identifying candidate biomarkers for nephronophthisis using global proteomics analysis of urinary EVs in 12 NPH-RC patients compared to 12 control individuals. The identification of biomarkers for nephronophthisis gives us opportunities to develop a non-invasive diagnostic test for children suspected of nephronophthisis and thereby improve the care for NPH-RC patients. When confirmed in larger patient series, we see promising applications in diagnostics and prognostics and, thereby, translation to clinical practice.

6.2 MATERIALS AND METHODS

6.2.1 Patients and urine collection

Twelve patients with NPH-RC and 12 age- and gender-matched control subjects were recruited at the Department of Pediatric Nephrology of the University Medical Center Utrecht, the Department of Genetics of the University Medical Center Utrecht, and the Department of Human Genetics of the Radboudumc Nijmegen. NPH-RC patients and controls were included in the AGORA (Aetiologic research into Genetic and Occupational/environmental Risk factors for congenital Anomalies) data- and biobank project, approved by the regional Committee on Research involving Human Subjects (CMO Arnhem-Nijmegen 2006/048 and METC UMC Utrecht 12-473). Signed informed consent was obtained for all subjects included in this study. Inclusion criteria for patients were a molecularly confirmed diagnosis of NPH-RC or a high suspicion thereof, based on clinical features including presence of polyuria, absence of recurrent urinary tract infections, CKD stage 1-5 [Kidney Disease: Improving Global Outcomes (KDIGO) CKD Work Group, 2013], renal ultrasound showing parenchymal damage but absence of malformation of the kidneys and urinary tract, urinalysis showing absence of hematuria, erythrocyte casts and proteinuria in the nephrotic range, and exclusion of other causes of early-onset renal failure. Age and gender-matched control subjects were acquaintances of the researchers and showed no signs or symptoms of NPH-RC, no family history of pediatric-onset renal disease, no known congenital anomalies of the kidney and urinary tract, no consanguinity, and a protein/creatinine ratio within the normal range (i.e. <20 mg/mmol in individuals over 2 years of age). Control urine samples were anonymized after collection and matching.

Urine samples (40 to 400 ml) were collected from all subjects using sterile urine containers and kept on ice for a maximum of five hours until processing. We did not use the first morning void to minimize the chance for an enrichment of EVs derived from the urinary bladder. A 4 µl aliquot of fresh urine was stored at -20°C for determination of protein/creatinine ratio using the Bradford Protein Assay (Bio-Rad, Hercules, CA, USA) and the Creatinine PAP FS kit (DiaSys Diagnostic Systems, Holzheim, Germany) according to manufacturers' instructions. The remainder of the urine was centrifuged at 500 g for 10 minutes at 4°C and at 2,000 g for 20 minutes at 4°C. Supernatants were stored at -80°C until further use.

when the signal is lost_marijn_8072018.indd 128 08/07/2018 10:50

6.2.2 EV isolation

Supernatants were processed in three batches of eight subjects with equal numbers of patients and controls, male and female subjects and uniform mean subject age to preclude batch effects. Thawed supernatants were centrifuged at 2,000 g for 20 minutes at 4°C. 0.05% NP-40 (Sigma-Aldrich, Zwijndrecht, The Netherlands) was added to each supernatant as a detergent [Bijnsdorp et al., 2017]. The samples were concentrated to 1 ml by centrifugation at 4,000 g at room temperature using Amicon Ultracel 100kDa cut-off centrifugal filters (Merck Millipore, Billerica, MA, USA). Concentrated samples were diluted to 1.9 ml using PBS (BBraun, Melsungen, Germany). Subsequently, 100 µl cOmplete™, Mini, EDTA-free Protease Inhibitor Cocktail (PIC) (Roche, Basel, Switzerland) in 525µl PBS was added to each sample. Urine was centrifuged for 16,000 g for 30 minutes at 4°C to remove debris. Next, Vn96 peptide (ME-kit, New England Peptide, Gardner, MA, USA) was added to the supernatant to aggregate EVs including exosomes as previously described [Ghosh et al., 2014; Knol et al., 2016]. The Vn96 peptide binds heat shock proteins present on the surface of EVs, allowing 'miniprep' isolation. Samples were incubated for 60 minutes at room temperature and centrifuged at 16,000 g for 15 minutes at 4°C. The full pellets were washed with 5% cOmplete™ PIC in PBS, centrifuged at 16,000 g for 15 minutes at 4°C and resuspended in 2 ml NuPAGE Sample Buffer (Life Technologies, Thermo Fisher Scientific, Carlsbad, CA, USA).

6.2.3 Western blot

Immunoblotting was performed in additional control urine samples to verify the isolation of EVs. Antibodies were directed against EV markers PDCD6IP (Alix, Mouse monoclonal; 1:1,000; Cell signaling Technology, Danvers, MA, USA) and TSG101 (Rabbit polyclonal; 1:500; Atlas Antibodies, Bromma, Sweden) (**Supplementary Figure S1**).

6.2.4 Gel electrophoresis and in-gel tryptic digestion

Sonified EV samples were size separated on NuPAGe Novex 4-12% Bis-Tris Protein Gels (Life Technologies, Thermo Fisher Scientific, Carlsbad, CA, USA) using one-dimensional gel electrophoresis. This eliminates contaminants and reduces sample complexity to improve peptide identification. Gels were processed with reducing and alkylating agents. Gels were cut prior to in-gel digestion with trypsin followed by peptide extraction as previously described [Knol et al., 2016; Piersma et al., 2013]. Extracts were stored at -20 °C until further use.

6.2.5 Nano-LC-MS/MS and database searching

Extracted peptides were concentrated in a vacuum centrifuge and the volume was adjusted using 4% acetonitrile in 0.5% trifluoro-acetic acid (TFA) to achieve equal protein loading based on gel images. Peptides were separated using nanoscale liquid chromatography and analyzed using tandem mass spectrometry (GelC-MS/MS) as previously described [Pham et al., 2012; Piersma et al., 2010; Chiasserini et al., 2014]. MS/MS spectra were searched against the Swissprot database (2015-09, 42,122 entries) using MaxQuant software (version 1.5.2.8) [Cox and Mann, 2008],

when the signal is lost_marijn_8072018.indd 129 08/07/2018 10:50

with a maximum allowed deviation of 4.5 ppm for the precursor mass and 20 ppm the for fragment masses. Cysteine carboxamidomethylation was treated as fixed modification and N-acetylation and methionine oxidation were treated as variable modifications. Identified peptides and proteins were filtered to a false discovery rate of 1% using the target-decoy method [Elias and Gygi, 2007]. Raw spectral counts of identified protein groups were processed using R for further analysis.

6.2.6 Data mining and statistical analyses

Spectral counts were normalized using the average of the sum of raw counts across all samples as previously described [Warmoes et al., 2016]. Protein expression differences between patients and controls were calculated using the beta-binominal test for unpaired data [Pham et al., 2009; Pham and Jimenez, 2012]. The P-values <0.05 were considered statistically significant. R package gplots was used to perform hierarchical clustering [Warnes et al., 2016].

Differentially expressed proteins were identified using stringent selection criteria: P<0.05, fold change ≥4 for down- and ≥3 for upregulated proteins, detected in at least 8 of 12 samples and a mean normalized count in positive samples of ≥2. Human gene symbols corresponding to protein identifiers of differentially expressed proteins were imported into the STRING tool (version 10.0) to examine protein-protein interactions [Szklarczyk et al., 2015]. Interaction networks were annotated using Cytoscape (version 3.4.0) [Shannon et al., 2003]. The PANTHER overrepresentation test in AmiGO 2 (version 2.4.24) was used for GO term enrichment analysis [Carbon et al., 2009; Mi et al., 2016]. Bonferroni-corrected P-values <0.05 were considered statistically significant. ConsensusPathDB (version 31) was used to analyze enriched biological pathways per annotated gene cluster [Kamburov et al., 2011]. Interaction databases that contained >50% drug-target and biochemical interactions were excluded from pathway enrichment analyses because they were considered irrelevant to the aims of the present study. Further statistical analyses, including correlation analyses of protein expression with CKD stage, were performed using Graph Pad Prism (Version 7.02). Finally, a PubMed literature search was performed for comparison of proteins that were previously associated with CKD with discriminating markers identified in the current study (**Supplementary Methods S1**).

when the signal is lost_marijn_8072018.indd 130 08/07/2018 10:50

6.3 RESULTS

6.3.1 Differentially expressed proteins discriminate between NPH-RC patients and controls

Twelve patients with NPH-RC and 12 age-and gender-matched control subjects, age 6 to 25 years, were recruited for urine collection (**Table 1**). Patients' phenotypes included isolated nephronophthisis (NPH; n=6), Bardet-Biedl syndrome (BBS; n=2), Sensenbrenner syndrome (CED; n=2), and Joubert syndrome (JBTS; n=2). Urine protein/creatinine ratio was determined in each subject to confirm patient or control status with a normal range of <20 mg/mmol in individuals over 2 years of age. The mean protein/creatinine ratio was 58.0 ± 64.2 mg/mmol in NPH-RC patients compared to 11.6 ± 8.5 mg/mmol in control individuals.

Table 1. Subject and urine characteristics

Subject characteristics	**Patients**	**Controls**
Number (n)	12	12
Gender (M/F)	6/6	6/6
Age (years; mean ± SD)	14.8 (± 4.7)	14.7 (± 4.7)
Diagnosis	Isolated NPH (n=6) BBS (-like) (n=2) CED (n=2) JBTS (n=2)	NA
CKD stage	I (n=1) II (n=3) III (n=4) IV (n=3) V (n=1)	NA
Urine characteristics	**Patients**	**Controls**
Amount (ml; mean ± SD)	113.3 (± 98.0)	90.0 (± 14.3)
Processing time (minutes; mean ± SD)	103.8 (± 79.0)	46.7 (± 41.1)
Storage time (days; mean ± SD)	119.6 (± 62.3)	95.0 (± 63.9)
Protein/creatinine ratio (mg/mmol mean ± SD)	58.0 (± 64.2)	11.6 (± 8.5)

NPH: nephronophthisis; BBS: Bardet-Biedl syndrome; CED: cranioectodermal dysplasia (Sensenbrenner syndrome); JBTS: Joubert syndrome; NA: not applicable.

when the signal is lost_marijn_8072018.indd 131 08/07/2018 10:50

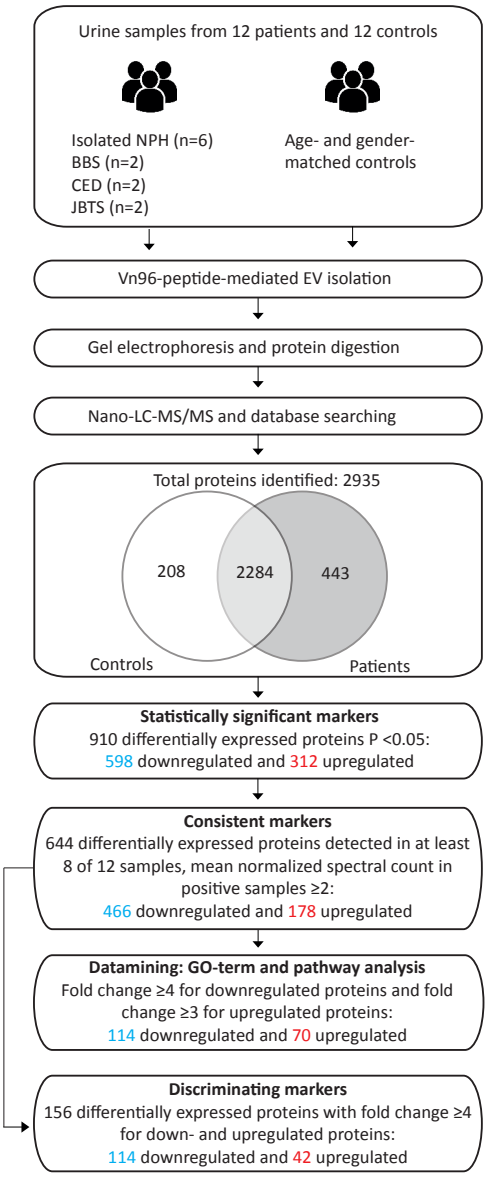

Figure 1. Study methodology to identify differentially expressed proteins in nephronophthisis patients compared to age- and gender-matched controls. Venn diagram shows total number of proteins identified in controls and in patients based on raw spectral counts. NPH: isolated nephronophthisis; BBS: Bardet-Biedl syndrome; CED: cranioectodermal dysplasia (Sensenbrenner syndrome); JBTS: Joubert syndrome.

when the signal is lost_marijn_8072018.indd 132 08/07/2018 10:50

Proteomic profiles of urinary EVs were determined in each patient and control individual by using EV protein fractionation by gel electrophoresis in conjunction with nanoLC-MS/MS. In total, 2,935 unique EV proteins were identified, of which 2,284 proteins were present in both patients and controls (**Figure 1**). Nine hundred ten proteins were differentially expressed in NPH-RC patients compared to controls (P<0.05), of which 598 proteins were downregulated and 312 proteins were upregulated. Out of 910 statistically significant differentially expressed urinary EV proteins, 156 proteins met stringent criteria for potential biomarker selection (fold change ≥4, detected in at least 8 of 12 samples and a mean normalized count in positive samples of ≥2) (**Figure 2**). Of the proteins that met these criteria, 114 proteins were downregulated and 42 proteins were upregulated (**Supplementary Table S1**).

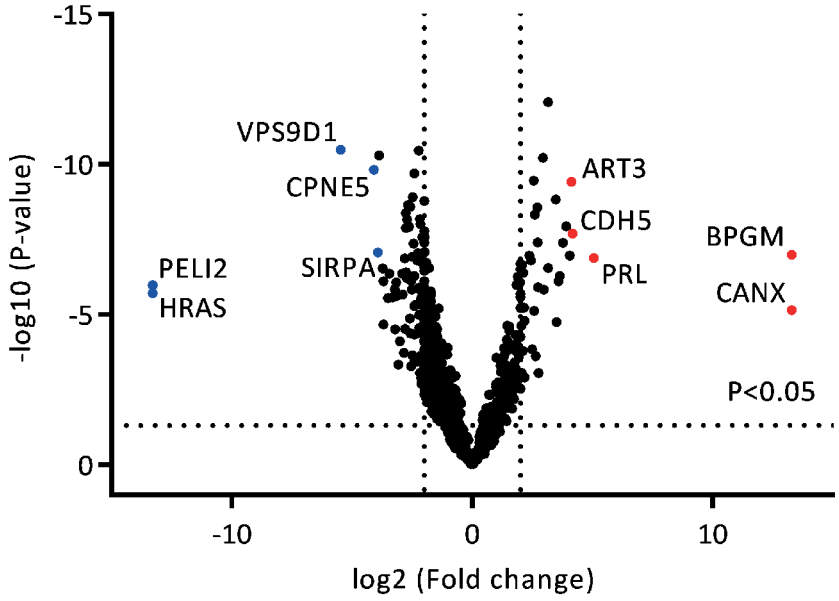

Figure 2. Volcano plot of differentially regulated proteins in patients compared to controls. Dots represent individual proteins. Proteins were detected in at least 8 of 12 samples and had a mean normalized count in positive samples of ≥2. Vertical dashed lines mark fold change = 4 and horizontal dashed line marks the significance threshold P<0.05. Top 5 most downregulated proteins (blue) and upregulated proteins (red) by fold change were highlighted and labeled with protein names.

when the signal is lost_marijn_8072018.indd 133 08/07/2018 10:50

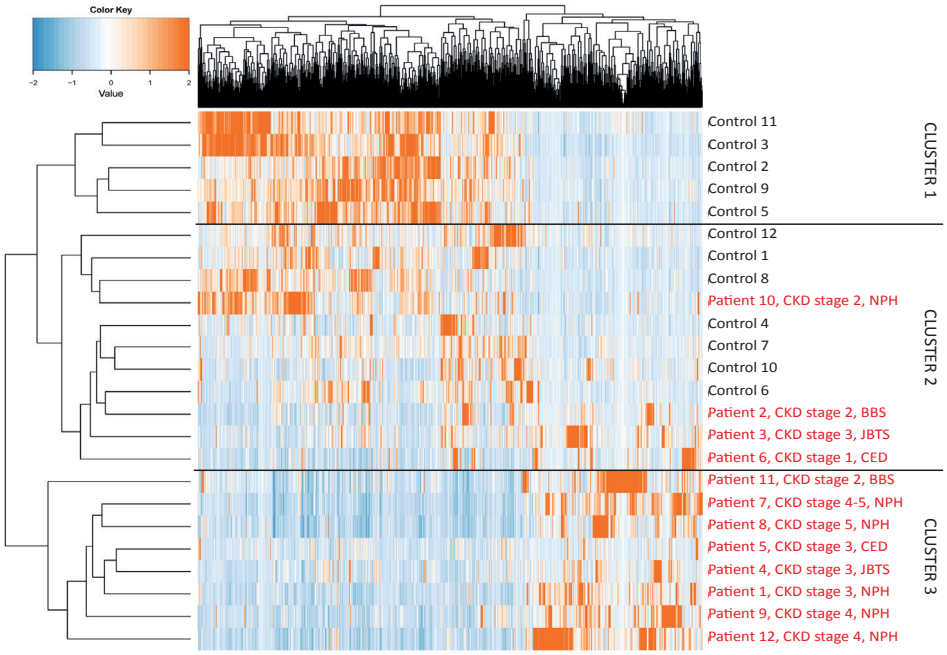

Figure 3. Supervised hierarchical clustering of normalized protein counts (P< 0.05) separates NPH-RC patients from controls. Three separate clusters (marked 1,2 and 3) can be discerned. Blue represents downregulated proteins and orange represents upregulated proteins. NPH: isolated nephronophthisis; BBS: Bardet-Biedl syndrome; CED: cranioectodermal dysplasia (Sensenbrenner syndrome); JBTS: Joubert syndrome.

Supervised hierarchical clustering of normalized protein counts showed a near-complete separation of patient and control samples (**Figure 3**). Three separate clusters were discerned: 1) a cluster of 5 control samples, 2) a central cluster of 4 patients (patient 2, 3, 6 and 10) positioned among 7 controls, and 3) a cluster of 8 patient samples. The average CKD stage of patients in cluster 3 comprising 8 patient samples was higher compared to the mean CKD stage of patients in the central cluster (CKD stage 3-4 versus CKD stage 2, respectively), suggesting that proteomic profiles from patients with a more advanced CKD stage cluster together. Patient 10 with a tentative genetic diagnosis (a mutation and a variant of unknown significance (VUS) in *NPHP4*, **Supplementary Table S2**) clustered in the central cluster among controls. Patients without a molecular diagnosis (patients 1 and 8) clustered together with patients with a molecular diagnosis in the third cluster. In addition, protein-clustering analyses after stratification into different diagnostic subgroups (i.e. isolated nephronophthisis, Bardet-Biedl syndrome, Sensenbrenner syndrome, and Joubert syndrome) showed separation between patients and matched controls except in isolated nephronophthisis, in which patient 10 grouped among controls (**Supplementary Figure S2**).

when the signal is lost_marijn_8072018.indd 134 08/07/2018 10:50

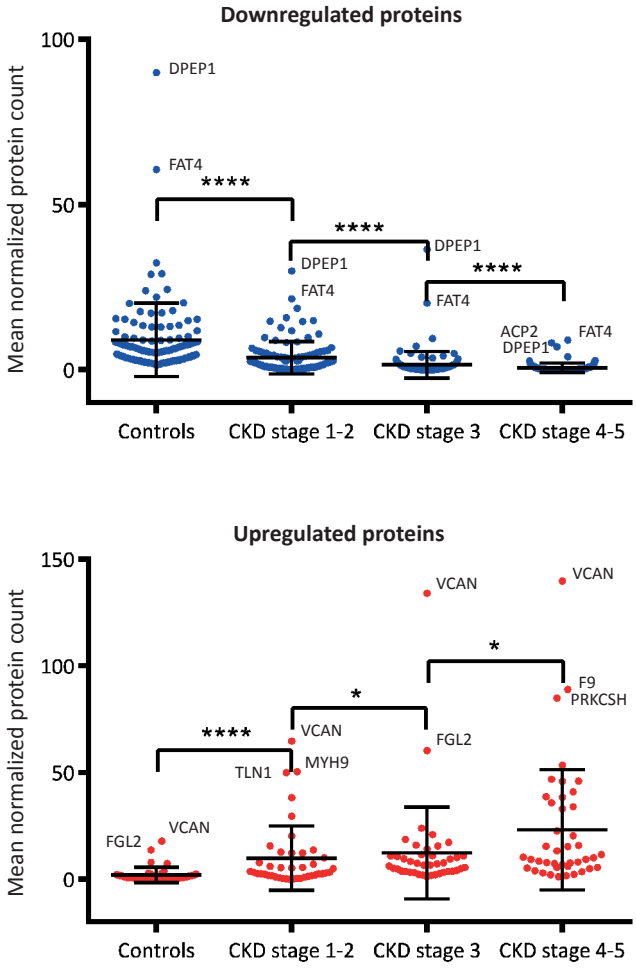

Figure 4. Differentially expressed proteins relate to chronic kidney disease stage. Mean normalized protein count of downregulated proteins (blue) and upregulated proteins (red) is associated with stage of CKD in NPH-RC patients. Dots represent individual proteins. Lines and error bars show mean and standard deviation, respectively. The most highly abundant proteins are labeled with protein names. *P<0.05, ****P<0.0001, calculated using Mann-Whitney test. CKD: chronic kidney disease.

6.3.2 Expression levels of differentiating proteins are correlated with CKD stage

To assess the relationship between the expression level of discriminating proteins and CKD stage in NPH-RC patients, mean normalized counts of individual proteins were compared between controls and patients with CKD stage 1-2 (n=4), CKD

when the signal is lost_marijn_8072018.indd 135 08/07/2018 10:50

stage 3 (n=4) and CKD stage 4-5 (n=4), respectively. The mean normalized protein counts of down- and upregulated proteins were correlated with CKD stage in NPH-RC patients by showing increasing downregulation or upregulation with advancing disease stage ($P<0.05$) (**Figure 4**). The expression levels of the most highly abundant downregulated proteins (DPEP1 and FAT4) and upregulated protein (VCAN) clearly illustrated this correlation. These findings indicate enhanced deregulation of proteins within urinary EVs of patients with advanced CKD stage and suggest a prognostic value for the discriminating proteins.

6.3.3 Differentially expressed proteins show enrichment for signaling pathways and response to tissue damage

Enrichment analysis for gene ontology (GO) terms related to 1) biological processes, 2) cellular components, and 3) molecular functions as well as pathway analysis was performed to gain insight into the functionality of 156 discriminating markers in NPH-RC patients. Sixty-eight GO terms related to biological processes were significantly enriched among 114 downregulated proteins in patients. Top enriched GO terms included multiple signaling pathways, 'regulation of actin cytoskeleton reorganization' and 'regulation of endocytosis' (**Figure 5A**). Signaling pathways included 'insulin receptor signaling', 'FC-gamma receptor signaling' and 'small GTPase-mediated signal transduction'. Forty-two out of 156 proteins were upregulated. This number was too small for GO term and pathway analyses. To enable broader GO term and pathway analyses, a less stringent fold change of ≥3 was applied for upregulated proteins, resulting in 70 instead of 42 upregulated proteins. Among 70 upregulated proteins, 31 GO terms related to biological processes were significantly enriched, including 'positive regulation of cell-substrate adhesion', 'extracellular matrix organization' and 'response to wounding'. These results seem to reflect kidney damage in general, present in the NPH-RC patients, rather than ciliopathy-specific processes.

Overrepresented GO terms related to cellular components corresponding to both down- and upregulated proteins included 'extracellular exosome' and 'cytoplasmic vesicle', which are both related to EVs, 'adherens junction' and 'cortical cytoskeleton' (**Figure 5B**). Of note, there was a two- to threefold decrease in mean normalized spectral counts of EV markers TSG101 and PDCD6IP in patients compared to controls ($P=0.0025$, calculated using Mann-Whitney test), possibly accounting for the overrepresentation of EV-related GO terms among downregulated proteins. Enriched GO terms related to molecular function showed mainly terms related to enzymatic and binding activity (**Figure 5C**).

Pathway analysis was performed using ConsensusPathDB to identify overrepresented pathways among differentially expressed proteins [Kamburov et al., 2011]. Two major clusters of highly connected downregulated proteins were identified based on GO term analyses (**Supplementary Figure S3A**). Pathway analyses per cluster revealed an enrichment for pathways related to 'signaling', 'transport' and 'phagocytosis' (with overlapping genes involved), 'endocytosis' and 'adherens junctions' among downregulated proteins in both clusters (**Supplementary Figure S3B**). In the subgroup of patients with isolated

when the signal is lost_marijn_8072018.indd 136 08/07/2018 10:50

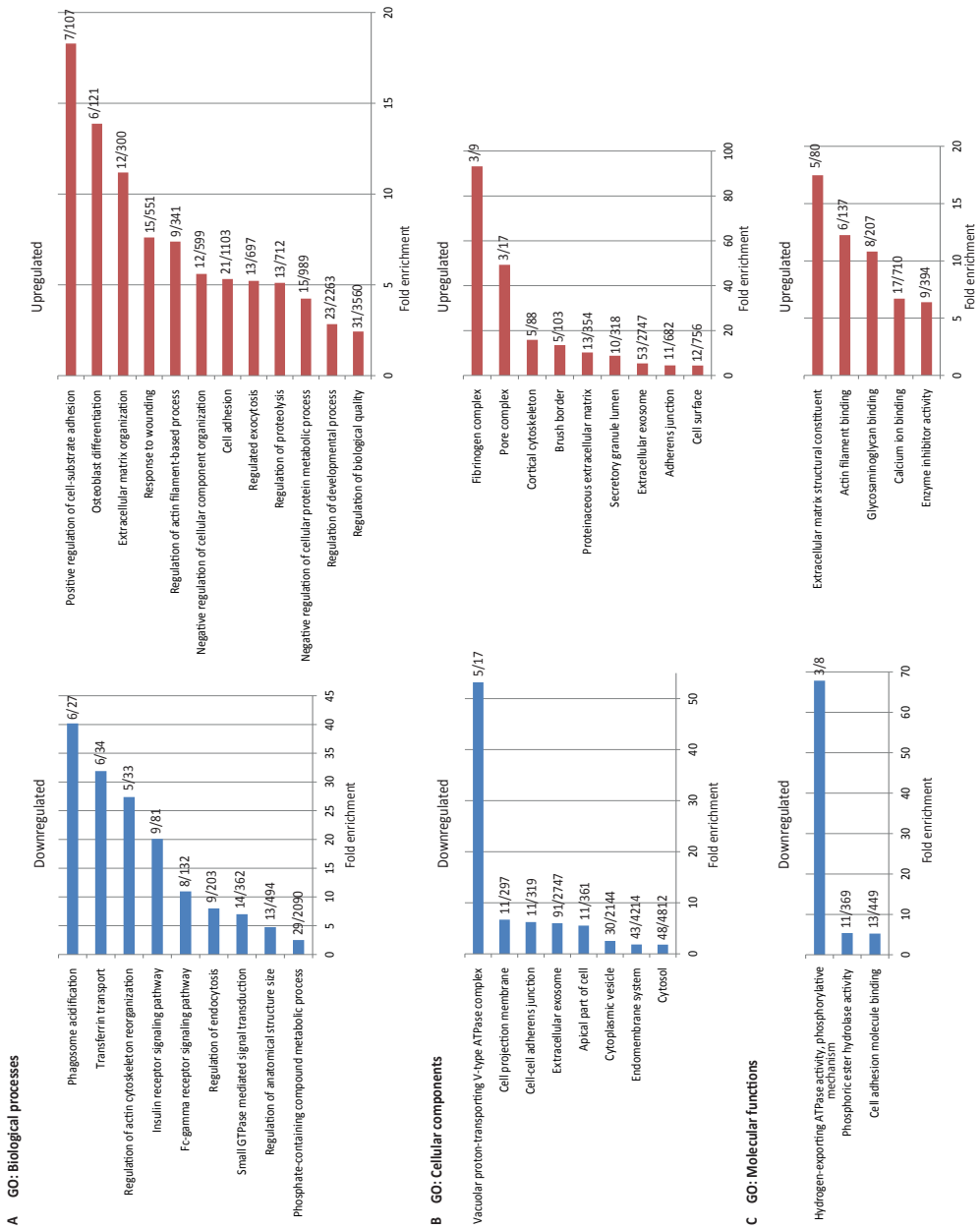

Figure 5. Results from gene ontology (GO) term enrichment analysis of differentially expressed proteins in urinary extracellular vesicles (EVs) from NPH-RC patients. GO terms related to **A.** overrepresented biological processes, **B.** cellular components, and **C.** molecular functions were

when the signal is lost_marijn_8072018.indd 137 08/07/2018 10:50

significantly associated with differentially expressed proteins in NPH-RC patients compared to controls by fold enrichment (P<0.05). Fraction represents the number of genes detected/ number of reference genes per GO term.

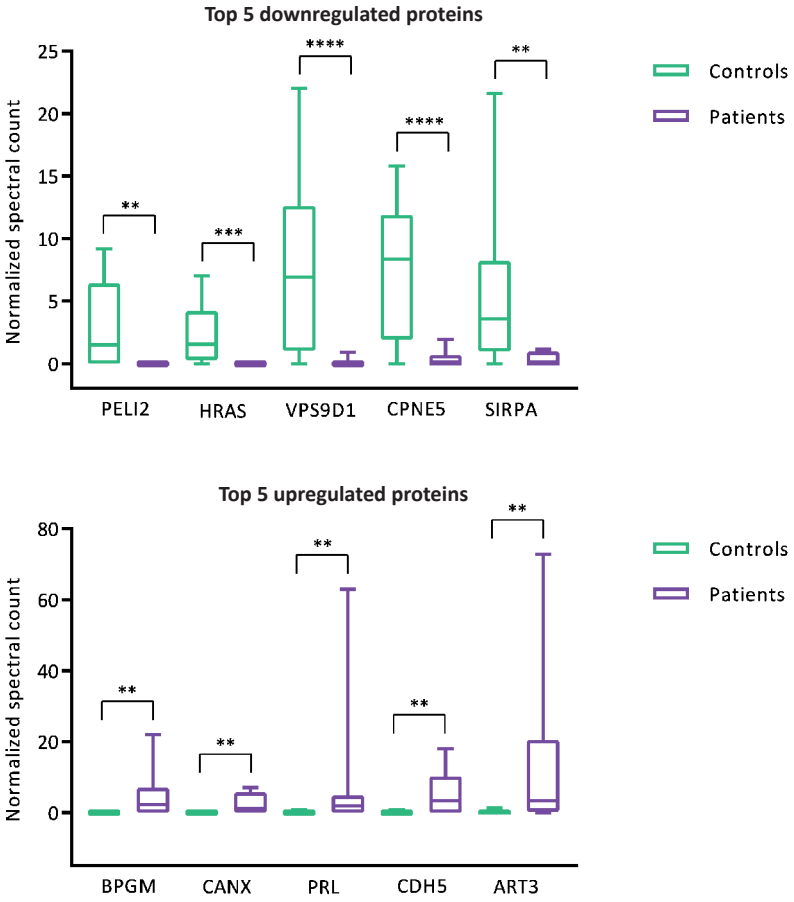

Figure 6. Box plots of top 5 most differentially expressed proteins in patients and controls based on normalized spectral counts. Lines and whiskers show mean, minimum and maximum values. **P<0.01, ***P<0.001, ****P<0.0001, calculated using Mann-Whitney test.

when the signal is lost_marijn_8072018.indd 138 08/07/2018 10:50

NPH (n=6), pathways enriched among downregulated proteins included specific cilia-associated pathways such as 'cargo trafficking to the periciliary membrane' (P=0.002) and the 'polycystic kidney disease pathway' (P=0.004) (data not shown). Significantly enriched pathways among three clusters of upregulated proteins comprised 'signaling', 'extracellular matrix organization', and 'coagulation and complement cascades' (**Supplementary Figure S3C** and **D**). These findings from pathway analyses, including overrepresentation of 'signaling' and 'endocytosis' pathways among downregulated proteins and 'extracellular matrix organization' pathways among upregulated proteins, were consistent with down- and upregulated GO terms.

6.3.4 Candidate biomarkers for nephronophthisis

The top five most discriminating downregulated proteins (PELI2, HRAS, VPS9D1, CPNE5, and SIRPA) and upregulated proteins (BPGM, CANX, PRL, CDH5, and ART3) based on fold change included two proteins (CANX and PRL) that have previously been reported to be upregulated in plasma and urine of patients with kidney diseases (**Figure 6**) [Kaneko et al., 2013; Triebel et al., 2015]. The other eight most discriminating proteins have not previously been described in the context of CKD and are potential novel biomarkers for ciliopathy-related CKD.

To assess the occurrence of cilia-associated proteins among potential biomarkers for NPH-RH, we used the SysCilia Gold Standard (Version 1) list of 303 confirmed ciliary genes (**Supplementary Table S3**) [Van Dam et al., 2013]. Five out of 156 differentially expressed proteins corresponded to known ciliary genes. Four proteins (PKD1, ARL13B, SMO, and RP2; **Supplementary Figure S4A-D**) were downregulated (average fold changes 9.9, 6.8, 4.5, and 4.1 respectively; $P<0.05$) and one protein (FLNA) was upregulated (fold change 4.0) in urinary EVs of NPH-RC patients (**Supplementary Figure S4E**). Ciliopathy genes that were mutated in the NPH-RC patients (**Supplementary Table S2**) were not represented in the downregulated ciliary proteins, suggesting that gene mutations globally affect ciliary pathways and are not restricted to a narrow effect.

A PubMed literature search was performed to list proteins expressed in whole urine that were previously associated with CKD (**Supplementary Methods S1** and **Supplementary Table S4**). Comparison of 70 CKD-associated proteins acquired from the literature with the 156 discriminating markers in our NPH-RC cohort showed that 3/156 proteins correspond to known CKD-associated urinary proteins. Of these, two proteins (MMP7 and PLTP) were upregulated in NPH-RC patients described in the current study, corresponding to the direction of fold change described in literature [Zhou et al., 2016; Craciun et al., 2016]. One downregulated protein in NPH-RC patients (ACE2) showed a different direction of fold change in urinary EVs compared to the direction of fold change described in literature [Abe et al., 2015]. This could be the result of the different compartment that was analyzed, namely urinary EVs instead of whole urine.

when the signal is lost_marijn_8072018.indd 139 08/07/2018 10:50

6.4 DISCUSSION

Here we report that protein expression profiles in urinary EVs can distinguish NPH-RC patients (n=12) from healthy controls (n=12) that were analyzed as individual samples. By using an in-depth proteomics analysis using 140 nanoLC-MS/MS runs on a high resolution fast scanning tandem mass spectrometer, combined with statistical and quantitative filtering, we identified 156 promising candidate protein biomarkers. Importantly, expression levels of the most discriminating proteins were associated with CKD stage in patients, suggesting a relation to disease-state and a potential prognostic value. Thus, urinary EVs form a promising non-invasive source of biomarkers for early detection and prognostics of nephronophthisis. Further research is needed to determine the specificity of these candidate biomarkers for NPH-RC.

Underscoring the validity of our systematic and unbiased interrogation of differentially expressed proteins in biofluid of NPH-RC patients, we found a significant upregulation of neutrophil gelatinase-associated lipocalin (NGAL) protein in NPH-RC patients (fold change 2.4, $P<0.05$). NGAL is the only biomarker for kidney injury in general that was previously identified in NPH-RC patients. An elevation of serum and whole urine NGAL protein levels has been reported in three patients with nephronophthisis-related Joubert syndrome [Lacquaniti et al., 2012]. This makes NGAL an interesting biomarker for further investigation.

GO terms and pathways enriched among proteins downregulated in NPH-RC patients were related to signaling, actin cytoskeleton reorganization and endocytosis. This could reflect a role for these proteins in cilia formation and in ciliary signaling pathways including the mTOR signaling pathway that was enriched among downregulated proteins. Alternatively, these GO terms and pathways could reflect a role in the (EV-mediated) response to kidney damage in general, similar to enriched GO terms and pathways among upregulated proteins, which were associated with extracellular matrix organization and response to wounding. Consequently, it is unclear whether the overrepresented pathways identified in this study point towards ciliopathy-specific disease mechanisms. Although cilia-associated pathways were overrepresented among downregulated proteins in patients with isolated nephronophthisis, including 'cargo trafficking to the periciliary membrane' and the 'polycystic kidney disease pathway', the limited number of patients per NPH-RC subgroup precludes firm conclusions about differences in pathogenesis of various NPH-RC syndromes.

The 114 discriminating downregulated proteins in urinary EVs of patients included cilia-associated proteins ARL13B, PKD1, RP2 and SMO. In addition, the top 20 downregulated proteins included the recently validated ciliary protein serine/threonine-protein kinase 11 (STK11) [Mick et al., 2015; Boehlke et al., 2010]. Previous studies in polycystic kidney disease (PKD) patients have demonstrated significantly different expression levels of cilia-specific membrane proteins in urine EVs of patients compared to controls, supporting our finding that ciliary proteins are present in urine EVs and that their abundance can reflect disease state [Hogan et al., 2015; Chacon-Heszele et al., 2014]. Although the 156 discriminating markers

when the signal is lost_marijn_8072018.indd 140 08/07/2018 10:50

could contain novel ciliary proteins, these proteins are also in part associated with CKD in general. As a result, the single cilia-associated proteins discussed above could be more specific biomarkers for nephronophthisis than the discriminating set of 156 proteins.

Two of the top five most discriminating upregulated proteins, calnexin (CANX) and prolactin (PRL), have previously been implicated in kidney diseases. CANX is a calcium-binding protein involved in the retention of incorrectly folded proteins within the endoplasmatic reticulum. CANX showed higher expression levels in plasma of renal cell carcinoma patients compared to controls [Kaneko et al., 2013]. A study in patients with diabetic nephropathy demonstrated increased levels of PRL in urine of patients compared to controls [Triebel et al., 2015]. Our study corroborates that CANX and PRL are CKD-associated markers and identifies additional discriminating proteins including ART3 and CDH5 as candidate biomarkers for (ciliopathy-related) CKD. These highly differentially expressed proteins should be investigated further in larger NPH-RC patient cohorts.

The upregulated proteins that showed a strong correlation with CKD stage included Versican core protein (VCAN) (**Figure 3**). VCAN is an extracellular matrix proteoglycan with normally low expression in kidneys [Uhlen et al., 2015]. Higher mRNA expression of VCAN in renal biopsies was reported to be correlated to histologic damage and progression of CKD [Rudnicki et al., 2012]. By contrast, Dipeptidase 1 (DPEP1) and Protocadherin Fat 4 (FAT4) were decreased in urinary EVs of patients. DPEP1 is a kidney-specific protein that is involved in the metabolism of several proteins by dipeptide hydrolysis. In line with our findings, DPEP1 was found to be downregulated in the urine of focal segmental glomerulosclerosis (FSGS) patients compared to controls [Nafar et al., 2014]. FAT4 is a planar cell polarity protein that localizes to cilia in kidney cells [Saburi et al., 2008]. Importantly, loss of *Fat4* causes cystic kidney disease in mice [Saburi et al., 2008]. The connection to cilia and cystic kidney disease makes FAT4 an interesting candidate biomarker for nephronophthisis. In addition, although FAT4 is not among the top five most discriminating markers based on fold change, its association with disease severity indicates potential prognostic value.

This study has several limitations. First, we did not investigate the specificity of the differentially expressed proteins. Therefore, comparison with a cohort of patients with early-onset CKD due to other causes is required to discern whether our findings are specific for NPH-RC or reflect CKD in general. Second, the identified markers need to be validated in larger patient cohorts in order to be able to stratify for disease subgroups. Third, longitudinal follow-up of individuals will establish whether urinary EV protein signatures can accurately predict disease onset in individuals with biallelic NPH-mutations and serve as prognostic markers.

when the signal is lost_marijn_8072018.indd 141 08/07/2018 10:50

6.5 CONCLUSIONS

To our knowledge this is the first report on an in-depth clinical proteomics dataset of global urinary EVs proteomics in well-characterized NPH-RC patients. Our data show that measuring protein profiles in urinary EVs is a promising approach for non-invasive early diagnostics and prognostics in patients with NPH-RC. Since the current diagnostics and prognostics toolbox for nephronophthisis is far from complete, early biomarkers indicative of disease will be of great benefit to NPH-RC patients and their relatives.

Acknowledgments
We thank the patients, healthy control individuals, and parents for participation in this study and donating urine samples. The authors thank Albertien M. van Eerde (Department of Genetics, UMC Utrecht), Marie-Jose H. van den Boogaard (Department of Genetics, UMC Utrecht), Hester Y. Kroes (Department of Genetics, UMC Utrecht), Mandy G. Keijzer-Veen (Department of Pediatric Nephrology, UMC Utrecht) and Mieke M. van Haelst (Department of Medical Genetics, VUMC) for their clinical contribution and Adele van Dijk (Department of Nephrology, UMC Utrecht) for measurement of protein and creatinine in urine samples. This study was financially supported by an Impulsion Grant of the ERA-EDTA Working Group on Inherited Kidney Disorders (WGIKD) to K.Y.R. The researchers received funding from the Dutch Kidney Foundation under grant agreement CP11.18; Kouncil to N.V.A.M.K. and the European Community's Seventh Framework Programme (FP7/2009) under grant agreement 305608; EURenOmics to N.V.A.M.K.

when the signal is lost_marijn_8072018.indd 142 08/07/2018 10:50

SUPPLEMENTARY MATERIAL

A.

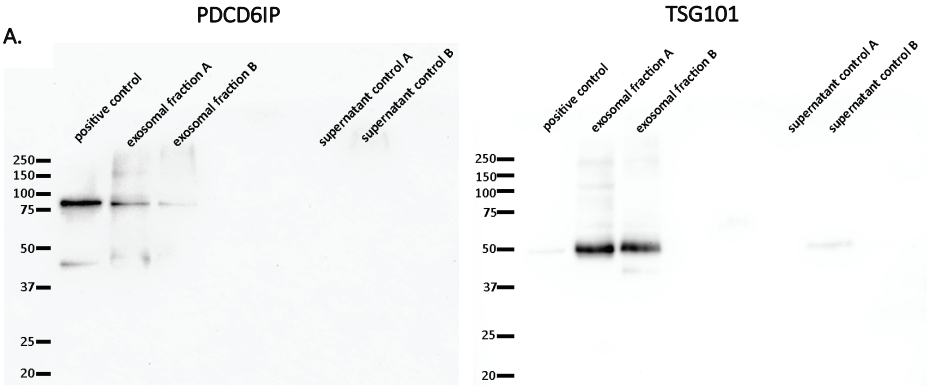

B.

Protein description	Gene symbol	Mean spectral count controls	Mean spectral count patients	Fold change	P-value
Programmed cell death 6-interacting protein	PDCD6IP	440.63	221.23	-2.05	9.43E-04
Tumor susceptibility gene 101 protein	TSG101	118.51	48.27	-2.64	6.19E-06

Supplementary Figure S1. Detection of extracellular vesicle markers. **A.** Western blot showing detectable levels of extracellular vesicle (EV)-related proteins PDCD6IP and TSG101 in EVs isolated from urine samples of control subjects A and B. Levels of EV-related proteins were low in the EV-depleted urine fraction, indicative of a near complete EV-isolation. **B.** Levels of EV markers quantified with LC-MS/MS.

when the signal is lost_marijn_8072018.indd 143 08/07/2018 10:50

Supplementary Methods S1. *Known CKD-associated genes*

A PubMed search was performed on November 6th 2016 using the following search terms: ("Proteomics"[Title/Abstract] OR "protein*"[Title/Abstract] OR "peptide*"[Title/Abstract]) AND ("urine"[Title/Abstract] OR "urinary"[Title/Abstract]) AND ("CKD"[Title/Abstract] OR "kidney disease"[Title/Abstract] OR "renal disease"[Title/Abstract] OR "kidney failure"[Title/Abstract] OR "renal failure"[Title/Abstract]). The search yielded 719 articles. Subsequent selection of English language articles describing studies in humans investigating CKD in general, kidney fibrosis, tubulointerstitial kidney disease or NPH-RC but no other subclassifications of kidney disease yielded 14 articles published since 2015. Many studies contained validations of discriminating proteins previously identified by Good et al. and included in the CKD273 classifier [Good et al., 2010]. The CKD273 classifier comprises 273 peptides corresponding to 30 proteins that differentiate healthy subjects from patients with CKD. Proteins included in the CKD273 classifier that were not recently validated (n=7) were also included (**Supplementary Table S4**).

when the signal is lost_marijn_8072018.indd 144 08/07/2018 10:50

when the signal is lost_marijn_8072018.indd 145

Supplementary Table S1. *Differentially expressed proteins (n=156)*

Accession Number	Gene Symbol	Fold change	P-value	Positive patient samples (of 12)	Positive control samples (of 12)	Mean counts positive patients	Mean counts positive controls	Mean counts all patients	Mean counts all controls
Q9HAT8	PELI2	∞	1.0E-06	0	8	Only in controls	4.8	0.0	3.2
P01112	HRAS	∞	1.9E-06	0	9	Only in controls	3.4	0.0	2.5
Q9Y2B5	VPS9D1	-44.3	3.2E-11	1	10	0.9	8.7	0.1	7.3
Q9HCH3	CPNE5	-17.1	1.5E-10	3	11	1.3	8.3	0.3	7.6
P78324	SIRPA	-15.2	8.4E-08	4	10	1.0	6.6	0.3	5.5
Q9HBH0	RHOF	-14.7	5.0E-11	5	12	1.2	8.5	0.5	8.5
Q9Y334-2	VWA7	-13.2	2.9E-07	2	12	1.4	3.3	0.2	3.3
Q9NQE9	HINT3	-12.9	7.8E-07	3	12	1.0	3.2	0.3	3.2
P31937	HIBADH	-12.9	2.1E-05	1	8	1.0	3.6	0.1	2.4
Q16864	ATP6V1F	-11.4	2.8E-06	3	9	1.1	5.8	0.3	4.3
A6NDG6	PGP	-10.8	4.3E-07	3	11	1.4	4.8	0.4	4.4
P98161-2	PKD1	-9.9	2.6E-06	2	10	1.4	4.7	0.2	3.9
Q9H173	SIL1	-9.3	1.4E-06	1	10	3.0	4.4	0.2	3.6
P13598	ICAM2	-9.2	3.1E-05	2	10	1.0	2.6	0.2	2.2
O15194	CTDSPL	-8.9	8.5E-07	2	10	1.9	4.9	0.3	4.1
Q15831-2	STK11	-8.9	2.4E-06	2	9	1.4	5.4	0.2	4.0
O60613	SEP15	-8.4	4.6E-04	1	9	1.3	2.0	0.1	1.5
Q9GZU7-2	CTDSP1	-8.0	7.8E-05	2	9	0.8	3.0	0.1	2.3
Q9HAC8	UBTD1	-7.5	4.3E-07	4	11	2.1	6.3	0.7	5.8
Q9P2R3	ANKFY1	-7.4	2.2E-06	4	8	2.3	10.9	0.8	7.2
P0C7U0	ELFN1	-7.4	2.1E-06	3	12	2.2	3.6	0.6	3.6
Q6B0K9	HBM	-7.2	1.9E-04	4	10	1.0	3.3	0.3	2.8
Q8NFZ8	CADM4	-7.0	1.3E-07	3	9	2.5	9.3	0.6	7.0
O00757	FBP2	-6.9	3.0E-05	3	12	1.8	2.8	0.4	2.8
Q3SXY8	ARL13B	-6.8	1.3E-08	7	12	2.2	9.0	1.3	9.0

08/07/2018 10:50

Q96H20	SNF8	-6.7	4.2E-09	5	11	3.2	12.6	1.3	11.6
O60704	TPST2	-6.7	3.9E-07	4	12	2.6	5.8	0.9	5.8
O95630	STAMBP	-6.6	6.0E-07	1	8	4.5	8.1	0.4	5.4
Q86VN1	VPS36	-6.5	6.8E-09	8	12	2.0	13.5	1.4	13.5
O95398-3	RAPGEF3	-6.4	2.3E-09	6	12	3.5	13.4	1.8	13.4
Q6PHR2	ULK3	-6.2	1.2E-08	7	12	4.2	13.0	2.4	13.0
Q96F10	SAT2	-6.1	1.3E-05	3	9	3.1	6.2	0.8	4.7
P06870-2	KLK1	-6.0	2.5E-09	10	12	3.7	17.9	3.1	17.9
Q9C0K7-2	STRADB	-6.0	4.2E-05	5	11	1.1	3.3	0.5	3.0
Q96LB4	ATP6V1G3	-5.8	5.2E-04	2	8	1.5	3.3	0.2	2.2
Q53TN4-3	CYBRD1	-5.8	7.4E-07	6	12	3.0	7.6	1.5	7.6
Q96BJ3	AIDA	-5.8	5.6E-04	1	8	1.5	2.5	0.1	1.7
P45381	ASPA	-5.7	1.5E-06	2	11	4.4	5.2	0.7	4.8
P16066	NPR1	-5.6	2.3E-04	3	10	1.5	2.7	0.4	2.3
Q9H7P6	MVB12B	-5.6	1.2E-07	3	10	3.4	8.5	0.8	7.1
Q8WW52	FAM151A	-5.6	1.2E-09	6	12	5.4	15.5	2.7	15.5
Q6P1N0-2	CC2D1A	-5.4	4.3E-08	2	8	6.0	14.4	1.0	9.6
P35270	SPR	-5.3	4.0E-04	3	10	1.4	2.5	0.4	2.1
Q9UQB8-5	BAIAP2	-5.3	2.0E-10	5	11	14.6	26.5	6.1	24.3
P21926	CD9	-5.3	4.5E-05	4	9	2.0	5.3	0.7	4.0
O60658	PDE8A	-5.3	5.1E-06	3	9	2.3	7.9	0.6	5.9
P15151-3	PVR	-5.3	5.2E-07	9	12	2.7	9.6	2.0	9.6
Q86UN3	RTN4RL2	-5.1	1.3E-07	4	11	4.7	8.8	1.6	8.1
Q9UKG1	APPL1	-5.1	4.7E-06	3	10	6.2	10.5	1.6	8.7
Q9UKW4-3	VAV3	-4.9	2.8E-04	2	9	2.3	3.3	0.4	2.5
P07948	LYN	-4.9	1.6E-07	8	12	4.9	14.3	3.3	14.3
Q16651	PRSS8	-4.9	4.1E-05	5	10	2.1	5.2	0.9	4.3
P05981	HPN	-4.8	3.6E-04	3	10	1.9	2.9	0.5	2.4
Q9BQ51	PDCD1LG2	-4.8	3.6E-04	4	9	1.7	4.0	0.6	3.0

when the signal is lost_marijn_8072018.indd 146 08/07/2018 10:50

Q9BYF1	ACE2	-4.8	8.9E-08	4	11	3.6	9.0	1.2	8.2
Q9UBR1	UPB1	-4.7	3.8E-04	2	9	4.6	4.5	0.8	3.4
Q9HBG4	ATP6V0A4	-4.7	3.5E-11	7	12	9.7	29.1	5.7	29.1
Q9UBP0-3	SPAST	-4.6	1.3E-06	1	9	8.1	7.5	0.7	5.6
P62330	ARF6	-4.6	2.8E-05	6	11	2.6	7.0	1.3	6.4
P41181	AQP2	-4.6	1.0E-05	5	11	4.2	7.4	1.7	6.8
Q8TF65	GIPC2	-4.5	8.8E-04	4	10	1.3	2.8	0.4	2.3
Q9UHR4	BAIAP2L1	-4.5	6.7E-09	9	12	6.1	23.9	4.6	23.9
Q99835	SMO	-4.5	3.3E-06	8	12	4.2	11.8	2.8	11.8
P09467	FBP1	-4.5	9.5E-09	10	12	7.6	32.4	6.4	32.4
Q96PU5-4	NEDD4L	-4.5	1.5E-06	2	8	3.8	10.1	0.6	6.8
Q8IZF2-2	ADGRF5	-4.5	3.7E-06	5	11	2.5	6.5	1.1	6.0
O75348	ATP6V1G1	-4.5	3.5E-06	8	11	2.1	8.2	1.4	7.5
P46108-2	CRK	-4.4	2.3E-04	1	8	3.6	4.4	0.3	2.9
Q4KMG9-2	TMEM52B	-4.4	3.9E-06	3	11	6.7	6.8	1.7	6.2
P61018	RAB4B	-4.4	1.3E-03	3	9	1.3	2.7	0.3	2.0
Q9Y5K8	ATP6V1D	-4.4	1.8E-07	9	11	2.8	16.7	2.1	15.3
P07947	YES1	-4.3	2.9E-06	7	12	4.4	9.1	2.5	9.1
P61224-3	RAP1B	-4.3	2.0E-03	4	10	1.0	2.0	0.3	1.7
P16444	DPEP1	-4.2	2.6E-08	12	12	24.4	90.0	24.4	90.0
Q8N8Y2	ATP6V0D2	-4.2	1.8E-06	3	12	5.0	5.8	1.2	5.8
Q9BUH6	C9orf142	-4.2	1.4E-03	3	10	1.9	2.6	0.5	2.1
P20339-2	RAB5A	-4.1	8.0E-04	4	10	1.9	3.4	0.6	2.8
P51580	TPMT	-4.1	3.1E-04	3	9	1.8	3.7	0.4	2.8
O75695	RP2	-4.1	1.5E-03	2	8	3.1	4.0	0.5	2.7
Q99523-2	SORT1	-4.0	6.1E-04	4	10	2.1	3.5	0.7	3.0
P11117	ACP2	-4.0	8.7E-08	10	12	10.3	22.0	8.6	22.0
Q8N392	ARHGAP18	-4.0	1.6E-09	3	10	11.8	24.1	2.9	20.1
P08582	MELTF	-4.0	1.7E-08	4	9	10.4	20.5	3.5	15.4

when the signal is lost_marijn_8072018.indd 147 08/07/2018 10:50

P54289-4	CACNA2D1	-4.0	2.4E-08	4	12	6.8	13.1	2.3	13.1
Q6V0I7-3	FAT4	-4.0	2.9E-08	8	12	25.3	60.6	16.9	60.6
Q9Y5K6	CD2AP	-4.0	4.0E-08	3	9	20.3	19.8	5.1	14.9
Q12923-3	PTPN13	-4.0	8.5E-08	5	8	12.6	30.5	5.2	20.3
P34913	EPHX2	-4.0	2.7E-07	8	12	6.5	17.2	4.4	17.2
Q8TE68	EPS8L1	-4.0	3.5E-07	10	11	9.0	31.6	7.5	28.9
Q7Z4W1	DCXR	-4.0	7.7E-07	9	12	6.9	17.6	5.2	17.6
Q8WZ75-2	ROBO4	-4.0	1.3E-06	8	12	8.7	17.3	5.8	17.3
P51178	PLCD1	-4.0	2.5E-06	6	12	6.5	10.0	3.3	10.0
Q8NI35	PATJ	-4.0	4.8E-06	3	8	9.0	11.9	2.3	8.0
Q8NBJ4-2	GOLM1	-4.0	5.8E-06	6	10	2.7	9.2	1.3	7.6
Q9NQA5	TRPV5	-4.0	9.8E-06	7	12	8.7	12.9	5.1	12.9
Q8N3R9	MPP5	-4.0	1.1E-05	7	11	4.7	9.8	2.7	9.0
Q9Y274	ST3GAL6	-4.0	1.4E-05	4	9	2.9	7.0	1.0	5.3
Q8N307-3	MUC20	-4.0	1.5E-05	7	11	4.5	11.0	2.6	10.1
Q12794-2	HYAL1	-4.0	1.6E-05	3	10	3.8	6.3	1.0	5.2
O43511	SLC26A4	-4.0	1.8E-05	4	10	8.1	10.1	2.7	8.4
Q9P0V3	SH3BP4	-4.0	2.9E-05	3	10	7.5	9.4	1.9	7.8
Q99747	NAPG	-4.0	4.6E-05	4	10	4.8	7.7	1.6	6.4
Q9Y6W5	WASF2	-4.0	5.0E-05	4	10	3.3	6.8	1.1	5.6
O43895	XPNPEP2	-4.0	5.4E-05	5	10	5.3	7.7	2.2	6.5
P16885	PLCG2	-4.0	6.9E-05	3	9	8.7	10.9	2.2	8.2
O96013	PAK4	-4.0	8.1E-05	5	8	3.5	10.6	1.5	7.1
P05937	CALB1	-4.0	8.1E-05	2	8	9.2	8.0	1.5	5.3
O00401	WASL	-4.0	1.5E-04	3	10	4.6	4.5	1.2	3.7
P12955	PEPD	-4.0	1.9E-04	2	11	6.1	3.5	1.0	3.2
Q9UJJ9	GNPTG	-4.0	2.1E-04	6	10	1.8	5.4	0.9	4.5
Q9NVS9-3	PNPO	-4.0	2.9E-04	5	10	3.0	6.2	1.3	5.1
O75144	ICOSLG	-4.0	4.1E-04	4	11	3.8	4.1	1.3	3.7
P57735	RAB25	-4.0	1.8E-03	2	11	2.8	2.1	0.5	1.9
P32754-2	HPD	-4.0	4.5E-03	2	9	2.3	2.1	0.4	1.6

when the signal is lost_marijn_8072018.indd 148 08/07/2018 10:50

when the signal is lost_marijn_8072018.indd 149

P07738	BPGM	∞	1.0E-07	8	0	6.7	Only in patients	4.5	0.0
P27824	CANX	∞	7.1E-06	8	0	3.8	Only in patients	2.5	0.0
P01236	PRL	33.2	1.3E-07	8	1	11.4	0.9	7.6	0.1
P33151	CDH5	18.0	2.0E-08	8	2	8.2	0.9	5.5	0.1
Q13508	ART3	17.4	3.8E-10	9	3	19.1	1.2	14.3	0.3
Q92688-2	ANP32B	16.7	1.1E-07	10	2	4.7	0.9	3.9	0.2
P19338	NCL	15.0	1.1E-08	8	2	11.0	0.9	7.3	0.2
P39687	ANP32A	13.8	4.1E-08	8	3	9.8	1.2	6.5	0.3
P09237	MMP7	12.4	5.2E-07	10	4	7.4	1.2	6.1	0.4
P02792	FTL	12.1	7.8E-07	10	3	6.0	1.1	5.0	0.3
O60234	GMFG	11.4	1.7E-05	8	3	6.2	0.9	4.1	0.2
Q01082	SPTBN1	11.1	1.5E-09	11	5	10.7	1.5	9.8	0.6
Q13421-4	MSLN	8.9	2.8E-07	8	1	10.1	3.9	6.7	0.3
P00740	F9	8.9	8.3E-13	12	6	39.0	5.4	39.0	2.7
P13866	SLC5A1	7.9	1.5E-06	9	5	8.9	1.7	6.7	0.7
P14314-2	PRKCSH	7.7	6.0E-11	9	5	57.4	9.2	43.1	3.8
Q92530	PSMF1	6.7	8.8E-04	9	2	2.5	0.9	1.8	0.2
Q13813	SPTAN1	6.7	1.2E-06	8	3	12.3	1.9	8.2	0.5
P24821	TNC	6.6	3.9E-08	8	5	29.9	2.7	19.9	1.1
P23142	FBLN1	6.5	2.7E-09	9	6	30.8	3.1	23.1	1.6
O75367-2	H2AFY	6.2	2.4E-04	8	3	4.3	1.3	2.9	0.3
Q01105	SET	6.1	4.7E-09	12	7	12.6	3.2	12.6	1.8
P07360	C8G	6.0	7.4E-06	10	4	6.0	2.3	5.0	0.8
P13611	VCAN	5.9	3.4E-10	12	9	112.9	23.8	112.9	17.8
Q8WXI7	MUC16	5.6	1.4E-04	8	2	4.8	2.6	3.2	0.4

08/07/2018 10:50

P98095	FBLN2	5.4	1.6E-07	8	3	23.6	9.6	15.7	2.4
Q99972	MYOC	5.2	1.1E-07	8	3	19.6	3.6	13.1	0.9
P09382	LGALS1	4.5	1.6E-05	10	8	7.3	1.1	6.1	0.8
P22223-2	CDH3	4.5	1.2E-03	8	4	4.0	1.5	2.7	0.5
P09871	C1S	4.5	5.9E-06	11	6	10.3	2.6	9.4	1.3
P49747	COMP	4.4	4.1E-07	10	8	15.8	2.7	13.2	1.8
P55058	PLTP	4.3	1.6E-04	12	7	4.2	1.5	4.2	0.9
P07225	PROS1	4.2	2.2E-07	8	6	28.2	4.2	18.8	2.1
P08519	LPA	4.1	8.7E-04	8	5	5.2	1.6	3.5	0.7
Q99878	HIST1H2AJ	4.1	2.3E-05	12	7	7.5	3.6	7.5	2.1
Q14314	FGL2	4.0	2.0E-07	12	10	43.7	16.6	43.7	13.8
P35579	MYH9	4.0	3.1E-07	11	8	41.8	12.1	38.3	8.0
Q9BXP8	PAPPA2	4.0	2.0E-06	11	8	28.9	11.1	26.5	7.4
Q9Y490	TLN1	4.0	2.6E-06	11	9	32.5	3.2	29.8	2.4
P06737-2	PYGL	4.0	6.1E-06	10	7	22.2	3.1	18.5	1.8
P21333-2	FLNA	4.0	5.4E-05	8	5	29.3	7.0	19.5	2.9
Q96S37-2	SLC22A12	4.0	2.9E-03	8	3	3.6	1.3	2.4	0.3

Differentially expressed proteins showed 114 downregulated proteins (fold change in blue) and 42 upregulated proteins (fold change in red) in urinary extracellular vesicles (EVs) from patients with nephronophthisis-related ciliopathy (NPH-RC) compared to matched controls ($P<0.05$, fold change ≥ 4, detected in at least 8 of 12 patient samples, with a mean normalized count in positive samples of ≥ 2). ∞ Protein uniquely present in controls (blue) or patients (red).

when the signal is lost_marijn_8072018.indd 150 08/07/2018 10:50

Supplementary Table S2. *Genetic findings in patients*

Patient	Sex	Age	CKD stage	Diagnosis	Gene	Mutation	Reference	Matched control #
1	M	15	3	NPH	NA	NA	NA	10
2	M	12	2	BBS	*BBS10*	c.[271dupT];[271dupT] p.[(Cys91SerfsX5)];[(Cys91SerfsX5)]	[Stoetzel et al., 2006]	3
3	M	12	3	JBTS	*NPHP1*	150kb homozygous deletion[b]	NA	4
4	M	24	3	JBTS	*AHI1*	c.[910_911insA];[2057_2060delAAAC] p.[(Thr304fs0];[(Asn686fs)]	[Kroes et al., 2008; Valente et al., 2006]	6
5[a]	M	16	3	CED	*WDR35*	c.[2891delT];[2623G>A] p.[(Pro964LeufsX15)];[(p.Ala875Thr)]	[Gilissen et al., 2010]	8
6[a]	F	11	1	CED	*WDR35*	c.[2891delT];[2623G>A] p.[(Pro964LeufsX15)];[(p.Ala875Thr)]	[Gilissen et al., 2010]	9
7	F	17	4-5	NPH	*NPHP1*	c.[?_-94_*455_?del];[?_-94_*455_?del] p.[(?)];[(?)]	NA	2
8	F	21	5	NPH	NA	NA	NA	7
9	M	10	4	NPH	*NPHP1*	c.[1027G>A];[1-?_2034+?del] p.[(Gly343Arg)];[(?)]	[Caridi et al., 2006b]	5
10	F	18	2	NPH	*NPHP4*	c.[271T>C];[122C>T][c] p.[(Phe91Leu)];[(Pro41Leu)]	[Hoefele et al., 2005]	1
11	F	14	2	BBS	*BBS1*	c.[1169T>G];[1169T>G] p.[(Met390Arg)];[(Met390Arg)]	[Mykytyn et al., 2002]	11
12	F	6	4	NPH	*NPHP1*	c.[1-?_2202+?del];[1-?_2202+?del] p.[(?)];[(?)]	NA	12

M: male; F: female; NPH: isolated nephronophthisis; BBS: Bardet-Biedl syndrome; CED: cranioectodermal dysplasia (Sensenbrenner syndrome); JBTS: Joubert syndrome; NA: not available. [a]Patient 5 and 6 are siblings. [b]Location of deletion is not reported in medical records. [c]Variant of unknown significance.

when the signal is lost_marijn_8072018.indd 151 08/07/2018 10:50

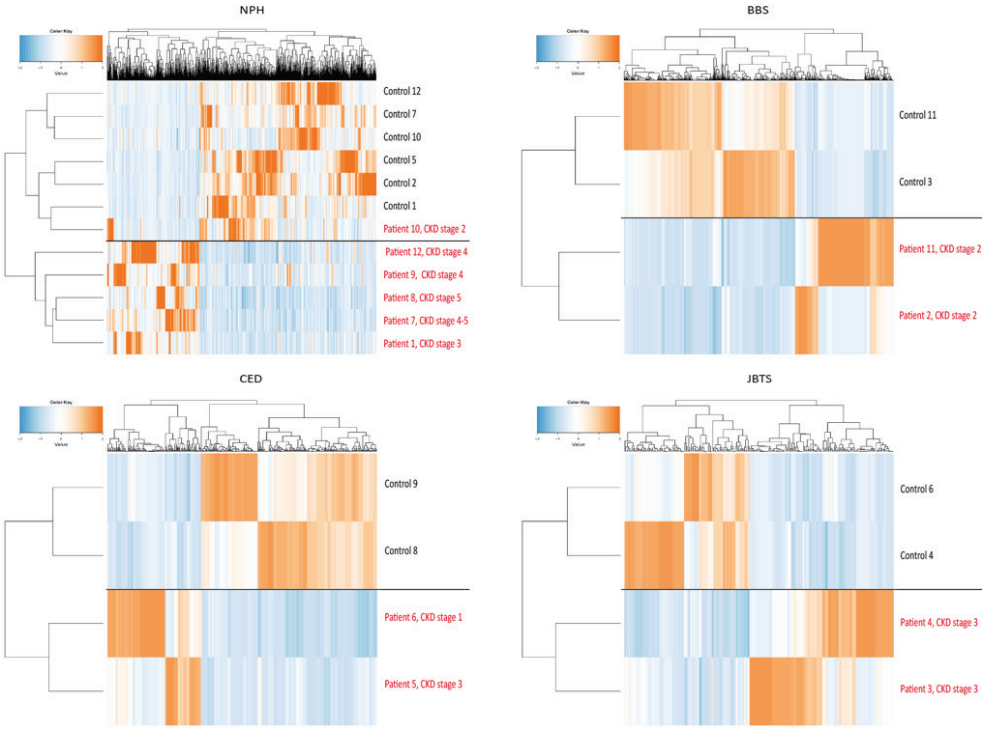

Supplementary Figure S2. Supervised hierarchical clustering of normalized protein counts in patients from stratified nephronophthisis-related ciliopathy (NPH-RC) subgroups and controls. Cluster analysis shows near-complete separation between patients and controls based on proteomic profiles in all diagnostic subgroups. Within the NPH subgroup, patient 10 clusters with controls. Blue color represents downregulated proteins and orange color represents upregulated proteins. NPH: isolated nephronophthisis; BBS: Bardet-Biedl syndrome; CED: cranioectodermal dysplasia (Sensenbrenner syndrome); JBTS: Joubert syndrome.

when the signal is lost_marijn_8072018.indd 152 08/07/2018 10:50

A. Downregulated proteins

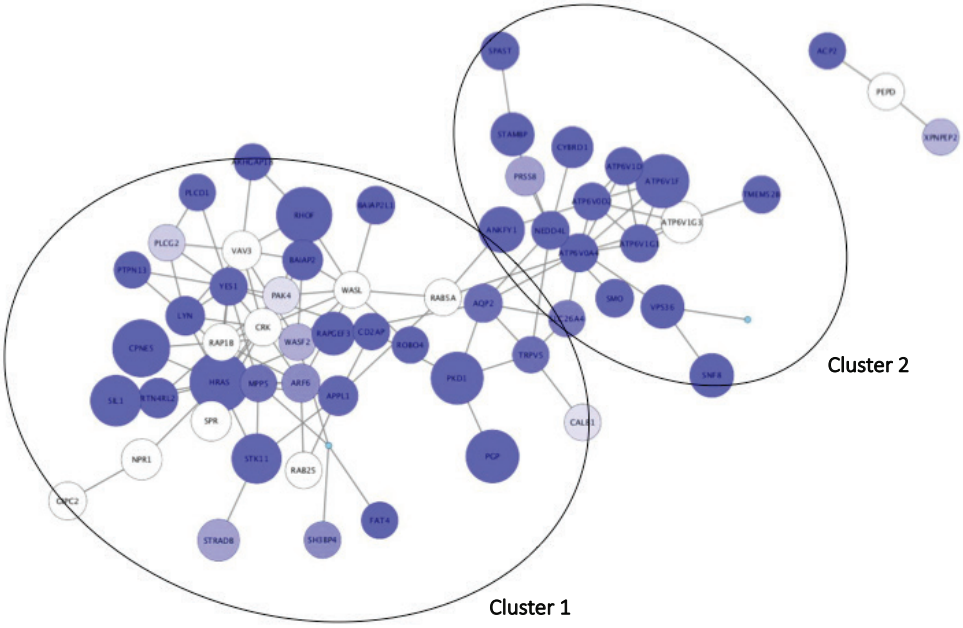

B. Cluster 1 - downregulated proteins

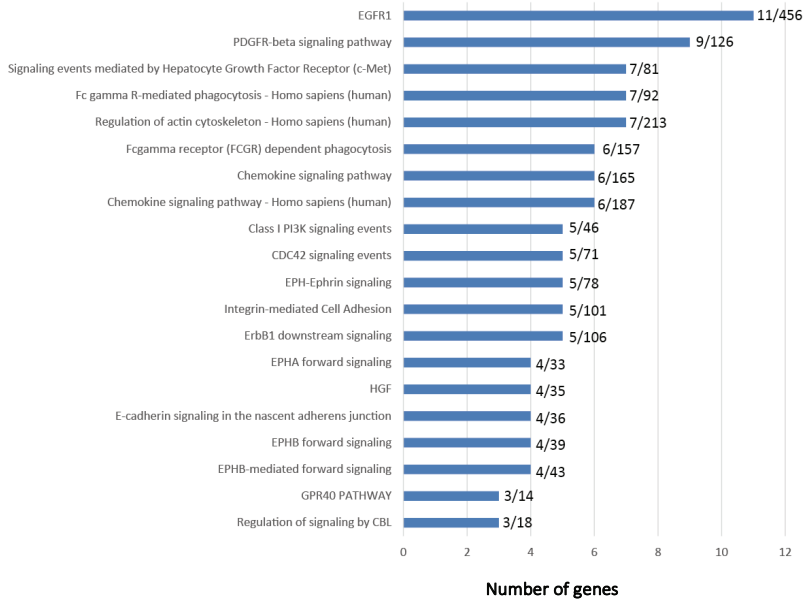

when the signal is lost_marijn_8072018.indd 153 08/07/2018 10:50

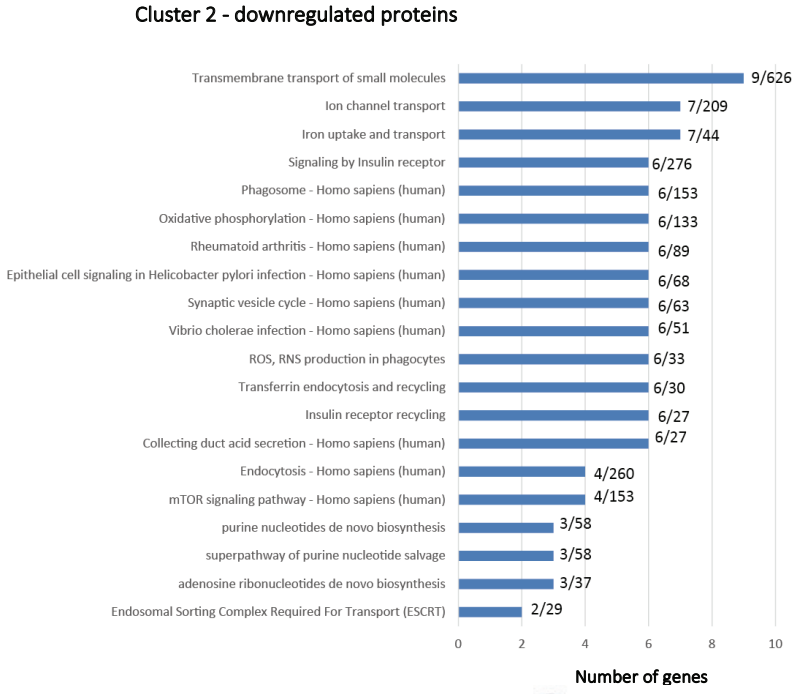

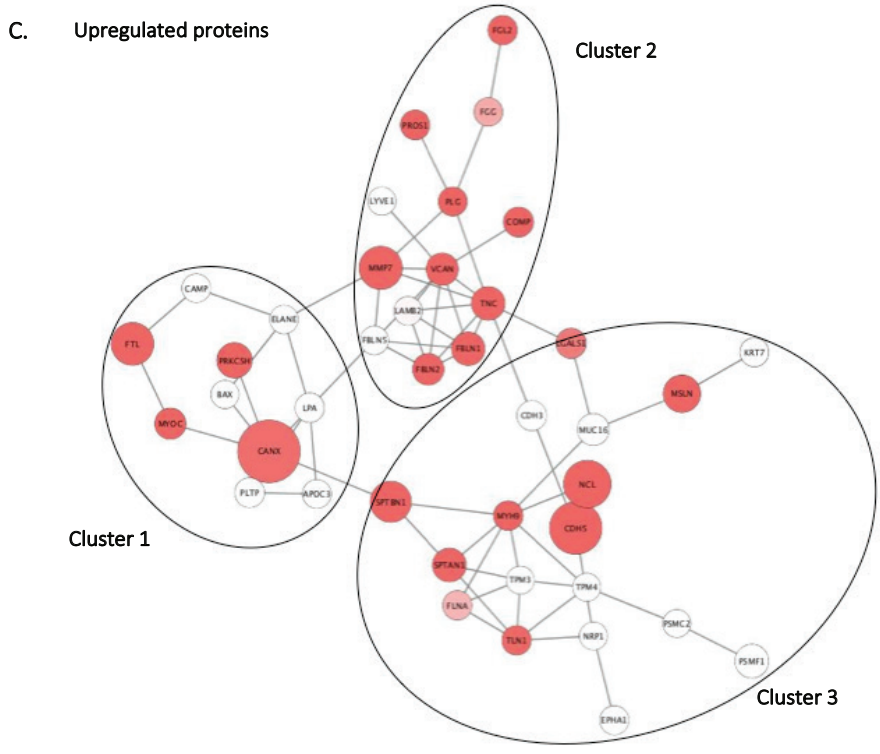

when the signal is lost_marijn_8072018.indd 154 08/07/2018 10:50

D. Cluster 1 - upregulated proteins

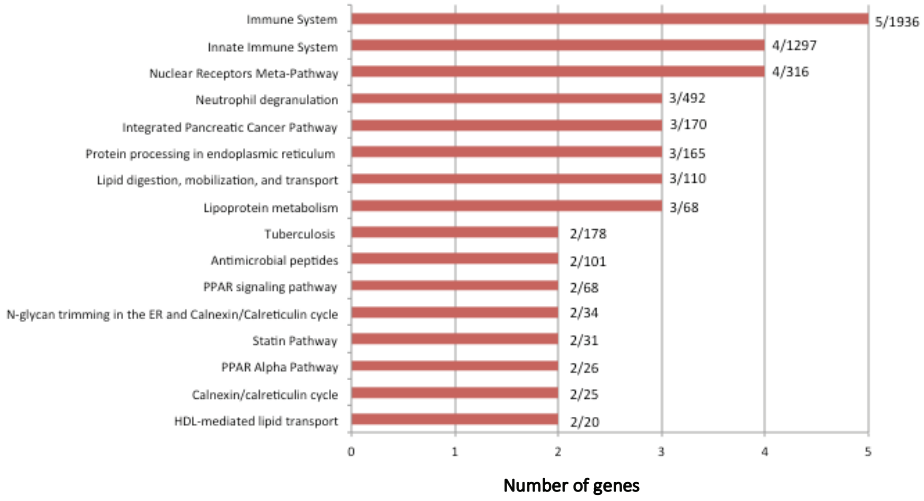

Cluster 2 - upregulated proteins

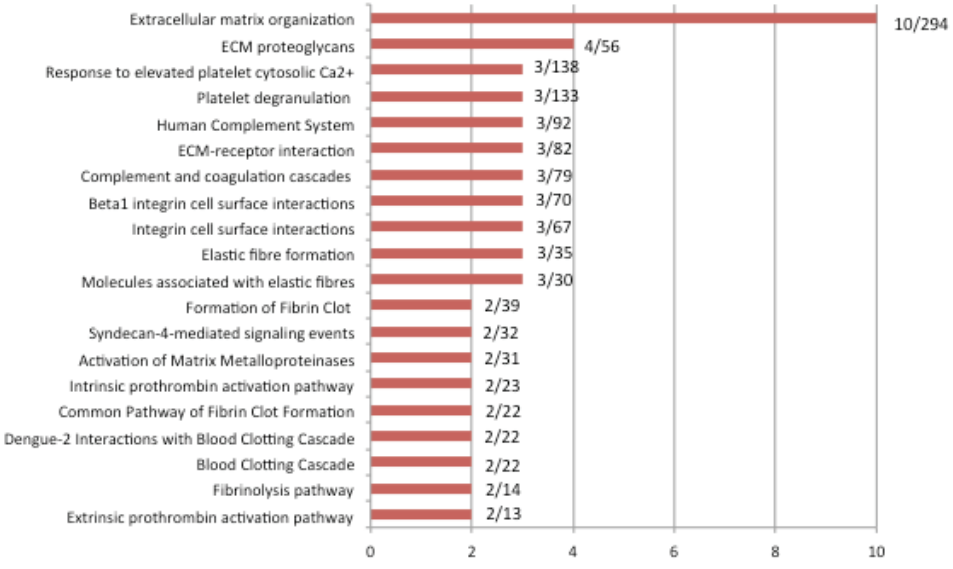

when the signal is lost_marijn_8072018.indd 155 08/07/2018 10:50

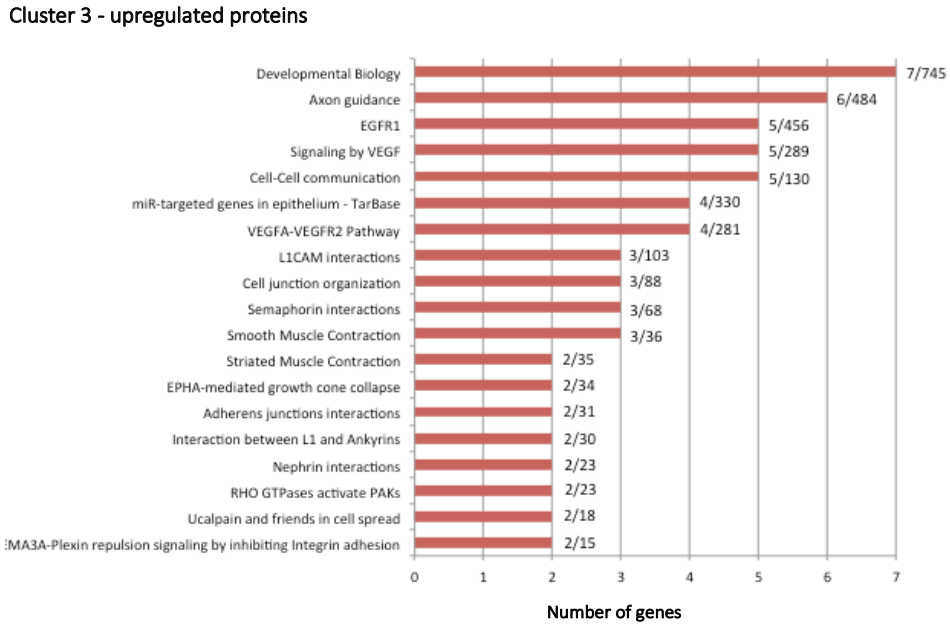

Supplementary Figure S3. Interaction networks and enriched pathways associated with differentially expressed proteins in urinary extracellular vesicles (EVs) of nephronophthisis-related ciliopathy (NPH-RC) patients compared to controls. **A.** Clusters of downregulated proteins based on GO term analyses. Interaction networks were generated in STRING and visualized in Cytoscape [Szklarczyk et al., 2015; Shannon et al., 2003]. Blue nodes represent proteins. Node size relates to fold change and node color relates to significance (blue is more significant, white is less significant). Edges represent interactions. **B.** Top 20 of most significantly downregulated pathways by number of genes per cluster (P<0.01). Fraction represents number of genes detected/number of reference genes per pathway. **C.** Clusters of upregulated proteins. Red nodes represent proteins. Node size relates to fold change and node color relates to significance (red is more significant, white is less significant). Edges represent interactions. **D.** Top 20 of most significantly upregulated pathways by number of genes per cluster (P<0.01). Fraction represents number of genes detected/number of reference genes per pathway.

when the signal is lost_marijn_8072018.indd 156 08/07/2018 10:50

Supplementary Table S3. *SysCilia Gold Standard list of 303 confirmed ciliary genes [Van Dam et al., 2013]*

ALMS1	*CLDN2*	*FAM161A*	*KIF27*	*PAFAH1B1*	*SEPT2*
ARF4	*CLUAP1*	*FBF1*	*KIF3A*	*PARD3*	*SEPT7*
ARL13B	*CNGA2*	*FLNA*	*KIF3B*	*PARD6A*	*SGK196*
ARL3	*CNGA4*	*FOPNL*	*KIF3C*	*PCDH15*	*SHH*
ARL6	*CNGB1*	*FOXJ1*	*KIF7*	*PCM1*	*SLC47A2*
ASAP1	*CP110*	*FUZ*	*LCA5*	*PDE6D*	*SMO*
ATXN10	*CRB3*	*GAS8*	*LRRC6*	*PDZD7*	*SNAP25*
AZI1	*CROCC*	*GLI1*	*LZTFL1*	*PHF17*	*SNX10*
B9D1	*CTNNB1*	*GLI2*	*MAK*	*PIBF1*	*SPA17*
B9D2	*DCDC2*	*GLI3*	*MAL*	*PKD1*	*SPAG16*
BBS1	*DCDC2*	*GLIS2*	*MAPRE1*	*PKD1L1*	*SPAG17*
BBS10	*DFNB31*	*GPR161*	*MCHR1*	*PKD2*	*SPAG6*
BBS12	*DISC1*	*GPR98*	*MDM1*	*PKHD1*	*SPATA7*
BBS2	*DNAAF1*	*GSK3B*	*MKKS*	*PLK1*	*SPEF2*
BBS4	*DNAAF2*	*HAP1*	*MKS1*	*POC1A*	*SSNA1*
BBS5	*DNAAF3*	*HEATR2*	*MLF1*	*PTCH1*	*SSTR3*
BBS7	*DNAH1*	*HNF1B*	*MNS1*	*PTPDC1*	*STIL*
BBS9	*DNAH10*	*HSPA8*	*MYO15A*	*RAB11A*	*STK36*
C21orf2	*DNAH11*	*HSPB11*	*MYO7A*	*RAB11FIP3*	*STK38L*
C2CD3	*DNAH2*	*HTR6*	*NEK1*	*RAB17*	*STOML3*
C2orf71	*DNAH5*	*HTT*	*NEK2*	*RAB23*	*STX3*
C8orf37	*DNAH6*	*HYDIN*	*NEK4*	*RAB3IP*	*SUFU*
CBY1	*DNAI1*	*HYLS1*	*NEK8*	*RAB8A*	*SYNE2*
CC2D2A	*DNAI2*	*IFT122*	*NGFR*	*RABL5*	*TBC1D30*
CCDC103	*DNAL1*	*IFT140*	*NIN*	*RAN*	*TBC1D7*
CCDC114	*DNALI1*	*IFT172*	*NINL*	*RANBP1*	*TCTN1*
CCDC164	*DPCD*	*IFT20*	*NME5*	*RFX3*	*TCTN2*
CCDC28B	*DPYSL2*	*IFT27*	*NME7*	*RILPL1*	*TCTN3*
CCDC37	*DRD1*	*IFT43*	*NME8*	*RILPL2*	*TEKT2*
CCDC39	*DRD2*	*IFT46*	*NOTO*	*ROPN1L*	*TEKT4*
CCDC40	*DRD5*	*IFT52*	*NPHP1*	*RP1*	*TEKT5*
CCDC41	*DVL1*	*IFT57*	*NPHP3*	*RP2*	*TMEM138*
CDH23	*DYNC2H1*	*IFT74*	*NPHP4*	*RPGR*	*TMEM216*
CENPJ	*DYNLT1*	*IFT80*	*NUP214*	*RPGRIP1*	*TMEM231*
CEP104	*DYX1C1*	*IFT81*	*NUP35*	*RPGRIP1L*	*TMEM237*
CEP135	*EFHC1*	*IFT88*	*NUP37*	*RSPH1*	*TMEM67*
CEP164	*EVC*	*INPP5E*	*NUP62*	*RSPH3*	*TNPO1*
CEP250	*EVC2*	*INTU*	*NUP93*	*RSPH4A*	*TOPORS*
CEP290	*EXOC3*	*INVS*	*OCRL*	*RSPH9*	*TPPP2*

when the signal is lost_marijn_8072018.indd 157 08/07/2018 10:50

TRAF3IP1	*TTC21B*	*TTLL6*	*TUBE1*	*ULK4*	*WDR35*
TRAPPC10	*TTC26*	*TTLL9*	*TUBGCP2*	*USH1C*	*WDR60*
TRAPPC3	*TTC29*	*TUBA1A*	*TUBGCP3*	*USH1G*	*WDR78*
TRAPPC9	*TTC30A*	*TUBA1C*	*TUBGCP4*	*USH2A*	*XPNPEP3*
TRIM32	*TTC30B*	*TUBA4A*	*TUBGCP5*	*VDAC3*	*ZNF423*
TRIP11	*TTC8*	*TUBB2A*	*TUBGCP6*	*VHL*	
TTBK2	*TTK*	*TUBB2B*	*TULP1*	*WDPCP*	
TTC12	*TTLL3*	*TUBB3*	*TULP3*	*WDR19*	

when the signal is lost_marijn_8072018.indd 158 08/07/2018 10:50

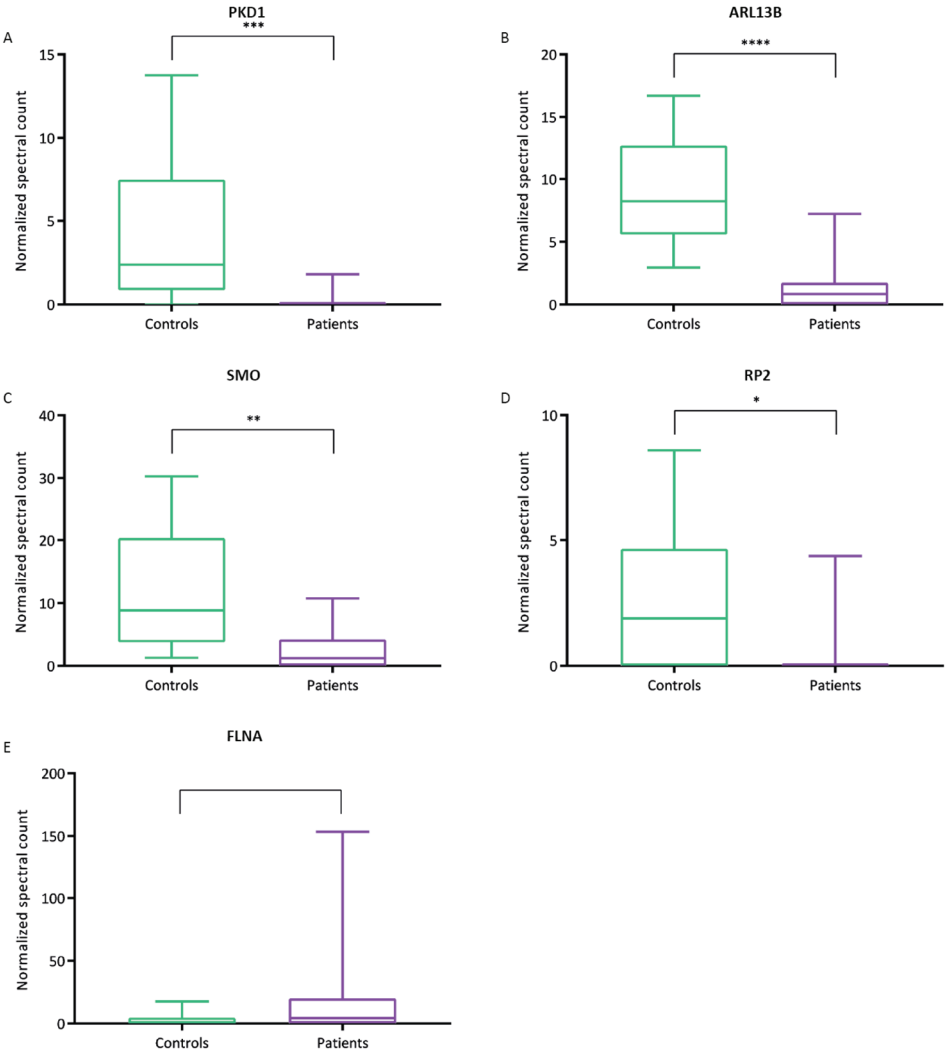

Supplementary Figure S4. Known cilia-associated proteins that were differentially expressed in nephronophthisis-related ciliopathy (NPH-RC) patients. Cilia-associated proteins were derived from the SysCilia Gold Standard (Version 1) [Van Dam et al., 2013]. **A.** PKD1, **B.** ARL13B, **C.** SMO, and **D.** RP2 proteins are significantly downregulated in patients. **E.** FLNA protein is upregulated in patients. Box plots based on normalized spectral counts. Lines and whiskers show mean, minimum and maximum values. *P<0.05, **P<0.01, ***P<0.001, ****P<0.0001, calculated using Mann-Whitney test.

when the signal is lost_marijn_8072018.indd 159 08/07/2018 10:50

Supplementary Table S4. *Known CKD-associated proteins and direction of fold change in CKD patients*

Protein ID	Direction*	In CKD273 classifier [Good et al., 2010]	References
COL1A1	up	Yes	[Schanstra et al., 2015; Øvrehus et al., 2015]
COL3A1	up	Yes	[Schanstra et al., 2015; Øvrehus et al., 2015]
FXYD2	up	Yes	[Schanstra et al., 2015; Øvrehus et al., 2015]
APOA1	down	Yes	[Schanstra et al., 2015; Øvrehus et al., 2015]
ALB	down	Yes	[Schanstra et al., 2015; Øvrehus et al., 2015]
SERPINA1	down	Yes	[Schanstra et al., 2015; Øvrehus et al., 2015]
B2M	down	Yes	[Schanstra et al., 2015; Øvrehus et al., 2015]
UMOD	down	Yes	[Schanstra et al., 2015]
SPP1	down	Yes	[Schanstra et al., 2015; Øvrehus et al., 2015]
LMAN2	down	No	[Schanstra et al., 2015]
PI16	down	No	[Schanstra et al., 2015]
A1BG	down	Yes	[Schanstra et al., 2015]
PCSK1N	down	Yes	[Schanstra et al., 2015]
COL2A1	up	Yes	[Schanstra et al., 2015; Øvrehus et al., 2015]
VGF	down	Yes	[Schanstra et al., 2015; Øvrehus et al., 2015]
MASP2	down	No	[Schanstra et al., 2015]
SERPINA5	down	No	[Schanstra et al., 2015]
COL1A2	up	Yes	[Schanstra et al., 2015]
PLG	down	No	[Schanstra et al., 2015]
HPGDS	down	Yes	[Schanstra et al., 2015]
ANXA1	down	No	[Schanstra et al., 2015]
PGRMC1	up	Yes	[Schanstra et al., 2015; Øvrehus et al., 2015]
CLU	down	Yes	[Schanstra et al., 2015]
CD99	up	Yes	[Schanstra et al., 2015; Øvrehus et al., 2015]
CFB	down	No	[Schanstra et al., 2015]
KRT2	down	No	[Schanstra et al., 2015]
S100A9	down	No	[Schanstra et al., 2015]
AHSG	down	Yes	[Schanstra et al., 2015; Øvrehus et al., 2015]
SERPINC1	down	Yes	[Schanstra et al., 2015]
APOA2	down	No	[Schanstra et al., 2015]
APOA4	down	No	[Schanstra et al., 2015]
FGA	up	Yes	[Schanstra et al., 2015; Øvrehus et al., 2015]
HBA1	down	No	[Schanstra et al., 2015]
HBB	down	No	[Schanstra et al., 2015]
TTR	down	Yes	[Schanstra et al., 2015]
COL16A1	up	No	[Schanstra et al., 2015]
COL11A2	up	No	[Schanstra et al., 2015]
IGKC	down	No	[Schanstra et al., 2015]
IGHG1	down	No	[Schanstra et al., 2015]
ITIH4	down	No	[Schanstra et al., 2015]
CRNN	down	No	[Schanstra et al., 2015]

when the signal is lost_marijn_8072018.indd 160 08/07/2018 10:50

ZYX	down	No	[Schanstra et al., 2015]
GAPDH	down	No	[Schanstra et al., 2015]
KRT13	down	No	[Schanstra et al., 2015]
KRT9	down	No	[Schanstra et al., 2015]
ACE2	up	No	[Abe et al., 2015]
L-FABP	up	No	[Abe et al., 2015; Kamijo-Ikemori et al., 2016; Matsui et al., 2016]
CDH11	up	No	[Craciun et al., 2016]
MRC1	up	No	[Craciun et al., 2016]
PLTP	up	No	[Craciun et al., 2016]
TFF1	up	No	[Lebherz-Eichinger et al., 2015]
TFF3	up	No	[Lebherz-Eichinger et al., 2015]
NGAL	up	No	[Lin et al., 2015; Patel et al., 2015; Tummalapalli et al., 2016]
CST3	up	No	[Mischak et al., 2015]
PFLC	up	No	[Mischak et al., 2015]
PIGR	down	Yes	[Øvrehus et al., 2015]
RBP	up	No	[Domingos et al., 2016]
BST1	up	No	[Konvalinka et al., 2016]
P3NP	up	No	[Tummalapalli et al., 2016]
VIM	up	No	[Tummalapalli et al., 2016]
CCL2	up	No	[Tummalapalli et al., 2016]
HAVCR1	up	No	[Tummalapalli et al., 2016]
MMP7	up	No	[Zhou et al., 2016]
CSTB	NA	Yes	[Good et al., 2010]
COL17A1	NA	Yes	[Good et al., 2010]
COL5A1	NA	Yes	[Good et al., 2010]
COL8A2	NA	Yes	[Good et al., 2010]
ORM1	NA	Yes	[Good et al., 2010]
IGLC1	NA	Yes	[Good et al., 2010]
PSORS1C2	NA	Yes	[Good et al., 2010]

*Direction of regulation in patients compared to controls. Up, upregulation; down, downregulation. For the proteins uniquely identified in the CKD273 classifier, the direction of regulation is provided for composing peptides in the original article [Good et al., 2010].

when the signal is lost_marijn_8072018.indd 161 08/07/2018 10:50

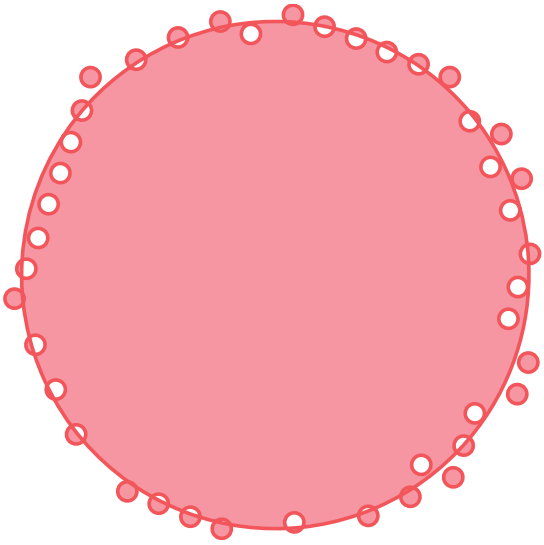

when the signal is lost_marijn_8072018.indd 162 08/07/2018 10:50

CHAPTER 7

The expanding phenotypic spectra of kidney diseases: insights from genetic studies

Stokman MF, Renkema KY, Giles RH, Schaefer F, Knoers NVAM, Van Eerde AM

2016. Nat. Rev. Nephrol. 12: 472-483
DOI:10.1038/nrneph.2016.87

when the signal is lost_marijn_8072018.indd 163 08/07/2018 10:50

ABSTRACT

Next-generation sequencing (NGS) has led to the identification of previously unrecognized phenotypes associated with classic kidney disease genes. In addition to improving diagnostics for genetically heterogeneous diseases and enabling a faster rate of gene discovery, NGS has enabled an expansion and redefinition of nephrogenetic disease categories. Findings from these studies raise the question of whether disease diagnoses should be made on clinical grounds, on genetic evidence or a combination thereof. Here, we discuss the major kidney disease-associated genes and gene categories for which NGS has expanded the phenotypic spectrum. For example, *COL4A3-5* genes, which are classically associated with Alport syndrome are now understood to also be involved in the aetiology of FSGS and *DGKE*, which is associated with nephrotic syndrome is also mutated in patients with atypical haemolytic uraemic syndrome. We examine how a shared genetic background between diverse clinical phenotypes can provide insight into the function of genes and novel links with essential pathophysiological mechanisms. In addition, we consider genetic and epigenetic factors that contribute to the observed phenotypic heterogeneity of kidney diseases and discuss the challenges in the interpretation of genetic data. Finally, we discuss the implications of the expanding phenotypic spectra related to kidney disease genes for clinical practice, genetic counselling and personalized care, and present our recommendations for the use of NGS-based tests in routine nephrology practice.

when the signal is lost_marijn_8072018.indd 164 08/07/2018 10:50

7.1 INTRODUCTION

The introduction of next-generation sequencing (NGS) has revolutionized the field of genetics over the past ten years. Rapidly decreasing costs and the increasing speed and availability of NGS technologies have paved the way for routine genetic testing in nephrogenetic diseases such as polycystic kidney disease [Eisenberger et al., 2015; Tavira et al., 2015] and familial haematuric nephropathies [Morinière et al., 2014; Lohmann and Klein, 2014]. NGS has increased the applicability of genetic testing in genetically heterogeneous kidney diseases such as nephrotic syndrome [Sampson et al., 2015] (OMIM 256300) and has provided a time and cost-efficient strategy to aid the diagnosis of diseases that are technically challenging to diagnose genetically, such as autosomal dominant polycystic kidney disease (ADPKD, OMIM 173900), for which multiple pseudogenes exist [Eisenberger et al., 2015]. NGS has also boosted gene discovery in numerous kidney disease categories including renal ciliopathies [Otto et al., 2010], nephrotic syndrome [Gupta et al., 2013; Gee et al., 2014a], focal segmental glomerulosclerosis [Gbadegesin et al., 2014] (FSGS, OMIM 603278) and congenital anomalies of the kidney and urinary tract (CAKUT; OMIM 610805) [Saisawat et al., 2014; Humbert et al., 2014]. A monogenic cause can now be identified in approximately 20% of patients with early-onset chronic kidney disease (CKD), depending on the population structure [Vivante and Hildebrandt, 2016]. In addition to enabling faster and more comprehensive molecular testing for genetic kidney diseases, NGS also has potential for clinical application through urinary biomarker-based diagnosis of renal tubular injury [Nassirpour et al., 2014], for tumour classification and pharmacogenomics in onconephrology [Gerlinger et al., 2012; Marsaud et al., 2015] and for histocompatibility assays in renal transplantation [Lan and Zhang, 2015].

In both research and diagnostic settings, NGS has evolved from an approach used to sequence panels of known and candidate kidney-disease associated genes, to whole-exome sequencing and whole-genome sequencing to identify causal disease-associated genes [Sun et al., 2015]. The progression of NGS towards increasingly untargeted approaches has resulted in the emergence of surprising findings, leading to reclassification of clinical diagnoses and broadening our understanding of the phenotypic spectrum of classic kidney disease-associated genes. Reclassification of clinical diagnoses on the basis of molecular findings from NGS is particularly relevant for renal diseases such as ADPKD [Bergmann, 2014] and nephronophthisis [Gee et al., 2014b] (OMIM 256100), for which phenotypically similar conditions exist. For diseases such as these, the identification of disease-causative genes has the potential to result in an unequivocal diagnosis.

In cases where a clinical diagnosis is unequivocal, findings from NGS have led to improved insights into phenotypic variability related to mutations in known kidney disease-associated genes. Clinical phenotypes with genetic overlap can be within the same disease category, for example renal ciliopathies. However, phenotypes can also be clinically unrelated; for example mutations in *DGKE* can cause both nephrotic syndrome type 7 with membranoproliferative

when the signal is lost_marijn_8072018.indd 165 08/07/2018 10:50

glomerulonephritis (MPGN; OMIM 615008) and atypical haemolytic-uraemic syndrome (aHUS; OMIM 235400), diseases that are considered clinically unrelated [Lemaire et al., 2013; Mele et al., 2015; Westland et al., 2014]. In these and other apparently distinct phenotypes, shared genetic aetiology can provide insight into common underlying pathophysiological processes.

In this Review we discuss examples of genes and gene categories in which NGS has led to an expansion in our understanding of the phenotypic spectrum, both across and within current kidney disease categories (**Table 1**). We examine how these findings can provide insight into gene function and underlying pathophysiological mechanisms, and consider the genetic and epigenetic factors that contribute to kidney disease heterogeneity. Finally, we highlight the implications of broader phenotypic spectra of classic kidney disease-associated genes for clinical practice, genetic counselling and personalized medicine, and present our current approach for the use of NGS-based tests in routine nephrology practice.

when the signal is lost_marijn_8072018.indd 166 08/07/2018 10:50

Table 1. Summary of genes discussed in this Review

Gene	Associated diseases (mode of inheritance*)	References	Potential mechanisms
Across disease categories			
COL4A3–5	FSGS (AD) TBMN (AD) Alport syndrome (AD, AR, XL)	[Xie et al., 2014; Malone et al., 2014; Gast et al., 2015] [Lemmink et al., 1996; Badenas et al., 2002] [Mochizuki et al., 1994; Barker et al., 1990]	FSGS could arise secondary to unrecognized TBMN through complex mechanisms involving cross-talk between components of the glomerular filtration barrier, through defects in the GBM that result in podocyte foot-process effacement and GBM scarring, and the actions of modifier genes [Miner, 2014; Deltas et al., 2015].
DGKE	MPGN (AR) aHUS (AR)	[Ozaltin et al., 2013] [Lemaire et al., 2013; Mele et al., 2015; Westland et al., 2014; Sánchez Chinchilla et al., 2014]	- aHUS could arise secondary to MPGN and *vice versa* because loss of *DGKE* function and complement activation both cause sustained diacylglycerol signalling [Ozaltin et al., 2013; Noris et al., 2015], which induces glomerular epithelial cell injury, proteinuria, upregulation of prothrombotic factors and platelet activation [Lemaire et al., 2013; Offermanns, 2006; Takano and Cybulsky, 2000; Noris et al., 2015] and increases TRPC6 channel activity, which is associated with podocyte foot-process effacement and nephrotic syndrome [Winn et al., 2006; Noris et al., 2015]. - In *DGKE*-mediated aHUS, the main prothrombotic effect is mediated through upregulation of the pro-inflammatory p38–MAPK pathway that causes impaired endothelial cell proliferation and angiogenesis [Bruneau et al., 2015].
TTC21B	Ciliopathies (AR) Glomerulopathies (AR)	[Davis et al., 2011] [Huynh Cong et al., 2014; Bullich et al., 2016]	- Most patients with *TTC21B*-related glomerulopathy reported to date carry biallelic p.Pro209Leu mutations. This mutation has also been identified in patients with nephronophthisis [Huynh Cong et al., 2014; Bullich et al., 2016; Davis et al., 2011]. - Glomerulopathies could result from *TTC21B*-mediated alterations in cytoskeletal architecture in mature podocytes, which affects cell size and migration, actin and microtubule networks and cell nucleation [Huynh Cong et al., 2014]. - Tubular lesions characteristic of nephronophthisis suggest a concomitant ciliary defect in glomerulopathy patients [Huynh Cong et al., 2014; Bullich et al., 2016].
PAX2	RCS (AD) CAKUT (AD) FSGS (AD)	[Sanyanusin et al., 1995] [Nishimoto et al., 2001] [Barua et al., 2014]	- Truncating PAX2 mutations are more frequently associated with RCS, while missense mutations are more frequently associated with isolated CAKUT or FSGS [Barua et al., 2014]. - Location of the mutation within the gene is associated with the phenotype [Barua et al., 2014].

when the signal is lost_marijn_8072018.indd 167 08/07/2018 10:50

			- FSGS could develop secondary to subtle renal developmental anomalies or through dysregulation of PAX2 targets (for example WT1) involved in podocyte development and/or function [Barua et al., 2014].
HNF1B	RCAD (AD) CAKUT (AD)	[Horikawa et al., 1997] [Weber et al., 2006; Hwang et al., 2014]	- *HNF1B* is involved in regulation of renal tubular epithelial cell proliferation and differentiation, and expression of cystic kidney disease-associated genes [Thomas et al., 2011; Hiesberger et al., 2004; Gresh et al., 2004]. - There are no clear genotype-phenotype correlations in *HNF1B*-related renal disease [Heidet et al., 2010].
Within disease categories			
MKS1, *B9D1*, *CEP290*	MKS and JBTS (AR)	[Kyttälä et al., 2006; Romani et al., 2014; Hopp et al., 2011; Sayer et al., 2006; Baala et al., 2007a]	- Both *MKS1*-related INPP5E mislocalization and mutations in *INPP5E* can cause Joubert syndrome, suggesting that INPP5E dysfunction is central to the pathogenesis of Joubert syndrome [Slaats et al., 2016a; Thomas et al., 2014; Bielas et al., 2009]. - In MKS, a complete loss of MKS1 leads to a marked defect in cilia formation and could result in more severe mislocalization of ciliary proteins [Slaats et al., 2016a].
WT1	Wilms tumour, DDS and SRNS (AD, SM)	[Haber et al., 1990; Hastie, 1992; Jeanpierre et al., 1998]	Mutation type and location within the gene affect the risks of Wilms tumour and SRNS [Lipska et al., 2014; Royer-Pokora et al., 2004]. The exact mechanisms are unclear.
Within phenotypes			
HNF4A	MODY1 and Fanconi renal tubular transport disorder (AD)	[Yamagata et al., 1996; Stanescu et al., 2012; Hamilton et al., 2014]	HNF4A is a known regulator of *SLC2A2*, which encodes the glucose transporter GLUT2, and mutations in *SLC2A2* cause Fanconi–Bickel syndrome, suggesting that defective HNF4A could lead to impaired renal tubular transport [Stanescu et al., 2012; Hamilton et al., 2014].
LMX1B	NPS and glomerulopathy (AD)	[Dreyer et al., 1998; Edwards et al., 2015; Isojima et al., 2014; Boyer et al., 2013]	Mutations associated with an isolated glomerulopathy are located in the homeodomain of *LMX1B*, possibly disrupting the interaction between LMX1B and (podocyte specific) DNA targets [Boyer et al., 2013; Edwards et al., 2015; Isojima et al., 2014]. however, mutations in this domain have been reported in NPS patients as well [Bongers et al., 2005].
OCRL1	Lowe syndrome and Dent-2 disease (XL)	[Bailey et al., 1992; Hoopes et al., 2005]	- Phenotypic variability could arise from different locations of mutations within *OCRL1*, differential splicing of *OCRL1* resulting in different isoforms and the presence of genetic modifiers [Shrimpton et al., 2009; Hichri et al., 2011]. - Pathophysiological mechanisms hypothesized to underlie Lowe syndrome and Dent-2 disease include cilia and cell polarity defects, and aberrant endocytic trafficking [Mehta et al., 2014].

when the signal is lost_marijn_8072018.indd 168 08/07/2018 10:50

FRAS1, FREM2 GRIP1	Fraser syndrome and CAKUT (AR)	[McGregor et al., 2003; Jadeja et al., 2005; Vogel et al., 2012; Kohl et al., 2014]	Biallelic truncating mutations cause Fraser syndrome, while biallelic missense mutation are associated with isolated CAKUT [Kohl et al., 2014]. - Missense mutations could result in a partial loss of function, which might be compensated for in the development of extrarenal tissues but not in development of the kidneys [Kohl et al., 2014].

AD: autosomal dominant; aHUS: atypical hemolytic uremic syndrome; AR: autosomal recessive; CAKUT: congenital anomalies of the kidney and urinary tract; DDS: Denys-Drash syndrome; FSGS: focal segmental glomerulosclerosis; JBTS: Joubert syndrome; MKS: Meckel-Gruber syndrome; MODY1: maturity-onset diabetes of the young type 1; MPGN: membranoproliferative glomerulosclerosis; NPS: nail–patella syndrome; RCAD: renal cysts and diabetes syndrome; RCS: Renal-coloboma syndrome; SM: somatic mutation; SRNS: steroid-resistant nephrotic syndrome; TBMN: thin basement membrane nephropathy; XL: X-linked. *Inheritance pattern is provided in the context of the affected gene. Sequencing techniques such as whole-exome sequencing have expanded the phenotypic spectrum associated with kidney disease genes. The subgroups contain selected examples from this review.

7.2 EXPANDING RENAL DISEASE PHENOTYPES

7.2.1 Expansions across disease categories

7.2.1.1 COL4A3-5 mutations in Alport syndrome and FSGS

NGS has indisputably broadened the phenotypic spectrum of diseases associated with mutations in *COL4A3–5*, which encode the α-chains of glomerular basement membrane collagen type IV. Mutations in these genes are classically associated with Alport syndrome (OMIM 301050), a glomerulonephropathy associated with variable sensorineural hearing loss and ocular anomalies. Clinically, Alport syndrome is characterized by microscopic haematuria with proteinuria and, eventually, renal failure [Kashtan, 2015]. Inheritance of Alport syndrome is X-linked in 65% of cases (only in patients with mutations in *COL4A5*) and dominant (20%) or recessive (15%) in other cases (that is, in patients with mutations in *COL4A3* and *COL4A4*) [Kashtan, 2015]. Several studies have shown the practical benefits of NGS in the diagnostic workup of patients with Alport syndrome [Artuso et al., 2012; Braun et al., 2016].

The allelic disease thin basement membrane nephropathy (TBMN, OMIM# 141200) is also characterized by persistent microscopic haematuria. Contrary to Alport syndrome, however, TBMN is rarely reported in combination with progressive proteinuria and end-stage renal disease (ESRD), although this milder phenotype might reflect a lack of longitudinal studies of patients with TBMN [Kashtan, 2015; Nogueira et al., 2000; Voskarides et al., 2007; Pierides et al., 2009]. Studies from 2007 and 2009 described families with TBMN caused by heterozygous mutations in *COL4A3* and *COL4A4* [Voskarides et al., 2007; Pierides et al., 2009]. In these studies, nearly all patients with microhaematuria, proteinuria

when the signal is lost_marijn_8072018.indd 169 08/07/2018 10:50

and CKD showed FSGS on examination of renal biopsy samples, suggesting that specific heterozygous mutations in *COL4A3-4* or unknown genetic modifiers might cause concurrent FSGS lesions in addition to TBMN [Voskarides et al., 2007; Pierides et al., 2009].

Later studies using NGS identified mutations in *COL4A3-5* genes in patients who had a primary diagnosis of FSGS but on closer clinical evaluation, exhibited features of Alport syndrome, such as characteristic findings on electron microscopy and hearing loss [Chatterjee et al., 2013; McCarthy et al., 2013; Gibson et al., 2013]. In addition, targeted sequencing of 26 glomerular genes in 50 patients with steroid-resistant nephrotic syndrome (SRNS) and/or FSGS identified three patients with mutations in genes known to cause SRNS and/or FSGS in combination with a heterozygous mutation in *COL4A3*, suggesting a modifier effect of *COL4A3* that might aggravate the phenotype of SRNS and/or FSGS [Bullich et al., 2015].

NGS has also led to the detection of *COL4A* variants in patients with isolated FSGS. For example, heterozygous missense *COL4A3* variants were identified in five of 40 Chinese families with hereditary FSGS and one of 50 Chinese patients with sporadic FSGS [Xie et al., 2014]. *COL4A3* and *COL4A4* missense and truncating mutations were also identified in seven of 70 families with a primary diagnosis of FSGS accompanied by proteinuria and haematuria. Clinical and pathological findings were inconsistent with Alport syndrome in four of these families [Malone et al., 2014]. Finally, *COL4A3–5* mutations were detected in 38% of families with FSGS (n = 8) and in 3% of patients with sporadic FSGS (n = 67) [Gast et al., 2015]. Although one patient with familial FSGS developed hearing loss consistent with Alport syndrome, the researchers claimed that their findings show that *COL4A3–5* mutations are the most frequent cause of FSGS in adults [Gast et al., 2015].

Whether the above-described cases of FSGS should be considered to be familial FSGS or rather a secondary effect of undiagnosed TBMN is a matter of debate [Deltas et al., 2015]. FSGS occurs in at least 5% of patients with TBMN [Savige et al., 2003]. TBMN could potentially lead to secondary FSGS through complex mechanisms involving cross-talk between components of the glomerular filtration barrier, through defects in the glomerular basement membrane (GBM) that result in podocyte foot-process effacement and GBM scarring, or through the actions of modifier genes, such as *NPHS2* [Miner, 2014; Deltas et al., 2015]. In the studies described above [Xie et al., 2014; Malone et al., 2014; Gast et al., 2015], most patients were diagnosed with FSGS well into adulthood; the possibility of these patients having secondary FSGS cannot therefore be excluded [Miner, 2014]. As an erroneous diagnosis of primary FSGS can lead to inaccurate counselling and unwarranted corticosteroid treatment [Deltas et al., 2015], the value of redefining the *COL4A* phenotypic spectrum to include both Alport syndrome and FSGS warrants serious discussion [Malone et al., 2014]. An alternative proposal is to redefine the Alport spectrum by including benign familial haematuria and TBMN (caused by heterozygous *COL4A3/4* mutations) at the mild end, secondary FSGS and late ESRD in the middle and early ESRD with extrarenal features (caused by biallelic *COL4A3/4* mutations or hemizygous *COL4A5* mutations) at the severe end of the spectrum [Miner, 2014] (**Figure 1**). Large, genetic studies with

when the signal is lost_marijn_8072018.indd 170 08/07/2018 10:50

longitudinal follow-up are required to confirm genotype–phenotype correlations in *COL4A* mutations, which will only realistically be achieved through collaborative multicentre networks.

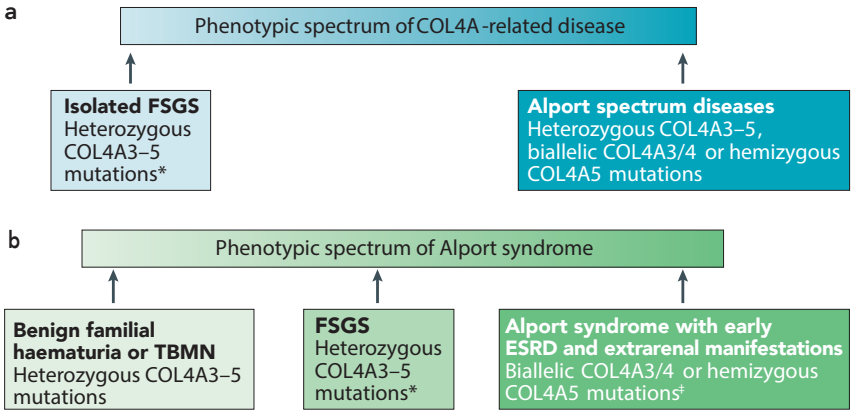

Figure 1. The phenotypic spectrum of *COL4A3–5* mutations. Two proposals exist as to how *COL4A* mutations that cause focal segmental glomerulosclerosis (FSGS) might be considered in the classical Alport paradigm. The first proposal **A.** is to revise the phenotypic spectrum of *COL4A*-related disease to include both isolated FSGS and Alport syndrome-related phenotypes (including benign familial haematuria, thin basement membrane nephropathy (TBMN) and Alport syndrome). The second **B.** proposes that FSGS exists as part of the phenotypic spectrum of Alport syndrome because it cannot be excluded that FSGS occurs secondarily to (as yet) undiagnosed TBMN or Alport syndrome [Miner, 2014]. *Women with heterozygous mutations in *COL4A5* can develop end-stage renal disease and/or hearing loss depending on (tissue specific) X-chromosome inactivation [Jais et al., 2003].

7.2.1.2 DGKE mutations in MPGN and aHUS

Homozygous truncating mutations in *DGKE*, which encodes diacylglycerol kinase ε, were first identified by whole-exome sequencing in a Turkish family with nephrotic syndrome type 7 with MPGN-like glomerular microangiopathy, and subsequently in two other families with MPGN [Ozaltin et al., 2013]. Histologically, biopsy samples from these patients exhibited hypertrophic, hyperlobulated and hypercellular glomeruli, thickening and splitting of the basement membrane, podocyte foot-process effacement and swelling of endothelial cells with obstruction of the capillary lumen [Ozaltin et al., 2013].

Whole-exome sequencing also revealed biallelic missense and truncating mutations in *DGKE* in two families with childhood-onset aHUS. *DGKE* mutations were subsequently identified in six of 47 additional unrelated probands who also had childhood-onset aHUS [Lemaire et al., 2013]. In addition, a study using whole-genome sequencing identified a biallelic intronic *DGKE* mutation that segregated with paediatric-onset aHUS in two unrelated families. Subsequent

when the signal is lost_marijn_8072018.indd 171 08/07/2018 10:50

cDNA sequencing showed that the intronic mutation causes aberrant splicing of the *DGKE* transcript, which is predicted to alter the protein catalytic domain that phosphorylates diacylglycerol [Mele et al., 2015]. In a study of 83 patients with early-onset aHUS, four patients had biallelic *DGKE* mutations of whom three showed additional heterozygous mutations in the genes encoding thrombomodulin and complement component C3 [Sánchez Chinchilla et al., 2014]. Finally, homozygous truncating mutations in *DGKE* were also reported in two of 1,783 families with SRNS [Sadowski et al., 2014].

aHUS can develop secondary to MPGN and vice versa. For example, patients with a primary diagnosis of MPGN caused by mutations in genes that regulate the alternative complement pathway (for example *CFH* and *C3*), can develop secondary aHUS [Noris et al., 2010; Licht and Fremeaux-Bacchi, 2009]. Multiple mechanisms link *DGKE* mutations to podocyte dysfunction, complement activation and thrombotic microangiopathy [Noris et al., 2015; Bruneau et al., 2015]. Diacylglycerol kinase ε phosphorylates diacylglycerol and is expressed in the endothelium of glomerular capillaries and podocytes [Lemaire et al., 2013; Ozaltin et al., 2013]. Both loss of DGKE function and complement activation cause sustained diacylglycerol signalling [Ozaltin et al., 2013; Noris et al., 2015], which induces glomerular epithelial cell injury, proteinuria, upregulation of prothrombotic factors and platelet activation [Lemaire et al., 2013; Offermanns, 2006; Takano and Cybulsky, 2000; Noris et al., 2015]. Furthermore, sustained diacylglycerol signalling increases TRPC6 channel activity, which is associated with podocyte foot-process effacement and nephrotic syndrome [Noris et al., 2015; Winn et al., 2006]. Based on the above-described mechanisms, one could expect that aHUS could develop during the course of *DGKE*-associated MPGN or could even precede the manifestations of MPGN. However, in the above-described families with MPGN caused by *DGKE* mutations, no signs of aHUS preceded the onset of MPGN, rendering it unlikely that MPGN occurred secondary to aHUS [Ozaltin et al., 2013].

Strikingly, most of the families with aHUS caused by *DGKE* mutations without additional mutations in *THBD* or *C3* did not show abnormal complement activation [Lemaire et al., 2013; Mele et al., 2015; Sánchez Chinchilla et al., 2014], and patients who received anticomplement therapy (eculizumab or plasma infusion) experienced an acute episode of aHUS while on treatment, suggesting the presence of a complement-independent mechanism with major implications for treatment [Lemaire et al., 2013]. Studies into the mechanism of *DGKE*-associated aHUS showed that although *DGKE* knockdown moderately downregulates expression of the complement inhibitory protein membrane cofactor protein (MCP), no increase in endothelial C3 deposition occurs [Bruneau et al., 2015]. Rather, the main prothrombotic effect is mediated through DGKE-mediated upregulation of the pro-inflammatory p38–MAPK pathway with impaired endothelial cell proliferation and angiogenesis that occurs in a complement-independent manner [Bruneau et al., 2015]. However, exceptions to this mechanism of action exist; a report of a family with *DGKE*-related aHUS with substantial serum complement activation and apparent responsiveness to plasma infusion therapy suggests that some patients

when the signal is lost_marijn_8072018.indd 172 08/07/2018 10:50

with *DGKE*-associated aHUS can benefit from complement-blocking agents [Westland et al., 2014]. Alternatively, the activation of serum complement in these patients could be the result of a transient effect of microparticles that are released from apoptotic endothelial cells and that augment DGKE-mediated damage [Bruneau et al., 2015; Renner et al., 2013]. Although this last possibility suggests that *DGKE* mutations might not preclude efficacy of complement blocking therapy, it does illustrate the value of a pharmacogenomic perspective in the management of patients with hereditary kidney disease.

7.2.1.3 TTC21B mutations in ciliopathies and glomerulopathies

TTC21B encodes the ciliary protein tetratricopeptide repeat domain-containing protein 21B (also known as IFT139), which is required for retrograde intraflagellar transport [Tran et al., 2008]. Using targeted sequencing of *TTC21B* in a cohort of 753 patients with diverse ciliopathies, biallelic mutations in *TTC21B* were identified in five families with nephronophthisis (OMIM 613820) and in one family with another ciliopathy, Jeune asphyxiating thoracic dystrophy (OMIM 613819) [Davis et al., 2011]. In addition, heterozygous pathogenic missense and truncating variants in *TTC21B* were found in 5% (n = 38) of the cohort. One-third of these mutations were found in combination with biallelic mutations in other known ciliopathy-associated genes. Although rare variants of *TTC21B* were not enriched in patients with ciliopathies compared to controls, pathogenic variants were, however, significantly enriched in patients, suggesting a modifier role of *TTC21B* in ciliopathies [Davis et al., 2011].

The association between pathogenic *TTC21B* variants and ciliopathies is not surprising, given the known role of *TTC21B* in regulating ciliary function; however, whole-exome sequencing also identified homozygous missense mutations in *TTC21B* in seven of 46 families with a primary diagnosis of late-onset FSGS [Huynh Cong et al., 2014]. The p.Pro209Leu mutation identified in these families was previously reported in patients with nephronophthisis [Davis et al., 2011]. In addition, biallelic mutations in *TTC21B* (p.Pro209Leu, p.His426Asp) were identified in three of 15 families with childhood-onset nephrotic proteinuria, renal biopsy findings of FSGS and tubulointerstitial lesions [Bullich et al., 2017]. Although secondary glomerulosclerosis has been observed in patients with advanced nephronophthisis, these reports constitute the first evidence of a ciliary gene being involved in a hereditary glomerulopathy.

The p.Pro209Leu mutation has a hypomorphic effect on cilia formation in undifferentiated podocytes; however, the glomerular defects seem to be mediated by a non-ciliary effect of the mutation on cytoskeletal architecture in mature podocytes, which affects cell size and migration, as well as actin and microtubule networks and cell nucleation [Huynh Cong et al., 2014]. Histological examination of biopsy samples from patients with *TTC21B*-associated FSGS showed tubular lesions characteristic of nephronophthisis in addition to classic FSGS lesions, suggesting a concomitant ciliary defect in renal tubular epithelial cells [Huynh Cong et al., 2014; Bullich et al., 2017]. Other ciliary genes that function in the podocyte cytoskeleton, for example the glycogen synthase kinase 3β, might well give rise

when the signal is lost_marijn_8072018.indd 173 08/07/2018 10:50

to primary FSGS as well providing a molecular link between tubulointerstitial and glomerular phenotypes.

7.2.2 Expansions within disease categories

7.2.2.1 Phenotypic heterogeneity in ciliopathies

The most striking example of a situation in which NGS findings have challenged the categorization of renal diseases is with the ciliopathies, in which mutations in *MKS1* and *B9D1*, previously associated with the embryonic lethal Meckel–Gruber syndrome (OMIM 249000), were identified in patients with the less severe and viable Joubert syndrome (OMIM 213300), indicating that these syndromes represent two ends of a phenotypic spectrum [Romani et al., 2014]. Biallelic truncating mutations in *MKS1* cause Meckel–Gruber syndrome; if at least one of the mutations is a hypomorphic missense mutation, Joubert syndrome results due to malfunction of MKS1 at the ciliary transition zone at the base of cilia and a subsequent reduction in ARL13B and INPP5E inside the cilium [Slaats et al., 2016a]. Both *MKS1*-related INPP5E mislocalization and mutations in *INPP5E* can cause Joubert syndrome, suggesting that INPP5E dysfunction is central to the pathogenesis of Joubert syndrome [Slaats et al., 2016a; Thomas et al., 2014; Bielas et al., 2009]. In Meckel-Gruber syndrome, a complete loss of MKS1 leads to a marked defect in cilia formation and could result in more severe mislocalization of ciliary proteins [Slaats et al., 2016a]. This example is characteristic of the phenotypic variability seen with mutations in ciliopathy-associated genes [Fehrenbach et al., 2014; Habbig and Liebau, 2015]. Nonsense-associated alternative splicing, a mechanism whereby detrimentally mutated exons are spliced out of the final gene transcript, partially explains phenotypic variability in patients with *CEP290*-related ciliopathies [Drivas et al., 2015; Littink et al., 2010] (**Figure 2**). This mechanism of basal exon skipping is expected to extend beyond ciliopathies and apply to other diseases with considerable phenotypic heterogeneity as well [Drivas et al., 2015]. In addition to the variation in the degree of protein impairment, genetic modifiers, such as heterozygous mutations in *TTC21B* [Davis et al., 2011], also contribute to phenotypic heterogeneity in ciliopathies [Hoefele et al., 2007].

when the signal is lost_marijn_8072018.indd 174 08/07/2018 10:50

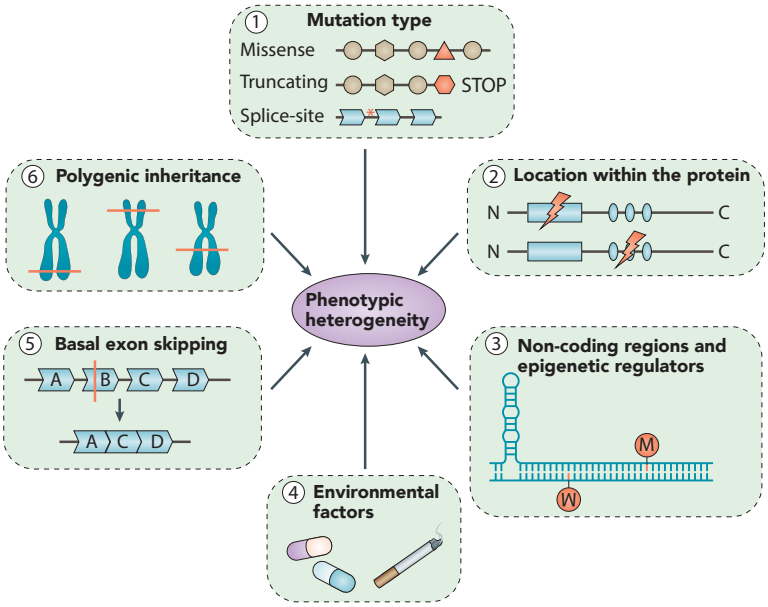

Figure 2. Sources of phenotypic heterogeneity in nephrogenetic disease. **1.** In general, truncating and splice-site mutations are expected to be more detrimental to protein function than are missense mutations. **2.** The phenotype can vary according to the location of the mutation within the gene. For example, mutations in important functional protein domains are more likely to affect protein function than are mutations outside functional domains. **3.** The expression of genes is regulated by non-coding factors such as microRNAs and by epigenetic modifications such as methylation. **4.** Environmental factors such as nutrition and medication have a role in the expression of multifactorial phenotypes. **5.** Basal exon skipping is a mechanism by which severely mutated exons can be selectively spliced out of the gene transcript. The resulting shortened transcript escapes nonsense-mediated decay and can retain partial function if the skipped exon was outside an important functional domain. **6.** Variants in multiple genes can influence the type and severity of phenotypic features. Modifier variants can have an additive pathogenic or a protective effect.

7.2.2.2 Phenotypic variability in WT1-related syndromes

Similar to ciliopathies, mutation type determines phenotypic outcome in *WT1*-related syndromes. In a cohort of 117 patients with Wilms tumour (OMIM 194070) associated with *WT1* mutations, truncating mutations were associated with the highest risk of early-onset bilateral Wilms tumour, followed by missense mutations and then deletions, which were most frequently associated with a syndromic phenotype [Royer-Pokora et al., 2004]. Missense mutations in exon 8 and exon 9 were associated with Denys–Drash syndrome (OMIM 194080), which is typically associated with early-onset, unilateral Wilms tumour [Dome and Huff, 2013; Royer-Pokora et al., 2004]. In a cohort of 61 patients with *WT1*-related SRNS, truncating

when the signal is lost_marijn_8072018.indd 175 08/07/2018 10:50

mutations were associated with a high risk of developing Wilms tumour (78%) and late-onset SRNS. Conversely, missense mutations were associated with diffuse mesangial sclerosis and early-onset SRNS and ESRD, and intronic (exon 9 splice site) mutations were associated with early-onset SRNS, FSGS on renal biopsy and a very low tumour risk [Lipska et al., 2014]. This example also illustrates that isolated presentations, such as early-onset SRNS or genitourinary anomalies, can be indicative of a tumour predisposition syndrome, which is relevant for genetic counselling [Nielsen et al., 2016].

7.2.3 Different presentations of the same phenotype

Some phenotypes differ only by the presence of renal or extra renal features. This phenotypic heterogeneity can be caused by the inheritance pattern of the causative gene, the mutation type, the presence of genetic modifiers or other, often unknown, factors. Contrary to expanding phenotypes across and within disease categories, patients with different presentations of the same phenotype share core (in this instance extra renal) features. For example, a heterozygous missense mutation in *HNF4A*, associated with maturity-onset diabetes of the young (MODY) type 1 (OMIM 125850) without renal involvement, has also been identified in patients with primary Fanconi renal tubular transport disorder (OMIM 616026) co-presenting with MODY [Stanescu et al., 2012; Hamilton et al., 2014]. HNF4A is a known regulator of *SLC2A2*, which encodes the glucose transporter GLUT2, and mutations in *SLC2A2* cause Fanconi–Bickel syndrome (OMIM 227810), suggesting that defective HNF4A could lead to impaired renal tubular transport [Stanescu et al., 2012]. We expect that *HNF4A* mutations in patients with primary Fanconi renal tubular transport disorder and MODY will be identified more frequently with increasing use of NGS, which will confirm the role of *HNF4A* in this phenotype.

Finally, different inheritance patterns or mutation types in genes involved in syndromic kidney disease can cause an isolated kidney phenotype at the mild end of the phenotypic spectrum. Examples are mutations in *LMX1B*, which are associated with nail–patella syndrome (OMIM 161200) but can also cause an isolated glomerulopathy [Edwards et al., 2015; Isojima et al., 2014; Boyer et al., 2013], and mutations in *OCRL1*, which cause Lowe oculocerebrorenal syndrome (OMIM 309000), but also cause Dent disease 2 (OMIM 300555) [Hoopes et al., 2005]. Another example is provided by *FRAS1* and *FREM2*, biallelic truncating mutations in which cause Fraser syndrome (OMIM 219000). A 2012 study identified heterozygous missense mutations in *FRAS1* and *FREM2* in patients with isolated unilateral renal agenesis [Saisawat et al., 2012]; however, a more extensive study by the same group in 2014 showed that biallelic missense mutations, rather than heterozygous missense mutations, in six genes associated with the Fraser–MOTA (manitoba-oculo-tricho-anal)–BNAR (bifid nose with or without anorectal and renal anomalies) spectrum of diseases, including *FRAS1* and *FREM2*, were responsible for 2.2% cases of CAKUT in 590 affected families [Kohl et al., 2014]. The frequency of heterozygous truncating variants in *FRAS1* and *FREM2* in a large control dataset was also found to be higher than expected if these mutations were to cause dominantly inheriting CAKUT, confirming that heterozygous mutations were

when the signal is lost_marijn_8072018.indd 176 08/07/2018 10:50

unlikely to cause CAKUT. Understanding exactly how these disease phenotypes correlate with inheritance and mutation type can have important consequences for diagnosis, clinical management and genetic counselling.

7.3 RECLASSIFYING KIDNEY DISEASE

Genetic findings from NGS can also lead to reclassification of kidney disease in individual patients. For example, patients with Alport syndrome have been misdiagnosed as having MPGN and patients with congenital chloride diarrhoea caused by *SLC26A3* mutations have been misdiagnosed as having Bartter syndrome [Adam et al., 2014; Choi et al., 2009]. Clinical phenotyping can confirm a molecular diagnoses, in one example revealing hearing loss and retinal anomalies in a patient with Alport syndrome, illustrating the importance of 'reverse phenotyping' [Adam et al., 2014].

Genetic diagnostics can aid clinical phenotyping especially for diseases with variable or incomplete expression. For example, missense and truncating mutations in *CLCN5* were detected in patients presenting with a Bartter-like phenotype (OMIM 601678) in whom mutations in known disease-associated genes were excluded [Besbas et al., 2005; Bogdanovic et al., 2010; Okamoto et al., 2012] and in patients with focal segmental and/or global glomerulosclerosis [Sethi et al., 2015; Copelovitch et al., 2007; Frishberg et al., 2009; Valina et al., 2013; Cramer et al., 2014]. *CLCN5* encodes the voltage-gated chloride channel ClC-5, which is classically associated with Dent disease (OMIM 300009). Dysfunctional CLCN5 is hypothesized to disrupt the endocytosis pathway in the proximal tubule and consequently increased sodium delivery to the distal tubule might induce hypovolemia, thereby activating the renin–angiotensin–aldosterone axis to cause Bartter-like features of hypokalemic metabolic alkalosis, hypercalciuria and hyperreninaemic hyperaldosteronism [Besbas et al., 2005; Bogdanovic et al., 2010], even though the clinical presence of low molecular weight proteinuria excluded a diagnosis of Bartter syndrome. Similarly, patients who presented with nephrotic range proteinuria and focal segmental and/or global glomerulosclerosis had selective albuminuria with normal serum albumin level, an absence of oedema, and minimal podocyte foot-process effacement on renal biopsy, suggesting a tubular rather than a glomerular aetiology and a missed diagnosis of Dent disease, which was confirmed by genetic findings [Copelovitch et al., 2007; Frishberg et al., 2009; Valina et al., 2013; Cramer et al., 2014; Sethi et al., 2015]. A diagnosis of Dent disease in patients with proteinuria has major consequences for treatment because immunosuppressive therapy, which can have considerable adverse effects, can be discontinued. In a patient with SRNS and a hemizygous truncating *CLCN5* mutation, treatment was changed from immunosuppressive therapy to an angiotensin-converting-enzyme (ACE) inhibitor in combination with citrate and thiazide supplementation [Sethi et al., 2015], demonstrating the clinical relevance of a molecular diagnosis for the management of kidney disease.

Another example in which NGS has enabled reclassification of clinical

when the signal is lost_marijn_8072018.indd 177 08/07/2018 10:50

diagnoses is provided by a study in which whole-exome sequencing was performed in 79 consanguineous and familial cases with paediatric onset of CKD with suspect nephronophthisis on the basis of renal ultrasound criteria. A causal mutation was identified in 50 cases, and led to reclassifications of the disease in 18: eight were reclassified as renal tubulopathy, four as Alport syndrome, three as CAKUT, two as autosomal-recessive polycystic kidney disease (OMIM 263200) and one as autoimmune polyendocrinopathy-candidiasis-ectodermal dystrophy (APECED) syndrome (OMIM 240300) [Braun et al., 2016]. Here too, reclassification can have important consequences for therapy and clinical monitoring of disease manifestations [Johnston et al., 2015].

7.4 OLIGOGENIC INHERITANCE AND REGULATORY REGIONS

Oligogenic inheritance, whereby a phenotype is determined by a combination of multiple genes, is increasingly recognized to explain at least a component of interfamilial and intrafamilial phenotypic variability. Simultaneous sequencing of genes associated with kidney diseases using NGS has uncovered many genes that contribute modifier alleles to a variety of nephrogenetic disorders, including manifestations outside their original phenotypic spectrum. An example is *HNF1B*, a gene that is involved in a plethora of cystic and noncystic kidney diseases with associated extra-renal manifestations [Verhave et al., 2015]. Heterozygous *HNF1B* mutations have also been detected in combination with mutations in *PKD1* or *PKD2* in familial cases of ADPKD [Bergmann et al., 2011]. In these patients, modifier variants in *HNF1B* result in a more severe, early-onset form of ADPKD, which presents antenatally with Potter sequence or enlarged, hyperechoic kidneys. In ciliopathies, heterozygous mutations in *TTC21B*, *RPGRIP1L* and *TMEM67* contribute to mutational load across the ciliopathy spectrum [Davis et al., 2011; Khanna et al., 2009; Leitch et al., 2008].

Although NGS has boosted gene discovery and significantly improved the diagnostic yield of genetic studies [Renkema et al., 2014; Braun et al., 2016; Sadowski et al., 2014], the origins of many nephrogenetic diseases remain unsolved. The aetiologies of approximately 50% of nephronophthisis cases remain unexplained and genes discovered after the first gene for nephronophthisis, *NPHP1*, in 1997 [Saunier et al., 1997; Hildebrandt et al., 1997a], individually explain the disease in only a very small percentage of patients [Arts and Knoers, 2013b]. Some patients with nephronophthisis have heterozygous mutations in genes associated with recessive disease in which a second mutation remains elusive [Schueler et al., 2016]. These cases warrant new sequencing approaches, such as whole-genome sequencing to study non-coding regulatory regions and microRNAs [Renkema et al., 2014]; chromosome conformation capture [Kubiak and Lewandowska, 2015] or chromatin immunoprecipitation sequencing (in combination with RNA-sequencing or proteomics) [Mimura et al., 2014] to study the regulation of gene expression and epigenetic modifications. An example of a noncoding modifier is an intronic polymorphism in *NOS3* that has been

when the signal is lost_marijn_8072018.indd 178 08/07/2018 10:50

associated with the rate of CKD progression in various populations of patients with ADPKD [Elumalai et al., 2014a; Merta et al., 2002]. In a cohort of patients with Alport syndrome, three of 24 identified causal *COL4A5* mutations were intronic [King et al., 2002]. Similarly, whole-genome sequencing in conjunction with mRNA sequencing identified intronic *DGKE* mutations that segregated with aHUS in two independent families [Mele et al., 2015]. These findings support whole-genome sequencing as a promising approach in genetically unsolved cases [Mele et al., 2015; Goodwin et al., 2016], although the discovery of noncoding mutations brings with them new challenges in interpreting their functional relevance [van de Hoek et al., 2015].

7.5 DIAGNOSTIC OPPORTUNITIES AND CHALLENGES

Advances in molecular diagnostics could potentially signal the end of the diagnostic renal biopsy. Indeed, molecular diagnostics has many advantages over histopathology, being less invasive and less prone to sampling errors and subjective assessment, which can lead to inconclusive results, especially in advanced stages of disease [Yao et al., 2012]. In contrast to histopathology, molecular testing requires only venepuncture and has the potential to pinpoint the aetiology of a disease regardless of the disease stage. The advantages of molecular diagnostics are evident in female carriers of Alport syndrome, where the distinction between a hemizygous mutation in the X-linked *COL4A5* gene and a heterozygous mutation in *COL4A3/4* can have important implications for prenatal counselling [Adam et al., 2014]. In addition, the type of *COL4A* mutation can provide prognostic information regarding renal and extrarenal phenotypes and the risk of post-transplantation anti-glomerular basement membrane glomerulonephritis [Adam et al., 2014; Jais et al., 2000], demonstrating that DNA testing can yield a diagnosis and guide prognostic and therapeutic decision-making in patients with nephrogenetic diseases.

An obvious limitation of genetic diagnostics, however, is that they cannot be used to diagnose acquired diseases, such as immune-mediated glomerulonephritis. In the absence of evidence for a genetic cause a renal biopsy should therefore be performed if indicated.

One challenge in integrating genetic findings into clinical practice is how to interpret specific genetic variants uncovered by molecular testing. Although many *in silico* tools exist to predict variant pathogenicity, variants that are termed 'pathogenic' in the literature have now also been found in control populations, such as those in the ExAC database (http://exac.broadinstitute.org), questioning the pathogenicity of these variants. For example, in a patient with ADPKD we observed a p.Arg4154Cys variant in *PKD1* (A.M. van Eerde, unpublished work), which is listed in the Human Gene Mutation Database (HGMD; www.biobase-international.com/product/hgmd) as a pathogenic mutation on the basis of findings from two publications [Stenson et al., 2014; The 1000 Genomes Project Consortium, 2010; Perrichot et al., 1999]. However, the allele frequency for this

when the signal is lost_marijn_8072018.indd 179 08/07/2018 10:50

variant of 0.001 reported in the ExAC database results in a carrier frequency that is tenfold higher than expected based on the prevalence of ADPKD, the contribution of *PKD1* mutations and the de novo mutation rate [Harris and Torres, 2015]. Carrier frequencies of this variant in populations of African and South Asian descent are even higher, approaching 1% and 0.6% respectively. These observations render it highly unlikely that the p.Arg4154Cys variant caused the dominant disease in our patient. Although non-penetrance and variability in age of ADPKD onset have been described, these findings prompt reinterpretation of published 'pathogenic' variants based on their occurrence in control datasets. Genome sequencing is estimated to generate up to 800 putative loss-of-function (LOF) mutations per individual genome (including incorrectly annotated hypomorphic mutations, heterozygous LOF mutations in genes associated with recessive disease and LOF mutations whose effect will be minimal because of gene redundancy), 100 of which are predicted to be true LOF mutations [Johnston et al., 2015]. In a study that investigated LOF mutations in 951 participants between 45 and 65 years of age from the ClinSeq cohort [Biesecker et al., 2009], 103 exomes contained putative LOF variants of which 34 could be related to a phenotype through deeper phenotyping or a detailed analysis of family history. The remainder of the LOF mutations, including mutations in *OFD1* (which is typically associated with oral-facial-digital syndrome type 1; OMIM 311200) and *TRPC6* (which is typically associated with FSGS2; OMIM 603965) were also identified in healthy individuals [Johnston et al., 2015], although the possibility that the patient with the *TRPC6* mutation might develop manifestations of FSGS later in life cannot be excluded. Similarly, targeted NGS of 208 candidate genes in 453 patients with CAKUT detected no significant excess of rare variants in these genes compared to control cohorts [Nicolaou et al., 2015a]. These findings illustrate that the genetic background of kidney diseases is more complex than previously thought. General considerations with regard to the interpretation of sequence variants in kidney disease and the concomitant ethical implications has been reviewed previously [Renkema et al., 2014].

Another point to bear in mind is that 'pathogenic' mutations are not always causal mutations for the disease of interest. Consequently, molecular testing in an index patient should be followed by segregation analysis in the family to determine whether the findings fit the expected inheritance pattern. If so, further validation of the findings should be performed to obtain clinical and functional proof of involvement of the variant in disease pathogenesis, for example, by performing deeper phenotyping to confirm the genetic diagnosis. Deeper phenotyping can include a revision of the renal biopsy and clinical evaluation of renal and extra-renal symptoms. Mutations in novel genes or novel mutations (especially missense mutations) in known genes require validation in a larger patient cohort and confirmation of their function, for example in patient-derived cells or model organisms [van de Hoek et al., 2015]. Of note, the presence of mutations in other genes known to be associated with a particular disease must be excluded before causality can be attributed to a new candidate variant [Braun et al., 2016; Roversi et al., 2015].

when the signal is lost_marijn_8072018.indd 180 08/07/2018 10:50

Diverse phenotypes are associated with mutations in canonical kidney disease genes. The examples discussed here show that phenotypic boundaries of disease can shift and that genotype–phenotype correlations are not clear cut [Chaki et al., 2011]. However, the ability to accurately predict the phenotype or outcome of a particular disease is relevant for genetic and reproductive counselling, for instance in decisions regarding preimplantation genetic diagnostics. Consequently, well-maintained international registries that combine extensive genotypic and phenotypic patient data, for example Decipher [Firth et al., 2009] (http://decipher.sanger.ac.uk) and ClinVar [Landrum et al., 2016] (www.ncbi.nlm.nih.gov/clinvar/), are imperative to establish clinically useful genotype–phenotype correlations.

Thus, although molecular diagnostics is a valuable addition to the diagnostic toolbox, its diagnostic utility is limited to diseases with a genetic aetiology and the interpretation of genetic variants can be challenging. Genetic counselling and disease management will become increasingly individualized on the basis of specific combinations of clinical findings together with the identification of disease gene mutations, modifiers and epigenetic factors [Nicolaou et al., 2015b; Prakash and Gharavi, 2015].

7.6 PERSONALIZED TREATMENT OF KIDNEY DISEASE

The ultimate goal of studies into the genetic aetiology of kidney phenotypes, next to genetic counselling, is the development and potential application of personalized approaches to treatment. The identification of mutations in podocyte-specific genes can influence decisions on immunosuppressive treatment in patients with FSGS and inform post-transplantation prognostics [Liebau, 2014; Weber and Tonshoff, 2005]. Similarly, the post-transplantation recurrence rate of aHUS is much lower in patients with mutations in *MCP* and *DGKE* than in patients with mutations in other genes [Noris et al., 2010, 2013] and ACE inhibitors can be used to slow the progression of renal failure in patients with Alport syndrome without the need for immunosuppressants [Gross et al., 2012; Webb et al., 2013]. Improved understanding of the genes and mechanisms underlying kidney disease can open new therapeutic routes. For example, the discovery of the role of DNA replication stress in the pathogenesis of nephronophthisis has led to the suggestion that antifibrotic agents such as paclitaxel might represent a promising new therapy [Slaats et al., 2016b]. Despite these successes, the variable response to complement inhibitors in patients with *DGKE*-related nephropathy illustrates that a monogenic paradigm can be too simplistic when considering pharmacogenomics. Large case-control studies are needed to establish real correlations between genetic, epigenetic and environmental factors in relation to response to therapy.

when the signal is lost_marijn_8072018.indd 181 08/07/2018 10:50

7.7 CONCLUSIONS

The explosive increase in the availability of high-throughput sequencing techniques has revolutionized the field of nephrogenetics. Large-scale implementation of NGS in research and diagnostics of kidney disease has led to a surprising shift in the phenotypic boundaries of diseases, connecting phenotypes within and across current disease categories and leading to new aetiological insights. For example, the identification of mutations in *DGKE*, a gene that is typically associated with MGPN, in patients with aHUS inspired the investigation of complement-dependent and complement-independent mechanistic links between both *DGKE*-associated diseases. The exploration of common aetiologies of diseases will thus continuously improve our understanding of the pathophysiology of inherited kidney disease and expose novel targets for personalized therapies.

An important question is whether molecular diagnostics will eventually replace clinical diagnostic tools. Although genetics can lead to an accurate diagnosis of hereditary kidney diseases, the phenotypic heterogeneity associated with genes described in this Review demonstrates that the aetiology of kidney disease is complex in many cases. We therefore cannot base diagnosis and therapeutic decisions solely on genetic findings (**Box 1**). Several mechanisms exist to explain phenotypic heterogeneity, including the type and location of the mutation [Romani et al., 2014], the presence or absence of basal exon skipping [Drivas et al., 2015], whether oligogenic inheritance is present [Bergmann et al., 2011; Davis et al., 2011], and the influence of non-coding regions and epigenetic regulators [Mele et al., 2015; Mimura et al., 2014]. While all these factors might influence disease outcome, therapy responsiveness depends on additional genetic factors (such as the presence of Cytochrome P450 polymorphisms, which can affect drug metabolism) and environmental factors (such as diet). The foundation of hereditary kidney disease management should therefore be based on molecular genetic analyses closely coupled with clinical evaluation and treatment (**Figure 3**). Emerging complex inheritance patterns and new challenges with regard to the interpretation of genetic data require multidisciplinary approaches, innovative computational tools, deeper and consistent phenotyping and international data sharing. A 'genome first' approach, whereby genetic testing is performed at the start of the diagnostic workup and the results integrated into all stages of routine clinical practice, will help to optimize care for patients with kidney disease.

when the signal is lost_marijn_8072018.indd 182 08/07/2018 10:50

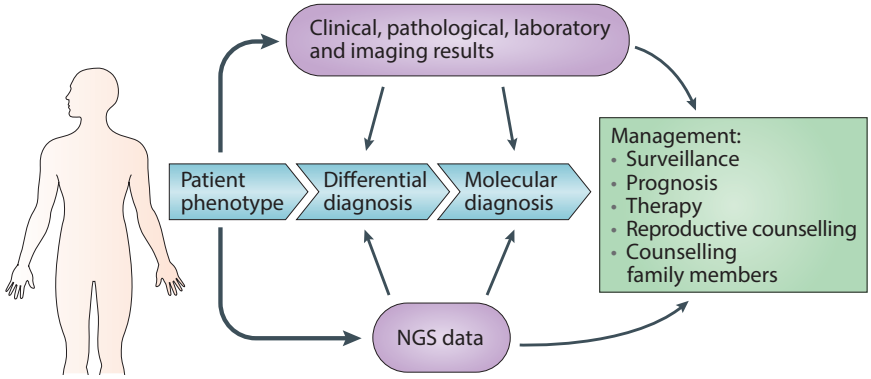

Figure 3. Implementation of next-generation sequencing (NGS) data in routine nephrology practice. When patients enter the nephrology outpatient clinic, NGS will be performed as part of the routine diagnostic workup. NGS results will be considered in combination with the phenotype and additional clinical investigations, including laboratory tests and renal ultrasonography. In the absence of evidence for a genetic cause a renal biopsy can be performed if indicated, for example for suspected immune-mediated glomerulonephritis. Detection of possibly causal genetic variants should be followed by segregation analysis in the family, deeper clinical phenotyping and, in case of novel variants, validation in larger cohorts and/or functional models before a definite molecular diagnosis can be made. NGS data, coupled with clinical data, can be used as a resource to guide and monitor personalized treatments, prognosis and surveillance in patients and family members, and can be used for reproductive counselling.

when the signal is lost_marijn_8072018.indd 183 08/07/2018 10:50

Box 1. Current approach for using next-generation sequencing (NGS)-based tests in nephrology

Requesting genetic tests by non-clinical geneticists

- Nephrologists can order genetic testing of symptomatic patients if the nephrologist is well informed about the associated phenotype and inheritance pattern of the likely genes involved and has counselled the patient. When gene panels contain large numbers of genes (or the entire exome) with a considerable potential of incidental findings, consider consulting or referring the patient to an expert centre for pre-test counselling.
- Determine the number of genes to be analysed, weighing the chance of finding the causal mutation against the risk of incidental findings.

Pre-test counselling

- Discuss the possibility of finding 'variants of unknown significance' and incidental findings with patients before testing, and explain the hospital's policy with regard to incidental findings. If the implication of an incidental finding in one of the genes in the test is unclear, consult a clinical geneticist.

Post-test counselling

- Correct interpretation of the NGS findings often takes a multidisciplinary approach involving nephrologists, clinical geneticists and laboratory specialists. Consider consulting an expert centre before communicating results to patients.

General considerations

- A diagnosis should be based on a combination of genetic and clinical findings.
- Genetic testing can confirm but not rule out a diagnosis owing to factors such as technical limitations and the presence of unknown causative genes. Some genes (such as *PKD1* and *MUC1*) are notoriously difficult to test. Large copy number variations are often not routinely picked up in diagnostic NGS.
- A genetic diagnosis should be viewed as a starting point that directs further clinical phenotyping.
- If heterozygous mutations in a particular recessive gene can cause a (subtle) phenotype, additional investigations (such as renal ultrasonography or urinalysis) should be considered in carrier parents.
- Oligogenic inheritance should be taken into account to explain interfamilial and intrafamilial variability and in counselling relatives.
- Functional validation, consistent phenotyping and data sharing are essential for the correct interpretation of variants in kidney disease genes.
- A clinical geneticist should be involved in presymptomatic genetic testing of family members.
- Genetic testing of family members, prenatal and preimplantation genetic diagnostics can only be offered if causality of a variant is established. As

when the signal is lost_marijn_8072018.indd 184 08/07/2018 10:50

the total process from mutation to establishing causality can be lengthy, we recommend timely genetic testing.

Acknowledgments
The researchers receive funding from the Dutch Kidney Foundation under grant agreements CP11.18 Kouncil (N.V.A.M.K. and R.H.G.) and KSTP12 010 (A.M.v.E.), the European Community's Seventh Framework Programme (FP7/2009) under grant agreement 305608 EURenOmics (N.V.A.M.K., F.S. and K.Y.R.) and Fonds NutsOhra grant 1303-070 (A.M.v.E.).

when the signal is lost_marijn_8072018.indd 185 08/07/2018 10:50

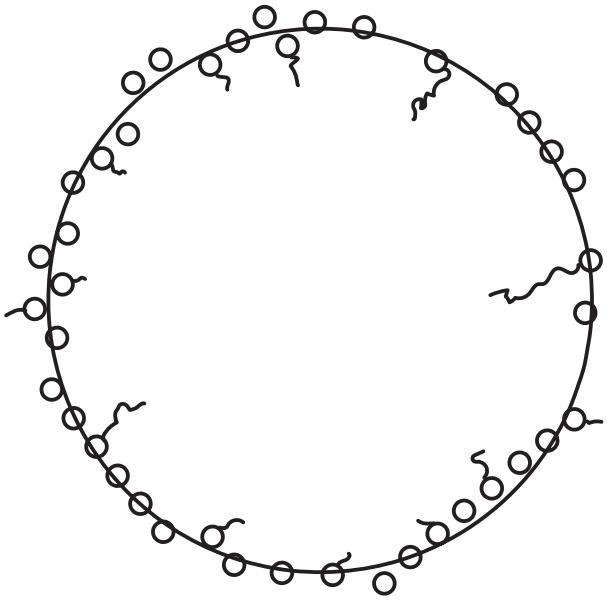

CHAPTER 8

General discussion

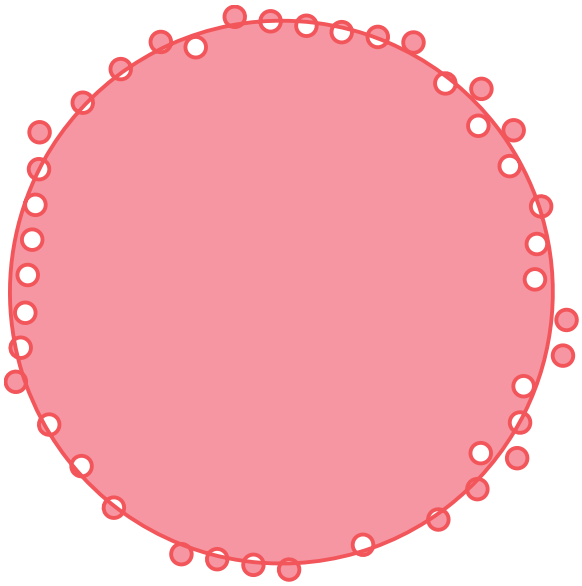

when the signal is lost_marijn_8072018.indd 187 08/07/2018 10:50

SUMMARY

In this thesis, I have investigated the phenotypes, genetic etiology and molecular mechanisms of a group of diseases called 'renal ciliopathies'. Although renal ciliopathies are considered rare diseases, they are the most important monogenic cause of pediatric end-stage renal disease (ESRD). To improve early diagnostics and prognostics, the Nephronophthisis Registry was created to identify presenting signs and symptoms and to investigate gene-phenotype associations in a cohort of 40 Dutch patients with a nephronophthisis-related ciliopathy (NPH-RC). Novel genetic variants and candidate genes for NPH-RC were identified. Two candidate genes for ciliopathies (*NEK1* and *KIF14*) were functionally characterized in cell models, and support was added for nonsense-associated alternative splicing as a mechanism behind phenotypic heterogeneity in ciliopathies. In addition, proteomics of urinary extracellular vesicles was used as a novel method for non-invasive diagnostic and prognostic biomarker discovery in patients with NPH-RC. Early detection and more accurate prognostics will improve timely treatment, genetic counseling and overall clinical care for patients with NPH-RC. Here, I will discuss the main findings of the research presented in this thesis in the context of the changing genetics landscape, renal ciliopathy research and the future of clinical genetics.

when the signal is lost_marijn_8072018.indd 188 08/07/2018 10:50

8.1 THE PROMISE OF NEXT-GENERATION SEQUENCING IN DIAGNOSTICS OF RENAL CILIOPATHIES

8.1.1 Genetic findings in a Dutch renal ciliopathy cohort

In **Chapter 2**, I describe a cohort of 52 Dutch patients from 45 families with a renal ciliopathy. Forty out of 52 patients met diagnostic criteria of NPH-RC and were included in the Nephronophthisis Registry. We detected causal biallelic mutations in the *NPHP1* gene in 38% of 13 NPH-RC patients who underwent genetic testing within this study. Biallelic variants in *TMEM67* were detected in three additional patients. Through whole-exome sequencing (WES) followed by cilia assays in fibroblasts, we identified *NEK1* as the first gene for oral-facial-digital syndrome type II (**Chapter 4**), expanding the phenotypic spectrum associated with mutations in *NEK1*. In addition, we confirmed mutations in the candidate gene *KIF14* as a cause for a severe Meckel-Gruber syndrome-like phenotype (**Chapter 5**). We also identified variants in novel candidate genes for ciliopathies, including *NINL*, *CLASP1* and *CNTRL*, for which functional characterization studies are still ongoing. In all cases described above, bioinformatic filtering prioritized candidate variants for functional characterization.

In patients without clear candidate variants, functional assays can also direct further bioinformatic filtering. For example, cilia characterizing assays in patient-derived fibroblasts were used to confirm that the phenotype was indicative of a ciliopathy in a patient with skeletal and cardiac defects and a heterozygous deletion encompassing *IFT43* (**Chapter 3**), and in a patient with a skeletal ciliopathy phenotype without suitable candidate variants after WES. In fibroblasts derived from the latter patient, the microtubule phenotype was consistent with that described for mutations in specific ciliopathy-associated genes (e.g. *IFT88, TRAF3IP1* and *NEK1*) [Bizet et al., 2015; Berbari et al., 2013; Thiel et al., 2011]. As a result, variants in these genes and their interactors were considered interesting candidate variants in this patient. Thus, bioinformatics and cilia characterizing assays in cell models can complement each other to reach a molecular diagnosis in NPH-RC patients.

Nevertheless, 62% of NPH-RC patients remained unsolved in our cohort, reflecting the <50% mutation detection rate reported in literature [Schueler et al., 2016]. Two patients (15%) showed single heterozygous predicted deleterious variants in known ciliopathy-associated genes after excluding deletions on the other allele. Similarly, a study using molecular inversion probe (MIP)-based targeted sequencing of 34 ciliopathy-associated genes in 384 NPH-RC patients yielded molecular diagnoses in only 21% of patients after excluding homozygous deletions of *NPHP1* [Schueler et al., 2016a]. Single heterozygous gene mutations were detected in 26 patients. CNV analysis and Sanger sequencing of all exons of the implicated genes revealed additional heterozygous mutations in only two patients [Schueler et al., 2016], demonstrating the high frequency of single heterozygous mutations in NPH-RC patients.

Assuming autosomal recessive inheritance in renal ciliopathies (the only known exception is OFD type 1, which is X-linked), heterozygous variants

when the signal is lost_marijn_8072018.indd 189 08/07/2018 10:50

detected in multiple ciliopathy-associated genes could point towards digenic or oligogenic inheritance. Digenic and oligogenic inheritance have been described in several ciliopathies [Katsanis, 2001; Bandano et al., 2003; Baala et al., 2007b; Helou et al., 2007; Tory et al., 2007; Leitch et al., 2008; Louie et al., 2010; Davis et al., 2011; Lin et al., 2013; Zhang et al., 2014]. However, the pathogenicity of some proposed modifier alleles is debated because they occur frequently in control populations, revealed for example using the ExAC browser [Lek et al., 2016]. Conversely, if heterozygous variants are detected in single ciliopathy-associated genes, and other ciliopathy-associated genes show excellent sequence coverage, detected variants could be modifiers to biallelic mutations in as yet unidentified cilia genes, or the second variant could be located outside the coding regions. Whole-genome sequencing (WGS) is then required to investigate the contribution of noncoding and regulatory regions. Noncoding variants have been implicated in other monogenic kidney diseases (**Chapter 7**) and could partly explain unsolved NPH-RC patients.

8.1.2 Diagnostic challenges in NPH-RC

NPH-RC can be challenging to diagnose clinically for several reasons. First, NPH-RC phenotypes are highly variable, even within families. This is illustrated in **Chapter 2** in which ESRD-onset in two siblings with a homozygous *NPHP1* deletion ranged from age 15 to age 28 years and the phenotypes of two siblings with *BBS1* mutations ranged from prenatally lethal cystic kidney disease in one sibling to mild developmental delay and polydactyly in the other sibling. Secondly, there is phenotypic overlap between different NPH-RC, for example NPH can occur in Joubert syndrome and in Bardet-Biedl syndrome. Third, as discussed in the introduction, symptoms and imaging findings in NPH are non-specific and overlap with other (cystic) kidney diseases including *MUC1*-related autosomal dominant tubulointerstitial kidney disease and autosomal recessive polycystic kidney disease (ARPKD) [Braun et al., 2016; Gee et al., 2014b]. Consequently, the diagnosis of NPH is often one per exclusionem. Fourth, the classification of NPH as a renal ciliopathy is called into question by the recent publication of biallelic mutations in *MAPKBP1* as a cause of cilia-independent NPH [Macia et al., 2017]. Although MAPKBP1 does not localize to cilia and no ciliary defects were observed in patient-derived fibroblasts, the combination of ESRD, histologic findings (including thickened tubular basement membrane, interstitial fibrosis, interstitial infiltrate, dilated tubules and cysts) and increased DNA damage response signaling resulted in the diagnosis NPH [Macia et al., 2017]. As a result, ciliary defects are no longer an obligatory feature in NPH, rendering the absence of defects in cilia assays inconclusive in patients with ESRD due to an unknown cause.

In addition to phenotypic variability, renal ciliopathies are highly genetically heterogeneous, limiting the utility of targeted sequencing approaches. While mutations in the first-discovered NPH gene, *NPHP1*, account for 20-25% of cases of isolated NPH, more recently published NPH genes (e.g. *ZNF423* and *DCDC2*) explain only 1-2% of cases or single families [Chaki et al., 2012; Schueler et al., 2015; Perrault et al., 2015]. It can take years to identify additional families with

when the signal is lost_marijn_8072018.indd 190 08/07/2018 10:50

genotypic and phenotypic overlap, as was the case for mutations in *KIF14* (**Chapter 5**), which were initially described in a single family with two fetuses with a Meckel-Gruber-like phenotype in 2014 [Filges et al., 2014]. Consequently, international data sharing and initiatives such as Gene Matcher [Sobreira et al., 2015] and Matchmaker Exchange [Philippakis et al., 2015], which connect clinicians and researchers working on similar genes and phenotypes, are indispensable to novel gene identification and molecular diagnostics in renal ciliopathies.

8.1.3 Next-generation sequencing in NPH-RC

Next-generation sequencing (NGS) has radically transformed research and diagnostics of genetically heterogeneous diseases during the past ten years because it enables mutation analysis of multiple genes at once, for example the targeted testing of a selected set of genes (gene-panel sequencing), the entire exome (whole-exome sequencing; WES), or the unbiased interrogation of the whole genome (whole-genome sequencing; WGS). In the context of renal ciliopathies, this means that all ciliopathy-associated genes and candidate genes can be examined simultaneously, allowing assessment of modifier alleles as well as facilitating discovery of novel genes. WES has proven to be a cost-effective strategy in a variety of disorders including intellectual disability, inborn errors of metabolism [Monroe et al., 2016; Valencia et al., 2015] and pediatric-onset chronic kidney disease [Vivante and Hildebrandt, 2016], and compared favorably with Sanger sequencing in Joubert syndrome [Tsurusaki et al., 2013].

However, the relatively high percentage of unsolved NPH-RC patients in this thesis and in literature [Braun et al., 2016; Schueler et al., 2016] necessitates the implementation of WGS to further improve diagnostics of renal ciliopathies. Although interpretation of WGS data is currently challenging, advantages are that WGS provides information about noncoding pathogenic variation [Elumalai et al., 2014b; Merta et al., 2002], structural variation and somatic mosaicism [King et al., 2016]. WGS shows improved mapping of repetitive elements and pseudogenes compared to WES. Furthermore, WGS yields a more uniform coverage of the exome than WES because it is less sensitive to GC content, which is especially high in first exons [Meienberg et al., 2016; Sun et al., 2015]. WGS has identified *C8ORF37* as a novel gene for Bardet-Biedl syndrome [Heon et al., 2016] and the ciliary gene *CEP78* as a novel gene for Usher syndrome [Fu et al., 2017]. Moreover, WGS in 16 unrelated patients with autosomal recessive retinitis pigmentosa (ARRP) uncovered a homozygous frameshift mutation in *NEK2* as a new cause in one patient and a deletion and inverted duplication in known ARRP-associated genes in two other patients [Nishiguchi et al., 2013]. These structural variants would have gone undetected with WES, underscoring the diagnostic utility of WGS.

when the signal is lost_marijn_8072018.indd 191 08/07/2018 10:50

8.2 CILIOPATHIES IN THE CONTEXT OF THE CHANGING GENETICS LANDSCAPE

8.2.1 Low hanging fruits in ciliopathies

As discussed above, genetic heterogeneity has caused the diagnostic slope in NPHP-RC patients to flatten. One interpretation in the field is that the 'low hanging fruits', i.e. variants that explain a relatively large percentage of patients, have been picked. A review of 150 studies using WES-based gene discovery in a broad range of patients' phenotypes revealed a decline in the proportion of cases explained by variants in newly identified genes over the past five years [Cirulli, 2016]. Fifty percent of the genes discovered in 2014-2015 showed variants in fewer than 5% of patients with a particular disease, suggesting that this could be a general trend in genetics of rare diseases [Cirulli, 2016]. The prediction made in 2011 that NGS would solve all monogenic diseases within the next few years has been proven to be too optimistic [Bamshad et al., 2011]. The findings in ciliopathies could therefore be symptomatic of a changing genetics landscape, in which geneticists are forced to consider different (non-monogenic) inheritance patterns and employ different (non-patient-based) methods of gene discovery in genetically heterogeneous diseases.

Large-scale efforts have identified numerous candidate genes for ciliopathies. Approaches range from siRNA screens [Wheway et al., 2015] and protein-protein interaction-based studies in cell lines [Dona et al., 2015; Coene et al., 2011; Boldt et al., 2009] to *in silico* modelling followed by functional characterization studies in zebrafish or other model systems [Shim et al., 2016]. A bioinformatic prediction model based on co-expression and co-evolution identified *TMEM107* as a ciliopathy candidate gene, which was subsequently confirmed by the detection of pathogenic mutations in *TMEM107* in three out of 238 patients with Joubert syndrome or OFD type VI [Lambacher et al., 2016]. A recent study using systematic tandem affinity purifications in combination with mass spectrometry for 217 ciliary proteins in HEK293T cells identified 1,319 proteins (of which 1,008 are currently not known to be ciliary), 4,905 interactions and 52 complexes [Boldt et al., 2016]. Among the interactors were three 3M syndrome-associated proteins, suggesting that 3M syndrome is a new ciliopathy phenotype [Boldt et al., 2016]. These studies help to elucidate the key players and pathways disrupted in ciliopathies, which will facilitate causal gene identification in patients.

8.2.2 Towards comprehensive molecular testing in NPH-RC

Until all NPH-RC patients can be explained with rapid genome sequencing techniques, integration of different types of -omics data from sequencing, proteomics and information about candidate genes and pathways obtained through methods described above can advance early diagnostic and prognostic testing. For example, we have shown for the first time that proteomics of urinary extracellular vesicles from NPH-RC patients can differentiate patients from controls (**Chapter 6**). If validated in larger independent cohorts, the discriminating proteins could serve as non-invasive biomarkers for diagnosis of NPH. In addition,

when the signal is lost_marijn_8072018.indd 192 08/07/2018 10:50

proteomics findings could point towards disrupted ciliary pathways and aid bioinformatic filtering in NPH-RC patients without a molecular diagnosis. Similarly, a discovery study investigating the urinary proteome in eight patients with ureteropelvic junction obstruction (UPJO) and eight control subjects identified 76 discriminating proteins, which could be used in the future to identify patients who require surgical intervention [Froehlich et al., 2016]. Overrepresentation of the oxidative stress pathway among discriminating proteins corroborated a previously described pathophysiological mechanism and could pinpoint candidate genes for UPJO [Froehlich et al., 2016]. An example of the benefit of integrating sequencing approaches is the improved mutation detection rate in NPH-RC patients through the combined application of high-throughput targeted molecular inversion probe (MIP) technology and array-based microfluidic PCR [Schueler et al., 2016]. Likewise, a combination of WGS, chromosome conformation capture and RNA sequencing could be employed to evaluate the role of (epigenetic) regulatory mechanisms in the etiology of NPH-RC. Cilia-specific databases such as Cildb and the curated SYSCILIA Gold Standard are essential to integrate and exploit data obtained through different (high-throughput) techniques [Arnaiz et al., 2009; Van Dam et al., 2013; Arnaiz et al., 2014].

8.2.3 Future directions in renal ciliopathy research

There are five major areas in renal ciliopathy research in which ongoing technological progress can further our biological understanding of this heterogeneous category of diseases and identify novel therapeutic targets.

First, the above described advances in the applications of WGS and other sequencing techniques, coupled with functional assays using CRISPR-Cas-mediated targeted mutagenesis, will help to elucidate the genetic etiology in the remaining 50% of NPH-RC patients.

Second, expanding the scope of NPH-RC research to extracellular vesicle-mediated intercellular communication and modifications of extracellular vesicle content in vitro can expose novel pathophysiological mechanisms and applications in kidney regeneration and targeted drug delivery. For example, extracellular vesicle-mediated communication between renal tubular epithelial cells and interstitial fibroblasts is thought to play an important role in epithelial-to-mesenchymal transition (EMT) and in tubulointerstitial fibrosis in chronic kidney disease [Tan et al., 2016; Borges et al., 2013; Bruno et al., 2012; Vella, 2014]. As tubulointerstitial damage is a key determinant of renal insufficiency in NPH-RC, the role of extracellular vesicle-based information transfer should be investigated alongside ciliary signaling pathways and the nuclear function of ciliary proteins (below) to elucidate the pathogenesis of nephronophthisis (**Figure 1**). This could be especially relevant because cilia secrete extracellular vesicles with cilia-specific proteins as cargo, which are thought to mediate ciliary signaling and have been implicated in ciliopathies [Chacon-Heszele et al., 2014; Wang and Barr, 2016; Dixon-Salazar et al., 2012; Nager et al., 2017]. Extracellular vesicles are also interesting in the context of targeted therapies for NPH, either through blocking of extracellular vesicles involved in EMT or through targeted delivery of wild-type

when the signal is lost_marijn_8072018.indd 193 08/07/2018 10:50

mRNA or drugs to kidney cells [Pomatto et al., 2017; Lener et al., 2015].

Third, innovations in cell biology will continue to unravel the pathophysiological mechanisms underlying ciliopathies, in particular the dual role of cilia proteins in cell-cycle regulation, DNA damage response signaling and microtubule dynamics [Choi et al., 2013; Chaki et al., 2012; Slaats and Giles, 2015; Kim et al., 2004; Hernandez-Hernandez et al., 2013]. Interestingly, *KIF14*-, *NEK1*- and *PKD1*-deficient cells show increased aneuploidy [Carleton et al., 2006; Chen et al., 2011a; AbouAlaiwi et al., 2014]. Aneuploidy is a hallmark feature of cancer cells. The association between ciliary defects and aneuploidy is also evident in cells from patients with *BUBR1*-mediated mosaic variegated aneuploidy [Miyamoto et al., 2011], which is a cancer predisposition syndrome, and in cells from patients with *ATR*- and *CPAP*-mediated Seckel syndrome, which show defects in cilia formation, disassembly and signaling [Stiff et al., 2016; Gabriel et al., 2016; Kalay et al., 2011]. These examples indicate important links between ciliopathies and fundamental cancer research (reviewed in [Gerhardt et al., 2016; Castresana, 2015]). Moreover, the role of spinocerebellar ataxia type 11-associated *TTBK2* in ciliogenesis [Goetz et al., 2012] and the recent discovery of *NEK1* risk variants in 3% of patients with amyotrophic lateral sclerosis [Kenna et al., 2016] support ciliary dysfunction in neurodegenerative disorders. These findings suggest that ciliopathies are more prevalent than previously assumed and that collaboration with researchers from other fields could unveil novel therapeutic targets for a wide range of cilia-associated diseases.

Fourth, the availability of organoids as model systems allows researchers to study the effect of mutations in ciliopathy-associated genes at an organ level. Kidney organoids containing both tubular and glomerular cell types have been developed from embryonic stem cells and induced pluripotent stem cells (iPSC) by several groups [Takasato et al., 2015; Xinaris et al., 2016; Yamaguchi et al., 2016]. In a recent study in which *REEP6* was identified as a novel gene for autosomal recessive retinitis pigmentosa, expression of a retina-specific isoform of *REEP6* was confirmed in human optic cup organoids [Arno et al., 2016]. In addition to increasing pathophysiological understanding, organoids are excellent tools to screen drugs that could benefit NPH-RC patients [Fatehullah et al., 2016].

Finally, advances in regenerative medicine are opening up new treatment options for ciliopathy patients. For example, clinical trials have demonstrated that gene-replacement therapy by using subretinal injection of an adeno-associated viral (AAV) vector containing *RPE65* caused improvement of visual acuity in patients with severe Leber congenital amaurosis due to *RPE65* mutations [Bainbridge et al., 2008; Hauswirth et al., 2008; Maguire et al., 2008]. Targeted delivery of genes or genome editing tools such as the CRISPR-Cas system to the kidney is a lot more challenging than delivery to the eye because the eye is a closed compartment. However, it has been proposed that CRISPR-Cas could be employed to generate exogenous human kidneys from human PCS in large animals [Higashijima et al., 2017]. Although technically challenging and subject to ethical debate, this latter approach could partly solve the shortage of kidneys for transplantation. Additionally, the knowledge of reprogramming cells gained from

when the signal is lost_marijn_8072018.indd 194 08/07/2018 10:50

organoid research (described above) could be applied to reseed decellularized kidney scaffolds or to populate 3D bioprinted kidneys as future alternatives for dialysis and transplantation [McKee and Wingert, 2016].

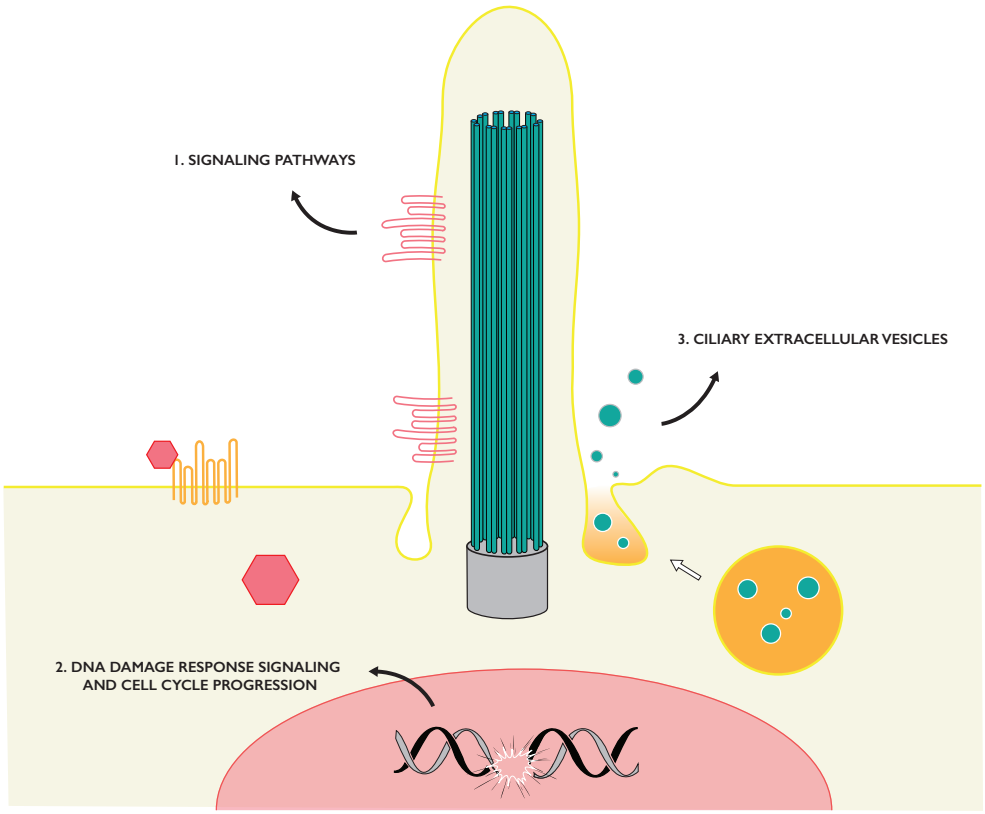

Figure 1. The role of ciliary extracellular vesicles in the pathophysiology of nephronophthisis should be studied in combination with ciliary signaling pathways and the function of ciliary proteins in DNA damage response signaling and cell cycle progression. Ciliary extracellular vesicles also represent an additional targetable mechanism for future treatment of nephronophthisis-related ciliopathies.

8.3 THE FUTURE OF GENETIC DIAGNOSTICS AND THE EVOLVING ROLE OF THE CLINICAL GENETICIST

8.3.1 Expanding territory of clinical genetics

Implementation of the above-described developments in personalized medicine depends on close collaborations between researchers, physicians and patients. One such collaborative effort in the Netherlands is the Parelsnoer Institute,

when the signal is lost_marijn_8072018.indd 195 08/07/2018 10:50

which provides researchers and physicians with the infrastructure for uniform collection of clinical data and biobanking of patient materials for biomedical research including kidney research (www.parelsnoer.org). Another example is the Center for Personalized Cancer Treatment, which aims at repurposing anti-cancer medication based on NGS profiles from tumor biopsies (www.cpct.nl). The latter example shows that clinical genetics is expanding from rare Mendelian syndromes into the domain of common diseases like cancer, obesity, cardiovascular disease and neuropsychiatric disorders. Consequently, clinical geneticists will increasingly participate in multidisciplinary teams with other (organ) specialists, lab specialists, bioinformaticians and ethicists [Bowdin et al., 2016].

Whereas clinical genetics is currently the ultimate diagnostic specialty, there is a growing appreciation among other medical specialists that genetic testing cannot only improve prognostics and genetic and reproductive counseling, it can also guide therapeutic decision-making (see pharmacogenetics, **Chapter 7**). This holds true for both rare genetic diseases and for complex traits [Zaiou and El Amri, 2017]. For example, sodium channel-blocking anticonvulsants such as carbamazepine are contraindicated in patients with *SCN1A*-related Dravet syndrome [Wallace et al., 2016] and the discovery of mutations in the ATP-dependent potassium channel subunit-encoding gene *ABCC9* in patients with Cantú syndrome suggested beneficial effects of treatment with ABCC9 antagonists [Harakalova et al., 2012]. Correspondingly, elucidation of fibrotic pathways in the pathogenesis of nephronophthisis suggested a role for anti-fibrotic agents including paclitaxel in the treatment of NPH-RC [Slaats et al., 2016b]. In common disease, a genome-wide association study (GWAS) of plasma lipid levels identified the *HMGCR* locus, marking a common variant with a modest effect on LDL cholesterol levels. However, the HMGCR protein is the target of the widely-used statins, which demonstrates that a GWAS variant of modest effect size can prove a disproportionately effective drug target [Global Lipids Genetics Consortium, 2013]. These examples highlight the utility of considering genetics in patient management.

8.3.2 The clinical geneticist as a treating physician

As a result of the advances in genome editing, especially the arrival of CRISPR-Cas technology, causal treatment of genetic diseases including NPH-RC will become feasible in the future. Originally part of the bacterial adaptive immune system, RNA-guided Cas9 nucleases can introduce targeted double-strand breaks in mutated genes, which can be repaired by non-homologous end joining (inactivating the gene) or by homology-directed repair using a DNA template (inserting the correct sequence) [Cong et al., 2009]. In their position paper entitled 'Genome Editing' published in November 2016, the Royal Netherlands Academy of Arts and Sciences (KNAW) states that genome editing using the CRISPR-Cas system is more precise, cheaper and more efficient than ever before [KNAW, 2016].

When CRISPR-Cas-based gene therapy becomes part of patient care, clinical geneticists are best equipped to inform patients about expected health benefits and potential risks and side effects, and coordinate and monitor the

when the signal is lost_marijn_8072018.indd 196 08/07/2018 10:50

treatment. As a first step, clinical geneticists are essential partners in the selection of patients with genetic disease with the highest potential benefits and the lowest potential risks for the first gene therapy clinical trials. The first clinical application of CRISPR-Cas-based gene therapy will likely be the editing of tissue-specific, somatic stem cells. Accordingly, the KNAW proposes editing of somatic stem cells of patients with inherited hematologic, metabolic or immunological diseases, or enhancing immune cell capacity to treat cancer, as the first clinical applications [KNAW, 2016]. Interestingly, a Chinese phase I clinical trial investigating CRISPR-Cas9-based knockout of *PD-1* in immune cells for the treatment of patients with metastatic non-small cell lung cancer was the first human CRISPR-Cas-based trial to receive ethical approval in 2016 [Cyranoski, 2016]. Recent reports of somatic applications of gene therapy for Hunter syndrome en junctional epidermolysis bullosa (using techniques other than CRISPR-Cas) have gained a lot of positive attention in regular media, which demonstrates an increasingly favorable attitude towards gene therapy [Hirsch et al., 2017; Voormolen, 2017]. The KNAW advises against clinical use of genome editing of the germline until technical, judicial and ethical issues have been addressed [KNAW, 2016]. For example, the Clinical Trials Regulation EU No. 536/2014 Article 90 prohibits gene therapy clinical trials that result in modification of the subject's germ line genetic identity. Additionally, although pre-implantation WGS of edited embryos would be advisable to exclude off-target effects, broader analysis of the obtained data would raise complex ethical concerns [De Wert et al., 2016].

Importantly, in NPH-RC patients, an early diagnosis would create a therapeutic window of three to four years to prevent severe kidney fibrosis. However, before clinical application of CRISPR-Cas would become a potential reality in Europe, technical hurdles must be taken including increasing the efficiency of editing by homology-directed repair, elimination of off-target and pleiotropic effects, circumventing an immune response against Cas9 and, for some somatic uses, (tissue-specific) gene delivery *in vivo* [Wang et al., 2016; Paquet et al., 2016; Chu et al., 2015]. Taken together, it will take many years before CRISPR-Cas-based therapy becomes a feasible treatment option for NPH-RC patients. Until then, *ex vivo* treatments that combine CRISPR-Cas technology and patient-derived PSC (discussed in section 8.2.3) are promising areas of personalized medicine.

8.3.3 Genetics in a societal context

The above described examples show that the position of genetics is changing, both inside the hospital and in society. The KNAW calls for an international societal debate between ethicists, scientists, physicians, patients, policymakers and the public on how genome editing can be applied clinically so that it promotes moral values such as equality and respect for diversity [KNAW, 2016]. The decision to change the human genome, especially in ways that affect future generations, is too big to be made by a select committee or to be guided by technological possibilities. Rather, it requires broad public engagement, as do other areas in genetics where technology has surpassed current policies (for example questions regarding ownership of genetic data, incidental findings and the duty to recontact).

when the signal is lost_marijn_8072018.indd 197 08/07/2018 10:50

The growing role of patient advocacy organizations in funding committees and in the establishment of European Reference Networks and Centers of Expertise [Hollak et al., 2016] shows that patients and informed public are valuable partners in decisions about genetic research and its clinical applications, for which public support is paramount.

8.4 CONCLUDING REMARKS

The chapters in this thesis demonstrate that renal ciliopathies are a complex field, characterized by vast genetic heterogeneity, overlapping syndromic entities, and a large percentage of unsolved patients using targeted sequencing techniques. WGS and especially the combined application of various sequencing techniques, *in silico* prediction models and proteomics-based candidate gene identification approaches (discussed in section 8.2.1) are likely to resolve (part of) the remaining cases. Furthermore, the emerging role of cilia proteins in cell cycle checkpoints and DNA damage response signaling points towards new avenues in diagnostics (including candidate genes and functional assays) and novel therapeutic targets. For the research in this thesis, both primary patient-derived cells, including fibroblasts and urine-derived renal epithelial cells (URECS), and cell lines were used to investigate the effect of variants in ciliopathy-associated genes *in vitro*. Innovations in extracellular vesicle isolation and manipulation, CRISPR-Cas technology and organoids allow researchers to study the pathophysiology of renal ciliopathies and drug response in an organ system, and bring gene therapy and kidney regeneration one step closer. For now, the combination of deep phenotyping and different molecular techniques including genome sequencing, RNA sequencing and proteomics will yield the best diagnostic and prognostic care for NPH-RC patients.

when the signal is lost_marijn_8072018.indd 198 08/07/2018 10:50

when the signal is lost_marijn_8072018.indd 199 08/07/2018 10:50

APPENDICES

NEDERLANDSE SAMENVATTING

REFERENCES

ACKNOWLEDGMENTS / DANKWOORD

LIST OF PUBLICATIONS

CURRICULUM VITAE

when the signal is lost_marijn_8072018.indd 200 08/07/2018 10:50

when the signal is lost_marijn_8072018.indd 201 08/07/2018 10:50

NEDERLANDSE SAMENVATTING
OOK VOOR NIET-INGEWIJDEN

GENETICA VAN NEFRONOFTISE EN AANVERWANTE CILIOPATHIEËN

De nierziekte nefronoftise is één van de belangrijkste erfelijke oorzaken van nierfalen op de kinderleeftijd. De diagnose wordt vaak pas in een gevorderd stadium van de aandoening gesteld omdat de klinische verschijnselen (bijvoorbeeld bloedarmoede) en echobevindingen (bijvoorbeeld cysten) niet specifiek zijn. Op dit moment kan in slechts 40 tot 50% van de patiënten de diagnose met DNA-onderzoek worden bevestigd. Bovendien is het niet mogelijk om betrouwbare voorspellingen te doen over het ziektebeloop van nefronoftise in een individuele patiënt op basis van een specifieke DNA mutatie. In dit proefschrift beschrijf ik mijn onderzoek naar de erfelijke achtergrond van nefronoftise, ziektemechanismen en nieuwe methoden om nefronoftise te detecteren en te vervolgen.

Op dit moment zijn er 20 genen bekend voor nefronoftise. Deze genen coderen voor eiwitten die belangrijk zijn voor de vorming en de functie van de primaire cilia. Cilia zijn haarvormige antennes die op cellen aanwezig zijn en signalen uit de omgeving oppikken. Ze spelen een rol in de signaaloverdracht binnen en tussen de cellen. Deze signalen zijn belangrijk voor de vorming en instandhouding van weefsels en organen. Door defecten van de cilia kan de signaaloverdracht verstoord zijn en kunnen organen niet goed worden aangelegd of geleidelijk beschadigd raken. Nefronoftise wordt een 'ciliopathie', oftewel 'ziekte van de cilia', genoemd omdat defecten van de cilia samenhangen met deze aandoening.

Daarnaast heeft een aantal eiwitten die we kennen uit de cilia ook een functie in de celkern waar het erfelijk materiaal (DNA) ligt opgeslagen. Het is gebleken dat deze eiwitten betrokken zijn bij de reactie van de cel op DNA schade en bij de regulatie van de celcyclus. Een verstoring van deze functies kan leiden tot verlittekening van het nierweefsel (fibrose) en daardoor tot het verslechteren van de nierfunctie.

Nefronoftise gaat in 10 tot 20% van de patiënten gepaard met problemen in andere organen, al dan niet in het kader van een syndroom. We spreken dan van 'aan nefronoftise gerelateerde ciliopathieën' (in dit proefschrift afgekort als NPH-RC). Inmiddels zijn er defecten in meer dan 90 verschillende genen geïdentificeerd die betrokken zijn bij NPH-RC. Met behulp van uitgebreid DNA onderzoek genaamd 'next-generation sequencing' kunnen bekende en potentieel nieuwe genen voor nefronoftise tegelijkertijd worden onderzocht.

Deel 1 gaat over de symptomen, de genetische achtergrond en de onderliggende mechanismen van nefronoftise en daaraan verwante ciliopathieën.

when the signal is lost_marijn_8072018.indd 202 08/07/2018 10:50

NEFRONOFTISE IN EEN NEDERLANDS COHORT

In **Hoofdstuk 2** beschrijven we een Nederlands cohort van 40 patiënten met aan nefronoftise gerelateerde ciliopathieën. We hebben de klinische gegevens van alle patiënten zorgvuldig gedocumenteerd in de Nephronophthisis Registry. Vervolgens hebben we de defecten in het DNA die betrokken zijn bij de ciliopathieën onderzocht en gekeken naar mogelijke verbanden tussen deze defecten en de ziekteverschijnselen van de patiënten (gen-fenotype associaties). We hebben mutaties aangetoond in bekende nefronoftise genen, maar ook in potentieel nieuwe nefronoftise genen. Wat betreft de klinische bevindingen was toename van witte gebieden (verhoogde echogeniciteit) een frequenter voorkomende echobevinding bij patiënten met nefronoftise dan niercysten. Dit verschil was extra groot bij patiënten met nefronoftise door mutaties in het *NPHP1*-gen. Vermoeidheid, meer drinken en meer plassen, en hoge bloeddruk waren de meest voorkomende eerste verschijnselen van nefronoftise. Meer kennis van eerste verschijnselen van nefronoftise kan bijdragen aan vroege opsporing van de nierziekte in de toekomst. Daarnaast zouden we op basis van de bevindingen in ons cohort aanraden om bij patiënten met een ciliopathie en zonder nierziekte de nierfunctie preventief te blijven controleren tot minimaal de leeftijd van 30 jaar.

VERANDERINGEN IN CELLEN VAN CILIOPATHIE PATIËNTEN

In **Hoofdstuk 3, 4** en **5** beschrijf ik experimenten die aantonen dat veranderingen in het DNA van patiënten ook daadwerkelijk leiden tot de nierziekte nefronoftise.

In **Hoofdstuk 3** wordt het verband onderzocht tussen een stukje ontbrekend DNA op chromosoom 14 (de novo 14q24.2-q24.3 microdeletie) en het fenotype van de patiënt dat wordt gekenmerkt door milde verstandelijke beperking, skeletafwijkingen, een hartafwijking en bijziendheid. De microdeletie bevatte het cilia-gen *IFT43*. Huidcellen (fibroblasten) van de patiënt toonden een transportdefect van cilia-eiwitten. Het is onduidelijk of de deletie van *IFT43* de oorzaak is van het fenotype in fibroblasten, omdat ciliopathieën meestal veroorzaakt worden door veranderingen in beide kopieën van een cilia-gen (de microdeletie betreft slechts één kopie). Dit zou verder onderzocht kunnen worden in cellen van ouders die drager zijn van een defect in een cilia-gen (bij hen is ook slechts één kopie van het gen aangedaan).

In **Hoofdstuk 4** worden mutaties in het *NEK1*-gen beschreven die zijn aangetoond in twee broers met oro-facial-digital syndroom type II (Mohr syndroom). Het *NEK1*-gen is het eerste gen beschreven voor OFD type II. NEK1 komt tot uiting in de cilia. Onderzoek in fibroblasten van de patiënt toonde een verstoring aan in de vorming van de cilia. De fenotypes van de patiënten met OFD type II weerspiegelen de dubbele rol van cilia-eiwitten in de vorming van cilia en in de reactie van de cel op DNA schade. Een verstoring in de vorming van cilia leidt tot verminderde signaaloverdracht (specifiek de sonic hedgehog signalering) wat

when the signal is lost_marijn_8072018.indd 203 08/07/2018 10:50

kan resulteren in de ledemaatafwijkingen bij deze patiënten. Een verstoring van NEK1 in de reactie op DNA schade kan leiden tot een gehemeltespleet door verlies van voorlopercellen en tot nefronoftise door dedifferentiatie van de niercellen met verlittekening van het nierweefsel als gevolg. Onderzoek van het RNA uit de cellen van de patiënt heeft aangetoond dat één van de mutaties in het *NEK1*-gen resulteert in het overslaan van een stuk van de DNA code voor NEK1. Dit noemen we "nonsense-associated alternative splicing". Dat wil zeggen dat het gedeelte van het DNA (exon) met de mutatie wordt overgeslagen in het uiteindelijke transcript. Hierdoor ontstaat een korter eiwit dat wel deels zijn functie behoudt. Mogelijk verklaart dit het relatief milde fenotype in onze patiënten vergeleken met de eerder beschreven patiënten met *NEK1*-mutaties (met een lethale ciliopathie genaamd short-rib polydactyly type Majewski).

De oorzakelijke rol van mutaties in het *KIF14*-gen in het ontstaan van het lethale Meckel-Gruber syndroom wordt bevestigd in **Hoofdstuk 5**. We beschrijven een familie met vier aangedane foetussen met nier- en hersenaanlegstoornissen ten gevolge van mutaties in het *KIF14*-gen. Onze bevindingen illustreren wederom de dubbele rol van cilia-eiwitten in zowel de ciliavorming als in de celdeling. Onderzoek van nierweefsel van een aangedane foetus toonde de afwezigheid van cilia en van het KIF14-eiwit. Daarnaast toonde onderzoek van fibroblasten afkomstig van patiënten meer cellen die mogelijk 'vastzaten' in de celdeling vergeleken met fibroblasten afkomstig van controles. Door de afwezigheid van KIF14-eiwit kan de deling van de cellen in twee dochtercellen worden verhinderd. Deze verstoorde celdeling ligt mogelijk ten grondslag aan de aanlegstoornissen van de nieren en de hersenen bij patiënten met Meckel-Gruber syndroom.

In **Deel 2** van dit proefschrift beschrijf ik nieuwe manieren om de diagnostiek van nefronoftise en andere nierziekten te verbeteren.

BIOMARKERS IN DE URINE VAN NEFRONOFTISEPATIËNTEN

In **Hoofdstuk 6** identificeren we welke eiwitten aanwezig zijn in de urine van nefronoftisepatiënten. Deze eiwitten kunnen in de toekomst gebruikt worden als biomarkers, oftewel signalen voor de vroege detectie van nefronoftise. In dit pilot onderzoek maken we gebruik van eiwitdetectie in extracellular vesicles die we uit de urine hebben geïsoleerd. Extracellular vesicles zijn blaasjes afkomstig van cellen van de nieren en urinewegen die worden uitgescheiden in de urine. We vergelijken de eiwitprofielen van twaalf nefronoftise patiënten met die van twaalf gezonde controle personen met dezelfde leeftijd en hetzelfde geslacht. We tonen aan dat deze eiwitprofielen nauwkeurig patiënten van controlepersonen kunnen onderscheiden. Daarnaast hangt de hoeveelheid van de onderscheidende eiwitten samen met het stadium van chronisch nierfalen in de patiënten. De mechanismen waarin de onderscheidende eiwitten functioneren zijn geassocieerd met nierziekten en extracellular vesicles in het algemeen. Vervolgstudies moeten uitwijzen of onze bevindingen specifiek zijn voor nefronoftise en dus nefronoftise

when the signal is lost_marijn_8072018.indd 204 08/07/2018 10:50

nauwkeurig kunnen aantonen in patiënten met verdenking op nefronoftise. Bovendien moet vervolgonderzoek aantonen of de eiwitten in de urine iets kunnen zeggen over het beloop (prognose) van de nierziekte. Onze resultaten zijn een eerste stap in de richting van een test die nefronoftise aantoont waarbij geen gebruik gemaakt wordt van invasieve methoden zoals bloedafname of een nierbiopt.

GENETICA VERANDERT DE INDELING VAN NIERZIEKTEN

Hoofdstuk 7 beschrijft hoe nieuwe genetische technieken zoals whole-exome sequencing en whole-genome sequencing (waarmee respectievelijk alle voor eiwit coderende delen van het genoom en het hele genoom kunnen worden afgelezen) op een revolutionaire manier hebben geleid tot een verandering van de klassieke indeling van nierziekten. Door veel genen tegelijk te onderzoeken ontdekken we DNA veranderingen in genen waar we ze niet verwacht hadden en zien we dat veranderingen in hetzelfde gen ten grondslag kunnen liggen aan heel uiteenlopende nierziekten. De ciliopathieën zijn hier een voorbeeld van. Door deze genetische bevindingen leren we meer over de ontstaansmechanismen van nierziekten, en uiteindelijk ook over nieuwe aangrijpingspunten voor behandeling.

TOEKOMSTPERSPECTIEVEN

In **Hoofdstuk 8** bespreek ik de uitdagingen van genetisch onderzoek naar nefronoftise en andere ciliopathieën. Whole-exome sequencing heeft de diagnostiek en de identificatie van nieuwe genen verbeterd in genetisch heterogene aandoeningen zoals nefronoftise. Toch wordt bij meer dan 50% van de nefronoftise patiënten de genetische oorzaak niet geïdentificeerd. Dan moeten andere technieken, zoals whole-genome sequencing en RNA sequencing, en andere manieren van overerving, zoals polygene overerving - waarbij mutaties in meerdere genen bijdragen aan het fenotype -, worden overwogen. Daarnaast zal het ciliaonderzoek gebaat zijn bij ontwikkelingen in de isolatie en manipulatie van extracellular vesicles uit de urine, het gebruik van organoïden (gekweekte "miniorganen") en de samenwerking met andere disciplines, zoals kankeronderzoek. Fundamenteel kankeronderzoek kan meer inzicht verschaffen in de manier waarop cilia-eiwitten de celcyclus beïnvloeden.

Technologische vooruitgang op het gebied van DNA sequencing en de mogelijkheden van het aanpassen van het DNA met behulp van CRISPR/Cas (genome editing), vooral wanneer die zouden worden toegepast in de kiembaan, maken dat genetica ons allemaal aangaat. Ontwikkelingen in de genetica vereisen daarom maatschappelijk debat en een breed draagvlak.

when the signal is lost_marijn_8072018.indd 205 08/07/2018 10:50

REFERENCES

Abe M, Maruyama N, Oikawa O, Maruyama T, Okada K, Soma M. 2015. Urinary ACE2 is associated with urinary L-FABP and albuminuria in patients with chronic kidney disease. Scand. J. Clin. Lab. Invest. 75: 421–427.

AbouAlaiwi W, Muntean B, Ratnam S, Joe B, Liu L, Booth R, Rodriguez I, Herbert B, Bacallao R, Fruttiger M, Mak T, Zhou J, Nauli S. 2014. Survivin-Induced Abnormal Ploidy Contributes to Cystic Kidney and Aneurysm Formation. Circulation 129: 660–672.

Adam J, Connor TMF, Wood K, Lewis D, Naik R, Gale DP, Sayer J a. 2014. Genetic testing can resolve diagnostic confusion in Alport syndrome. Clin. Kidney J. 7: 197–200.

Adly N, Alhashem A, Ammari A, Alkuraya FS. 2014. Ciliary Genes TBC1D32/C6orf170 and SCLT1 are Mutated in Patients with OFD Type IX. Hum. Mutat. 35: 36–40.

Adzhubei IA, Schmidt S, Peshkin L, Ramensky VE, Gerasimova A, Bork P, Kondrashov AS, Sunyaev SR. 2010. A method and server for predicting damaging missense mutations. Nat. Methods 7: 248–249.

Airik R, Slaats GG, Guo Z, Weiss A-C, Khan N, Ghosh A, Hurd TW, Bekker-Jensen S, Schroder JM, Elledge SJ, Andersen JS, Kispert A, Castelli M, Boletta A, Giles RH, Hildebrandt F. 2014. Renal-Retinal Ciliopathy Gene Sdccag8 Regulates DNA Damage Response Signaling. J. Am. Soc. Nephrol. 25: 2573–2583.

Aken B, Achuthan P, Akanni W, Amode M, Bernsdorff F, Bhai J, Billis K, Carvalho-Silva D, Cummins C, Clapham P, Gil L, García Girón C, Gordon L, Hourlier T, Hunt S, Janacek S, Juettemann T, Keenan S, Laird M, Lavidas I, Maurel T, McLaren W, Moore B, Murphy D, Nag R, Newman V, Nuhn M, Kee Ong C, Parker A, Patricio M, Singh Riat H, Sheppard D, Sparrow H, Taylor K, Thormann A, Vullo A, Walts B, Wilder S, Zadissa A, Kostadima M, Martin F, Muffato M, Perry E, Ruffier M, Staines D, Trevanion S, Cunningham F, Yates A, Zerbino D, Flicek P. 2017. Ensembl 2017. Nucleic Acids Res. Database issue: D635–D642.

Ala-Mello S, Kivivuori SM, Rönnholm KAR, Koskimies O, Siimes MA. 1996. Mechanism underlying early anaemia in children with familial juvenile nephronophthisis. Pediatr. Nephrol. 10: 578–581.

Arnaiz O, Cohen J, Tassin A-M, Koll F. 2014. Remodeling Cildb, a popular database for cilia and links for ciliopathies. Cilia 3: 9.

Arnaiz O, Malinowska A, Klotz C, Sperling L, Dadlez M, Koll F, Cohen J. 2009. Cildb: A knowledgebase for centrosomes and cilia. Database: 1–14.

Arno G, Agrawal SA, Eblimit A, Bellingham J, Xu M, Wang F, Chakarova C, Parfitt DA, Lane A, Burgoyne T, Hull S, Carss KJ, Fiorentino A, Hayes MJ, Munro PM, Nicols R, Pontikos N, Holder GE, Black G, Hall G, Ingram S, Gillespie R, Manson F, Sergouniotis P, Inglehearn C, Toomes C, Ali M, McKibbin M, Poulter J, Khan K, Lord E, Nemeth A, Downes S, Yu J, Lise S, Arno G, Fiorentino A, Ponitkos N, Plagnol V, Michaelides M, Hardcastle AJ, Cheetham ME, Webster AR, van Heyningen V, Asomugha C, Raymond FL, Moore AT, Plagnol V, Michaelides

when the signal is lost_marijn_8072018.indd 206 08/07/2018 10:50

M, Hardcastle AJ, Li Y, Cukras C, Webster AR, Cheetham ME, Chen R. 2016. Mutations in REEP6 Cause Autosomal-Recessive Retinitis Pigmentosa. Am. J. Hum. Genet. 99: 1305–1315.

Arts H, Knoers N. 2013a. Cranioectodermal Dysplasia. GeneReviews® [Internet]. Seattle Univ. Washington, Seattle; 1993-2017: 1–28.

Arts HH, Bongers EMHF, Mans DA, van Beersum SEC, Oud MM, Bolat E, Spruijt L, Cornelissen EAM, Schuurs-Hoeijmakers JHM, de Leeuw N, Cormier-Daire V, Brunner HG, Knoers NVAM, Roepman R. 2011. C14ORF179 encoding IFT43 is mutated in Sensenbrenner syndrome. J. Med. Genet. 48: 390–395.

Arts HH, Knoers NVAM. 2013b. Current insights into renal ciliopathies: What can genetics teach us? Pediatr. Nephrol. 28: 863–874.

Artuso R, Fallerini C, Dosa L, Scionti F, Clementi M, Garosi G, Massella L, Epistolato MC, Mancini R, Mari F, Longo I, Ariani F, Renieri A, Bruttini M. 2012. Advances in Alport syndrome diagnosis using next-generation sequencing. Eur. J. Hum. Genet. 20: 50–57.

Ashkinadze E, Rosen T, Brooks S, Katsanis N, Davis E. 2013. Combining fetal sonography with genetic and allele pathogenicity studies to secure a neonatal diagnosis of Bardet– Biedl syndrome. Clin. Genet. 83: 553–559.

Attanasio M, Uhlenhaut NH, Sousa VH, O'Toole JF, Otto E, Anlag K, Klugmann C, Treier AC, Helou J, Sayer JA, Seelow D, Nurnberg G, Becker C, Chudley AE, Nurnberg P, Hildebrandt F, Treier M. 2007. Loss of GLIS2 causes nephronophthisis in humans and mice by increased apoptosis and fibrosis. Nat. Genet. 39: 1018–1024.

Van der Auwera G, Carneiro M, Hartl C. 2014. From FastQ Data to High-Confidence Variant Calls: The Genome Analysis Toolkit Best Practices Pipeline. Curr. Protoc. Bioinforma. 11: 358-366.

Baala L, Audollent S, Martinovic J, Ozilou C, Babron M-C, Sivanandamoorthy S, Saunier S, Salomon R, Gonzales M, Rattenberry E, Esculpavit C, Toutain A, Moraine C, Parent P, Marcorelles P, Dauge M-C, Roume J, Le Merrer M, Meiner V, Meir K, Menez F, Beaufrère A-M, Francannet C, Tantau J, Sinico M, Dumez Y, MacDonald F, Munnich A, Lyonnet S, Gubler M-C, Génin E, Johnson CA, Vekemans M, Encha-Razavi F, Attié-Bitach T. 2007a. Pleiotropic effects of CEP290 (NPHP6) mutations extend to Meckel syndrome. Am. J. Hum. Genet. 81: 170–179.

Baala L, Romano S, Khaddour R, Saunier S, Smith UM, Audollent S, Ozilou C, Faivre L, Laurent N, Foliguet B, Munnich A, Lyonnet S, Salomon R, Encha-Razavi F, Gubler MC, Boddaert N, de Lonlay P, Johnson CA, Vekemans M, Antignac C, Attie-Bitach T. 2007b. The Meckel-Gruber syndrome gene, MKS3, is mutated in Joubert syndrome. Am. J. Hum. Genet. 80: 186–194.

Bachmann-Gagescu R, Dona M, Hetterschijt L, Tonnaer E, Peters T, de Vrieze E, Mans DA, van Beersum SEC, Phelps IG, Arts HH, Keunen JE, Ueffing M, Roepman R, Boldt K, Doherty D, Moens CB, Neuhauss SCF, Kremer H, van Wijk E. 2015. The Ciliopathy Protein CC2D2A Associates with NINL and Functions in RAB8-MICAL3-Regulated Vesicle Trafficking. PLoS Genet. 11: 1–28.

when the signal is lost_marijn_8072018.indd 207 08/07/2018 10:50

Badenas C, Praga M, Tazón B, Heidet L, Arrondel C, Armengol A, Andrés A, Morales E, Camacho JA, Lens X, Dávila S, Milà M, Antignac C, Darnell A, Torra R. 2002. Mutations in theCOL4A4 and COL4A3 genes cause familial benign hematuria. J. Am. Soc. Nephrol. 13: 1248–1254.

Bailey LJ, Olivos I, Leahey A, Attree O, Okabe I, Lewis R, MacInnes R, Spinner N, Nelson D, Nussbaum R. 1992. Characterization of a candidate gene for OCRL. Am. J. Hum. Genet. 51: 1.

Bainbridge JWB, Smith AJ, Barker SS, Robbie S, Henderson R, Balaggan K, Viswanathan A, Holder GE, Stockman A, Tyler N, Petersen-Jones S, Bhattacharya SS, Thrasher AJ, Fitzke FW, Carter BJ, Rubin GS, Moore AT, Ali RR. 2008. Effect of gene therapy on visual function in Leber's congenital amaurosis. N. Engl. J. Med. 358: 2231–2239.

Bamshad MJ, Ng SB, Bigham AW, Tabor HK, Emond MJ, Nickerson DA, Shendure J. 2011. Exome sequencing as a tool for Mendelian disease gene discovery. Nat. Rev. Genet. 12: 745–755.

Bandano JL, Kim JC, Hoskins BE, Lewis RA, Ansley SJ, Cutler DJ, Castellan C, Beales PL, Leroux MR, Katsanis N. 2003. Heterozygous mutations in BBS1, BBS2 and BBS6 have a potential epistatic effect on Bardet-Beidl patients with two mutations at a second BBS locus. Hum. Mol. Genet. 12: 1651–1659.

Barker AR, Thomas R, Dawe HR. 2014. Meckel-Gruber syndrome and the role of primary cilia in kidney, skeleton, and central nervous system development. Organogenesis 10: 96–107.

Barker D, Hostikka S, Zhou J, Chow L, Oliphant A, Gerken S, Gregory M, Skolnick M, Atkin C, Tryggvason K. 1990. Identification of mutations in the COL4A5 collagen gene in Alport syndrome. Science (80-.). 248: 1224–1227.

Barua M, Stellacci E, Stella L, Weins A, Genovese G, Muto V, Caputo V, Toka HR, Charoonratana VT, Tartaglia M, Pollak MR. 2014. Mutations in PAX2 Associate with Adult-Onset FSGS. J. Am. Soc. Nephrol.: 1–12.

Basavarajappa H, Corson T. 2012. KIF14 as an oncogene in retinoblastoma: a target for novel therapeutics? Futur. Med Chem 4: 2149–2152.

Basten S. 2013. Functional aspects of cilia and tumor suppressors.

Benzing T, Schermer B. 2012. Clinical spectrum and pathogenesis of nephronophthisis. Curr. Opin. Nephrol. Hypertens. 21: 272–278.

Berbari NF, Sharma N, Malarkey EB, Pieczynski JN, Boddu R, Gaertig J, Guay-Woodford L, Yoder BK. 2013. Microtubule modifications and stability are altered by cilia perturbation and in cystic kidney disease. Cytoskeleton 70: 24–31.

Bergmann C. 2014. ARPKD and early manifestations of ADPKD: the original polycystic kidney disease and phenocopies. Pediatr. Nephrol. 30: 1–16.

Bergmann C, von Bothmer J, Ortiz Bruchle N, Venghaus a., Frank V, Fehrenbach H, Hampel T, Pape L, Buske a., Jonsson J, Sarioglu N, Santos a., Ferreira JC, Becker JU, Cremer R, Hoefele J, Benz MR, Weber LT, Buettner R, Zerres K. 2011. Mutations in Multiple PKD Genes May Explain Early and Severe Polycystic Kidney Disease. J. Am. Soc. Nephrol. 22: 2047–2056.

Besbas N, Ozaltin F, Jeck N, Seyberth H, Ludwig M. 2005. CLCN5 mutation (R347X)

when the signal is lost_marijn_8072018.indd 208 08/07/2018 10:50

associated with hypokalaemic metabolic alkalosis in a Turkish child: an unusual presentation of Dent's disease. Nephrol. Dial. Transplant. 20: 1476–1479.

Bielas SL, Silhavy JL, Brancati F, Kisseleva M V, Al-Gazali L, Sztriha L, Bayoumi RA, Zaki MS, Abdel-Aleem A, Rosti RO, Kayserili H, Swistun D, Scott LC, Bertini E, Boltshauser E, Fazzi E, Travaglini L, Field SJ, Gayral S, Jacoby M, Schurmans S, Dallapiccola B, Majerus PW, Valente EM, Gleeson JG. 2009. Mutations in INPP5E, encoding inositol polyphosphate-5-phosphatase E, link phosphatidyl inositol signaling to the ciliopathies. Nat. Genet. 41: 1032–1036.

Biesecker LG, Mullikin JC, Facio FM, Turner C, Cherukuri PF, Blakesley RW, Bouffard GG, Chines PS, Cruz P, Hansen NF, Teer JK, Maskeri B, Young AC, Comparative N, Program S, Manolio TA, Wilson AF, Finkel T, Hwang P, Arai A, Remaley AT, Sachdev V, Shamburek R, Cannon RO, Green ED. 2009. The ClinSeq Project : Piloting large-scale genome sequencing for research in genomic medicine. Genome Res. 19: 1665–1674.

Bijnsdorp I V, Maxouri O, Kardar A, Schelfhorst T, Sander R, Pham T V, Vis A, Moorselaar RJ Van, Connie R, Bijnsdorp I V, Maxouri O, Kardar A, Schelfhorst T, Piersma R, Pham T V, Vis A, Moorselaar RJ Van, Jimenez CR. 2017. Feasibility of urinary extracellular vesicle proteome profiling using a robust and simple , clinically applicable isolation method. J. Extracell. Vesicles 6.

Billingsley G, Vincent A, Deveault C, Héon E. 2012. Mutational Analysis of SDCCAG8 in Bardet-Biedl Syndrome Patients with Renal Involvement and Absent Polydactyly. Ophthalmic Genet. 33: 150–154.

Bimonte S, De Angelis A, Quagliata L, Giusti F, Tammaro R, Dallai R, Ascenzi MG, Diez-Roux G, Franco B. 2011. Ofd1 is required in limb bud patterning and endochondral bone development. Dev. Biol. 349: 179–191.

Bizet A a., Becker-Heck A, Ryan R, Weber K, Filhol E, Krug P, Halbritter J, Delous M, Lasbennes M-C, Linghu B, Oakeley EJ, Zarhrate M, Nitschké P, Garfa-Traore M, Serluca F, Yang F, Bouwmeester T, Pinson L, Cassuto E, Dubot P, Elshakhs N a. S, Sahel J a., Salomon R, Drummond I a., Gubler M-C, Antignac C, Chibout S, Szustakowski JD, Hildebrandt F, Lorentzen E, Sailer AW, Benmerah A, Saint-Mezard P, Saunier S. 2015. Mutations in TRAF3IP1/IFT54 reveal a new role for IFT proteins in microtubule stabilization. Nat. Commun. 6: 8666.

Blowey D, Querfeld U, Geary D, Warady B, Alon U. 1996. Ultrasound findings in juvenile nephronophthisis. Pediatr. Nephrol. 10: 22–24.

Boehlke C, Kotsis F, Patel V, Braeg S, Voelker H, Bredt S, Beyer T, Janusch H, Hamann C, Gödel M, Müller K, Herbst M, Hornung M, Doerken M, Köttgen M, Nitschke R, Igarashi P, Walz G, Kuehn EW. 2010. Primary cilia regulate mTORC1 activity and cell size through Lkb1. Nat. Cell Biol. 12: 1115–1122.

Bogdanovic R, Draaken M, Toromanovic A, Dordevic M, Stajic N, Ludwig M. 2010. A novel CLCN5 mutation in a boy with Bartter-like syndrome and partial growth hormone deficiency. Pediatr. Nephrol. 25: 2363–2368.

Boldt K, van Reeuwijk J, Gloeckner CJ, Ueffing M, Roepman R. 2009. Tandem affinity purification of ciliopathy-associated protein complexes. Elsevier

when the signal is lost_marijn_8072018.indd 209 08/07/2018 10:50

Masson SAS. 143-160 p.
Boldt K, van Reeuwijk J, Lu Q, Koutroumpas K, Nguyen T-MT, Texier Y, van Beersum SEC, Horn N, Willer JR, Mans DA, Dougherty G, Lamers IJC, Coene KLM, Arts HH, Betts MJ, Beyer T, Bolat E, Gloeckner CJ, Haidari K, Hetterschijt L, Iaconis D, Jenkins D, Klose F, Knapp B, Latour B, Letteboer SJF, Marcelis CL, Mitic D, Morleo M, Oud MM, Riemersma M, Rix S, Terhal PA, Toedt G, van Dam TJP, de Vrieze E, Wissinger Y, Wu KM, Apic G, Beales PL, Blacque OE, Gibson TJ, Huynen MA, Katsanis N, Kremer H, Omran H, van Wijk E, Wolfrum U, Kepes F, Davis EE, Franco B, Giles RH, Ueffing M, Russell RB, Roepman R. 2016. An organelle-specific protein landscape identifies novel diseases and molecular mechanisms. Nat. Commun. 7: 11491.
Bongers EMHF, Huysmans FT, Levtchenko E, de Rooy JW, Blickman JG, Admiraal RJC, Huygen PLM, Cruysberg JRM, Toolens P a MP, Prins JB, Krabbe PFM, Borm GF, Schoots J, van Bokhoven H, van Remortele AMF, Hoefsloot LH, van Kampen A, Knoers NV a M. 2005. Genotype-phenotype studies in nail-patella syndrome show that LMX1B mutation location is involved in the risk of developing nephropathy. Eur. J. Hum. Genet. 13: 935–946.
Borges FT, Melo SA, Ozdemir BC, Kato N, Revuelta I, Miller CA, Gattone VH, LeBleu VS, Kalluri R. 2013. TGF- 1-Containing Exosomes from Injured Epithelial Cells Activate Fibroblasts to Initiate Tissue Regenerative Responses and Fibrosis. J. Am. Soc. Nephrol. 24: 385–392.
Bowdin S, Gilbert A, Bedoukian E, Carew C, Adam MP, Belmont J, Bernhardt B, Biesecker L, Bjornsson HT, Blitzer M, D'Alessandro LCA, Deardorff MA, Demmer L, Elliott A, Feldman GL, Glass IA, Herman G, Hindorff L, Hisama F, Hudgins L, Innes AM, Jackson L, Jarvik G, Kim R, Korf B, Ledbetter DH, Li M, Liston E, Marshall C, Medne L, Meyn MS, Monfared N, Morton C, Mulvihill JJ, Plon SE, Rehm H, Roberts A, Shuman C, Spinner NB, Stavropoulos DJ, Valverde K, Waggoner DJ, Wilkens A, Cohn RD, Krantz ID. 2016. Recommendations for the integration of genomics into clinical practice. Genet. Med. 18: 1075–1084.
Boyer O, Woerner S, Yang F, Oakeley EJ, Linghu B, Gribouval O, Tête M-J, Duca JS, Klickstein L, Damask AJ, Szustakowski JD, Heibel F, Matignon M, Baudouin V, Chantrel F, Champigneulle J, Martin L, Nitschké P, Gubler M-C, Johnson KJ, Chibout S-D, Antignac C. 2013. LMX1B mutations cause hereditary FSGS without extrarenal involvement. J. Am. Soc. Nephrol. 24: 1216–1222.
Braun DA, Hildebrandt F. 2017. Ciliopathies. Cold Spring Harb. Perspect. Biol. 9: 1–28.
Braun DA, Schueler M, Halbritter J, Gee HY, Porath JD, Lawson JA, Airik R, Shril S, Allen SJ, Stein D, Al Kindy A, Beck BB, Cengiz N, Moorani KN, Ozaltin F, Hashmi S, Sayer JA, Bockenhauer D, Soliman NA, Otto EA, Lifton RP, Hildebrandt F. 2016. Whole exome sequencing identifies causative mutations in the majority of consanguineous or familial cases with childhood-onset increased renal echogenicity. Kidney Int. 89: 468–475.
Bredrup C, Saunier S, Oud MM, Fiskerstrand T, Hoischen A, Brackman D, Leh SM, Midtbo M, Filhol E, Bole-Feysot C, Nitschke P, Gilissen C, Haugen OH,

when the signal is lost_marijn_8072018.indd 210 08/07/2018 10:50

Sanders JS, Stolte-Dijkstra I, Mans DA, Steenbergen EJ, Hamel BC, Matignon M, Pfundt R, Jeanpierre C, Boman H, Rodahl E, Veltman JA, Knappskog PM, Knoers N V, Roepman R, Arts HH. 2011. Ciliopathies with skeletal anomalies and renal insufficiency due to mutations in the IFT-A gene WDR19. Am. J. Hum. Genet. 89: 634–643.

Bruneau S, Néel M, Roumenina LT, Frimat M, Laurent L, Frémeaux-Bacchi V, Fakhouri F. 2015. Loss of DGKe induces endothelial cell activation and death independently of complement activation. Blood: 1–10.

Bruno S, Grange C, Collino F, Deregibus MC, Cantaluppi V, Biancone L, Tetta C, Camussi G. 2012. Microvesicles derived from mesenchymal stem cells enhance survival in a lethal model of acute kidney injury. PLoS One 7.

Brynychova V, Ehrlichova M, Hlavac V, Nemcova-Furstova V, Pecha V, Leva J, Trnkova M, Mrhalova M, Kodet R, Vrana D, Kovar J, Vaclavikova R, Gut I, Soucek P. 2016. Genetic and functional analyses do not explain the association of high PRC1 expression with poor survival of breast carcinoma patients. Biomed Pharmacother: 857–864.

Bullich G, Trujillano D, Santín S, Ossowski S, Mendizábal S, Fraga G, Madrid Á, Ariceta G, Ballarín J, Torra R, Estivill X, Ars E. 2015. Targeted next-generation sequencing in steroid- resistant nephrotic syndrome : mutations in multiple glomerular genes may influence disease severity. Eur. J. Hum. Genet. 23: 1192–1199.

Bullich G, Vargas I, Trujillano D, Mendizábal S, Piñero-fernández JA, Fraga G, García-solano J, Ballarín J. 2017. Contribution of the TTC21B gene to glomerular and cystic kidney diseases. Nephrol. Dial. Transpl. 32: 151-156.

Caravaca F, Gonzales B, Bayo MÁ, Luna E. 2016. Musculoskeletal pain in patients with chronic kidney disease. Nefrol. (English Ed). 36: 433–440.

Carbon S, Ireland A, Mungall CJ, Shu S, Marshall B, Lewis S, Lomax J, Mungall C, Hitz B, Balakrishnan R, Dolan M, Wood V, Hong E, Gaudet P. 2009. AmiGO: Online access to ontology and annotation data. Bioinformatics 25: 288–289.

Caridi G, Dagnino M, Rossi A, Valente EM, Bertini E, Fazzi E, Emma F, Murer L, Verrina E, Ghiggeri GM. 2006a. Nephronophthisis type 1 deletion syndrome with neurological symptoms: prevalence and significance of the association. Kidney Int. 70: 1342–1347.

Caridi G, Dagnino M, Trivelli A, Emma F, Perfumo F, Ghiggeri GM. 2006b. Stop codon at arginine 586 is the prevalent nephronopthisis type 1 mutation in Italy. Nephrol. Dial. Transplant. 21: 2301–2303.

Carleton M, Mao M, Biery M, Warrener P, Kim S, Buser C, Marshall CG, Fernandes C, Annis J, Linsley PS. 2006. RNA Interference-Mediated Silencing of Mitotic Kinesin KIF14 Disrupts Cell Cycle Progression and Induces Cytokinesis Failure. Mol. Cell. Biol. 26: 3853–3863.

Castresana J. 2015. Cancer as a Ciliopathy : The Primary Cilium as a New Therapeutic Target. Carcinog. Mutagen. 6: 2517–2519.

Chacon-Heszele MF, Choi SY, Zuo X, Baek J-I, Ward C, Lipschutz JH. 2014. The exocyst and regulatory GTPases in urinary exosomes. Physiol. Rep. 2: e12116.

A

when the signal is lost_marijn_8072018.indd 211 08/07/2018 10:50

Chaki M, Airik R, Ghosh AK, Giles RH, Chen R, Slaats GG, Wang H, Hurd TW, Zhou W, Cluckey A, Gee HY, Ramaswami G, Hong CJ, Hamilton BA, Cervenka I, Ganji RS, Bryja V, Arts HH, van Reeuwijk J, Oud MM, Letteboer SJ, Roepman R, Husson H, Ibraghimov-Beskrovnaya O, Yasunaga T, Walz G, Eley L, Sayer JA, Schermer B, Liebau MC, Benzing T, Le Corre S, Drummond I, Janssen S, Allen SJ, Natarajan S, O'Toole JF, Attanasio M, Saunier S, Antignac C, Koenekoop RK, Ren H, Lopez I, Nayir A, Stoetzel C, Dollfus H, Massoudi R, Gleeson JG, Andreoli SP, Doherty DG, Lindstrad A, Golzio C, Katsanis N, Pape L, Abboud EB, Al-Rajhi AA, Lewis RA, Omran H, Lee EY, Wang S, Sekiguchi JM, Saunders R, Johnson CA, Garner E, Vanselow K, Andersen JS, Shlomai J, Nurnberg G, Nurnberg P, Levy S, Smogorzewska A, Otto EA, Hildebrandt F. 2012. Exome capture reveals ZNF423 and CEP164 mutations, linking renal ciliopathies to DNA damage response signaling. Cell 150: 533–548.

Chaki M, Hoefele J, Allen SJ, Ramaswami G, Janssen S, Bergmann C, Heckenlively JR, Otto EA, Hildebrandt F. 2011. Genotype-phenotype correlation in 440 patients with NPHP-related ciliopathies. Kidney Int. 80: 1239–1245.

Chatterjee R, Hoffman M, Cliften P, Seshan S, Liapis H, Jain S. 2013. Targeted exome sequencing integrated with clinicopathological information reveals novel and rare mutations in atypical, suspected and unknown cases of Alport syndrome or proteinuria. PLoS One 8: e76360.

Chen CP, Chang TY, Chen CY, Wang TY, Tsai FJ, Wu PC, Chern SR, Wang W. 2012. Short rib-polydactyly syndrome type II (Majewski): Prenatal diagnosis, perinatal imaging findings and molecular analysis of the NEK1 gene. Taiwan. J. Obstet. Gynecol. 51: 100–105.

Chen Y, Chen CF, Chiang HC, Pena M, Polci R, Wei RL, Edwards RA, Hansel DE, Chen PL, Riley DJ. 2011a. Mutation of NIMA-related kinase 1 (NEK1) leads to chromosome instability. Mol. Cancer 10: 5.

Chen Y, Chen CF, Riley DJ, Chen PL. 2011b. Nek1 kinase functions in DNA damage response and checkpoint control through a pathway independent of ATM and ATR. Cell Cycle 10: 655–663.

Chiasserini D, Van Weering JRT, Piersma SR, Pham T V., Malekzadeh A, Teunissen CE, De Wit H, Jiménez CR. 2014. Proteomic analysis of cerebrospinal fluid extracellular vesicles: A comprehensive dataset. J. Proteomics 106: 191–204.

Choi HJ, Lin JR, Vannier JB, Slaats GG, Kile AC, Paulsen RD, Manning DK, Beier DR, Giles RH, Boulton SJ, Cimprich KA. 2013. NEK8 links the ATR-regulated replication stress response and S phase CDK activity to renal ciliopathies. Mol. Cell 51: 423–439.

Choi M, Scholl UI, Ji W, Liu T, Tikhonova IR, Zumbo P, Nayir A, Bakkaloğlu A, Ozen S, Sanjad S, Nelson-Williams C, Farhi A, Mane S, Lifton RP. 2009. Genetic diagnosis by whole exome capture and massively parallel DNA sequencing. Proc. Natl. Acad. Sci. U. S. A. 106: 19096–19101.

Chu VT, Weber T, Wefers B, Wurst W, Sander S, Rajewsky K, Kühn R. 2015. Increasing the efficiency of homology-directed repair for CRISPR-Cas9-induced precise gene editing in mammalian cells. Nat. Biotechnol. 33: 543–548.

Cirulli ET. 2016. The Increasing Importance of Gene-Based Analyses. PLoS Genet.

when the signal is lost_marijn_8072018.indd 212 08/07/2018 10:50

12: 1–12.
Coene KLM, Mans DA, Boldt K, Gloeckner CJ, van Reeuwijk J, Bolat E, Roosing S, Letteboer SJF, Peters TA, Cremers FPM, Ueffing M, Roepman R. 2011. The ciliopathy-associated protein homologs RPGRIP1 and RPGRIP1L are linked to cilium integrity through interaction with Nek4 serine/threonine kinase. Hum. Mol. Genet. 20: 3592–3605.
Conde-Vancells J, Falcon-Perez JM. 2012. Isolation of Urinary Exosomes from Animal Models to Unravel Noninvasive Disease Biomarkers. In: Josic D, Hixson DC, editors. Liver Proteomics: Methods and Protocols. Totowa, NJ: Humana Press, 321–340.
Cong L, Ran F, Cox D, Lin S, Barretto R, Habib N, Hsu P, Wu X, Jiang W, Marraffini L, Zhang F. 2009. Multiplex genome engineering using CRISPR/Cas systems. Science 339: 819–823.
Cooper G, Stone E, Asimenos G, Comparative N, Program S, Green E, Batzoglou S, Sidow A. 2005. Distribution and intensity of constraint in mammalian genomic sequence. Genome Res.: 901–913.
Copelovitch L, Nash MA, Kaplan BS. 2007. Hypothesis : Dent Disease Is an Underrecognized Cause of Focal Glomerulosclerosis. J. Am. Soc. Nephrol. 2: 914–918.
Corbit KC, Shyer AE, Dowdle WE, Gaulden J, Singla V, Reiter JF. 2008. Kif3a constrains β-catenin-dependent Wnt signalling through dual ciliary and non-ciliary mechanisms. Nat. Cell Biol. 10: 70–76.
Cox J, Mann M. 2008. MaxQuant enables high peptide identification rates, individualized p.p.b.-range mass accuracies and proteome-wide protein quantification. Nat. Biotechnol. 26: 1367–1372.
Craciun FL, Bijol V, Ajay AK, Rao P, Kumar RK, Hutchinson J, Hofmann O, Joshi N, Luyendyk JP, Kusebauch U, Moss CL, Srivastava A, Himmelfarb J, Waikar SS, Moritz RL, Vaidya VS. 2016. RNA Sequencing Identifies Novel Translational Biomarkers of Kidney Fibrosis. J. Am. Soc. Nephrol. 27: 1702–1713.
Cramer MT, Charlton JR, Fogo AB, Fathallah-shaykh SA, Askenazi DJ, Guay-woodford LM. 2014. Expanding the phenotype of proteinuria in Dent disease . A case series. Pediatr. Nephrol. 29: 2051–2054.
Cyranoski D. 2016. CRISPR gene-editing tested in a person for the first time. Nature 539: 479.
Dam, van TJ, Kennedy J, Van der Lee R, De Vrieze E, Wunderlich KA, Rix S, Dougherty GW, Lambacher NJ, Li C, Jensen VL, Leroux MR, Hjeij R, Horn N, Texier Y, Wissinger Y, Van Reeuwijk J, Wheway G, Knapp B, Scheel JF, Franco B, Mans DA, Van Wijk E, Kepes F, Slaats GG, Toedt G, Kremer H, Omran H, Szymanska K, Koutroumpas K, Ueffing M, Nguyen TMT, Letteboer SJF, Oud MM, Van Beersum SEC, Schmidts M, Beales PL, Lu Q, Giles RH, Szklarczyk R, Russel RB, Gibson TJ, Johnson CA, Blaque OE, Wolfrum U, Boldt K, Roepman R, Hernandez-Hernandez V, Huynen MA. 2017. CiliaCarta: An integrated and validated compendium of ciliary genes. BioRxiv.
Davis EE, Zhang Q, Liu Q, Diplas BH, Davey LM, Hartley J, Stoetzel C, Szymanska K, Ramaswami G, Logan C V, Muzny DM, Young AC, Wheeler DA, Cruz P, Morgan

when the signal is lost_marijn_8072018.indd 213 08/07/2018 10:50

M, Lewis LR, Cherukuri P, Maskeri B, Hansen NF, Mullikin JC, Blakesley RW, Bouffard GG, Program NCS, Gyapay G, Rieger S, Tonshoff B, Kern I, Soliman NA, Neuhaus TJ, Swoboda KJ, Kayserili H, Gallagher TE, Lewis RA, Bergmann C, Otto EA, Saunier S, Scambler PJ, Beales PL, Gleeson JG, Maher ER, Attie-Bitach T, Dollfus H, Johnson CA, Green ED, Gibbs RA, Hildebrandt F, Pierce EA, Katsanis N. 2011. TTC21B contributes both causal and modifying alleles across the ciliopathy spectrum. Nat. Genet. 43: 189–196.

Delous M, Baala L, Salomon R, Laclef C, Vierkotten J, Tory K, Golzio C, Lacoste T, Besse L, Ozilou C, Moutkine I, Hellman NE, Anselme I, Silbermann F, Vesque C, Gerhardt C, Rattenberry E, Wolf MT, Gubler MC, Martinovic J, Encha-Razavi F, Boddaert N, Gonzales M, Macher MA, Nivet H, Champion G, Bertheleme JP, Niaudet P, McDonald F, Hildebrandt F, Johnson CA, Vekemans M, Antignac C, Ruther U, Schneider-Maunoury S, Attie-Bitach T, Saunier S. 2007. The ciliary gene RPGRIP1L is mutated in cerebello-oculo-renal syndrome (Joubert syndrome type B) and Meckel syndrome. Nat. Genet. 39: 875–881.

Delous M, Hellman NE, Gaude HM, Silbermann F, Le Bivic A, Salomon R, Antignac C, Saunier S. 2009. Nephrocystin-1 and nephrocystin-4 are required for epithelial morphogenesis and associate with PALS1/PATJ and Par6. Hum. Mol. Genet. 18: 4711–4723.

Deltas C, Savva I, Voskarides K, Papazachariou L, Pierides A. 2015. Carriers of Autosomal Recessive Alport Syndrome with Thin Basement Membrane Nephropathy Presenting as Focal Segmental Glomerulosclerosis in Later Life. Nephron 130: 271–280.

Dixon-Salazar TJ, Silhavy JL, Udpa N, Schroth J, Bielas S, Schaffer AE, Olvera J, Bafna V, Zaki MS, Abdel-Salam GH, Mansour LA, Selim L, Abdel-Hadi S, Marzouki N, Ben-Omran T, Al-Saana NA, Sonmez FM, Celep F, Azam M, Hill KJ, Collazo A, Fenstermaker AG, Novarino G, Akizu N, Garimella K V., Sougnez C, Russ C, Gabriel SB, Gleeson JG. 2012. Exome Sequencing Can Improve Diagnosis and Alter Patient Management. Sci. Transl. Med. 4.

Dome J, Huff V. 2013. Wilms Tumor Overview. GeneReviews® [Internet]. Seattle Univ. Washington, Seattle; 1993-2015.: 1–24.

Domingos MAM, Moreira SR, Gomez L, Goulart A, Lotufo PA, Bensenor I, Titan S. 2016. Urinary retinol-binding protein: Relationship to renal function and cardiovascular risk factors in chronic kidney disease. PLoS One 11: 1–10.

Dona M, Bachmann-Gagescu R, Texier Y, Toedt G, Hetterschijt L, Tonnaer EL, Peters TA, van Beersum SEC, Bergboer JGM, Horn N, de Vrieze E, Slijkerman RWN, van Reeuwijk J, Flik G, Keunen JE, Ueffing M, Gibson TJ, Roepman R, Boldt K, Kremer H, van Wijk E. 2015. NINL and DZANK1 Co-function in Vesicle Transport and Are Essential for Photoreceptor Development in Zebrafish. PLoS Genet. 11: 1–28.

Donaldson JC, Dise RS, Ritchie MD, Hanks SK. 2002. Nephrocystin-conserved domains involved in targeting to epithelial cell-cell junctions, interaction with filamins, and establishing cell polarity. J. Biol. Chem. 277: 29028–29035.

Dreyer SD, Zhou G, Baldini a, Winterpacht a, Zabel B, Cole W, Johnson RL, Lee

when the signal is lost_marijn_8072018.indd 214 08/07/2018 10:50

B. 1998. Mutations in LMX1B cause abnormal skeletal patterning and renal dysplasia in nail patella syndrome. Nat. Genet. 19: 47–50.

Drivas TG, Wojno AP, Tucker BA, Stone EM, Bennett J. 2015. Basal exon skipping and genetic pleiotropy: A predictive model of disease pathogenesis. Sci. Transl. Med. 7.

Drmanac R. 2011. The advent of personal genome sequencing. Genet. Med. 13: 188–190.

Edwards N, Rice SJ, Raman S, Hynes a. M, Srivastava S, Moore I, Al-Hamed M, Xu Y, Santibanez-Koref M, Thwaites DT, Gale DP, Sayer J a. 2015. A novel LMX1B mutation in a family with end-stage renal disease of "unknown cause." Clin. Kidney J. 8: 113–119.

Eisenberger T, Decker C, Hiersche M, Hamann RC, Decker E, Neuber S, Frank V, Bolz HJ, Fehrenbach H, Pape L, Toenshoff B, Mache C, Latta K, Bergmann C. 2015. An Efficient and Comprehensive Strategy for Genetic Diagnostics of Polycystic Kidney Disease - fetchObject.action. PLoS One 10: e0116680.

Elias JE, Gygi SP. 2007. Target-decoy search strategy for increased confidence in large-scale protein identifications by mass spectrometry. Nat. Methods 4: 207–214.

Elumalai R, Periasamy S, Ramanathan G, Lakkakula BV, Soundararajan P. 2014b. Role of endothelial nitric oxide synthase VNTR (intron 4 a/b) polymorphism on the progression of renal disease in autosomal dominant polycystic kidney disease. J. Ren. Inj. Prev. 3: 69–73.

Fatehullah A, Tan SH, Barker N. 2016. Organoids as an in vitro model of human development and disease. Nat. Cell Biol. 18: 246–254.

Fehrenbach H, Decker C, Eisenberger T, Frank V, Hampel T, Walden U, Amann KU, Krüger-Stollfuß I, Bolz HJ, Häffner K, Pohl M, Bergmann C. 2014. Mutations in WDR19 encoding the intraflagellar transport component IFT144 cause a broad spectrum of ciliopathies. Pediatr. Nephrol. 29: 1451–6.

Ferrante MI, Feather SA, Bulfone A, Wright V, Ghiani M, Selicorni A, Gammaro L, Scolari F, Woolf AS, Sylvie O, Bernard LM, Malcolm S, Winter R, Ballabio A, Giorgio G, Franco B. 2001. Identification of the Gene for Oral-Facial-Digital Type I Syndrome. Am. J. Hum. Genet. 68: 569–576.

Ferrante MI, Romio L, Castro S, Collins JE, Goulding DA, Stemple DL, Woolf AS, Wilson SW. 2009. Convergent extension movements and ciliary function are mediated by ofd1, a zebrafish orthologue of the human oral-facial-digital type 1 syndrome gene. Hum. Mol. Genet. 18: 289–303.

Ferrante MI, Zullo A, Barra A, Bimonte S, Messaddeq N, Studer M, Dollé P, Franco B. 2006. Oral-facial-digital type I protein is required for primary cilia formation and left-right axis specification. Nat. Genet. 38: 112–117.

Filges I, Nosova E, Bruder E, Tercanli S, Townsend K, Gibson WT, Röthlisberger B, Heinimann K, Hall JG, Gregory-Evans CY, Wasserman WW, Miny P, Friedman JM. 2014. Exome sequencing identifies mutations in KIF14 as a novel cause of an autosomal recessive lethal fetal ciliopathy phenotype. Clin. Genet. 86: 220–228.

Firth H V, Richards SM, Bevan AP, Clayton S, Corpas M, Rajan D, Vooren S Van, Moreau Y, Pettett RM, Carter NP. 2009. REPORT DECIPHER : Database

when the signal is lost_marijn_8072018.indd 215 08/07/2018 10:50

of Chromosomal Imbalance and Phenotype in Humans Using Ensembl Resources. Am. J. Hum. Genet. 84: 524–533.

Fliegauf M, Horvath J, von Schnakenburg C, Olbrich H, Muller D, Thumfart J, Schermer B, Pazour GJ, Neumann HP, Zentgraf H, Benzing T, Omran H. 2006. Nephrocystin specifically localizes to the transition zone of renal and respiratory cilia and photoreceptor connecting cilia. J. Am. Soc. Nephrol. 17: 2424–2433.

Forsythe E, Beales P. 2015. Bardet-Biedl syndrome. GeneReviews® [Internet]. Seattle Univ. Washington, Seattle; 1993-2017.: 1–39.

Franceschini P, Guala A, Vardeu M, Signorile F, Franceschini D, Bolgiani M. 1995. Short rib-dysplasia group (with/without polydactyly): report of a patient suggesting the existence of a continuous spectrum. Am. J. Med. Genet.: 359–364.

Frishberg Y, Dinour D, Belostotsky R, Becker-cohen R, Rinat C, Feinstein S. 2009. Dent ' s disease manifesting as focal glomerulosclerosis : Is it the tip of the iceberg? Pediatr. Nephrol. 24: 2369–2373.

Froehlich JW, Kostel SA, Cho PS, Briscoe AC, Steen H, Vaezzadeh AR, Lee RS. 2016. Urinary Proteomics Yield Pathological Insights for Ureteropelvic Junction Obstruction. Mol. Cell. Proteomics 15: 2607–2615.

Fry AM, Leaper MJ, Bayliss R. 2014. The primary cilium: Guardian of organ development and homeostasis. Organogenesis 10: 62–68.

Fry AM, O'Regan L, Sabir SR, Bayliss R. 2012. Cell cycle regulation by the NEK family of protein kinases. J. Cell Sci. 125: 4423–4433.

Fu Q, Xu M, Chen X, Sheng X, Yuan Z, Liu Y, Li H, Sun Z, Li H, Yang L, Wang K, Zhang F, Li Y, Zhao C, Sui R, Chen R. 2017. CEP78 is mutated in a distinct type of Usher syndrome. J. Med. Genet. 54: 190–195.

Gabriel E, Wason A, Ramani A, Gooi LM, Keller P, Pozniakovsky A, Poser I, Noack F, Telugu NS, Calegari F, Saric T, Hescheler J, Hyman AA, Gottardo M, Calliani G, Alkuraya FS, Gopalakrishnan J. 2016. CPAP promotes timely cilium disassembly to maintain neural progenitor pool. EMBO J. 35: 699–791.

Gast C, Pengelly RJ, Lyon M, Bunyan DJ, Seaby EG, Graham N, Venkat-Raman G, Ennis S. 2015. Collagen (COL4A) mutations are the most frequent mutations underlying adult focal segmental glomerulosclerosis. Nephrol. Dial. Transplant.: 1–10.

Gbadegesin RA, Hall G, Adeyemo A, Hanke N, Tossidou I, Burchette J, Wu G, Homstad A, Sparks MA, Gomez J, Jiang R, Alonso A, Lavin P, Conlon P, Korstanje R, Stander MC, Shamsan G, Barua M, Spurney R, Singhal PC, Kopp JB, Haller H, Howell D, Pollak MR, Shaw AS, Schiffer M, Winn MP. 2014. Mutations in the Gene That Encodes the F-Actin Binding Protein Anillin Cause FSGS. JASN: 1991–2002.

Gee HY, Ashraf S, Wan X, Vega-warner V, Esteve-rudd J, Lovric S, Fang H, Hurd TW, Sadowski CE, Allen SJ, Otto EA, Korkmaz E, Washburn J, Levy S, Williams DS, Bakkaloglu SA, Zolotnitskaya A, Ozaltin F, Zhou W. 2014a. Mutations in EMP2 Cause Childhood-Onset Nephrotic Syndrome. Am. J. Hum. Genet. 94: 884–890.

when the signal is lost_marijn_8072018.indd 216 08/07/2018 10:50

Gee HY, Otto EA, Hurd TW, Ashraf S, Chaki M, Cluckey A, Vega-Warner V, Saisawat P, Diaz KA, Fang H, Kohl S, Allen SJ, Airik R, Zhou W, Ramaswami G, Janssen S, Fu C, Innis JL, Weber S, Vester U, Davis EE, Katsanis N, Fathy HM, Jeck N, Klaus G, Nayir A, Rahim KA, Al Attrach I, Al Hassoun I, Ozturk S, Drozdz D, Helmchen U, O'Toole JF, Attanasio M, Lewis RA, Nürnberg G, Nürnberg P, Washburn J, MacDonald J, Innis JW, Levy S, Hildebrandt F. 2014b. Whole-exome resequencing distinguishes cystic kidney diseases from phenocopies in renal ciliopathies. Kidney Int. 85: 880–7.

Gerhardt C, Leu T, Lier JM, Rüther U. 2016. The cilia-regulated proteasome and its role in the development of ciliopathies and cancer. Cilia 5: 14.

Gerlinger M, Rowan AJ, Horswell S, Larkin J, Endesfelder D, Gronroos, E, Pierre Martinez, Ph.D., Nicholas Matthews BS, Aengus Stewart, M.Sc., Patrick Tarpey, Ph.D., Ignacio Varela, Ph.D., Benjamin Phillimore, B.Sc., Sharmin Begum MS, Neil Q. McDonald, Ph.D., Adam Butler, B.Sc., David Jones, M.Sc., Keiran Raine, M.Sc., Calli Latimer BS, Claudio R. Santos, Ph.D., Mahrokh Nohadani, H.N.C., Aron C. Eklund, Ph.D., Bradley Spencer-Dene PD, Graham Clark, B.Sc., Lisa Pickering, M.D., Ph.D., Gordon Stamp, M.D., Martin Gore, M.D., Ph.D., Zoltan Szallasi MD, Julian Downward, Ph.D., P. Andrew Futreal, Ph.D., and Charles Swanton, M.D. PD. 2012. Intratumor Heterogeneity and Branched Evolution Revealed by Multiregion Sequencing. N. Engl. J. Med. 366: 883–892.

Ghosh A, Davey M, Chute IC, Griffiths SG, Lewis S, Chacko S, Barnett D, Crapoulet N, Fournier S, Joy A, Caissie MC, Ferguson AD, Daigle M, Meli MV, Lewis SM, Ouellette RJ. 2014. Rapid isolation of extracellular vesicles from cell culture and biological fluids using a synthetic peptide with specific affinity for heat shock proteins. PLoS One 9.

Gibson J, Gilbert R, Bunyan D, Angus E, Fowler D, S E. 2013. Exome analysis resolves differential diagnosis of familial kidney disease and uncovers a potential confounding variant. Genet. Res. 95: 165–73.

Gilissen C, Arts HH, Hoischen A, Spruijt L, Mans DA, Arts P, Van Lier B, Steehouwer M, Van Reeuwijk J, Kant SG, Roepman R, Knoers NVAM, Veltman JA, Brunner HG. 2010. Exome sequencing identifies WDR35 variants involved in Sensenbrenner syndrome. Am. J. Hum. Genet. 87: 418–423.

Giorgio G, Alfieri M, Prattichizzo C, Zullo A, Cairo S, Franco B. 2007. Functional characterization of the OFD1 protein reveals a nuclear localization and physical interaction with subunits of a chromatin remodeling complex. Mol. Biol. Cell 18: 4397–4404.

Global Lipids Genetics Consortium. 2013. Discovery and refinement of loci associated with lipid levels. Nat. Genet. 45: 1274–1283.

Goetz SC, Liem KF, Anderson K V. 2012. The spinocerebellar ataxia-associated gene tau tubulin kinase 2 controls the initiation of ciliogenesis. Cell 151: 847–858.

Good DM, Zurbig P, Argiles A, Bauer HW, Behrens G, Coon JJ, Dakna M, Decramer S, Delles C, Dominiczak AF, Ehrich JH, Eitner F, Fliser D, Frommberger M, Ganser A, Girolami MA, Golovko I, Gwinner W, Haubitz M, Herget-Rosenthal

when the signal is lost_marijn_8072018.indd 217 08/07/2018 10:50

S, Jankowski J, Jahn H, Jerums G, Julian BA, Kellmann M, Kliem V, Kolch W, Krolewski AS, Luppi M, Massy Z, Melter M, Neususs C, Novak J, Peter K, Rossing K, Rupprecht H, Schanstra JP, Schiffer E, Stolzenburg JU, Tarnow L, Theodorescu D, Thongboonkerd V, Vanholder R, Weissinger EM, Mischak H, Schmitt-Kopplin P. 2010. Naturally occurring human urinary peptides for use in diagnosis of chronic kidney disease. Mol. Cell. Proteomics 9: 2424–2437.

Goodwin S, McPherson JD, McCombie WR. 2016. Coming of age: ten years of next-generation sequencing technologies. Nat. Rev. Genet. 17: 333–351.

Gorden NT, Arts HH, Parisi M a, Coene KLM, Letteboer SJF, van Beersum SEC, Mans D a, Hikida A, Eckert M, Knutzen D, Alswaid AF, Ozyurek H, Dibooglu S, Otto E a, Liu Y, Davis EE, Hutter CM, Bammler TK, Farin FM, Dorschner M, Topçu M, Zackai EH, Rosenthal P, Owens KN, Katsanis N, Vincent JB, Hildebrandt F, Rubel EW, Raible DW, Knoers NV a M, Chance PF, Roepman R, Moens CB, Glass I a, Doherty D. 2008. CC2D2A is mutated in Joubert syndrome and interacts with the ciliopathy-associated basal body protein CEP290. Am. J. Hum. Genet. 83: 559–71.

Gresh L, Fischer E, Reimann A, Tanguy M, Garbay S, Shao X, Hiesberger T, Fiette L, Igarashi P, Yaniv M, Pontoglio M. 2004. A transcriptional network in polycystic kidney disease. EMBO 23: 1657–68.

Gross O, Licht C, Anders HJ, Hoppe B, Beck B, Tönshoff B, Höcker B, Wygoda S, Ehrich JHH, Pape L, Konrad M, Rascher W, Dötsch J, Müller-Wiefel DE, Hoyer P, Knebelmann B, Pirson Y, Grunfeld J-P, Niaudet P, Cochat P, Heidet L, Lebbah S, Torra R, Friede T, Lange K, Müller G a, Weber M. 2012. Early angiotensin-converting enzyme inhibition in Alport syndrome delays renal failure and improves life expectancy. Kidney Int. 81: 494–501.

Gruneberg U, Neef R, Li X, Chan EHY, Chalamalasetty RB, Nigg EA, Barr FA. 2006. KIF14 and citron kinase act together to promote efficient cytokinesis. J. Cell Biol. 172: 363–372.

Gupta IR, Baldwin C, Auguste D, Ha KCH, Andalousi J El, Fahiminiya S, Bitzan M, Bernard C, Akbari MR, Narod SA, Rosenblatt DS, Majewski J, Takano T. 2013. ARHGDIA : a novel gene implicated in nephrotic syndrome. J. Med. Genet: 330–338.

Gurrieri F, Franco B, Toriello H, Neri G. 2007. Oral-facial-digital syndromes: Review and diagnostic guidelines. Am. J. Med. Genet. A 143A: 3314–3323.

Habbig S, Liebau MC. 2015. Ciliopathies - from rare inherited cystic kidney diseases to basic cellular function. Mol. Cell. Pediatr. 2: 8–13.

Haber DA, Buckler AJ, Glaser T, Call KM, Pelletier J, Sohn RL, Douglass EC, Housman DE. 1990. An internal deletion within an 11p13 zinc finger gene contributes to the development of Wilms' tumor. Cell 61: 1257–1269.

Haghighi A, Savaj S, Haghighi-Kakhki H, Benoit V, Grisart B, Dahan K. 2016. Identification of an NPHP1 deletion causing adult form of nephronophthisis. Ir. J. Med. Sci. 185: 589–595.

Haider NB, Carmi R, Shalev H, Sheffield VC, Landau D. 1998. A Bedouin kindred with infantile nephronophthisis demonstrates linkage to chromosome 9 by homozygosity mapping. Am. J. Hum. Genet. 63: 1404–1410.

when the signal is lost_marijn_8072018.indd 218 08/07/2018 10:50

Halbritter J, Porath JD, Diaz KA, Braun DA, Kohl S, Chaki M, Allen SJ, Soliman NA, Hildebrandt F, Otto EA. 2013. Identification of 99 novel mutations in a worldwide cohort of 1,056 patients with a nephronophthisis-related ciliopathy. Hum. Genet. 132: 865–884.

Hamilton AJ, Bingham C, McDonald TJ, Cook PR, Caswell RC, Weedon MN, Oram RA, Shields BM, Shepherd M, Inward CD, Hamilton-Shield JP, Kohlhase J, Ellard S, Hattersley AT. 2014. The HNF4A R76W mutation causes atypical dominant Fanconi syndrome in addition to a β cell phenotype. J. Med. Genet. 51: 165–169.

Hamiwka LA, Midgley JP, Wade AW, Martz KL, Grisaru S. 2008. Outcomes of kidney transplantation in children with nephronophthisis: An analysis of the North American Pediatric Renal Trials and Collaborative Studies (NAPRTCS) Registry. Pediatr. Transplant. 12: 878–882.

Harakalova M, van Harssel JJT, Terhal PA, van Lieshout S, Duran K, Renkens I, Amor DJ, Wilson LC, Kirk EP, Turner CLS, Shears D, Garcia-Minaur S, Lees MM, Ross A, Venselaar H, Vriend G, Takanari H, Rook MB, van der Heyden MAG, Asselbergs FW, Breur HM, Swinkels ME, Scurr IJ, Smithson SF, Knoers N V, van der Smagt JJ, Nijman IJ, Kloosterman WP, van Haelst MM, van Haaften G, Cuppen E. 2012. Dominant missense mutations in ABCC9 cause Cantú syndrome. Nat. Genet. 44: 793–796.

Harris PC, Torres VE. 2015. Polycystic Kidney Disease , Autosomal Dominant. GeneReviews: 1–46.

Hastie N. 1992. Dominant negative mutations in the Wilms tumour (WT1) gene cause Denys-Drash syndrome--proof that a tumour-suppressor gene plays a crucial role in normal genitourinary development. Hum. Molec. Genet. 1: 293–295.

Hauswirth WW, Aleman TS, Kaushal S, Cideciyan A V., Schwartz SB, Wang L, Conlon TJ, Boye SL, Flotte TR, Byrne BJ, Jacobson SG. 2008. Treatment of Leber Congenital Amaurosis Due to RPE65 Mutations by Ocular Subretinal Injection of Adeno-Associated Virus Gene Vector: Short-Term Results of a Phase I Trial. Hum. Gene Ther. 19: 979–990.

Heidet L, Decramer S, Pawtowski A, Moriniere V, Bandin F, Knebelmann B, Lebre AS, Faguer S, Guigonis V, Antignac C, Salomon R. 2010. Spectrum of HNF1B mutations in a large cohort of patients who harbor renal diseases. Clin. J. Am. Soc. Nephrol. 5: 1079–1090.

Helou J, Otto EA, Attanasio M, Allen SJ, Parisi MA, Glass I, Utsch B, Hashmi S, Fazzi E, Omran H, O 'toole JF, Sayer JA, Hildebrandt F. 2007. Mutation analysis of NPHP6/CEP290 in patients with Joubert syndrome and Senior–Løken syndrome. J Med Genet 44: 657–663.

Heon E, Kim G, Qin S, Garrison JE, Tavares E, Vincent A, Nuangchamnong N, Anthony Scott C, Slusarski DC, Sheffield VC. 2016. Mutations in C8ORF37 cause Bardet Biedl syndrome (BBS21). Hum. Mol. Genet. 25: 2283–2294.

Hernandez-Hernandez V, Pravincumar P, Diaz-Font A, May-Simera H, Jenkins D, Knight M, Beales PL. 2013. Bardet-biedl syndrome proteins control the cilia length through regulation of actin polymerization. Hum. Mol. Genet. 22:

when the signal is lost_marijn_8072018.indd 219 08/07/2018 10:50

3858–3868.
Hichri H, Rendu J, Monnier N, Coutton C, Dorseuil O, Poussou RV, Baujat G, Blanchard A, Nobili F, Ranchin B, Remesy M, Salomon R, Satre V, Lunardi J. 2011. From lowe syndrome to Dent disease: Correlations between mutations of the OCRL1 gene and clinical and biochemical phenotypes. Hum. Mutat. 32: 379–388.
Hiesberger T, Bai Y, Shao X, McNally BT, Sinclair AM, Tian X, Somlo S, Igarashi P. 2004. Mutation of hepatocyte nuclear factor-1B inhibits Pkhd1 gene expression and produces renal cysts in mice. J. Clin. Invest. 113: 814–825.
Higashijima Y, Hirano S, Nangaku M, Nureki O. 2017. Applications of the CRISPR-Cas9 system in kidney research. Kidney Int. 92: 324–335.
Hildebrandt F, Attanasio M, Otto E. 2009. Nephronophthisis: disease mechanisms of a ciliopathy. J. Am. Soc. Nephrol. 20: 23–35.
Hildebrandt F, Otto E, Rensing C, Nothwang HG, Vollmer M, Adolphs J, Hanusch H, Brandis M. 1997a. A novel gene encoding an SH3 domain protein is mutated in nephronophthisis type 1. Nat. Genet. 17: 149–153.
Hildebrandt F, Singh-Sawhney I, Schnieders B, Centofante L, Omran H, Pohlmann A, Schmaltz C, Wedekind H, Schubotz C, Antignac C. 1993. Mapping of a gene for familial juvenile nephronophthisis: refining the map and defining flanking markers on chromosome 2. APN Study Group. Am. J. Hum. Genet. 53: 1256–1261.
Hildebrandt F, Strahm B, Nothwang HG, Gretz N, Schnieders B, Singh-Sawhney I, Kutt R, Vollmer M, Brandis M. 1997b. Molecular genetic identification of families with juvenile nephronophthisis type 1: rate of progression to renal failure. APN Study Group. Arbeitsgemeinschaft fur Padiatrische Nephrologie. Kidney Int. 51: 261–269.
Hildebrandt F, Zhou W. 2007. Nephronophthisis-associated ciliopathies. J. Am. Soc. Nephrol. 18: 1855–1871.
Hilton LK, White MC, Quarmby LM. 2009. The NIMA-related kinase NEK1 cycles through the nucleus. Biochem. Biophys. Res. Commun. 389: 52–56.
Hirsch T, Rothoeft T, Teig N, Bauer JW, Pellegrini G, De Rosa L, Scaglione D, Reichelt J, Klausegger A, Kneisz D, Romano O, Seconetti AS, Contin R, Enzo E, Jurman I, Carulli S, Jacobsen F, Luecke T, Lehnhardt M, Fischer M, Kueckelhaus M, Quaglino D, Morgante M, Bicciato S, Bondanza S, De Luca M. 2017. Regeneration of the entire human epidermis using transgenic stem cells. Nature 551: 327–332.
Hoefele J, Sudbrak R, Reinhardt R, Lehrack S, Hennig S, Imm A, Muerb U, Utsch B, Attanasio M, O'Toole JF, Otto E, Hildebrandt F. 2005. Mutational analysis of the NPHP4 gene in 250 patients with nephronophthisis. Hum. Mutat. 25: 411.
Hoefele J, Wolf MT, O'Toole JF, Otto EA, Schultheiss U, Deschenes G, Attanasio M, Utsch B, Antignac C, Hildebrandt F. 2007. Evidence of oligogenic inheritance in nephronophthisis. J. Am. Soc. Nephrol. 18: 2789–2795.
Van De Hoek G, Nicolaou N, Giles RH, Knoers NVAM, Renkema KY, Bongers EMHF. 2015. Functional models for congenital anomalies of the kidney and urinary

when the signal is lost_marijn_8072018.indd 220 08/07/2018 10:50

tract. Nephron 129: 62–67.
Hogan MC, Bakeberg JL, Gainullin VG, Irazabal M V, Harmon AJ, Lieske JC, Charlesworth MC, Johnson KL, Madden BJ, Zenka RM, Mccormick DJ, Sundsbak JL, Heyer CM, Torres VE, Harris PC, Ward CJ. 2015. Identification of Biomarkers for PKD1 Using Urinary Exosomes. J. Am. Soc. Nephrol. 26: 1661–1670.
El Hokayem J, Huber C, Couvé A, Aziza J, Baujat G, Bouvier R, Cavalcanti DP, Collins FA, Cordier M-P, Delezoide A-L, Gonzales M, Johnson D, Le Merrer M, Levy-Mozziconacci A, Loget P, Martin-Coignard D, Martinovic J, Mortier GR, Perez M-J, Roume J, Scarano G, Munnich A, Cormier-Daire V. 2012. NEK1 and DYNC2H1 are both involved in short rib polydactyly Majewski type but not in Beemer Langer cases. J. Med. Genet. 49: 227–233.
Hollak CEM, Biegstraaten M, Baumgartner MR, Belmatoug N, Bembi B, Bosch A, Brouwers M, Dekker H, Dobbelaere D, Engelen M, Groenendijk MC, Lachmann R, Langendonk JG, Langeveld M, Linthorst G, Morava E, Poll-The BT, Rahman S, Rubio-Gozalbo ME, Spiekerkoetter U, Treacy E, Wanders R, Zschocke J, Hagendijk R. 2016. Position statement on the role of healthcare professionals, patient organizations and industry in European Reference Networks. Orphanet J. Rare Dis. 11: 7.
Hoopes RR, Shrimpton AE, Knohl SJ, Hueber P, Hoppe B, Matyus J, Simckes A, Tasic V, Toenshoff B, Suchy SF, Nussbaum RL, Scheinman SJ. 2005. Dent Disease with mutations in OCRL1. Am. J. Hum. Genet. 76: 260–267.
Hopp K, Heyer CM, Hommerding CJ, Henke SA, Sundsbak JL, Patel S, Patel P, Consugar MB, Czarnecki PG, Gliem TJ, Torres VE, Rossetti S, Harris PC. 2011. B9d1 is revealed as a novel Meckel syndrome (MKS) gene by targeted exon-enriched next-generation sequencing and deletion analysis. Hum. Mol. Genet. 20: 2524–2534.
Horikawa Y, Iwasaki N, Hara M, Futura H, Hinokio Y, Cockburn B. 1997. Mutation in hepatocyte nuclear factor-1B gene (TCF2) associated with MODY. Nat. Genet. 15: 57–61.
Huang W, Wang J, Zhang D, Chen W, Hou L, Wu X, Lu Y. 2015. Inhibition of KIF14 Suppresses Tumor Cell Growth and Promotes Apoptosis in Human Glioblastoma. Cell. Physiol. Biochem. 37: 1659–1670.
Huber C, Cormier-Daire V. 2012. Ciliary disorder of the skeleton. Am. J. Med. Genet. Part C Semin. Med. Genet. 160 C: 165–174.
Van Huis M. 2016. Quality of Care and Monitoring in Paediatric End Stage Renal Disease.
Humbert C, Silbermann F, Morar B, Parisot M, Zarhrate M, Cecile M, Tores F, Blanchet P, Perez M-J, Petrov Y, Khau Van Kien P, Roume J, Leroy B, Gribouval O, Kalaydjieva L, Heidet L, Salomon R, Antignac C, Benmerah A, Heidet L, Saunier S, Jeanpierre C. 2014. Integrin Alpha 8 Recessive Mutations Are Responsible for Bilateral Renal Agenesis in Humans. Am. J. Hum. Genet.: 288–294.
Huppke P, Wegener E, Böhrer-Rabel H, Bolz HJ, Zoll B, Gärtner J, Bergmann C. 2015. Tectonic gene mutations in patients with Joubert syndrome. Eur. J.

when the signal is lost_marijn_8072018.indd 221 08/07/2018 10:50

Hum. Genet. 23: 616–620.
Hurd TW, Hildebrandt F. 2011. Mechanisms of nephronophthisis and related ciliopathies. Nephron - Exp. Nephrol. 118: 9–14.
Huynh Cong E, Bizet A a, Boyer O, Woerner S, Gribouval O, Filhol E, Arrondel C, Thomas S, Silbermann F, Canaud G, Hachicha J, Ben Dhia N, Peraldi M-N, Harzallah K, Iftene D, Daniel L, Willems M, Noel L-H, Bole-Feysot C, Nitschké P, Gubler M-C, Mollet G, Saunier S, Antignac C. 2014. A Homozygous Missense Mutation in the Ciliary Gene TTC21B Causes Familial FSGS. J. Am. Soc. Nephrol.: 1–9.
Hwang D-Y, Dworschak GC, Kohl S, Saisawat P, Vivante A, Hilger AC, Reutter HM, Soliman N a, Bogdanovic R, Kehinde EO, Tasic V, Hildebrandt F. 2014. Mutations in 12 known dominant disease-causing genes clarify many congenital anomalies of the kidney and urinary tract. Kidney Int. 85: 1–5.
Isojima T, Harita Y, Furuyama M, Sugawara N, Ishizuka K, Horita S, Kajiho Y, Miura K, Igarashi T, Hattori M, Kitanaka S. 2014. LMX1B mutation with residual transcriptional activity as a cause of isolated glomerulopathy. Nephrol. Dial. Transplant. 29: 81–88.
Jadeja S, Smyth I, Pitera JE, Taylor MS, van Haelst M, Bentley E, McGregor L, Hopkins J, Chalepakis G, Philip N, Perez Aytes A, Watt FM, Darling SM, Jackson I, Woolf AS, Scambler PJ. 2005. Identification of a new gene mutated in Fraser syndrome and mouse myelencephalic blebs. Nat. Genet. 37: 520–525.
Jais JP, Knebelmann B, Giatras I, De Marchi M, Rizzoni G, Renieri a, Weber M, Gross O, Netzer KO, Flinter F, Pirson Y, Verellen C, Wieslander J, Persson U, Tryggvason K, Martin P, Hertz JM, Schröder C, Sanak M, Krejcova S, Carvalho MF, Saus J, Antignac C, Smeets H, Gubler MC. 2000. X-linked Alport syndrome: natural history in 195 families and genotype- phenotype correlations in males. J. Am. Soc. Nephrol. 11: 649–657.
Jais JP, Knebelmann B, Giatras I, De Marchi M, Rizzoni G, Renieri A, Weber M. 2003. X-Linked Alport Syndrome: Natural History and Genotype-Phenotype Correlations in Girls and Women Belonging to 195 Families: A "European Community Alport Syndrome Concerted Action" Study. J. Am. Soc. Nephrol. 14: 2603–2610.
Jeanpierre C, Denamur E, Henry I, Cabanis MO, Luce S, Cécille A, Elion J, Peuchmaur M, Loirat C, Niaudet P, Gubler MC, Junien C. 1998. Identification of constitutional WT1 mutations, in patients with isolated diffuse mesangial sclerosis, and analysis of genotype/phenotype correlations by use of a computerized mutation database. Am. J. Hum. Genet. 62: 824–833.
Johnston JJ, Lewis KL, Ng D, Singh LN, Wynter J, Brewer C, Brooks BP, Brownell I, Candotti F, Gonsalves SG, Hart SP, Kong HH, Rother KI, Sokolic R, Solomon BD, Zein WM, Cooper DN, Stenson PD, Mullikin JC, Biesecker LG. 2015. Individualized Iterative Phenotyping for Genome-wide Analysis of Loss-of-Function Mutations. Am. J. Hum. Genet. 96: 913–925.
De Jong OG, Verhaar MC, Chen Y, Vader P, Gremmels H, Posthuma G, Schiffelers RM, Gucek M, van Balkom BWM. 2012. Cellular stress conditions are reflected

when the signal is lost_marijn_8072018.indd 222 08/07/2018 10:50

in the protein and RNA content of endothelial cell-derived exosomes. J. Extracell. Vesicles 1: 1–12.

Kadioglu A. 2010. Renal measurements, including length, parenchymal thickness, and medullary pyramid thickness, in healthy children: What are the normative ultrasound values? Am. J. Roentgenol. 194: 509–515.

Kalay E, Yigit G, Aslan Y, Brown KE, Pohl E, Bicknell LS, Kayserili H, Li Y, Tüysüz B, Nürnberg G, Kiess W, Koegl M, Baessmann I, Buruk K, Toraman B, Kayipmaz S, Kul S, Ikbal M, Turner DJ, Taylor MS, Aerts J, Scott C, Milstein K, Dollfus H, Wieczorek D, Brunner HG, Hurles M, Jackson AP, Rauch A, Nürnberg P, Karagüzel A, Wollnik B. 2011. CEP152 is a genome maintenance protein disrupted in Seckel syndrome. Nat. Genet. 43: 23–26.

Kamburov A, Pentchev K, Galicka H, Wierling C, Lehrach H, Herwig R. 2011. ConsensusPathDB: Toward a more complete picture of cell biology. Nucleic Acids Res. 39: 712–717.

Kamijo-Ikemori A, Sugaya T, Yoshida M, Hoshino S, Akatsu S, Yamazaki S, Kimura K, Shibagaki Y. 2016. Clinical utility of urinary liver-type fatty acid binding protein measured by latex-enhanced turbidimetric immunoassay in chronic kidney disease. Clin. Chem. Lab. Med. 54: 1645–1654.

Kaneko N, Gotoh A, Okamura N, Matsuo E, Terao S, Watanabe M, Yamada Y, Hamami G, Nakamura T, Ikekita M. 2013. Potential tumor markers of renal cell carcinoma : a-Enolase for postoperative follow up, and galectin-1 and galectin-3 for primary detection. Int. J. Urol. 20: 530–535.

Kang HG, Lee HK, Ahn YH, Joung J-G, Nam J, Kim NKD, Ko JM, Cho MH, Shin J Il, Kim J, Park HW, Park YS, Ha I-S, Chung WY, Lee D-Y, Kim SY, Park WY, Cheong H Il. 2016. Targeted exome sequencing resolves allelic and the genetic heterogeneity in the genetic diagnosis of nephronophthisis-related ciliopathy. Exp. Mol. Med. 48: e251.

Karmous-Benailly H, Martinovic J, Gubler M, Sirot Y, Clech L, Ozilou C, Auge J, Brahimi N, Etchevers H, Detrait E, Esculpavit C, Audollent S, Goudefroye G, Gonzales M, Tantau J, Loget P, Joubert M, Gaillard D, Jeanne-Pasquier C, Delezoide A, Peter M, Plessis G, Simon-Bouy B, Dollfus H, Le Merrer M, Munnich A, Encha-Razavi F, Vekemans M, Attié-Bitach T. 2005. Antenatal presentation of Bardet-Biedl syndrome may mimic Meckel syndrome. Am J Hum Genet. 76: 493–504.

Kashtan C. 2015. Alport Syndrome and Thin Basement Membrane Nephropathy. GeneReviews.

Katsanis N. 2001. Triallelic Inheritance in Bardet-Biedl Syndrome, a Mendelian Recessive Disorder. Science 293: 2256–2259.

Kenna KP, van Doormaal PTC, Dekker AM, Ticozzi N, Kenna BJ, Diekstra FP, van Rheenen W, van Eijk KR, Jones AR, Keagle P, Shatunov A, Sproviero W, Smith BN, van Es MA, Topp SD, Kenna A, Miller JW, Fallini C, Tiloca C, McLaughlin RL, Vance C, Troakes C, Colombrita C, Mora G, Calvo A, Verde F, Al-Sarraj S, King A, Calini D, de Belleroche J, Baas F, van der Kooi AJ, de Visser M, ten Asbroek ALMA, Sapp PC, McKenna-Yasek D, Polak M, Asress S, Muñoz-Blanco JL, Strom TM, Meitinger T, Morrison KE, D'Alfonso S, Mazzini L,

when the signal is lost_marijn_8072018.indd 223 08/07/2018 10:50

Comi GP, Del Bo R, Ceroni M, Gagliardi S, Querin G, Bertolin C, Pensato V, Castellotti B, Corti S, Cereda C, Corrado L, Sorarù G, Lauria G, Williams KL, Leigh PN, Nicholson GA, Blair IP, Leblond CS, Dion PA, Rouleau GA, Pall H, Shaw PJ, Turner MR, Talbot K, Taroni F, Boylan KB, Van Blitterswijk M, Rademakers R, Esteban-Pérez J, García-Redondo A, Van Damme P, Robberecht W, Chio A, Gellera C, Drepper C, Sendtner M, Ratti A, Glass JD, Mora JS, Basak NA, Hardiman O, Ludolph AC, Andersen PM, Weishaupt JH, Brown RH, Al-Chalabi A, Silani V, Shaw CE, van den Berg LH, Veldink JH, Landers JE. 2016. NEK1 variants confer susceptibility to amyotrophic lateral sclerosis. Nat. Genet. 48: 1037–1042.

Kent WJ, Sugnet CW, Furey TS, Roskin KM. 2002. The Human Genome Browser at UCSC W. Genome Res. 12: 996–1006.

Khanna H, Davis EE, Murga-Zamalloa CA, Estrada-Cuzcano A, Lopez I, den Hollander AI, Zonneveld MN, Othman MI, Waseem N, Chakarova CF, Maubaret C, Diaz-Font A, MacDonald I, Muzny DM, Wheeler DA, Morgan M, Lewis LR, Logan C V, Tan PL, Beer MA, Inglehearn CF, Lewis RA, Jacobson SG, Bergmann C, Beales PL, Attié-Bitach T, Johnson CA, Otto EA, Bhattacharya SS, Hildebrandt F, Gibbs RA, Koenekoop RK, Swaroop A, Katsanis N. 2009. A common allele in RPGRIP1L is a modifier of retinal degeneration in ciliopathies. Nat. Genet. 41: 739–745.

Kidney Disease: Improving Global Outcomes (KDIGO) CKD Work Group. 2013. KDIGO 2012 Clinical Practice Guideline for the Evaluation and Management of Chronic Kidney Disease. Kidney Int. Suppl. 3: 1–150.

Kim JC, Badano JL, Sibold S, Esmail M a, Hill J, Hoskins BE, Leitch CC, Venner K, Ansley SJ, Ross AJ, Leroux MR, Katsanis N, Beales PL. 2004. The Bardet-Biedl protein BBS4 targets cargo to the pericentriolar region and is required for microtubule anchoring and cell cycle progression. Nat. Genet. 36: 462–470.

King DA, Sifrim A, Fitzgerald TW, Rahbari R, Hobson E, Homfray T, Mansour S, Mehta SG, Shehla M, Tomkins SE, Vasudevan PC, Hurles ME, Study TDDD. 2016. Detection of structural mosaicism from targeted and whole-genome sequencing data. BioRxiv: 62620.

King K, Flinter FA, Nihalani V, Green PM. 2002. Unusual deep intronic mutations in the COL4A5 gene cause X linked Alport syndrome. Hum. Genet. 111: 548–554.

KNAW. 2016. Genome Editing, Visiedocument KNAW. 1–6.

Knol JC, de Reus I, Schelfhorst T, Beekhof R, de Wit M, Piersma SR, Pham T V., Smit EF, Verheul HMW, Jiménez CR. 2016. Peptide-mediated "miniprep" isolation of extracellular vesicles is suitable for high-throughput proteomics. EuPA Open Proteomics 11: 11–15.

Kohl S, Hwang D-Y, Dworschak GC, Hilger AC, Saisawat P, Vivante A, Stajic N, Bogdanovic R, Reutter HM, Kehinde EO, Tasic V, Hildebrandt F. 2014. Mild Recessive Mutations in Six Fraser Syndrome-Related Genes Cause Isolated Congenital Anomalies of the Kidney and Urinary Tract. J. Am. Soc. Nephrol.: 1–6.

Köhler S, Vasilevsky NA, Engelstad M, Foster E, McMurry J, Aymé S, Baynam G,

when the signal is lost_marijn_8072018.indd 224 08/07/2018 10:50

Bello SM, Boerkoel CF, Boycott KM, Brudno M, Buske OJ, Chinnery PF, Cipriani V, Connell LE, Dawkins HJS, DeMare LE, Devereau AD, De Vries BBA, Firth H V., Freson K, Greene D, Hamosh A, Helbig I, Hum C, Jähn JA, James R, Krause R, Laulederkind SJF, Lochmüller H, Lyon GJ, Ogishima S, Olry A, Ouwehand WH, Pontikos N, Rath A, Schaefer F, Scott RH, Segal M, Sergouniotis PI, Sever R, Smith CL, Straub V, Thompson R, Turner C, Turro E, Veltman MWM, Vulliamy T, Yu J, Von Ziegenweidt J, Zankl A, Züchner S, Zemojtel T, Jacobsen JOB, Groza T, Smedley D, Mungall CJ, Haendel M, Robinson PN. 2017. The human phenotype ontology in 2017. Nucleic Acids Res. 45: 865–876.

König J, Kranz B, König S, Schlingmann KP, Titieni A, Tönshoff B, Habbig S, Pape L, Häffner K, Hansen M, Büscher A, Bald M, Billing H, Schild R, Walden U, Hampel T, Staude H, Riedl M, Gretz N, Lablans M, Bergmann C, Hildebrandt F, Omran H, Konrad M. 2017. Phenotypic Spectrum of Children with Nephronophthisis and Related Ciliopathies. Clin. J. Am. Soc. Nephrol. 12: 1974–1983.

Konvalinka A, Batruch I, Tokar T, Dimitromanolakis A, Reid S, Song X, Pei Y, Drabovich AP, Diamandis EP, Jurisica I, Scholey JW. 2016. Quantification of angiotensin II-regulated proteins in urine of patients with polycystic and other chronic kidney diseases by selected reaction monitoring. Clin. Proteomics 13: 16.

Kroes HY, Monroe GR, Van Der Zwaag B, Duran KJ, De Kovel CG, Van Roosmalen MJ, Harakalova M, Nijman IJ, Kloosterman WP, Giles RH, Knoers NVAM, Van Haaften G. 2016. Joubert syndrome: Genotyping a Northern European patient cohort. Eur. J. Hum. Genet. 24: 214–220.

Kroes HY, van Zon PHA, van de Putte DF, Nelen MR, Nievelstein RJ, Wittebol-Post D, van Nieuwenhuizen O, Mancini GMS, van der Knaap MS, Kwee ML, Maas SM, Cobben JM, De Nef JEE, Lindhout D, Sinke RJ. 2008. DNA analysis of AHI1, NPHP1 and CYCLIN D1 in Joubert syndrome patients from the Netherlands. Eur. J. Med. Genet. 51: 24–34.

Kubiak M, Lewandowska MA. 2015. Can chromatin conformation technologies bring light into human molecular pathology? Acta Biochim. Pol. 62: 483–489.

Kuechler A, Altmüller J, Nürnberg P, Kotthoff S, Kubisch C, Borck G. 2015. Exome sequencing identifies a novel heterozygous TGFB3 mutation in a disorder overlapping with Marfan and Loeys-Dietz syndrome. Mol. Cell. Probes 29: 330–334.

Kulon M. Pediatric Kidney Size Percentile Calculator. Radiol. Universe Inst.: 1.

Kumar P, Henikoff S, Ng PC. 2009. Predicting the effects of coding non-synonymous variants on protein function using the SIFT algorithm. Nat. Protoc. 4: 1073–1082.

Kyttälä M, Tallila J, Salonen R, Kopra O, Kohlschmidt N, Paavola-Sakki P, Peltonen L, Kestilä M. 2006. MKS1, encoding a component of the flagellar apparatus basal body proteome, is mutated in Meckel syndrome. Nat. Genet. 38: 155–7.

when the signal is lost_marijn_8072018.indd 225 08/07/2018 10:50

Lacquaniti A, Chirico V, Donato V, Briuglia S, Cernaro V, Gallizzi R, Salpietro CD, Buemi M. 2012. NGAL as an early biomarker of kidney disease in Joubert syndrome: three brothers compared. Ren. Fail. 34: 495–498.

Lambacher NJ, Bruel A-L, van Dam TJP, Szymańska K, Slaats GG, Kuhns S, McManus GJ, Kennedy JE, Gaff K, Wu KM, van der Lee R, Burglen L, Doummar D, Rivière J-B, Faivre L, Attié-Bitach T, Saunier S, Curd A, Peckham M, Giles RH, Johnson CA, Huynen MA, Thauvin-Robinet C, Blacque OE. 2016. TMEM107 recruits ciliopathy proteins to subdomains of the ciliary transition zone and causes Joubert syndrome. Nat. Cell Biol. 18: 122–131.

Lan J, Zhang Q. 2015. Clinical applications of next-generation sequencing in histocompatibility and transplantation. Curr. Opin. Organ Transplant. 20: 461–467.

Landrum MJ, Lee JM, Benson M, Brown G, Chao C, Chitipiralla S, Gu B, Hart J, Hoffman D, Hoover J, Jang W, Katz K, Ovetsky M, Riley G, Sethi A, Tully R, Villamarin-salomon R, Rubinstein W, Maglott DR. 2016. ClinVar : public archive of interpretations of clinically relevant variants. Nucleic Acids Res. 44: 862–868.

Lebherz-Eichinger D, Tudor B, Ankersmit HJ, Reiter T, Haas M, Roth-Walter F, Krenn CG, Roth GA. 2015. Trefoil factor 1 excretion is increased in early stages of chronic kidney disease. PLoS One 10: 1–11.

Leitch CC, Zaghloul N a, Davis EE, Stoetzel C, Diaz-Font A, Rix S, Alfadhel M, Al-Fadhel M, Lewis RA, Eyaid W, Banin E, Dollfus H, Beales PL, Badano JL, Katsanis N. 2008. Hypomorphic mutations in syndromic encephalocele genes are associated with Bardet-Biedl syndrome. Nat. Genet. 40: 443–448.

Lek M, Karczewski KJ, Minikel E V., Samocha KE, Banks E, Fennell T, O'Donnell-Luria AH, Ware JS, Hill AJ, Cummings BB, Tukiainen T, Birnbaum DP, Kosmicki JA, Duncan LE, Estrada K, Zhao F, Zou J, Pierce-Hoffman E, Berghout J, Cooper DN, Deflaux N, DePristo M, Do R, Flannick J, Fromer M, Gauthier L, Goldstein J, Gupta N, Howrigan D, Kiezun A, Kurki MI, Moonshine AL, Natarajan P, Orozco L, Peloso GM, Poplin R, Rivas MA, Ruano-Rubio V, Rose SA, Ruderfer DM, Shakir K, Stenson PD, Stevens C, Thomas BP, Tiao G, Tusie-Luna MT, Weisburd B, Won H-H, Yu D, Altshuler DM, Ardissino D, Boehnke M, Danesh J, Donnelly S, Elosua R, Florez JC, Gabriel SB, Getz G, Glatt SJ, Hultman CM, Kathiresan S, Laakso M, McCarroll S, McCarthy MI, McGovern D, McPherson R, Neale BM, Palotie A, Purcell SM, Saleheen D, Scharf JM, Sklar P, Sullivan PF, Tuomilehto J, Tsuang MT, Watkins HC, Wilson JG, Daly MJ, MacArthur DG. 2016. Analysis of protein-coding genetic variation in 60,706 humans. Nature 536: 285–291.

Lemaire M, Frémeaux-Bacchi V, Schaefer F, Choi M, Tang WH, Le Quintrec M, Fakhouri F, Taque S, Nobili F, Martinez F, Ji W, Overton JD, Mane SM, Nürnberg G, Altmüller J, Thiele H, Morin D, Deschenes G, Baudouin V, Llanas B, Collard L, Majid M a., Simkova E, Nürnberg P, Rioux-Leclerc N, Moeckel GW, Gubler MC, Hwa J, Loirat C, Lifton RP. 2013. Recessive mutations in DGKE cause atypical hemolytic-uremic syndrome. Nat. Genet. 45: 531–536.

Lemmink HH, Nillesen WN, Mochizuki T, Schröder CH, Brunner HG, Van Oost

when the signal is lost_marijn_8072018.indd 226 08/07/2018 10:50

BA, Monnens LAH, Smeets HJM. 1996. Benign familial hematuria due to mutation of the type IV collagen A4 gene. J. Clin. Invest. 98: 1114–1118.

Lener T, Gimona M, Aigner L, Börger V, Buzas E, Camussi G, Chaput N, Chatterjee D, Court FA, del Portillo HA, O'Driscoll L, Fais S, Falcon-Perez JM, Felderhoff-Mueser U, Fraile L, Gho YS, Görgens A, Gupta RC, Hendrix A, Hermann DM, Hill AF, Hochberg F, Horn PA, de Kleijn D, Kordelas L, Kramer BW, Krämer-Albers EM, Laner-Plamberger S, Laitinen S, Leonardi T, Lorenowicz MJ, Lim SK, Lötvall J, Maguire CA, Marcilla A, Nazarenko I, Ochiya T, Patel T, Pedersen S, Pocsfalvi G, Pluchino S, Quesenberry P, Reischl IG, Rivera FJ, Sanzenbacher R, Schallmoser K, Slaper-Cortenbach I, Strunk D, Tonn T, Vader P, van Balkom BWM, Wauben M, El Andaloussi S, Théry C, Rohde E, Giebel B. 2015. Applying extracellular vesicles based therapeutics in clinical trials - An ISEV position paper. J. Extracell. Vesicles 4: 1–31.

Li K, Qi Y, Xia T, Chan A, Zhang Z, Aibaidula A, Zhang R, Zhou L, Yao Y, Ng H. 2017. The kinesin KIF14 is overexpressed in medulloblastoma and downregulation of KIF14 suppressed tumor proliferation and induced apoptosis. Lab. Investig. 97: 946–961.

Licht C, Fremeaux-Bacchi V. 2009. Hereditary and acquired complement dysregulation in membranoproliferative glomerulonephritis. Thromb. Haemost. 101: 271–278.

Liebau MC. 2014. An emerging molecular understanding and novel targeted treatment approaches in pediatric kidney diseases. Front. Pediatr. 2: 68.

Lin AE, Traum AZ, Sahai I, Keppler-Noreuil K, Kukolich MK, Adam MP, Westra SJ, Arts HH. 2013. Sensenbrenner syndrome (Cranioectodermal dysplasia): Clinical and molecular analyses of 39 patients including two new patients. Am. J. Med. Genet. Part A 161: 2762–2776.

Lin HYH, Hwang DY, Lee SC, Kuo HT, Kuo MC, Chang J-M, Tsai JC, Hung CC, Hwang SJ, Chen HC. 2015. Urinary neutrophil gelatinase-associated lipocalin and clinical outcomes in chronic kidney disease patients. Clin. Chem. Lab. Med. 53: 73–83.

Lindstrand A, Davis EE, Carvalho CMB, Pehlivan D, Willer JR, Tsai IC, Ramanathan S, Zuppan C, Sabo A, Muzny D, Gibbs R, Liu P, Lewis RA, Banin E, Lupski JR, Clark R, Katsanis N. 2014. Recurrent CNVs and SNVs at the NPHP1 locus contribute pathogenic alleles to Bardet-Biedl syndrome. Am. J. Hum. Genet. 94: 745–754.

Lipska BS, Ranchin B, Iatropoulos P, Gellermann J, Melk A, Ozaltin F, Caridi G, Seeman T, Tory K, Jankauskiene A, Zurowska A, Szczepanska M, Wasilewska A, Harambat J, Trautmann A, Peco-Antic A, Borzecka H, Moczulska A, Saeed B, Bogdanovic R, Kalyoncu M, Simkova E, Erdogan O, Vrljicak K, Teixeira A, Azocar M, Schaefer F, Azocar M, Higuita LMS, Ranchin B, Fischbach M, Davitaia T, Gellermann J, Oh J, Melk A, Schaefer F, Wigger M, Printza N, Sallay P, Gheissari A, Noris M, Pasini A, Marco Ghiggeri G, Ardissino G, Benetti E, Emma F, Aoun B, Abou-Jaoudé P, Jankauskiene A, Wasilewska A, Gacka E, Zurowska A, Drozdz D, Tkaczyk M, Borzecka H, Silska M, Jarmolinski T, Firszt-Adamczyk A, Ksiazek J, Kuzma-Mroczkowska E, Medynska A, Szczepanska

when the signal is lost_marijn_8072018.indd 227 08/07/2018 10:50

M, Caldas Afonso A, Jardim H, Bogdanovic R, Krmar RT, Simonetti GD, Saeed B, Anarat A, Balat A, Baskin ZE, Cakar N, Erdogan O, Özcakar B, Ozaltin F, Sakallioglu O, Soylemezoglu O, Akman S, Gok F, Caliskan S, Candan C, Emre S, Mir S, Akil I, Ertan P, Özkaya O, Kalyoncu M, Simkova E, Alhammadi E, Sobko R. 2014. Genotype–phenotype associations in WT1 glomerulopathy. Kidney Int. 85: 1169–1178.

Littink KW, Pott JWR, Collin RWJ, Kroes HY, Verheij JBGM, Blokland EAW, Miró M de C, Hoyng CB, Klaver CCW, Koenekoop RK, Rohrschneider K, Cremers FPM, Ingeborgh van den Born L, den Hollander AI. 2010. A novel nonsense mutation in CEP290 induces exon skipping and leads to a relatively mild retinal phenotype. Investig. Ophthalmol. Vis. Sci. 51: 3646–3652.

Liu B, Chen S, Johnson C, Helms JA. 2014. A ciliopathy with hydrocephalus, isolated craniosynostosis, hypertelorism, and clefting caused by deletion of Kif3a. Reprod. Toxicol. 48: 88–97.

Logan C V., Abdel-Hamed Z, Johnson CA. 2011. Molecular genetics and pathogenic mechanisms for the severe ciliopathies: Insights into neurodevelopment and pathogenesis of neural tube defects. Mol. Neurobiol. 43: 12–26.

Lohmann K, Klein C. 2014. Next Generation Sequencing and the Future of Genetic Diagnosis. Neurotherapeutics 11: 699–707.

Lopez E, Thauvin-Robinet C, Reversade B, El Khartoufi N, Devisme L, Holder M, Ansart-Franquet H, Avila M, Lacombe D, Kleinfinger P, Kaori I, Takanashi JI, Le Merrer M, Martinovic J, Noël C, Shboul M, Ho L, Güven Y, Razavi F, Burglen L, Gigot N, Darmency-Stamboul V, Thevenon J, Aral B, Kayserili H, Huet F, Lyonnet S, Le Caignec C, Franco B, Rivière JB, Faivre L, Attié-Bitach T. 2014. C5orf42 is the major gene responsible for OFD syndrome type VI. Hum. Genet. 133: 367–377.

Louie CM, Caridi G, Lopes VS, Brancati F, Kispert A, Lancaster MA, Schlossman AM, Otto EA, Leitges M, Grone HJ, Lopez I, Gudiseva H V, O'Toole JF, Vallespin E, Ayyagari R, Ayuso C, Cremers FP, den Hollander AI, Koenekoop RK, Dallapiccola B, Ghiggeri GM, Hildebrandt F, Valente EM, Williams DS, Gleeson JG. 2010. AHI1 is required for photoreceptor outer segment development and is a modifier for retinal degeneration in nephronophthisis. Nat. Genet. 42: 175–180.

Macca M, Franco B. 2009. The molecular basis of oral-facial-digital syndrome, type 1. Am. J. Med. Genet. Part C Semin. Med. Genet. 151: 318–325.

Macia MS, Halbritter J, Delous M, Bredrup C, Gutter A, Filhol E, Mellgren AEC, Leh S, Bizet A, Braun DA, Gee HY, Silbermann F, Henry C, Krug P, Bole-Feysot C, Nitschké P, Joly D, Nicoud P, Paget A, Haugland H, Brackmann D, Ahmet N, Sandford R, Cengiz N, Knappskog PM, Boman H, Linghu B, Yang F, Oakeley EJ, Saint Mézard P, Sailer AW, Johansson S, Rødahl E, Saunier S, Hildebrandt F, Benmerah A. 2017. Mutations in MAPKBP1 Cause Juvenile or Late-Onset Cilia-Independent Nephronophthisis. Am. J. Hum. Genet. 100: 372.

Maguire AM, Simonelli F, Pierce EA, Pugh EN, Mingozzi F, Bennicelli J, Banfi S, Marshall KA, Testa F, Surace EM, Rossi S, Lyubarsky A, Arruda VR, Konkle B, Stone E, Sun J, Jacobs J, Dell'Osso L, Hertle R, Ma J, Redmond TM, Zhu

when the signal is lost_marijn_8072018.indd 228 08/07/2018 10:51

X, Hauck B, Zelenaia O, Shindler KS, Maguire MG, Wright JF, Volpe NJ, McDonnell JW, Auricchio A, High KA, Bennett J. 2008. Safety and Efficacy of Gene Transfer for Leber's Congenital Amaurosis. N. Engl. J. Med. 358: 2240–2248.

Mahjoub MR. 2005. NIMA-Related Kinases Defective in Murine Models of Polycystic Kidney Diseases Localize to Primary Cilia and Centrosomes. J. Am. Soc. Nephrol. 16: 3485–3489.

Malone AF, Phelan PJ, Hall G, Cetincelik U, Homstad A, Alonso AS, Jiang R, Lindsey TB, Wu G, Sparks MA, Smith SR, Webb NJA, Kalra PA, Adeyemo AA, Shaw AS, Conlon PJ, Jennette JC, Howell DN, Winn MP, Gbadegesin RA. 2014. Rare hereditary COL4A3/COL4A4 variants may be mistaken for familial focal segmental glomerulosclerosis. Kidney Int. 86: 1253–1259.

Marsaud A, Dadone B, Ambrosetti D, Baudoin C, Chamorey E, Rouleau E, Lefol C, Roussel J, Fabas T, Cristofari G, Carpentier X, Michiels J, Amiel J, Pedeutour F. 2015. Dismantling Papillary Renal Cell Carcinoma Classification: The Heterogeneity of Genetic Profiles Suggests Several Independent Diseases. Genes. Chromosomes Cancer 54: 369–382.

Marszalek JR, Ruiz-Lozano P, Roberts E, Chien KR, Goldstein LSB. 1999. Situs inversus and embryonic ciliary morphogenesis defects in mouse mutants lacking the KIF3A subunit of kinesin-II. Proc. Natl. Acad. Sci. U. S. A. 96: 5043–5048.

Mathivanan S, Ji H, Simpson RJ. 2010. Exosomes: Extracellular organelles important in intercellular communication. J. Proteomics 73: 1907–1920.

Matsui K, Kamijo-Ikemori A, Imai N, Sugaya T, Yasuda T, Tatsunami S, Toyama T, Shimizu M, Furuichi K, Wada T, Shibagaki Y, Kimura K. 2016. Clinical significance of urinary liver-type fatty acid-binding protein as a predictor of ESRD and CVD in patients with CKD. Clin. Exp. Nephrol. 20: 195–203.

Matyas G, Naef P, Tollens M, Oexle K. 2014. De novo mutation of the latency-associated peptide domain of TGFB3 in a patient with overgrowth and Loeys-Dietz syndrome features. Am. J. Med. Genet. Part A 164: 2141–2143.

McCarthy HJ, Bierzynska A, Wherlock M, Ognjanovic M, Kerecuk L, Hegde S, Feather S, Gilbert RD, Krischock L, Jones C, Sinha MD, Webb NJ a, Christian M, Williams MM, Marks S, Koziell A, Welsh GI, Saleem M a. 2013. Simultaneous sequencing of 24 genes associated with steroid-resistant nephrotic syndrome. Clin. J. Am. Soc. Nephrol. 8: 637–648.

McGregor L, Makela V, Darling SM, Vrontou S, Chalepakis G, Roberts C, Smart N, Rutland P, Prescott N, Hopkins J, Bentley E, Shaw A, Roberts E, Mueller R, Jadeja S, Philip N, Nelson J, Francannet C, Perez-Aytes A, Megarbane A, Kerr B, Wainwright B, Woolf AS, Winter RM, Scambler PJ. 2003. Fraser syndrome and mouse blebbed phenotype caused by mutations in FRAS1/Fras1 encoding a putative extracellular matrix protein. Nat. Genet. 34: 203–208.

McKee RA, Wingert RA. 2016. Repopulating decellularized kidney scaffolds: An avenue for ex vivo organ generation. Materials (Basel). 9.

McKenna A, Hanna M, Banks E. 2010. The Genome Analysis Toolkit: A MapReduce framework for analyzing next-generation DNA sequencing data. Genome

when the signal is lost_marijn_8072018.indd 229 08/07/2018 10:51

Res.: 1297–1303.
Mehta ZB, Pietka G, Lowe M. 2014. The cellular and physiological functions of the lowe syndrome protein OCRL1. Traffic 15: 471–487.
Meienberg J, Bruggmann R, Oexle K, Matyas G. 2016. Clinical sequencing: is WGS the better WES? Hum. Genet. 135: 359–362.
Meirelles GV, Perez AM, de Souza EE, Basei FL, Papa PF, Melo Hanchuk TD, Cardoso VB, Kobarg J. 2014. "Stop Ne(c)king around": How interactomics contributes to functionally characterize Nek family kinases. World J. Biol. Chem. 5: 141–160.
Mele C, Lemaire M, Iatropoulos P, Piras R, Bresin E, Bettoni S, Bick D, Helbling D, Veith R, Valoti E, Donadelli R, Murer L, Neunhäuserer M, Breno M, Frémeaux-Bacchi V, Lifton R, Remuzzi G, Noris M. 2015. Characterization of a New DGKE Intronic Mutation in Genetically Unsolved Cases of Familial Atypical Hemolytic Uremic Syndrome. Clin. J. Am. Soc. Nephrol. 10: 1011–9.
Merta M, Reiterová J, Tesař V, Štekrová J, Viklický O. 2002. Influence of the endothelial nitric oxide synthase polymorphism on the progression of autosomal dominant polycystic kidney disease and IgA nephropathy. Ren. Fail. 24: 585–593.
Mi H, Huang X, Muruganujan A, Tang H, Mills C, Kang D, Thomas PD. 2016. Panther version 11: expanded annotation data from Gene Ontology and Reactome pathways, and data analysis tool enhancements. Nucleic Acids Res. 45: 1–15.
Mick DU, Rodrigues RB, Leib RD, Adams CM, Chien AS, Gygi SP, Nachury M V. 2015. Proteomics of Primary Cilia by Proximity Labeling. Dev. Cell 35: 497–512.
Mimura I, Kanki Y, Kodama T, Nangaku M. 2014. Revolution of nephrology research by deep sequencing: ChIP-seq and RNA-seq. Kidney Int. 85: 31–8.
Miner JH. 2014. Pathology versus molecular genetics: (re)defining the spectrum of Alport syndrome. Kidney Int. 86: 1084–1086.
Mischak H, Delles C, Vlahou A, Vanholder R. 2015. Proteomic biomarkers in kidney disease: issues in development and implementation. Nat. Rev. Nephrol. 11: 221–232.
Miyamoto T, Porazinski S, Wang H, Borovina A, Ciruna B, Shimizu A, Kajii T, Kikuchi A, Furutani-Seiki M, Matsuura S. 2011. Insufficiency of BUBR1, a mitotic spindle checkpoint regulator, causes impaired ciliogenesis in vertebrates. Hum. Mol. Genet. 20: 2058–2070.
Moawia A, Shaheen R, Rasool S, Waseem SS, Ewida N, Budde B, Kawalia A, Motameny S, Khan K, Fatima A, Jameel M, Ullah F, Akram T, Ali Z, Abdullah U, Irshad S, Höhne W, Noegel AA, Al-Owain M, Hörtnagel K, Stöbe P, Baig SM, Nürnberg P, Alkuraya FS, Hahn A, Hussain MS. 2017. Mutations of KIF14 cause primary microcephaly by impairing cytokinesis. Ann. Neurol. 82: 562–577.
Mochizuki T, Lemmink HH, Mariyama M, Antignac C, Gubler M-C, Pirson Y, Verellen-Dumoulin C, Chan B, Schröder CH, Smeets HJ, Reeders ST. 1994. Identification of mutations in the α3(IV) and α4(IV) collagen genes in autosomal recessive Alport syndrome. Nat. Genet. 8: 77–82.
Monroe GR, Frederix GW, Savelberg SMC, de Vries TI, Duran KJ, van der Smagt JJ,

when the signal is lost_marijn_8072018.indd 230 08/07/2018 10:51

Terhal PA, van Hasselt PM, Kroes HY, Verhoeven-Duif NM, Nijman IJ, Carbo EC, van Gassen KL, Knoers N V., Hövels AM, van Haelst MM, Visser G, van Haaften G. 2016. Effectiveness of whole-exome sequencing and costs of the traditional diagnostic trajectory in children with intellectual disability. Genet. Med. 18: 949–956.

Morinière V, Dahan K, Hilbert P, Lison M, Lebbah S, Topa A, Bole-Feysot C, Pruvost S, Nitschke P, Plaisier E, Knebelmann B, Macher M-A, Noel L-H, Gubler M-C, Antignac C, Heidet L. 2014. Improving Mutation Screening in Familial Hematuric Nephropathies through Next Generation Sequencing. J. Am. Soc. Nephrol.: 1–12.

Mykytyn K, Nishimura DY, Searby CC, Shastri M, Yen H, Beck JS, Braun T, Streb LM, Cornier AS, Cox GF, Fulton AB, Carmi R, Lüleci G, Chandrasekharappa SC, Collins FS, Jacobson SG, Heckenlively JR, Weleber RG, Stone EM, Sheffield VC. 2002. Identification of the gene (BBS1) most commonly involved in Bardet-Biedl syndrome, a complex human obesity syndrome. Nat. Genet. 31: 435–438.

Nafar M, Kalantari S, Samavat S, Rezaei-tavirani M, Rutishuser D, Zubarev R . 2014. The Novel Diagnostic Biomarkers for Focal Segmental Glomerulosclerosis. Int. J. Nephrol. 574261: 1–10.

Nager AR, Goldstein JS, Herranz-Pérez V, Portran D, Ye F, Garcia-Verdugo JM, Nachury M V. 2017. An Actin Network Dispatches Ciliary GPCRs into Extracellular Vesicles to Modulate Signaling. Cell: 252–263.

Nassirpour R, Mathur S, Gosink MM, Li Y, Shoieb AM, Wood J, O'Neil SP, Homer BL, Whiteley LO. 2014. Identification of tubular injury microRNA biomarkers in urine: comparison of next-generation sequencing and qPCR-based profiling platforms. BMC Genomics 15: 485.

Need AC, Shashi V, Hitomi Y, Schoch K, Shianna K V, McDonald MT, Meisler MH, Goldstein DB. 2012. Clinical application of exome sequencing in undiagnosed genetic conditions. J. Med. Genet. 49: 353–361.

NHLBI GO Exome Sequencing Project (ESP). 2014. Exome Variant Server. Seattle, WA.

Niaudet P. 2013. Clinical manifestations, diagnosis, and treatment of nephronophthisis. UpToDate: 1–7.

Nicolaou N, Pulit SL, Nijman IJ, Monroe GR, Feitz WFJ, Schreuder MF, Eerde AM Van, Jong TPVM De, Giltay JC, Zwaag B Van Der, Havenith MR, Zwakenberg S, Zanden LFM Van Der, Poelmans G, Cornelissen EAM, Lilien MR, Franke B, Roeleveld N, Rooij IALM Van, Cuppen E, Bongers EMHF, Giles RH, Knoers NVAM, Renkema KY. 2015a. Prioritization and burden analysis of rare variants in 208 candidate genes suggest they do not play a major role in CAKUT. Kidney Int. 89: 476-486.

Nicolaou N, Renkema KY, Bongers EMHF, Giles RH, Knoers NV a. M. 2015b. Genetic, environmental, and epigenetic factors involved in CAKUT. Nat. Rev. Nephrol. 11: 720–731.

Nielsen SM, Rhodes L, Blanco I, Chung WK, Eng C, Maher ER, Richard S, Giles RH. 2016. Von Hippel-Lindau Disease: Genetics and Role of Genetic Counseling

when the signal is lost_marijn_8072018.indd 231 08/07/2018 10:51

in a Multiple Neoplasia Syndrome. J. Clin. Oncol. 34: 2172-2181.
Nishiguchi KM, Tearle RG, Liu YP, Oh EC, Miyake N, Benaglio P, Harper S, Koskiniemi-Kuendig H, Venturini G, Sharon D, Koenekoop RK, Nakamura M, Kondo M, Ueno S, Yasuma TR, Beckmann JS, Ikegawa S, Matsumoto N, Terasaki H, Berson EL, Katsanis N, Rivolta C. 2013. Whole genome sequencing in patients with retinitis pigmentosa reveals pathogenic DNA structural changes and NEK2 as a new disease gene. Proc. Natl. Acad. Sci. U. S. A. 110: 16139–16144.
Nishimoto K, Iijima K, Shirakawa T, Kitagawa K, Satomura K, Nakamura H, Yoshikawa N. 2001. PAX2 gene mutation in a family with isolated renal hypoplasia. J. Am. Soc. Nephrol. 12: 1769–1772.
Nogueira M, Cartwright JJ, Horn K, Doe N, Shappell S, Barrios R, Coroneos E, Truong L. 2000. Thin basement membrane disease with heavy proteinuria or nephrotic syndrome at presentation. Am. J. Kidney Dis. 35: E15.
Noris M, Bresin E, Mele C, Remuzzi G. 2013. Atypical Hemolytic-Uremic Syndrome. GeneReviews.
Noris M, Caprioli J, Bresin E, Mossali C, Pianetti G, Gamba S, Daina E, Fenili C, Castelletti F, Sorosina A, Piras R, Donadelli R, Maranta R, van der Meer I, Conway EM, Zipfel PF, Goodship TH, Remuzzi G. 2010. Relative Role of Genetic Complement Abnormalities in Sporadic and Familial aHUS and Their Impact on Clinical Phenotype. Clin. J. Am. Soc. Nephrol. 5: 1844–1859.
Noris M, Mele C, Remuzzi G. 2015. Podocyte dysfunction in atypical haemolytic uraemic syndrome. Nat. Rev. Nephrol. 11: 245–252.
Novarino G, Akizu N, Gleeson JG. 2011. Modeling human disease in humans: The ciliopathies. Cell 147: 70–79.
Oehl-Jaschkowitz B, Vanakker OM, De Paepe A, Menten B, Martin T, Weber G, Christmann A, Krier R, Scheid S, Mcnerlan SE, Mckee S, Tzschach A. 2014. Deletions in 14q24.1q24.3 are associated with congenital heart defects, brachydactyly, and mild intellectual disability. Am. J. Med. Genet. Part A 164: 620–626.
Offermanns S. 2006. Activation of Platelet Function Through G Protein – Coupled Receptors. Circ. Res. 99: 1293–1304.
Okamoto T, Tajima T, Hirayama T, Sasaki S. 2012. A patient with Dent disease and features of Bartter syndrome caused by a novel mutation of CLCN5. Eur. J. Pediatr. 171: 401–404.
Olbrich H, Fliegauf M, Hoefele J, Kispert A, Otto E, Volz A, Wolf MT, Sasmaz G, Trauer U, Reinhardt R, Sudbrak R, Antignac C, Gretz N, Walz G, Schermer B, Benzing T, Hildebrandt F, Omran H. 2003. Mutations in a novel gene, NPHP3, cause adolescent nephronophthisis, tapeto-retinal degeneration and hepatic fibrosis. Nat. Genet. 34: 455–459.
Omran H. 2010. NPHP proteins: gatekeepers of the ciliary compartment. J. Cell Biol. 190: 715–717.
Omran H, Fernandez C, Jung M, Haffner K, Fargier B, Villaquiran A, Waldherr R, Gretz N, Brandis M, Ruschendorf F, Reis A, Hildebrandt F. 2000. Identification of a new gene locus for adolescent nephronophthisis, on chromosome

when the signal is lost_marijn_8072018.indd 232 08/07/2018 10:51

3q22 in a large Venezuelan pedigree. Am. J. Hum. Genet. 66: 118–127.

Otto EA, Hurd TW, Airik R, Chaki M, Zhou W, Stoetzel C, Patil SB, Levy S, Ghosh AK, Murga-Zamalloa CA, van Reeuwijk J, Letteboer SJ, Sang L, Giles RH, Liu Q, Coene KL, Estrada-Cuzcano A, Collin RW, McLaughlin HM, Held S, Kasanuki JM, Ramaswami G, Conte J, Lopez I, Washburn J, Macdonald J, Hu J, Yamashita Y, Maher ER, Guay-Woodford LM, Neumann HP, Obermuller N, Koenekoop RK, Bergmann C, Bei X, Lewis RA, Katsanis N, Lopes V, Williams DS, Lyons RH, Dang C V, Brito DA, Dias MB, Zhang X, Cavalcoli JD, Nurnberg G, Nurnberg P, Pierce EA, Jackson PK, Antignac C, Saunier S, Roepman R, Dollfus H, Khanna H, Hildebrandt F. 2010. Candidate exome capture identifies mutation of SDCCAG8 as the cause of a retinal-renal ciliopathy. Nat. Genet. 42: 840–850.

Otto EA, Ramaswami G, Janssen S, Chaki M, Allen SJ, Zhou W, Airik R, Hurd TW, Ghosh AK, Wolf MT, Hoppe B, Neuhaus TJ, Bockenhauer D, Milford D V., Soliman NA, Antignac C, Saunier S, Johnson CA, Hildebrandt F. 2011. Mutation analysis of 18 nephronophthisis associated ciliopathy disease genes using a DNA pooling and next generation sequencing strategy. J. Med. Genet. 48: 105–116.

Otto EA, Schermer B, Obara T, O'Toole JF, Hiller KS, Mueller AM, Ruf RG, Hoefele J, Beekmann F, Landau D, Foreman JW, Goodship JA, Strachan T, Kispert A, Wolf MT, Gagnadoux MF, Nivet H, Antignac C, Walz G, Drummond IA, Benzing T, Hildebrandt F. 2003. Mutations in INVS encoding inversin cause nephronophthisis type 2, linking renal cystic disease to the function of primary cilia and left-right axis determination. Nat. Genet. 34: 413–420.

Oud MM, van Bon BW, Bongers EMHF, Hoischen A, Marcelis CL, de Leeuw N, Mol SJJ, Mortier G, Knoers NVAM, Brunner HG, Roepman R, Arts HH. 2014. Early presentation of cystic kidneys in a family with a homozygous INVS mutation. Am. J. Med. Genet. Part A 164: 1627–1634.

Øvrehus MA, Zürbig P, Vikse BE, Hallan SI. 2015. Urinary proteomics in chronic kidney disease: diagnosis and risk of progression beyond albuminuria. Clin. Proteomics 12: 21.

Ozaltin F, Li B, Rauhauser A, An S-W, Soylemezoglu O, Gonul II, Taskiran EZ, Ibsirlioglu T, Korkmaz E, Bilginer Y, Duzova A, Ozen S, Topaloglu R, Besbas N, Ashraf S, Du Y, Liang C, Chen P, Lu D, Vadnagara K, Arbuckle S, Lewis D, Wakeland B, Quigg RJ, Ransom RF, Wakeland EK, Topham MK, Bazan NG, Mohan C, Hildebrandt F, Bakkaloglu A, Huang C-L, Attanasio M. 2013. DGKE Variants Cause a Glomerular Microangiopathy That Mimics Membranoproliferative GN. J. Am. Soc. Nephrol. 24: 377–384.

Paquet D, Kwart D, Chen A, Sproul A, Jacob S, Teo S, Olsen KM, Gregg A, Noggle S, Tessier-Lavigne M. 2016. Efficient introduction of specific homozygous and heterozygous mutations using CRISPR/Cas9. Nature 533: 125–129.

Parisi M, Glass I. 2017. Joubert syndome. GeneReviews® [Internet]. Seattle Univ. Washington, Seattle; 1993-2017.: 1–51.

Patel ML, Sachan R, Misra R, Kamal R, Shyam R, Sachan P. 2015. Prognostic significance of urinary NGAL in chronic kidney disease. Int. J. Nephrol.

when the signal is lost_marijn_8072018.indd 233 08/07/2018 10:51

Renovasc. Dis. 8: 139–144.
Patil M, Pabla N, Huang S, Dong Z. 2013. Nek1 phosphorylates von Hippel-Lindau tumor suppressor to promote its proteasomal degradation and ciliary destabilization. Cell Cycle 12: 166–171.
Perrault I, Halbritter J, Porath JD, Gérard X, Braun DA, Gee HY, Fathy HM, Saunier S, Cormier-Daire V, Thomas S, Attié-Bitach T, Boddaert N, Taschner M, Schueler M, Lorentzen E, Lifton RP, Lawson JA, Garfa-Traore M, Otto EA, Bastin P, Caillaud C, Kaplan J, Rozet J-M, Hildebrandt F. 2015. IFT81 , encoding an IFT-B core protein, as a very rare cause of a ciliopathy phenotype. J. Med. Genet. 52: 657–665.
Perrault I, Saunier S, Hanein S, Filhol E, Bizet AA, Collins F, Salih MAM, Gerber S, Delphin N, Bigot K, Orssaud C, Silva E, Baudouin V, Oud MHM, Shannon N, Le Merrer M, Roche O, Pietrement C, Goumid J, Baumann C, Bole-Feysot C, Nitschke P, Zahrate M, Beales P, Arts HH, Munnich A, Kaplan J, Antignac C, Cormier-Daire V, Rozet JM. 2012. Mainzer-saldino syndrome is a ciliopathy caused by IFT140 mutations. Am. J. Hum. Genet. 90: 864–870.
Perrichot R, Mercier B, Simon P, Whebe B, Cledes J, Ferec C. 1999. DGGE screening of PKD1 gene reveals novel mutations in a large cohort of 146 unrelated patients. Hum. Genet. 105: 231–239.
Pham T V., Jimenez CR. 2012. An accurate paired sample test for count data. Bioinformatics 28: 596–602.
Pham T V., Piersma SR, Warmoes M, Jimenez CR. 2009. On the beta-binomial model for analysis of spectral count data in label-free tandem mass spectrometry-based proteomics. Bioinformatics 26: 363–369.
Pham T V, Piersma SR, Oudgenoeg G, Jimenez CR. 2012. Label-free mass spectrometry-based proteomics for biomarker discovery and validation. Expert Rev. Mol. Diagn. 12: 343–359.
Philippakis AA, Azzariti DR, Beltran S, Brookes AJ, Brownstein CA, Brudno M, Brunner HG, Orion J, Carey K, Doll C, Dumitriu S, Dyke SOM, Dunnen JT Den, Firth H V, Gibbs RA, Girdea M, Haendel MA, Hamosh A, Holm IA, Huang L, Hurles ME, Hutton B, Misyura A, Christopher J, Paschall J, Paten B, Robinson PN, Sobreira NL, Swaminathan GJ, Taschner PE, Terry SF, Washington NL, Boycott KM, Rehm HL, Hospital W, Medicine PP, Hospital W, Program GB, Medicine C, Division G, Berkeley L, Alliance G, Genesis T, Epidemiology C, Health O, Cruz S, Children B. 2015. The Matchmaker Exchange: A Platform for Rare Disease Gene Discovery. Hum. Mutat. 36: 915–921.
Pierides A, Voskarides K, Athanasiou Y, Ioannou K, Damianou L, Arsali M, Zavros M, Pierides M, Vargemezis V, Patsias C, Zouvani I, Elia A, Kyriacou K, Deltas C. 2009. Clinico-pathological correlations in 127 patients in 11 large pedigrees, segregating one of three heterozygous mutations in the COL4A3/ COL4A4 genes associated with familial haematuria and significant late progression to proteinuria and chronic kidney dis. Nephrol. Dial. Transplant 24: 2721–2729.
Piersma SR, Fiedler U, Span S, Lingnau A, Pham T V., Hoffmann S, Kubbutat MHG, Jiménez CR. 2010. Workflow comparison for label-free, quantitative

when the signal is lost_marijn_8072018.indd 234 08/07/2018 10:51

secretome proteomics for cancer biomarker discovery: Method evaluation, differential analysis, and verification in serum. J. Proteome Res. 9: 1913–1922.

Piersma SR, Warmoes MO, de Wit M, de Reus I, Knol JC, Jiménez CR. 2013. Whole gel processing procedure for GeLC-MS/MS based proteomics. Proteome Sci. 11: 17.

Polci R, Peng A, Chen P-L, Riley DJ, Chen Y. 2004. NIMA-related protein kinase 1 is involved early in the ionizing radiation-induced DNA damage response. Cancer Res. 64: 8800–8803.

Pomatto MAC, Gai C, Bussolati B, Camussi G. 2017. Extracellular Vesicles in Renal Pathophysiology. Front. Mol. Biosci. 4: 37.

Powles-Glover N. 2014. Cilia and ciliopathies: Classic examples linking phenotype and genotype-An overview. Reprod. Toxicol. 48: 98–105.

Prakash S, Gharavi AG. 2015. Diagnosing kidney disease in the genetic era. Curr. Opin. Nephrol. Hypertens. 24: 380–387.

Raposo G, Nijman HW, Stoorvogel W, Leijendekker R, Harding C V, Melief CJ, Geuze HJ. 1996. B Lymphocytes Secrete Antigen-presenting Vesicles. J. Exp. Med. 183: 1161–1172.

Van Reeuwijk J, Arts HH, Roepman R. 2011. Scrutinizing ciliopathies by unraveling ciliary interaction networks. Hum. Mol. Genet. 20: 149–157.

Renkema KY, Stokman MF, Giles RH, Knoers NVAM. 2014. Next-generation sequencing for research and diagnostics in kidney disease. Nat. Rev. Nephrol. 10: 433–444.

Renner B, Klawitter J, Goldberg R, Mccullough JW, Ferreira VP, Cooper JE, Christians U, Thurman JM. 2013. Cyclosporine Induces Endothelial Cell Release of complement-activating microparticles. J Am Soc Nephrol 24: 1849–1862.

Romani M, Micalizzi A, Kraoua I, Dotti MT, Cavallin M, Sztriha L, Ruta R, Mancini F, Mazza T, Castellana S, Hanene B, Carluccio MA, Darra F, Máté A, Zimmermann A, Gouider-Khouja N, Valente EM. 2014. Mutations in B9D1 and MKS1 cause mild Joubert syndrome: expanding the genetic overlap with the lethal ciliopathy Meckel syndrome. Orphanet J. Rare Dis. 9: 72.

Romio L. 2004. OFD1 Is a Centrosomal/Basal Body Protein Expressed during Mesenchymal-Epithelial Transition in Human Nephrogenesis. J. Am. Soc. Nephrol. 15: 2556–2568.

Roversi G, Picinelli C, Bestetti I, Crippa M, Perotti D, Ciceri S, Saccheri F, Collini P, Poliani PL, Catania S, Peissel B, Pagni F, Russo S, Peterlongo P, Manoukian S, Finelli P. 2015. Constitutional de novo deletion of the FBXW7 gene in a patient with focal segmental glomerulosclerosis and multiple primitive tumors. Sci. Rep. 5: 15454.

Royer-Pokora B, Beier M, Henzler M, Alam R, Weirich A, Huff V. 2004. Twenty-Four New Cases of WT1 Germline Mutations and Review of the Literature : Genotype / Phenotype Correlations for Wilms Tumor Development. Am. J. Med. Genet. 257: 249–257.

Rudnicki M, Perco P, Neuwirt H, Noppert S-J, Leierer J, Sunzenauer J, Eder S, Zoja

when the signal is lost_marijn_8072018.indd 235 08/07/2018 10:51

C, Eller K, Rosenkranz AR, Müller GA, Mayer B, Mayer G. 2012. Increased Renal Versican Expression Is Associated with Progression of Chronic Kidney Disease. PLoS One 7: e44891.

Saburi S, Hester I, Fischer E, Pontoglio M, Eremina V, Gessler M, Quaggin SE, Harrison R, Mount R, McNeill H. 2008. Loss of Fat4 disrupts PCP signaling and oriented cell division and leads to cystic kidney disease. Nat. Genet. 40: 1010–1015.

Sadowski CE, Lovric S, Ashraf S, Pabst WL, Gee HY, Kohl S, Engelmann S, Vega-Warner V, Fang H, Halbritter J, Somers MJ, Tan W, Shril S, Fessi I, Lifton RP, Bockenhauer D, El-Desoky S, Kari J a, Zenker M, Kemper MJ, Mueller D, Fathy HM, Soliman N a, Hildebrandt F. 2014. A Single-Gene Cause in 29.5% of Cases of Steroid-Resistant Nephrotic Syndrome. J. Am. Soc. Nephrol.: 1–11.

Saisawat P, Kohl S, Hilger AC, Hwang D, Gee HY, Dworschak GC, Tasic V, Pennimpede T, Natarajan S, Sperry E, Bogdanovic R, Blaauw I De, Marcelis CLM, Matassa DS, Wijers CHW, Bartels E, Schmiedeke E, Schmidt D, Grasshoff-derr S, Holland-cunz S, Ludwig M, Ma S, Herrmann BG, Solomon BD, Klein A De, Rooij IALM Van. 2014. Whole-exome resequencing reveals recessive mutations in TRAP1 in individuals with CAKUT and VACTERL association. Kidney Int.: 1310–1317.

Saisawat P, Tasic V, Vega-Warner V, Kehinde EO, Günther B, Airik R, Innis JW, Hoskins BE, Hoefele J, Otto E a, Hildebrandt F. 2012. Identification of two novel CAKUT-causing genes by massively parallel exon resequencing of candidate genes in patients with unilateral renal agenesis. Kidney Int. 81: 196–200.

Salomon R, Saunier S, Niaudet P. 2009. Nephronophthisis. Pediatr. Nephrol. 24: 2333–44.

Sampson MG, Gillies CE, Robertson CC, Crawford B, Vega-warner V, Otto EA, Kretzler M. 2015. Using Population Genetics to Interrogate the Monogenic Nephrotic Syndrome Diagnosis in a Case Cohort. J. Am. Soc. Nephrol. 27: 1–14.

Sánchez Chinchilla D, Pinto S, Hoppe B, Adragna M, Lopez L, Justa Roldan ML, Peña A, Lopez Trascasa M, Sánchez-Corral P, Rodríguez de Córdoba S. 2014. Complement mutations in diacylglycerol kinase-ε-associated atypical hemolytic uremic syndrome. Clin. J. Am. Soc. Nephrol. 9: 1611–9.

Sang L, Miller JJ, Corbit KC, Giles RH, Brauer MJ, Otto EA, Baye LM, Wen X, Scales SJ, Kwong M, Huntzicker EG, Sfakianos MK, Sandoval W, Bazan JF, Kulkarni P, Garcia-Gonzalo FR, Seol AD, O'Toole JF, Held S, Reutter HM, Lane WS, Rafiq MA, Noor A, Ansar M, Devi AR, Sheffield VC, Slusarski DC, Vincent JB, Doherty DA, Hildebrandt F, Reiter JF, Jackson PK. 2011. Mapping the NPHP-JBTS-MKS protein network reveals ciliopathy disease genes and pathways. Cell 145: 513–528.

Sanyanusin P, Schimmenti LA, McNoe LA, Ward TA, Pierpont MEM, Sullivan MJ, Dobyns WB, Eccles MR. 1995. Mutation of the PAX2 gene in a family with optic nerve colobomas, renal anomalies and vesicoureteral reflux. Nat. Genet. 9: 358–364.

when the signal is lost_marijn_8072018.indd 236 08/07/2018 10:51

Satir P, Pedersen LB, Christensen ST. 2010. The primary cilium at a glance. J. Cell Sci. 123: 499–503.

Saunier S, Calado J, Heilig R, Silbermann F, Benessy F, Morin G, Konrad M, Broyer M, Gubler MC, Weissenbach J, Antignac C. 1997. A novel gene that encodes a protein with a putative src homology 3 domain is a candidate gene for familial juvenile nephronophthisis. Hum. Mol. Genet. 6: 2317–2323.

Savige J, Rana K, Tonna S, Buzza M, Dagher H, Wang Y. 2003. Thin Basement Membrane Nephropathy. Kidney Int. 64: 1169–1178.

Sayer JA, Otto EA, O'Toole JF, Nurnberg G, Kennedy MA, Becker C, Hennies HC, Helou J, Attanasio M, Fausett B V, Utsch B, Khanna H, Liu Y, Drummond I, Kawakami I, Kusakabe T, Tsuda M, Ma L, Lee H, Larson RG, Allen SJ, Wilkinson CJ, Nigg EA, Shou C, Lillo C, Williams DS, Hoppe B, Kemper MJ, Neuhaus T, Parisi MA, Glass IA, Petry M, Kispert A, Gloy J, Ganner A, Walz G, Zhu X, Goldman D, Nurnberg P, Swaroop A, Leroux MR, Hildebrandt F. 2006. The centrosomal protein nephrocystin-6 is mutated in Joubert syndrome and activates transcription factor ATF4. Nat. Genet. 38: 674–681.

Schaefer E, Zaloszyc A, Lauer J, Durand M, Stutzmann F, Perdomo-Trujillo Y, Redin C, Bennouna Greene V, Toutain A, Perrin L, Gerard M, Caillard S, Bei X, Lewis RA, Christmann D, Letsch J, Kribs M, Mutter C, Muller J, Stoetzel C, Fischbach M, Marion V, Katsanis N, Dollfus H. 2011. Mutations in SDCCAG8/NPHP10 Cause Bardet-Biedl Syndrome and Are Associated with Penetrant Renal Disease and Absent Polydactyly. Mol. Syndromol. 1: 273–281.

Schanstra JP, Zürbig P, Alkhalaf A, Argiles A, Bakker SJL, Beige J, Bilo HJG, Chatzikyrkou C, Dakna M, Dawson J, Delles C, Haller H, Haubitz M, Husi H, Jankowski J, Jerums G, Kleefstra N, Kuznetsova T, Maahs DM, Menne J, Mullen W, Ortiz A, Persson F, Rossing P, Ruggenenti P, Rychlik I, Serra AL, Siwy J, Snell-Bergeon J, Spasovski G, Staessen JA, Vlahou A, Mischak H, Vanholder R. 2015. Diagnosis and Prediction of CKD Progression by Assessment of Urinary Peptides. J. Am. Soc. Nephrol. 26: 1999–2010.

Schmidts M, Frank V, Eisenberger T, Al Turki S, Bizet AA, Antony D, Rix S, Decker C, Bachmann N, Bald M, Vinke T, Toenshoff B, Di Donato N, Neuhann T, Hartley JL, Maher ER, Bogdanović R, Peco-Antić A, Mache C, Hurles ME, Joksić I, Guć-Šćekić M, Dobricic J, Brankovic-Magic M, UK10K, Bolz HJ, Pazour GJ, Beales PL, Scambler PJ, Saunier S, Mitchison HM, Bergmann C. 2013. Combined NGS Approaches Identify Mutations in the Intraflagellar Transport Gene IFT140in Skeletal Ciliopathies with Early Progressive Kidney Disease. Hum. Mutat. 34: 714–724.

Schueler M, Braun DA, Chandrasekar G, Gee HY, Klasson TD, Halbritter J, Bieder A, Porath JD, Airik R, Zhou W, Loturco JJ, Che A, Otto EA, Böckenhauer D, Sebire NJ, Honzik T, Harris PC, Koon SJ, Gunay-Aygun M, Saunier S, Zerres K, Bruechle NO, Drenth JPH, Pelletier L, Tapia-Páez I, Lifton RP, Giles RH, Kere J, Hildebrandt F. 2015. DCDC2 mutations cause a renal-hepatic ciliopathy by disrupting Wnt signaling. Am. J. Hum. Genet. 96: 81–92.

Schueler M, Halbritter J, Phelps IG, Braun DA, Otto EA, Porath JD, Gee HY, Shendure J, O'Roak BJ, Lawson JA, Nabhan MM, Soliman NA, Doherty D, Hildebrandt

when the signal is lost_marijn_8072018.indd 237 08/07/2018 10:51

F. 2016a. Large-scale targeted sequencing comparison highlights extreme genetic heterogeneity in nephronophthisis-related ciliopathies. J. Med. Genet. 53: 208–214.

Sethi SK, Otto EA, Ma S, Duggal R, Vega-Warner V, Kher V. 2015. A boy with proteinuria and focal global glomerulosclerosis: Answers. Pediatr. Nephrol. 30: 1945–1946.

Shalom O, Shalva N, Altschuler Y, Motro B. 2008. The mammalian Nek1 kinase is involved in primary cilium formation. FEBS Lett. 582: 1465–1470.

Shamseldin HE, Rajab A, Alhashem A, Shaheen R, Al-Shidi T, Alamro R, Al Harassi S, Alkuraya FS. 2013. Mutations in DDX59 implicate RNA helicase in the pathogenesis of orofaciodigital syndrome. Am. J. Hum. Genet. 93: 555–560.

Shannon P, Markiel A, Ozier O, Baliga NS, Wang JT, Ramage D, Amin N, Schwikowski B, Ideker T. 2003. Cytoscape: a software environment for integrated models of biomolecular interaction networks. Genome Res. 13: 2498–2504.

Shidham GB, Siddiqi N, Beres JA, Logan B, Nagaraja HN, Shidham SG, Piering WF. 2005. Clinical risk factors associated with bleeding after native kidney biopsy. Nephrology 10: 305–310.

Shim H, Kim JH, Kim CY, Hwang S, Kim H, Yang S, Lee JE, Lee I. 2016. Function-driven discovery of disease genes in zebrafish using an integrated genomics big data resource. Nucleic Acids Res. 44: 9611–9623.

Shrimpton AE, Hoopes RR, Knohl SJ, Hueber P, Reed AAC, Christie PT, Igarashi T, Lee P, Lehman A, White C, Milford D V., Sanchez MR, Unwin R, Wrong OM, Thakker R V., Scheinman SJ. 2009. OCRL1 mutations in dent 2 patients suggest a mechanism for phenotypic variability. Nephron - Physiol. 112: 27–36.

Silengo M, Bell G, Biagioli M, Franceschini P. 1987. Oro-facial-digital syndrome II. Transitional type between the Mohr and the Majewski syndromes: Report of two new cases. Clin. Genet.: 331–336.

Simms RJ, Hynes AM, Eley L, Sayer JA, Simms RJ, Hynes AM, Eley L, Sayer JA. 2011. Nephronophthisis: A Genetically Diverse Ciliopathy. Int. J. Nephrol. 2011: 1–10.

Simons M, Gloy J, Ganner A, Bullerkotte A, Bashkurov M, Kronig C, Schermer B, Benzing T, Cabello OA, Jenny A, Mlodzik M, Polok B, Driever W, Obara T, Walz G. 2005. Inversin, the gene product mutated in nephronophthisis type II, functions as a molecular switch between Wnt signaling pathways. Nat. Genet. 37: 537–543.

Slaats GG, Ghosh AK, Falke LL, Le Corre S, Shaltiel IA, van de Hoek G, Klasson TD, Stokman MF, Logister I, Verhaar MC, Goldschmeding R, Nguyen TQ, Drummond IA, Hildebrandt F, Giles RH. 2014. Nephronophthisis-Associated CEP164 Regulates Cell Cycle Progression, Apoptosis and Epithelial-to-Mesenchymal Transition. PLoS Genet. 10.

Slaats GG, Giles RH. 2015. Are renal ciliopathies (replication) stressed out? Trends Cell Biol. 25: 317–319.

Slaats GG, Isabella CR, Kroes HY, Dempsey JC, Gremmels H, Monroe GR, Phelps IG, Duran KJ, Adkins J, Kumar SA, Knutzen DM, Knoers N V, Mendelsohn

when the signal is lost_marijn_8072018.indd 238 08/07/2018 10:51

NJ, Neubauer D, Mastroyianni SD, Vogt J, Worgan L, Karp N, Bowdin S, Glass IA, Parisi MA, Otto EA, Johnson CA, Hildebrandt F, van Haaften G, Giles RH, Doherty D. 2016a. MKS1 regulates ciliary INPP5E levels in Joubert syndrome. J. Med. Genet. 53: 62-72.

Slaats GG, Lilien MR, Giles RH. 2016b. Nephronophthisis: should we target cysts or fibrosis? Pediatr. Nephrol. 31: 545–554.

Slaats GG, Saldivar JC, Bacal J, Zeman MK, Kile AC, Hynes AM, Srivastava S, Nazmutdinova J, Ouden K Den, Zagers MS, Foletto V, Verhaar MC, Miles C, Sayer J a, Cimprich K a, Giles RH. 2015. DNA replication stress underlies renal phenotypes in CEP290 -associated Joubert syndrome. J. Clin. Invest. 125: 1–10.

Sobreira N, Valle D, Hamosh A. 2015. GeneMatcher : A Matching Tool for Connecting Investigators with an Interest in the Same Gene. Hum. Mutat. 36: 928–930.

Soliman NA, Hildebrandt F, Otto EA, Nabhan MM, Allen SJ, Badr AM, Sheba M, Fadda S, Gawdat G, El-Kiky H. 2012. Clinical characterization and NPHP1 mutations in nephronophthisis and associated ciliopathies: a single center experience. Saudi J. kidney Dis. Transplant. 23: 1090–1098.

Srour M, Hamdan FF, Schwartzentruber JA, Patry L, Ospina LH, Shevell MI, Désilets V, Dobrzeniecka S, Mathonnet G, Lemyre E, Massicotte C, Labuda D, Amrom D, Andermann E, Sébire G, Maranda B, Consortium FC, Rouleau GA, Majewski J, Michaud JL. 2012. Mutations in TMEM231 cause Joubert syndrome in French Canadians. J. Med. Genet. 49: 636–641.

Stanescu DE, Hughes N, Kaplan B, Stanley C a., De León DD. 2012. Novel presentations of congenital hyperinsulinism due to mutations in the MODY genes: HNF1A and HNF4A. J. Clin. Endocrinol. Metab. 97: 1–5.

Stenson PD, Mort M, Ball E V, Shaw K, Phillips AD, Cooper DN. 2014. The Human Gene Mutation Database : building a comprehensive mutation repository for clinical and molecular genetics , diagnostic testing and personalized genomic medicine. Hum. Genet. 133: 1–9.

Stiff T, Tena TC, O'Driscoll M, Jeggo PA, Philipp M. 2016. ATR promotes cilia signalling: Links to developmental impacts. Hum. Mol. Genet. 25: 1574–1587.

Stoetzel C, Laurier V, Davis EE, Muller J, Rix S, Badano JL, Leitch CC, Salem N, Chouery E, Corbani S, Jalk N, Vicaire S, Sarda P, Hamel C, Lacombe D, Holder M, Odent S, Holder S, Brooks AS, Elcioglu NH, Da Silva E, Rossillion B, Sigaudy S, de Ravel TJL, Alan Lewis R, Leheup B, Verloes A, Amati-Bonneau P, Mégarbané A, Poch O, Bonneau D, Beales PL, Mandel J-L, Katsanis N, Dollfus H. 2006. BBS10 encodes a vertebrate-specific chaperonin-like protein and is a major BBS locus. Nat. Genet. 38: 521–524.

Stokman M, Lilien M, Knoers N. 2016a. Nephronophthisis. GeneReviews® [Internet]. Seattle Univ. Washington, Seattle; 1993-2017.: 1–40.

Stokman MF, Renkema KY, Giles RH, Schaefer F, Knoers NVAM, Van Eerde AM. 2016b. The expanding phenotypic spectra of kidney diseases: Insights from genetic studies. Nat. Rev. Nephrol. 12: 472–483.

when the signal is lost_marijn_8072018.indd 239 08/07/2018 10:51

Sun Y, Ruivenkamp CAL, Hoffer MJV, Vrijenhoek T, Kriek M, van Asperen CJ, den Dunnen JT, Santen GWE. 2015. Next-Generation Diagnostics: Gene Panel, Exome, or Whole Genome? Hum. Mutat. 36: 648–655.

Surpili MJ, Delben TM, Kobarg J. 2003. Identification of Proteins That Interact with the Central Coiled-Coil Region of the Human Protein Kinase NEK1. Biochemistry 42: 15369–15376.

Szklarczyk D, Franceschini A, Wyder S, Forslund K, Heller D, Huerta-Cepas J, Simonovic M, Roth A, Santos A, Tsafou KP, Kuhn M, Bork P, Jensen LJ, Von Mering C. 2015. STRING v10: Protein-protein interaction networks, integrated over the tree of life. Nucleic Acids Res. 43: D447–D452.

Takano T, Cybulsky A V. 2000. Complement C5b-9-Mediated Arachidonic Acid Metabolism in Glomerular Epithelial Cells Role of Cyclooxygenase-1 and -2. Am. J. Pathol. 156: 2091–2101.

Takasato M, Er PX, Chiu HS, Maier B, Baillie GJ, Ferguson C, Parton RG, Wolvetang EJ, Roost MS, Chuva de Sousa Lopes SM, Little MH. 2015. Kidney organoids from human iPS cells contain multiple lineages and model human nephrogenesis. Nature 526: 564–568.

Tan RJ, Zhou D, Liu Y. 2016. Signaling Crosstalk between Tubular Epithelial Cells and Interstitial Fibroblasts after Kidney Injury. Kidney Dis 2: 136–144.

Tassano E, Accogli A, Panigada S, Ronchetto P, Cuoco C, Gimelli G. 2014. Phenotypic and genetic characterization of a patient with a de novo interstitial 14q24.1q24.3 deletion. Mol. Cytogenet. 7: 49.

Tavira B, Gómez J, Málaga S, Santos F, Fernández-Aracama J, Alonso B, Iglesias S, Benavides A, Hernando I, Plasencia A, Alvarez V, Coto E. 2015. A labor and cost effective next generation sequencing of PKHD1 in autosomal recessive polycystic kidney disease patients. Gene 561: 165–169.

Thauvin-Robinet C. 2006. Clinical, molecular, and genotype-phenotype correlation studies from 25 cases of oral-facial-digital syndrome type 1: a French and Belgian collaborative study. J. Med. Genet. 43: 54–61.

Thauvin-Robinet C, Lee JS, Lopez E, Herranz-Pérez V, Shida T, Franco B, Jego L, Ye F, Pasquier L, Loget P, Gigot N, Aral B, Lopes CAM, St-Onge J, Bruel A-L, Thevenon J, González-Granero S, Alby C, Munnich A, Vekemans M, Huet F, Fry AM, Saunier S, Rivière J-B, Attié-Bitach T, Garcia-Verdugo JM, Faivre L, Mégarbané A, Nachury M V. 2014. The oral-facial-digital syndrome gene C2CD3 encodes a positive regulator of centriole elongation. Nat. Genet. 46: 905–911.

The 1000 Genomes Project Consortium. 2010. A map of human genome variation from population-scale sequencing. Nature 467: 1061–1073.

Thiel C, Kessler K, Giessl A, Dimmler A, Shalev SA, Von Der Haar S, Zenker M, Zahnleiter D, Stöss H, Beinder E, Abou Jamra R, Ekici AB, Schröder-Kreß N, Aigner T, Kirchner T, Reis A, Brandstätter JH, Rauch A. 2011. NEK1 mutations cause short-rib polydactyly syndrome type majewski. Am. J. Hum. Genet. 88: 106–114.

Thomas R, Sanna-Cherchi S, Warady BA, Furth SL, Kaskel FJ, Gharavi AG. 2011. HNF1B and PAX2 mutations are a common cause of renal hypodysplasia in

when the signal is lost_marijn_8072018.indd 240 08/07/2018 10:51

the CKiD cohort. Pediatr. Nephrol. 26: 897–903.
Thomas S, Legendre M, Saunier S, Bessières B, Alby C, Bonnière M, Toutain A, Loeuillet L, Szymanska K, Jossic F, Gaillard D, Yacoubi MT, Mougou-Zerelli S, David A, Barthez MA, Ville Y, Bole-Feysot C, Nitschke P, Lyonnet S, Munnich A, Johnson CA, Encha-Razavi F, Cormier-Daire V, Thauvin-Robinet C, Vekemans M, Attié-Bitach T. 2012. TCTN3 mutations cause Mohr-Majewski syndrome. Am. J. Hum. Genet. 91: 372–378.
Thomas S, Wright KJ, Corre S Le, Micalizzi A, Romani M, Abhyankar A, Saada J, Perrault I, Amiel J, Litzler J, Filhol E, Elkhartoufi N, Kwong M, Casanova JL, Boddaert N, Baehr W, Lyonnet S, Munnich A, Burglen L, Chassaing N, Encha-Ravazi F, Vekemans M, Gleeson JG, Valente EM, Jackson PK, Drummond IA, Saunier S, Atti-Bitach T. 2014. A Homozygous PDE6D Mutation in Joubert Syndrome Impairs Targeting of Farnesylated INPP5E Protein to the Primary Cilium. Hum. Mutat. 35: 137–146.
Toriello H, Franco B, Bruel A, Thauvin-Robinet C. 2016. Oral-facial-digital syndrome type I. GeneReviews® [Internet]. Seattle Univ. Washington, Seattle; 1993-2015.: 1–16.
Tory K, Lacoste T, Burglen L, Morinière V, Boddaert N, Macher M-A, Llanas B, Nivet H, Bensman A, Niaudet P, Antignac C, Salomon R, Saunier S. 2007. High NPHP1 and NPHP6 mutation rate in patients with Joubert syndrome and nephronophthisis: potential epistatic effect of NPHP6 and AHI1 mutations in patients with NPHP1 mutations. J. Am. Soc. Nephrol. 18: 1566–1575.
Tory K, Rousset-Rouviere C, Gubler MC, Moriniere V, Pawtowski A, Becker C, Guyot C, Gie S, Frishberg Y, Nivet H, Deschenes G, Cochat P, Gagnadoux MF, Saunier S, Antignac C, Salomon R. 2009. Mutations of NPHP2 and NPHP3 in infantile nephronophthisis. Kidney Int. 75: 839–847.
Tran P V, Haycraft CJ, Besschetnova TY, Turbe-doan A, Stottmann RW, Herron BJ, Chesebro AL, Qiu H, Scherz PJ, Shah J V, Yoder BK, Beier DR. 2008. THM1 negatively modulates mouse sonic hedgehog signal transduction and affects retrograde intraflagellar transport in cilia. Nat. Genet. 40: 403–410.
Triebel J, Moreno-Vega AI, Vázquez-Membrillo M, Nava G, García-Franco R, López-Star E, Baldivieso-Hurtado O, Ochoa D, Macotela Y, Bertsch T, De, Martinez la Escalera G, Clapp C. 2015. High Prolactin Excretion in Patients with Diabetes Mellitus and Impaired Renal Function. Clin. Lab. 61: 709–16.
Tsurusaki Y, Kobayashi Y, Hisano M, Ito S, Doi H, Nakashima M, Saitsu H, Matsumoto N, Miyake N. 2013. The diagnostic utility of exome sequencing in Joubert syndrome and related disorders. J. Hum. Genet. 58: 113–115.
Tummalapalli L, Nadkarni GN, Coca SG. 2016. Biomarkers for predicting outcomes in chronic kidney disease. Curr. Opin. Nephrol. Hypertens. 25: 480–486.
Uhlen M, Fagerberg L, Hallstrom BM, Lindskog C, Oksvold P, Mardinoglu A, Sivertsson A, Kampf C, Sjostedt E, Asplund A, Olsson I, Edlund K, Lundberg E, Navani S, Szigyarto CA-K, Odeberg J, Djureinovic D, Takanen JO, Hober S, Alm T, Edqvist P-H, Berling H, Tegel H, Mulder J, Rockberg J, Nilsson P, Schwenk JM, Hamsten M, von Feilitzen K, Forsberg M, Persson L, Johansson F, Zwahlen M, von Heijne G, Nielsen J, Ponten F. 2015. Tissue-based map of

when the signal is lost_marijn_8072018.indd 241 08/07/2018 10:51

the human proteome. Science 347: 1260419–1260419.
Ung PMU, Schlessinger A. 2015. DFGmodel: Predicting protein kinase structures in inactive states for structure-based discovery of type-II inhibitors. ACS Chem. Biol. 10: 269–278.
Upadhya P, Birkenmeier EH, Birkenmeier CS, Barker JE. 2000. Mutations in a NIMA-related kinase gene, Nek1, cause pleiotropic effects including a progressive polycystic kidney disease in mice. Proc. Natl. Acad. Sci. U. S. A. 97: 217–21.
Upadhya P, Churchill G, Birkenmeier EH, Barker JE, Frankel WN. 1999. Genetic Modifiers of Polycystic Kidney Disease in Intersubspecific KAT2J Mutants. Genomics 58: 129–137.
Vale RD, Fletterick RJ. 1997. The design plan of kinesin motors. Annu Rev Cell Dev Biol. 13: 745–777.
Valencia CA, Husami A, Holle J, Johnson JA, Qian Y, Mathur A, Wei C, Indugula SR, Zou F, Meng H, Wang L, Li X, Fisher R, Tan T, Hogart Begtrup A, Collins K, Wusik KA, Neilson D, Burrow T, Schorry E, Hopkin R, Keddache M, Harley JB, Kaufman KM, Zhang K. 2015. Clinical Impact and Cost-Effectiveness of Whole Exome Sequencing as a Diagnostic Tool: A Pediatric Center's Experience. Front. Pediatr. 3.
Valente EM, Brancati F, Silhavy JL, Castori M, Marsh SE, Barrano G, Bertini E, Boltshauser E, Zaki MS, Abdel-Aleem A, Abdel-Salam GMH, Bellacchio E, Battini R, Cruse RP, Dobyns WB, Krishnamoorthy KS, Lagier-Tourenne C, Magee A, Pascual-Castroviejo I, Salpietro CD, Sarco D, Dallapiccola B, Gleeson JG. 2006. AHI1 gene mutations cause specific forms of Joubert syndrome-related disorders. Ann. Neurol. 59: 527–534.
Valente EM, Logan C V, Mougou-Zerelli S, Lee JH, Silhavy JL, Brancati F, Iannicelli M, Travaglini L, Romani S, Illi B, Adams M, Szymanska K, Mazzotta A, Lee JE, Tolentino JC, Swistun D, Salpietro CD, Fede C, Gabriel S, Russ C, Cibulskis K, Sougnez C, Hildebrandt F, Otto EA, Held S, Diplas BH, Davis EE, Mikula M, Strom CM, Ben-Zeev B, Lev D, Sagie TL, Michelson M, Yaron Y, Krause A, Boltshauser E, Elkhartoufi N, Roume J, Shalev S, Munnich A, Saunier S, Inglehearn C, Saad A, Alkindy A, Thomas S, Vekemans M, Dallapiccola B, Katsanis N, Johnson CA, Attié-Bitach T, Gleeson JG. 2010. Mutations in TMEM216 perturb ciliogenesis and cause Joubert, Meckel and related syndromes. Nat. Genet. 42: 619–625.
Valina M, Larsen C, Kanosky S, Suchy S, Nield L, Onder A. 2013. A novel CLCN5 mutation in a boy with asymptomatic proteinuria and focal global glomerulosclerosis. Clin Nephrol 80: 377–384.
Veland I, Awan A, Pedersen L. 2009. Primary cilia and signaling pathways in mammalian development, health and disease. Nephron Physiol. 111: 39–53.
Vella LJ. 2014. The Emerging Role of Exosomes in Epithelial-Mesenchymal-Transition in Cancer. Front. Oncol. 4: 1–5.
Verhave JC, Bech AP, Wetzels JFM, Nijenhuis T. 2015. Hepatocyte Nuclear Factor 1 -Associated Kidney Disease: More than Renal Cysts and Diabetes. J. Am. Soc. Nephrol.: 1–9.
Vivante A, Hildebrandt F. 2016. Exploring the genetic basis of early-onset chronic

when the signal is lost_marijn_8072018.indd 242 08/07/2018 10:51

kidney disease. Nat Rev Nephrol doi: 10.10.
Vogel MJ, van Zon P, Brueton L, Gijzen M, van Tuil MC, Cox P, Schanze D, Kariminejad A, Ghaderi-Sohi S, Blair E, Zenker M, Scambler PJ, Ploos van Amstel HK, van Haelst MM. 2012. Mutations in GRIP1 cause Fraser syndrome. J. Med. Genet. 49: 303–6.
Voormolen S. 2017. Eerste genreparatie in het lichaam van een patiënt. nrc.nl: 1–7.
Voskarides K, Damianou L, Neocleous V, Zouvani I, Christodoulidou S, Hadjiconstantinou V, Ioannou K, Athanasiou Y, Patsias C, Alexopoulos E, Pierides A, Kyriacou K, Deltas C. 2007. COL4A3/COL4A4 Mutations Producing Focal Segmental Glomerulosclerosis and Renal Failure in Thin Basement Membrane Nephropathy. J. Am. Soc. Nephrol. 18: 3004–3016.
Wallace A, Wirrell E, Kenney-Jung DL. 2016. Pharmacotherapy for Dravet Syndrome. Pediatr. Drugs 18: 197–208.
Wang J, Barr MM. 2016. Ciliary Extracellular Vesicles: Txt Msg Organelles. Cell. Mol. Neurobiol. 36: 449–457.
Wang X, Huang X, Fang X, Zhang Y, Wang W. 2016. CRISPR-Cas9 System as a Versatile Tool for Genome Engineering in Human Cells. Mol. Ther. - Nucleic Acids 5: e388.
Warmoes M, Lam SW, Groep P Van Der, Jaspers JE, Boer L De, Pham TV, Piersma SR, Rottenberg S, Boven E, Jonkers J, Diest PJ Van, Connie R. 2016. Secretome proteomics reveals candidate biomarkers of BRCA1 deficiency in breast cancer. Oncotarget 7.
Warnes GR, Bolker B, Bonebakker L, Gentleman R, Huber W, Liaw A, Lumley T, Maechler M, Magnusson A, Moeller S, Schwartz M, Venable B. 2016. gplots: Various R Programming Tools for Plotting Data. https://CRAN.R-project.org/package=gplots.
Webb NJ a, Shahinfar S, Wells TG, Massaad R, Gleim GW, Sisk CM, Lam C. 2013. Losartan and enalapril are comparable in reducing proteinuria in children with Alport syndrome. Pediatr. Nephrol. 28: 737–743.
Weber S, Moriniere V, Knu T, Charbit M, Ghiggeri GM, Jankauskiene A, Mir S, Montini G, Peco-antic A, Wu E, Zurowska AM, Mehls O, Antignac C, Schaefer F, Salomon R. 2006. Prevalence of Mutations in Renal Developmental Genes in Children with Renal Hypodysplasia : Results of the ESCAPE Study. J Am Soc Nephrol 17: 2864–2870.
Weber S, Tonshoff B. 2005. Recurrence of Focal-Segmental Glomerulosclerosis in Children after Renal Transplantation: Clinical and Genetic Aspects. Transplantation 80: S128–S134.
De Wert G, Pennings G, Clarke A, Eichenlaub-ritter U, El CG Van, Forzano F. 2016. Human germ-line gene editing: Conclusions and recommendations. ESHG ESHRE: 1–5.
Westland R, Bodria M, Carrea A, Lata S, Scolari F, Fremeaux-Bacchi V, D'Agati VD, Lifton RP, Gharavi AG, Ghiggeri GM, Sanna-Cherchi S. 2014. Phenotypic Expansion of DGKE-Associated Diseases. J Am Soc Nephrol 25: 1408–1414.
Wheway G, Schmidts M, Mans D, Szymanska K, Nguyen T, Racher H, Phelps I, Toedt G, Kennedy J, Wunderlich K, Sorusch N, Abdelhamed Z, Natarajan S,

when the signal is lost_marijn_8072018.indd 243 08/07/2018 10:51

Herridge W, Van Reeuwijk J, Horn N, Boldt K, Parry D, Letteboer S, Roosing S, Adams M, Bell S, Bond J, Higgins J, Morrison E, Tomlinson D, Slaats G, Van Dam T, Huang L, Kessler K, Giessl A, Logan C, Boyle E, Shendure J, Anazi S, Aldahmesh M, Al Hazzaa S, Hegele R, Ober C, Frosk P, Mhanni A, Chodirker B, Chudley A, Lamont R, Bernier F, Beaulieu C, Gordon P, Pon R, Donahue C, Barkovich A, Wolf L, Toomes C, Thiel C, Boycott K, McKibbin M, Inglehearn C, Consortium U, Genomics U of WC for M, Stewart F, Omran H, Huynen M, Sergouniotis P, Alkuraya F, Parboosingh J, Innes A, Willoughby C, Giles R, Webster A, Ueffing M, Blaque O, Gleeson J, Wolfrum U, Beales P, Bibson T, Doherty D, Mitchison H, Roepman R, Johnson C. 2015. An siRNA-based functional genomics screen for the identification of regulators of ciliogenesis and ciliopathy genes. Nat Cell Biol 17: 1074–1087.

White MC, Quarmby LM. 2008. The NIMA-family kinase, Nek1 affects the stability of centrosomes and ciliogenesis. BMC Cell Biol. 9: 29.

Winn MP, Daskalakis N, Spurney RF, Middleton JP. 2006. Unexpected Role of TRPC6 Channel in Familial Nephrotic Syndrome : Does It Have Clinical Implications? J Am Soc Nephrol: 378–387.

Wolf MTF. 2015. Nephronophthisis and related syndromes. Curr. Opin. Pediatr. 27: 201–211.

Wolf MTF, Hildebrandt F. 2011. Nephronophthisis. Pediatr. Nephrol. 26: 181–194.

Xie J, Wu X, Ren H, Wang W, Wang Z, Pan X, Hao X, Tong J, Ma J, Ye Z, Meng G, Zhu Y, Kiryluk K, Kong X, Hu L, Chen N. 2014. COL4A3 mutations cause focal segmental glomerulosclerosis. J. Mol. Cell Biol. 6: 498–505.

Xinaris C, Benedetti V, Novelli R, Abbate M, Rizzo P, Conti S, Tomasoni S, Corna D, Pozzobon M, Cavallotti D, Yokoo T, Morigi M, Benigni A, Remuzzi G. 2016. Functional Human Podocytes Generated in Organoids from Amniotic Fluid Stem Cells. J. Am. Soc. Nephrol. 27: 1400–1411.

Xu M, Yang L, Wang F, Li H, Wang X, Wang W, Ge Z, Wang K, Zhao L, Li H, Li Y, Sui R, Chen R. 2015. Mutations in human IFT140 cause non-syndromic retinal degeneration. Hum. Genet. 134: 1069–1078.

Yamagata K, Furuta H, Oda N, Kaisaki P, Menzel S, Cox N, Fajans S, Signorini S, Stoffel M, Bell G. 1996. No Mutations in the hepatocyte nuclear factor-4alpha gene in maturity-onset diabetes of the young (MODY1). Nature 384: 458–460.

Yamaguchi S, Morizane R, Homma K, Monkawa T, Suzuki S, Fujii S, Koda M, Hiratsuka K, Yamashita M, Yoshida T, Wakino S, Hayashi K, Sasaki J, Hori S, Itoh H. 2016. Generation of kidney tubular organoids from human pluripotent stem cells. Sci. Rep. 6: 38353.

Yang T, Zhang X, Zheng Z. 2013a. Suppression of KIF14 expression inhibits hepatocellular carcinoma progression and predicts favorable outcome. Cancer Sci 104: 552–557.

Yang Y, Muzny DM, Reid JG, Bainbridge MN, Willis A, Ward PA, Braxton A, Beuten J, Xia F, Niu Z, Hardison M, Person R, Bekheirnia MR, Leduc MS, Kirby A, Pham P, Scull J, Wang M, Ding Y, Plon SE, Lupski JR, Beaudet AL, Gibbs RA, Eng CM. 2013b. Clinical Whole-Exome Sequencing for the Diagnosis of

when the signal is lost_marijn_8072018.indd 244 08/07/2018 10:51

Mendelian Disorders. N. Engl. J. Med. 369: 1502–1511.
Yao X-D, Chen X, Huang G-Y, Yu Y-T, Xu S-T, Hu Y-L, Wang Q-W, Chen H-P, Zeng C-H, Ji D-X, Hu W-X, Tang Z, Liu Z-H. 2012. Challenge in pathologic diagnosis of Alport syndrome: evidence from correction of previous misdiagnosis. Orphanet J. Rare Dis. 7: 100.
Yu J, Carroll TJ, McMahon AP. 2002. Sonic hedgehog regulates proliferation and differentiation of mesenchymal cells in the mouse metanephric kidney. Development 129: 5301–5312.
Yuan S, Sun Z. 2013. Expanding Horizons: Ciliary Proteins Reach Beyond Cilia. Annu. Rev. Genet. 47: 353–376.
Yunus J, Setsu T, Kikkawa S, Sakisaka T, Terashima T. 2014. Cytoarchitecture of the olfactory bulb in the laggard mutant mouse. Neuroscience: 259–271.
Zaghloul NA, Brugmann SA. 2011. The emerging face of primary cilia. Genesis 49: 231–246.
Zaiou M, El Amri H. 2017. Cardiovascular pharmacogenetics: a promise for genomically-guided therapy and personalized medicine. Clin. Genet. 91: 355–370.
Zalli D, Bayliss R, Fry AM. 2012. The Nek8 protein kinase, mutated in the human cystic kidney disease nephronophthisis, is both activated and degraded during ciliogenesis. Hum. Mol. Genet. 21: 1155–1171.
Zhang Y, Seo S, Bhattarai S, Bugge K, Searby CC, Zhang Q, Drack A V., Stone EM, Sheffield VC. 2014. BBS mutations modify phenotypic expression of CEP290-related ciliopathies. Hum. Mol. Genet. 23: 40–51.
Zhang Y, Yuan Y, Liang P, Zhang Z, Guo X, Xia L, Zhao Y, Shu X, Sun S, Ying Y, Cheng Y. 2017. Overexpression of a novel candidate oncogene KIF14 correlates with tumor progression and poor prognosis in prostate cancer. Oncotarget 8: 45459–45469.
Zhou D, Tian Y, Sun L, Zhou L, Xiao L, Tan RJ, Tian J, Fu H, Hou FF, Liu Y. 2016. Matrix Metalloproteinase-7 Is a Urinary Biomarker and Pathogenic Mediator of Kidney Fibrosis. J. Am. Soc. Nephrol. 28: 1–14.
Zollinger H, Mihatsch M, Edefonti A, Gaboardi F, Imbasciati E, Lennert T. 1980. Nephronophthisis (medullary cystic disease of the kidney). A study using electron microscopy, immunofluorescence, and a review of the morphological findings. Helv. Paediatr. Acta.: 509–530.
Zubiri I, Posada-Ayala M, Benito-Martin A, Maroto AS, Martin-Lorenzo M, Cannata-Ortiz P, De La Cuesta F, Gonzalez-Calero L, Barderas MG, Fernandez-Fernandez B, Ortiz A, Vivanco F, Alvarez-Llamas G. 2015. Kidney tissue proteomics reveals regucalcin downregulation in response to diabetic nephropathy with reflection in urinary exosomes. Transl. Res. 166: 474–484.

when the signal is lost_marijn_8072018.indd 245 08/07/2018 10:51

ACKNOWLEDGMENTS / DANKWOORD

Allereerst hartelijk dank aan de leescommissie bestaande uit Prof. dr. Roel Goldschmeding, Prof. dr. Marianne Verhaar, Prof. dr. Susanne Lens, Prof. dr. Ronald Roepman en Prof. dr. Dorien Peters voor het beoordelen van dit proefschrift.

Natuurlijk wil ik ook de vele mensen bedanken die direct en indirect hebben bijgedragen aan de totstandkoming van dit proefschrift. Allereerst mijn fantastische promotieteam: Nine, Rachel, Marc en Kirsten.

Beste **Nine**, ik ben je heel dankbaar voor de mogelijkheid om drie jaar full time onderzoek te kunnen doen, ingebed in een inspirerend team van nier onderzoekers, en in de wetenschap dat ik na afloop mijn opleiding zou kunnen hervatten. Door deze unieke ervaring en onder jouw betrokken begeleiding voel ik me echt opgeleid als onderzoeker. Dank voor de tijd voor overleg die je op miraculeuze wijze kon vrijmaken in je drukke agenda, de 'potjes' die aangeboord konden worden voor experimenten en voor je steun in het combineren van werk en gezin. Ik heb je oprechte interesse in de niet-werkgerelateerde zaken bijzonder gewaardeerd.

Rachel, jij hebt mijn onderzoeksperiode op talloze manieren verrijkt. Eén van de leukste aspecten van mijn onderzoek vond ik het functionele werk dat ik onder jouw begeleiding heb gedaan en waar ik heel veel van heb geleerd. Het getuigt van echte passie dat jij als PI ook nog regelmatig in het lab en achter de confocal microscoop te vinden bent. Je hebt me geintroduceerd in de wereld van patientenverenigingen, wat een waardevolle extra dimensie heeft gegeven aan mijn werk als onderzoeker en arts. Tenslotte ben je een ontzettend inspirerend en humorvol persoon, en altijd bereikbaar, onafhankelijk van de tijdszone waarin je je bevindt. Dank voor het organiseren van de 'pee party' om de laatste urines voor het extracellular vesicles project te verzamelen.

Marc, dank voor je betrokkenheid en scherpe klinische blik. Jij loopt net zo warm voor extracellular vesicles uit urine als ik! Eigenlijk ben je vanaf het begin betrokken geweest bij mijn onderzoek, en in de laatste paar maanden van mijn onderzoek is dat ook officieel erkend.

Kirsten, dankjewel voor je vrolijkheid, je openheid en je benaderbaarheid. Je hebt in jouw onderzoeksgroep een low-stress, veilige leeromgeving gecreëerd waarin alles gevraagd en besproken kan worden. Bedankt voor het vertrouwen dat je me vanaf de eerste dag hebt gegeven en voor de vrijheid om technieken te leren, samenwerkingen aan te gaan en me te ontwikkelen als onderzoeker.

Veel dank ook aan mijn supervisory committee, **Edwin Cuppen** en **Joost Frenkel** voor jullie kritische vragen en waardevolle adviezen.

when the signal is lost_marijn_8072018.indd 246 08/07/2018 10:51

Mieke, hoewel jij niet op papier betrokken was bij mijn onderzoek heb ik heel veel projecten en patiënten aan jou te danken. Je bent een voorbeeld in de manier waarop je kliniek en onderzoek combineert, een essentiele schakel die ik ook hoop te kunnen zijn in mijn verdere carrière. Bedankt dat je me twee keer hebt gewezen op een vacature voor arts-assistent bij de klinische genetica tijdens mijn onderzoeksstage in LA.

To all the members of the KOUNCIL consortium: **Nine, Kirsten, Marc, Bert, Rachel, Hester, Albertien, Tim, Gisela, Heleen, Ronald, Simone, Machteld, Ernie, Nicole, Miriam, Phil** and **Katia**, thank you for the fruitful collaboration! Jeroen, dank dat ik altijd laagdrempelig met je kon sparren over de database. I have enjoyed the informal atmosphere of our meetings. Thank you also to the members of AGORA for facilitating the patient inclusions in KOUNCIL.

Veel dank aan de **Nierstichting** voor het financieren van het onderzoek dat resulteerde in dit proefschrift.

Aan de onderzoekers, analisten, research verpleegkundigen en specialisten van de kindernefrologie, de nefrologie, de klinische genetica en de pathologie: **Mandy, Annelien, Maarten, Arjan, Elena, Gijs, Hester, Jacques, Paulien, Marie-Jose, Klaske, Jeske, Roel, Tri, Peter, Domenico, Petra, Jojanneke, Krista,** veel dank voor de fijne samenwerking in verschillende projecten. **Hans Kristian, Bert, Patrick** en **Rumo** bedankt voor de nauwe samenwerking en korte lijntjes met de sectie genoomdiagnostiek. **Joost van der Heijden**, bedankt voor de waardevolle samenwerking met de afdeling nefrologie van het VUmc. **Connie, Tim** en **Irene**, enorm bedankt voor de enthousiaste begeleiding bij het exosomenproject. Dankzij jullie inzet, en het doneren van urine door jouw kinderen, Irene, is dit project geslaagd. **John**, ik ben altijd onder de indruk als je uitlegt wat je doet. Dank voor het opzoeken van kandidaatgenen in de voorloper van CiliaCarta. Ik hoop dat we in de toekomst nog vaak zullen samenwerken.

Dank aan de VHL Vereniging (**Rachel** en **Barbara**), de Joubert Syndroom Ouder Contactgroep (**Susan**), de Joubert Stichting Nederland (**Jody** en **Brenda**), de Bardet Biedl Syndroom Stichting (**Bendert**) en de Nierpatienten Vereniging Nederland (de **Marjoleinen** en **Wouter**) voor de uitnodigingen om deel te nemen aan jullie bijeenkomsten en mijn onderzoek te presenteren, en natuurlijk voor de leuke activiteiten met de jeugd. Ik leer ontzettend veel van jullie en hoop dat ik nog lang betrokken kan blijven. Vooral ook heel veel dank aan de **patiënten** die hebben deelgenomen aan mijn onderzoek. En natuurlijk aan alle **gezonde vrijwilligers** voor het doneren van urine en melktanden. Zonder jullie was dit nooit gelukt! **Tony**, jij hebt ook inhoudelijk bijgedragen aan mijn onderzoek. Bedankt voor het toesturen van het artikel over nonsense-associated exon skipping op exact het juiste moment!

Beste **Wilmy**, **Monique** en **Simone**, veel dank voor jullie creativiteit bij het maken van afspraken in overvolle agenda's. **Saskia**, dank voor het vinden van vrije spreekkamers en het opvangen en inschrijven van mijn patienten. Ik waardeer je ontspannen

when the signal is lost_marijn_8072018.indd 247 08/07/2018 10:51

houding en je oplossingsgerichtheid.

Nine, Kirsten, Albertien, Edith, Nayia, Glenn, Rozemarijn en **Anukrati**, bedankt voor de fijne sfeer in onze groep. **Albertien**, dank voor alle soepele één-tweetjes die zoveel inclusies hebben opgeleverd. **Edith**, heel fijn dat jij mijn cel experimenten kon overnemen tijdens mijn verlof en daarna, en bedankt voor je hulp met het verzamelen van urine. **Nayia**, I am so glad of our friendship. We loved visiting you in Cyprus. **Glenn**, met jouw creatieve en populaire initiatieven zoals 'Sweet-treat Monday' en 'Discolab Friday' zorgde je altijd weer voor de nodige luchtigheid. **Rozemarijn** en **Anukrati**, heel veel succes met jullie PhDs! **Rachel, Gisela, Tim, Ive, Saskia, Zhiyong** en **Ka Man**, thank you for the productive meetings, the nice borrels and for your patience in teaching me cell culture. **Tim**, I really enjoyed climbing with you and your Hubrecht friends. Dank ook aan de studenten, **Joost** en **Chalana** die hebben bijgedragen aan de onderzoeken in dit proefschrift. Lieve **Elly**, bedankt voor je hulp bij het invoeren van medische gegevens in de database!

Iris en **Glen**, bedankt dat jullie mijn paranimfen wilden zijn. **Iris**, wat leuk dat jij een zelfde pad bewandelt en ook vanuit het WKZ in het Stratenum terecht kwam. Ik waardeer je vrolijkheid, humor en interesse. Ik weet zeker dat jij je PhD met heel veel success gaat afronden. Binnenkort ben je opnieuw mijn collega in de kliniek, en hopelijk snel ook als AIOS! **Glen**, I enjoyed the trips to Cologne, to Ghent with the Cypriots and the conference in Cardiff. It was great working with you on the NEK1 paper and brainstorming about ALS. You have an awesome personality AND the best taste in food!

Sanne, je bent het zonnetje in onze kamer. Bedankt voor je betrokkenheid en je Brabantse gezelligheid! **Mirjam**, je bent een voorbeeld in hoe je werk en privé combineert (en dan nog tientallen andere activiteiten maar dat doe ik je niet na)! Ik voel me vaak gesteund door de gesprekken met jou en ik waardeer enorm dat we weer collega's zijn in het WKZ. **Chris, Karen, Glen, Christina, Sanne, Iris, Edith, Rozemarijn, Helen, Vinicius, Daiane, Sakhsi, Mircea, Daniel, Jessica, Joske, Maarten, Ellen, Ivo, Ruben, Sander, Nicole, Lynne** thank you for the great atmosphere in our department and the interesting lunch conversations. **Martin, Mark, Robert, Flip, Ies, Gijs, Wigard** en **Jeroen**, bedankt dat ik altijd bij jullie binnen kon lopen met vragen. **Terry**, geen voorstel is te gek voor jou. Veel dank voor het organiseren van de inspiration meetings. Je bent een voorbeeld in hoe je de maatschappelijke rol van de geneticus vertolkt.

Eva, Carolien en **Bobby**, mijn eerste kennismaking met genetisch onderzoek was onder jullie begeleiding. Bedankt voor een interessante en leerzame stage. Beste **Eva**, vanaf mijn eerste coschap bij de klinische genetica kan ik bij jou terecht voor inspiratie en advies. Ik waardeer je betrokkenheid, ontspannenheid en pragmatisme. Je bent heel belangrijk geweest in mijn keuze voor de klinische genetica. Ik ben erg blij dat jij opleider bent geworden.

when the signal is lost_marijn_8072018.indd 248 08/07/2018 10:51

Roel, Anil, Simone, Jytte, Tina, Brian, bedankt voor de inspirerende tijd in LA. **Roel**, de geweldige ervaring in jouw lab heeft mij doen besluiten om een PhD te doen. Toen ik twijfelde tussen neurogenetisch en nefrogenetisch onderzoek zei je dat een interessant mechanisme belangrijker is dan een interessant orgaan, een heel waardevol advies! De manier waarop jij werk en gezin combineert zal altijd een voorbeeld zijn.

Aan de arts-assistenten Klinische Genetica uit het WKZ: **Charlotte, Saskia, Nienke, Danielle, Noor, Claire, Iris, Remco, Laura, Aster, Marten, Jette** en **Maaike**, heel fijn om weer deel uit te maken van onze gezellige assistenten groep. **Evelien**, je was een super fijne kamergenoot. Dank ook aan alle klinisch genetici en andere collega's voor de prettige sfeer op onze afdeling en de ruimte om af en toe aan onderzoek te werken. **Nienke Verbeek**, dank dat je mijn mentor wilde zijn. Ik waardeer onze gesprekken enorm.

Mark, Sanne, David, bedankt voor de vakanties, de ontspanning en de relativerende humor. **Saskia**, van het strijden voor de erkenning van tweede studies tot de chirurgie in Ede tot de koffies bij MiCafe tijdens onze PhDs, wat fijn om altijd synchroon met jou te lopen. Beste **Sybrand** en **Elsemarie**, bedankt voor de fijne tijd aan de Oudegracht, de unieke ontmoetingen en de interessante gesprekken. Jullie leven volgens jullie eigen idealen. Het is een voorrecht om deel uit te maken van jullie gemeenschap, ookal wonen we nu niet meer 'op stand'. Ik kom graag binnenkort een glaasje port drinken. Dank ook aan onze lieve ex-roomies, **Pien** en **Fleur**.

Nicole, Rudi, Carolien, Jan Willem, Robin, Lou, Annick en **Tom**, bedankt voor jullie steun, de interesse in mijn onderzoek, de maaltijden waar ik iets later kon aanschuiven en natuurlijk voor het klussen in ons huis. Het is een fijn idee dat onze community buiten de gracht weer opnieuw is opgebouwd en dat **Rafaël** opgroeit temidden van zijn 'extended family'. **Jan Willem**, bedankt voor het prachtige ontwerp van de KOUNCIL website www.kouncil.nl, en natuurlijk voor het ontwerpen van dit proefschrift.

Lieve **Papa, Mama, Tijs, Jen, Fieke** en **Karlien**, bedankt voor jullie onvoorwaardelijke steun en liefde. Dankzij jullie heb ik het vertrouwen om met veel enthousiasme dingen te ondernemen waarvan ik van te voren niet weet of ik ze kan. **Papa**, dank voor het vele klussen en voor je 'can do'-mentaliteit. **Mama** en **Fieke**, dank dat jullie zulke fijne oppassen zijn voor **Rafaël**. Daarmee hebben jullie natuurlijk ook bijgedragen aan het afronden van dit proefschrift.

Lieve **Remmelt**, ik heb ervan genoten om deze bijzondere PhD fase tegelijk met jou te doorlopen. Je amplificeerde mijn enthousiasme en als ik frustratie uitte kwam je met zulke radicale oplossingen dat ik weer met humor naar de situatie kon kijken. Lieve vrolijke **Rafaël**, ik ben zo blij dat jij geboren bent! Ik hou onbeschrijfelijk veel van jullie.

when the signal is lost_marijn_8072018.indd 249 08/07/2018 10:51

LIST OF PUBLICATIONS

Stokman MF, Renkema KY, Giles RH, Schaefer F, Knoers NVAM, Van Eerde AM. 2016. The expanding phenotypic spectra of kidney diseases: insights from genetic studies. Nat. Rev. Nephrol. 12: 472-483. DOI:10.1038/nrneph.2016.87.

Monroe GR*, Kappen IF*, **Stokman MF***, Terhal PA, Van den Boogaard MH, Savelberg SM, Van der Veken LT, Van Es RJ, Lens SM, Hengeveld RC, Creton MA, Janssen NG, Mink van der Molen AB, Ebbeling MB, Giles RH, Knoers NVAM, Van Haaften G. 2016. Compound heterozygous NEK1 variants in two sibs with oral-facial-digital syndrome II (Mohr syndrome). Eur. J. Hum. Genet. 24:1752-1760. DOI:10.1038/ejhg.2016.103.

*These authors contributed equally

Stokman MF, Lilien MR, Knoers NVAM. 2016. Nephronophthisis. In: Adam MP, Ardinger HH, Pagon RA, Wallace SE, Bean LJH, Stephens K, Amemiya A, editors. GeneReviews® [Internet]. Seattle Univ. of Washington, Seattle: 1-40.

Stokman MF, Oud MM, Van Binsbergen E, Slaats GG, Nicolaou N, Renkema KY, Nijman IJ, Roepman R, Giles RH, Arts HH, Knoers NVAM, Van Haelst MM. 2016. De novo 14q24.2q24.3 microdeletion including IFT43 is associated with intellectual disability, skeletal anomalies, cardiac anomalies and myopia. Am. J. Med. Genet. A. 170: 1566-1569. DOI: 10.1002/ajmg.a.37598.

Eshuis-Peters E, Versluys AB, **Stokman MF**, Van der Crabben S, Nij Bijvank SW, Van Wezel-Meijler G. 2016. Congenital amegakaryocytic thrombocytopenia type II presenting with multiple central nervous system anomalies. Neuropediatrics. 47: 128-131. DOI:10.1055/s-0036-1571800.

Ajzenberg H, Slaats GG, **Stokman MF**, Arts HH, Logister I, Kroes HY, Renkema KY, Van Haelst MM, Terhal PA, Van Rooij IA, Keijzer-Veen MG, Knoers NVAM, Lilien MR, Jewett MA, Giles RH. 2015. Non-invasive sources of cells with primary cilia from pediatric and adult patients. Cilia. 4: 8. DOI:10.1186/s13630-015-0017-x.

Slaats GG, Ghosh AK, Falke LL, Le Corre S, Shaltiel IA, Van de Hoek G, Klasson TD, **Stokman MF**, Logister I, Verhaar MC, Goldschmeding R, Nguyen TQ, Drummond IA, Hildebrandt F, Giles RH. 2014. Nephronophthisis-associated CEP164 regulates cell cycle progression, apoptosis and epithelial-to-mesenchymal transition. PloS Genet. 10: e1004594. DOI:10.1371/journal.pgen.1004594.

Renkema KY, **Stokman MF**, Giles RH, Knoers NV. 2014. Next-generation sequencing for research and diagnostics in kidney disease. Nat. Rev. Nephrol. 10: 433-44. DOI:10.1038/nrneph.2014.95.

when the signal is lost_marijn_8072018.indd 250 08/07/2018 10:51

Stokman MF, Van der Zwaag B, Van de Kar NCAJ, Van Haelst MM, Van Eerde AM, Van der Heijden JW, Kroes HY, Ippel E, Schulp JA, Van Gassen KL, Van Rooij IALM, Giles RH, Beales PL, Roepman R, Arts HH, Bongers EMHF, Renkema KY, Knoers NVAM, Van Reeuwijk J*, Lilien MR*. Clinical and genetic analyses of a Dutch cohort of 40 patients with a nephronophthisis-related ciliopathy. 2018. Pediatr. Nephrol. DOI:10.1007/s00467-018-3958-7.

*These authors contributed equally

Submitted manuscript

Stokman MF, Bijnsdorp IV, Schelfhorst T, Peters EDJ, Pham TV, Piersma SR, Knol JC, Giles RH, Bongers EMHF, Knoers NVAM, Lilien MR, Jimenez CR*, Renkema KY*. Changes in the urinary extracellular vesicle proteome are associated with nephronophthisis-related ciliopathies. (Manuscript submitted)

*These authors contributed equally

Manuscript in preparation

Stokman MF, Van Harssel JJ, Peters EDJ, Verduijn JM, Nguyen TQ, Castigliego D, Den Ouden K, Van Gassen KL, Van der Veken LT, Knoers NVAM, Filges I, Benmerah A, Giles RH. Mutations in KIF14 cause Meckel-Gruber syndrome and cytokinesis defects. (Manuscript in preparation)

when the signal is lost_marijn_8072018.indd 251 08/07/2018 10:51

CURRICULUM VITAE

Marijn Fijke Stokman was born in Utrecht on February 26th, 1987. She attended Ridge High School in Basking Ridge, New Jersey, and the Maaslandcollege in Oss. Marijn started Medicine at Utrecht University in 2006 and a bachelor English Language and Culture in 2007. In 2010, she did her gynaecology internship in 's Lands Hospitaal in Paramaribo, Surinam. In 2012, she did a six-month research internship in the lab of Prof. dr. Roel Ophoff at the Center for Neurobehavioral Genetics at UCLA in Los Angeles, California, investigating the expression of microRNAs from the 22q11.2 region in different brain regions from patients with psychotic disorder and healthy controls. This inspiring experience motivated her to do a PhD in human genetics. After obtaining her medical degree in 2012, Marijn started working as a resident at the Department of Genetics at the University Medical Center Utrecht and was accepted to become a clinical geneticist in training in 2013. In that same year she began her PhD research that was funded by the Dutch Kidney Foundation and has resulted in this thesis, under supervision of Prof. dr. Nine Knoers, Dr. Rachel Giles, Dr. Marc Lilien and Dr. Kirsten Renkema. She resumed her clinical training at the Department of Genetics in 2017. In the future, she aims to combine clinical genetics with ciliopathy research. Marijn lives in Utrecht with her partner Remmelt and their son Rafaël.

when the signal is lost_marijn_8072018.indd 252 08/07/2018 10:51

A

when the signal is lost_marijn_8072018.indd 253 08/07/2018 10:51